NASA CR-
141890

Calspan

(NASA-CR-141890) EXPERIMENTAL AND THEORETICAL STUDY OF SHUTTLE LEE-SIDE HEAT TRANSFER RATES (Calspan Corp., Buffalo, N.Y.) 203 p HC $7.25 CSCL 20D

N75-26309

Unclas
G3/34 27273

Experimental and Theoretical Study of Shuttle Lee-Side Heat Transfer Rates

Calspan Report No. ZC-5403-A-1

Prepared For:

National Aeronautics and Space Administration
Lyndon B. Johnson Space Center
Houston, Texas 77058

Contract No. NAS9-13707

March 1975

PREPARED BY: G. K. Mruk

J. Bertin (Univ. of Texas)

J. P. Lamb (Univ. of Texas)

APPROVED BY: C. E. Rogers

A. Ritter, Assistant Head
Aerodynamic Research Dept.

Calspan Corporation
Buffalo, New York 14221

TABLE OF CONTENTS

I. FOREWORD

This investigation was carried out by Calspan Corporation for the Lyndon B. Johnson Space Center of the National Aeronautics and Space Administration under Contract No. NAS 9-13707. The test program was conducted during the period of 7 November through 10 December 1974 in the Calspan 96-inch Hypersonic Shock Tunnel. The theoretical studies and data comparisons were performed by The University of Texas under subcontract to Calspan. Dr. John Bertin is the author of the section entitled "Discussion of Results - Orbiter Model" while Dr. J. P. Lamb is the author of "Discussion of Results - Fuselage Model".

The test model was fabricated at The University of Texas; the instrumentation was fabricated and installed by Calspan.

This model and the results of the test program are unclassified.

Dr. W. D. Goodrich of NASA - JSC monitored the program and contributed guidance during the test program and valuable comments regarding interpretation of the data.

II. INTRODUCTION

In order to determine the convective heat-transfer distribution over the leeward surface of space shuttle entry configurations, one must describe a three-dimensional flow-field, which includes extensive regions of separated flow and complex viscous:inviscid interactions. Because of its complexity, the separated flow to the leeward of an entry configuration is a function of many variables. The variables to be considered include:

(1) Reynolds number,

(2) Mach number,

(3) configuration (both forebody geometry and the afterbody geometry),

(4) angle-of-attack,

(5) heat-shield material and mass-addition,

(6) gas composition, and

(7) surface temperature.

Numerous investigators have studied the effect of these parameters on the leeward flow-field for entry configurations at hypersonic speeds. A survey of the relevant literature has been completed as part of the contractual effort and is given in Ref. 1.

The present report discusses the experimental program which was conducted in the Calspan 96-Inch Hypersonic Shock Tunnel to investigate what effect the windward surface temperature had on the heat transfer to the leeward surface of the space shuttle orbiter. Heat-transfer distributions, surface-pressure distributions, and schlieren photographs were obtained for an 0.01-scale model of the 139 configuration space shuttle orbiter at angles-of-attack of 30° and of 40°. Similar data were obtained for an 0.01 scale wingless model of the 139 configuration at angles-of-attack of 30° and of 90°. Data were obtained for Mach numbers from

10 to 19, for Reynolds numbers, $Re_{\infty,L}$, from 0.1×10^6 to 1.75×10^6, and for the following ranges of surface temperatures.

$$T_{wwd} = 0.09T_t \text{ to } 0.31T_t$$

$$T_{lee} = 0.09T_t \text{ to } 0.31T_t$$

The data are compared with theoretical results which are also discussed herein.

III. NOMENCLATURE AND SYMBOLS

SYMBOLS

c	Local sonic velocity
F	Dimensionless streamwise velocity function for the boundary layer (u/u_e)
h	Heat transfer coefficient, equations (4) and (12); also metric for three-dimensional boundary layer
H	Enthalpy, ft. lbs/slug
L	Fuselage length for model (1.075 ft)
M	Mach number
NSE	Normal shock expansion calculation
P	Pressure, psia
Pr	Prandtl number
PSE	Parallel shock expansion calculation
q	Dynamic pressure, psia
$\dot{q}$	Local heat-transfer rate
r	Recovery factor
Re	Reynolds number
s	Wetted distance along a streamline
St	Stanton number, equation (3)
T	Temperature, ^{o}R
t	Time, seconds
u	Streamwise velocity component
v	Normal velocity component
x	Axial coordinate
y	Coordinate measured normal to the model surface
α	Angle-of-attack, degrees
γ	Specific heat ratio
δ	Boundary-layer thickness
δ^*	Displacement thickness
θ	Momentum thickness, equation (16)

SYMBOLS

θ_{II}	Enthalpy thickness, equation (14)
μ	Absolute viscosity, slugs/ft-sec
ν	Kinetic viscosity, μ/ρ
ρ	Density, slugs/ft^3
τ	Shear stress
ϕ	Angular coordinate of the leeward gages, measured as a rotation about waterline z400

SUBSCRIPTS

b	Base flow conditions
e	Edge of boundary layer
i	Incident shock in driven gas
lee	Leeward surface of model
ns	Conditions behind normal shock wave
o	Nozzle supply conditions
o'	Stagnation conditions behind a normal shock
ref	Reference sphere (.01-ft radius)
s	Distance along streamline
t	Stagnation conditions in test section
ts	Test section initial conditions
w	Initial conditions at model surface
wwd	Windward surface of model
1	Initial driven gas condition
2	Conditions behind normal shock
4	Gas conditions behind reflected shock
∞	Free stream or test section conditions

IV. EXPERIMENTAL PROGRAM

The experimental program was conducted to investigate the effect of windward surface temperature on heat transfer to the leeward surface of the shuttle orbiter. Heat-transfer distributions, surface-pressure distributions, and schlieren photographs were obtained in the Calspan 96-Inch Hypersonic Shock Tunnel using an 0.01-scale model of the 139 configuration space shuttle orbiter. A horizontal sheet of insulation, running the entire length of the model at waterline z350, physically divided the model into two sections: the "windward" section and the "leeward" section. A second, wingless windward section was also designed so as to produce a fuselage-only configuration. The model was designed so that the temperature of the windward surface could be varied from 420°R (233°K) to 1400°R (800°K) while the temperature of the leeward surface could be varied from 420°R (233°K) to 530°R (294°K). The parameters of the experimental program included the free-stream Mach number, the free-stream Reynolds number, the angle-of-attack, and the temperature ratios: T_{wwd}/T_t and T_{wwd}/T_{lee}. The values of T_{wwd}/T_t used in the program were (nominally) 0.09, 0.18, and 0.31. The values for T_{wwd}/T_{lee} were (nominally) 1.00, 1.57, 2.70. The values chosen for these parameters were intended to simulate, at one extreme, the temperature ratios obtained during atmospheric entry and, at the other extreme, values typical of those obtained in continuous-flow wind tunnels.

A. Model

As noted above, the 0.01-scale model of the shuttle-orbiter was divided into a windward section and a leeward section. Sketches of the windward and of the leeward sections are presented in Fig. 1. The external body contours of the leeward section were constant in cross section aft of x = 0.334L. The model

did not include either the orbital maneuvering system (OMS) pods or the tail surface. Since the principal objective of the program was to investigate parameters which affect the heat transfer to the leeward surface, most of the instrumentation was concentrated there. All pressure transducers and 43 of the 48 heat-transfer gages were located on the leeward surface. The locations of these gages are presented in Table 1 and in Fig. 1. The angular coordinate of a heat-transfer gage is defined by a rotation with respect to an x-axis at the waterline z400 (see Fig. 1) with $\phi = 0^{\circ}$ at the leeward pitch-plane.

Because the gage locations were identical at the stations x = 0.335L and x = 0.420L, a single sketch is presented in Fig. 1b for these two stations. Although there was no gage at $\phi = 90^{\circ}$ for x = 0.500 L, the instrumentation both at x = 0.500L and at x = 0.600L were identical and one sketch is used for these two stations. An isometric sketch of the leeward surface of the orbiter illustrates the locations of these gages (Fig. 2). Two x-axes are shown in Fig. 2: (1) the waterline z400 which is the axis of rotation for the ϕ coordinate and (2) the waterline z338 which passes through the apex of the orbiter. A horizontal plane passing through the latter axis (i.e., z338) divides the windward surface from the leeward surface for the theoretical boundary-layer solutions. Furthermore, all five static-pressure orifices were located in the leeward pitch plane (See Table 2).

The locations of the five heat-transfer gages which were in the windward plane-of-symmetry, i.e., $\phi = 180^{\circ}$, are also given in Fig. 1 and in Table 1.

For some of the runs, an Incaloy heater-element was placed in the windward section to generate the desired high surface temperature. For other runs, freon was passed through a cooling coil located in the windward section to obtain the desired low surface temperature. For all runs, freon was passed through the cooling coil located in the leeward section. By controlling the mass-flow rate

of the freon, the leeward surface could be maintained at approximately 530°R (294°K) for those runs where the windward surface was heated and at approximately 420°R (233°K) for those runs with a cooled windward surface. The coils can be seen exiting the aft end of the model and constrained to the model-support sting in the installation photographs of Fig. 3.

An insulator plate ran the length of the model at waterline z350 (i.e., the model split line) to limit heat transfer from the relatively hot windward section to the leeward section. The insulator plate consisted of a metal layer to serve as a radiation shield and an asbestos layer to inhibit conduction. The asbestos layer is clearly evident in both views of the model which are presented in Fig. 3. Illustrated in the photograph of Fig. 4 are the various components of the model, including the leeward section, the heat shield (without the asbestos gasket), and the windward section. Of special interest is the geometry and location of the cooling coil. Typical cross-sections (Fig. 1c) of the windward section, fuselage-only model illustrate the contour formed by a nominal chine radius of 1/4 inch.

B. Instrumentation

1. Heat-Transfer Gages

The heat-transfer rates were determined from measurements of the transient surface temperature by means of thin-film resistance thermomenters (Refs. 2 and 3). The standard gage consisted of a Pyrex blank with a substrate thickness of 0.0625 in. (0.1588 cm). This thickness is more than adequate to satisfy semi-infinite slab requirements since the transient heat pulse does not penetrate much beyond 0.01 in. (0.03 cm) in ten milliseconds. A strip of Hanovia-05x bright platinum solution is handpainted along a diameter of the substrate. Upon heating to about 1250°F in a ventilated furnace, the volatile constituents are

driven off and a bright, specular, metallic film that is firmly bonded to the Pyrex is obtained. Film planform dimensions are approximately 1 mm in width by 5 mm in length. Several thin coatings are generally fired consecutively to achieve a room temperature resistance in the range from 75 to 125 ohms. Optical techniques have been used to measure the film thickness which typically is less than 0.1 micron.

To insulate the metallic film, a thin dielectric coating of magnesium fluoride is deposited on the surface of the gage. As the heat capacity of the gage is negligible, the film temperature is a measure of the instantaneous surface temperature of the pyrex and is related to the heat transfer rate by the classical equation of heat transfer into a semi-infinite slab of known thermal characteristics. Analysis has shown this technique to be valid for 0.1-micron-thick gages during the short duration of a shock-tunnel test.

The heat-transfer gages are calibrated prior to tests to determine the change in resistance of the elements with temperature. Since calibrations at very high temperatures are not practical, the gage constant at room temperature (K_{70}) is determined by measuring gage resistance at about 70°F and 150°F and calculating the gage sensitivity constant. Since K_{70} is applicable only to room temperature, a correction to appropriate ambient conditions is required. This conversion has been established by noting that for temperatures up to 1000°F, the resistance-temperature function is defined adequately by a second-degree equation.

$$R_T = a_o + b_o T - c_o T^2$$

Defining temperature T in the Fahrenheit scale, it is convenient to rewrite this equation in terms of a reference temperature of T = 70°F, i.e., room temperature.

$$R_T = a_1 + a_2(T - 70) - a_3(T - 70)^2$$

The constant a_1 is the value of gauge resistance at $T = 70^{\circ}F$.

$$R_T = R_{70} + a_2(T - 70) - a_3(T - 70)^2$$

By differentiating this equation, the value of the slope K at any temperature is obtained.

$$K_T = \left(\frac{dR}{dT}\right)_T = a_3 - 2a_3(T - 70)$$

The constant a_2 is the value of K at $T = 70^{\circ}F$, i.e., $a_2 = \left(\frac{dR}{dT}\right)_{70} = K_{70}$.

Thus the last equation may be written as follows.

$$K_T = K_{70}\,[1 - a_4(T - 70)]$$

where

$$a_4 = \frac{2a_3}{K_{70}}$$

A relationship is available, therefore, to define heat-transfer gage sensitivity at any temperature T in terms of the room temperature calibration value, K_{70}. For engineering purposes, a mean value for a_4 of 2.59×10^{-4} may be used for all gages. The resulting conversion is presented in graphical form in Fig. 5.

These calibrations are then used to set the recording equipment for the expected temperature increases. Calibrations to determine the heat-transfer gage's temperature resistance characteristics are conducted with an error potential of one percent. Far more significant than this is the repeatability of the heat transfer gage during testing. A series of shock tunnel tests designed to determine repeatability of the heat transfer data has shown that the RMS deviation of the repeatability is $\pm$ 3 percent. A combination of these errors indicated that the relative RMS deviation of the leeward heat transfer data is about $\pm$ 3.2 percent.

The data obtained by the five windward heat transfer gages are subject to large uncertainties. This is the result of a thermal instability in the gage resistance. The following reasons are the basis for this conclusion.

1. The use of these gages as steady state resistance thermometers results in disagreement with measurements of the model skin temperature made by Chromel-Alumel thermocouples. Since $R_T = R_{70} + a_2(T - 70) \cdot a_3(T - 70)^2$ (see the section on heat transfer instrumentation) where $a_2 = k_{T=70}$ and $a_4 = 2a_3/k_{70} = 2.59 \times 10^{-4}$, it follows that $R_T - R_{70} = a_2 \left[(T - 70) - (a_3/a_2)(T - 70)^2\right]$ and thus $(R_T - R_{70})/K_{70} = (T - 70) - .295 \times 10^{-4}(T - 70)^2$. Having calibrated the gage at T = 70°F and measuring the resistance, R_T, allows one to use the thin film resistance gage as a thermometer by calculating T in the preceding equation. The model wall temperature prior to a run computed by means of this equation is typically below the Chromel-Alumel thermocouple reading by 400°F in the highest temperature cases, i.e., 600°F instead of 1000°F.
2. Post test calibrations of the gages produced inexplicable changes in gage sensitivities at room temperature as well as changes in the gage resistances in some cases. Following these room temperature re-calibrations, several gages were heated to approximately 1000°F and held at this temperature for about 15 minutes which is similar to the wind tunnel run situation. Following a period of time, during which the gages returned to room temperature, the gage resistance was measured. It was determined that one gage open circuited after two such cycles and further that the resistance was not stable following those cycles for the other gages.
3. Plots of the Stanton Number versus $Re_{\infty/ft}$ and x/L for the data showed large scatter.

It is believed that poor performance of the joint between the platinum film and the lead wire embedded within the pryex substrate is the cause of the thermal instability displayed by the gages.

Because of these large uncertainties the data for the five windward heat transfer gages are not reported herein.

The theory of heat conduction in a nonhomogeneous body is used to relate the surface temperature to the rate of heat transfer. Since the resistance element has negligible effect on the pyrex substrate surface temperature, the substrate can be characterized as being semi-infinite, homogeneous and isotropic. The general heat conduction equation is:

$$\rho c(T) \frac{\partial T}{\partial t} = \frac{\partial}{\partial x} \left(K(T) \frac{\partial T}{\partial x} \right) \tag{1}$$

where ρ, c and k are substrate density, specific heat and thermal conductivity, respectively, and x is the substrate depth.

If the substrate properties are independent of temperature; i.e., if the temperature change is less than $100^{\circ}R$, a closed-form solution is obtained for the heat transfer rate:

$$\dot{q}(t) = \frac{1}{2} \left(\frac{\pi \rho c k}{t} \right)^{1/2} \left[T(t) + \frac{1}{\pi} \int_0^T \frac{\lambda^{1/2} T(t) - t^{1/2} T(\lambda)}{(t - \lambda)^{3/2}} \, d\lambda \right] . \tag{2}$$

This equation is solved directly by use of q-meters, which are passive electrical analog networks, in conjunction with the heat-transfer gage. The analog is based on the fact that the equation for heat conduction in a semi-infinite solid is identical to that for a semi-infinite electrical transmission line with distributed series resistance and shunt capacitance. In practice, it has been found feasible to construct the analog of a finite number of circuit elements

consisting of parallel resistor-capacitor elements in a series arrangement. For temperature changes greater than 100°F the variation of substrate properties and electrical properties of the resistance element with temperature causes a significant droop of the q-meter output which is corrected by a time and heat-transfer-rate dependent factor.

The heat-transfer data were normalized in terms of a Stanton number and heat-transfer coefficient based on free stream conditions. The relations used for the calculations are given by

$$St = \frac{778\ \dot{q}_w}{\rho_\infty U_\infty (r H_o - H_w)} = \frac{778\ \dot{q}_w}{\rho_{ns} U_{ns} (r H_o - H_w)} \tag{3}$$

$$h = 778(32.17)\frac{\dot{q}_w}{(r H_o - H_w)} \tag{4}$$

where the wall conditions are based on the appropriate initial model surface temperature. Heat transfer coefficients were generated for recovery factors of 1.0 and 0.85, whereas Stanton numbers were calculated for r = 1.0.

In addition, a theoretical stagnation heating rate for a 0.01 foot radius sphere was calculated for each run by the method of Fay and Riddell (Ref. 4) for the purpose of data normalization. The sphere temperature used to determine wall enthalpy was that of the windward or leeward model wall depending on the location of the gage whose data was normalized.

2. Pressure

The model pressures were measured by a system developed to meet the particular requirements of shock tunnel testing. The pressure transducers employ piezoelectric crystals, and their small size permits installation within the model. The transducers used in this test have a dual-element feature which reduces acceleration effects to an indicated pressure of 0.00015 psi/g. Pressures as low as 0.001 psi may be accurately measured by these transducers.

The pressure transducers measure the difference between the initial test section pressure and the applied local pressure. The initial pressure is of the order of 5 microns and is added to the measured pressure to obtain the absolute model pressure.

On the basis of calibration repeatability (see Fig. 6 for calibration curve) and on the consistency and repeatability of past pressure data obtained with the type of transducer used to measure model pressure in this test, it is estimated that these data have an accuracy of $\pm$ 5%.

3. Schlieren System

The schlieren system used was of the double-pass collimated type with the knife edge horizontal. This system was used for the sensitivity needed to obtain photographs of shock wave during the low density runs. Schlieren photographs were taken on most of the runs; representative photographs are presented in Appendix B.

4. Model Temperature

The model skin temperature was monitored by means of five Chromel-Alumel thermocouples which were operated with a room temperature reference function.

5. Model Attitude

The model attitude was set with an inclinometer at the desired angle of attack within $\pm$ 0.1°.

6. Data Acquisition

Forty-eight of the electrical outputs of heat transfer gages were sampled at 50-microsecond intervals and recorded on the magnetic storage drum of a Navigation Computer Corporation MCL-100 data acquisition system (NAVCOR). The stagnation-sphere heat-transfer gage and all pressures were recorded on oscilloscopes. The data stored on the magnetic drum were reproduced on a strip chart

recorded for manual reading. The output from each heat-transfer gage, as recorded on the NAVCOR drum, was additionally processed by a "q-meter", which is a passive electrical analog network that converts the analog voltage representation of the gage element temperature into an analog voltage representation of heat-transfer rate. These results were also reproduced on the strip chart. The electrical output of the stagnation heat-transfer gage was first processed by a q-meter and the resultant signal as well as those of the pressure transducers were then recorded on Polaroid film from the oscilloscopes. All measurements are tabulated in Appendix C.

C. The Calspan 96-Inch Hypersonic Shock Tunnel

The basic components of the Calspan 96-inch Hypersonic Shock Tunnel are shown in Fig. 7. This tunnel consists of a chambered shock tube with an area ratio (driver/driven) of 1.56. The 5-inch (12.70 cm) I.D. driver is 16 ft (4.87 m) long and is externally heated to 1260^{o}R (700^{o}K). The 4-inch (10.16) cm I.D. driven tube is 48.5 ft. (14.79 m) long. A helium-air mixture was used as the driver gas. Air was used as the test gas.

The tailored-interface mode of operation was used to provide the longest possible steady-state reservoir conditions. Maximum driver pressure is 30,000 psi (2.07×10^{8} N/m^{2}), which yields a maximum pressure behind the reflected shock of 20,000 psi (1.38×10^{8} N/m^{2}).

All test conditions were obtained using the "D"-nozzle, which is a contoured, axisymmetric nozzle whose exit diameter is 4.0 ft (1.22 m).

D. Test Program

The test conditions for the experimental program are presented in Table 3. Heat-transfer rates were measured over a range of free-stream Mach number from 10.0 to 18.6 and of free-stream Reynolds number from 0.1×10^{6} per foot to

1.6×10^6 per foot (0.3×10^6 per meter to 5.3×10^6 per meter). For the complete orbiter configuration data were obtained at angles-of-attack of 30° and 40°. For the wingless configuration, data were obtained at angles-of-attack of 30° and 90°. Note that, because of the irregular shape of the model, the surface temperature was not uniform for either the leeward section or the windward section. Heat transfer from one part of the model to another contributed to the temperature variations. Therefore, the surface temperatures presented in Table 3 merely represent a nominal value for a particular run.

Values of the freestream Mach number in the test section were determined from previous airflow calibrations in the nozzle. The test conditions of freestream pressure, temperature, and Reynolds number are computed by assuming isentropic expansion of the test gas from the conditions behind the reflected shock in the driven tube to the test section Mach number. The calculation of test section freestream parameters includes the effect of molecular vibration assuming a simple harmonic oscillator model for the diatomic constituents of air.

The stagnation enthalpy and temperature of the air behind the reflected shock are determined, respectively, from

$$H_o = H_1 \, (H_4/H_1) \tag{5}$$

and

$$T_o = T_1 \, (T_4/T_1) \tag{6}$$

where H_4/H_1 and T_4/T_1, are functions of U_i, the incident shock velocity (References 5-7). U_i is obtained by measuring the time taken by the shock wave to pass between two stations in the shock tube. H_1 is taken from Reference 8 and T_1 is measured prior to each run. Freestream static temperature is obtained from

$$T_\infty = \frac{H_o}{c_{P_{\infty AV}}} \left(1 + \frac{\gamma_\infty - 1}{2} \, \frac{c_{P_\infty}}{c_{P_{\infty AV}}} \, M_\infty^2 \right)^{-1} \tag{7}$$

where γ_∞ is a function of c_{P_∞} ; c_{P_∞} and $c_{P_{\infty AV}}$ include vibrational heat capacity and are functions of T_∞ , requiring an iteration between T_∞ and c_P. Freestream pressure is calculated using

$$P_\infty = \frac{P}{P_P} P_o \left(1 + \frac{\gamma_\infty - 1}{2} M_\infty^2 \right)^{-\frac{\gamma_\infty}{\gamma_\infty - 1}} \tag{8}$$

where $\frac{P}{P_P} = \frac{(P/P_o)\ \text{real}}{(P/P_o)\ \text{perfect}}$

is the real gas correction to the ideal static to total pressure ratio as described in Reference 9 but suitably modified to include vibrational specific heat in the test section, and P_o is the measured pressure behind the reflected shock. The source data used in this technique are References 8 and 10.

Freestream velocity, density and dynamic pressure are respectively calculated from

$$U_\infty = M_\infty \sqrt{\gamma_\infty R T_\infty} \tag{9}$$

$$\rho_\infty = P_\infty / \bar{R} T_\infty \tag{10}$$

$$q_\infty = \frac{1}{2} \rho_\infty U_\infty^2 \tag{11}$$

Values for absolute viscosity (μ) used to compute Reynolds numbers were obtained from Reference 11 for temperature below $500^\circ R$ and from Reference 12 for temperature about $500^\circ R$.

Stagnation conditions behind a normal shock in the test section are based on data of Reference 10.

The stagnation enthalpy and the test-section free-stream conditions were calculated, using the thermodynamic properties of real air, the incident shock wave velocity and the nozzle supply-pressure. The speed of the incident shock wave was measured to within $\pm$ 1 percent. Based on the agreement of pressure transducers, the nozzle supply pressure is considered accurate to within $\pm$ 2.6

percent. The test-section Mach number was determined from airflow calibrations made prior to the test program. The computed values of free stream Mach number from a large number of airflow calibrations for each nozzle-throat combination were used to calculate variation coefficients in Mach number of $\pm$ 1.0 percent. Accordingly, the determination of free stream static pressure is considered to be accurate to within $\pm$ 7 percent of the true values.

V. DISCUSSION OF RESULTS - ORBITER MODEL

A. Theoretical Solutions

Theoretical solutions for the viscous boundary-layer of the orbiter model at an angle-of-attack of 30° were generated to determine the effect of the test variables on the boundary-layer prior to separation. The theoretical solutions for the nonsimilar, laminar boundary-layer were computed using the code described in Ref. 13. Required as input for the code are the flow conditions at the edge of the boundary layer, the radius of the "equivalent" body-of-revolution, and the wall-temperature distribution.

The required inviscid solution was provided by Mr. K. Houston of Lockheed (Houston) (Ref. 14) using a code based on Newtonian theory. Representative streamlines for an orbiter configuration, whose geometry is essentially that of the model used in the present program except for the absence of the canopy, are presented in Fig. 8 for an angle-of-attack of 30°. Parametric boundary-layer solutions were obtained along the streamline represented by the unbroken line, since this streamline encounters the free-vortex-layer separation downstream of the canopy but is upstream of the influence of the wing. Therefore, numerical solutions for a nonsimilar, laminar boundary-layer were generated along this streamline for six of the test conditions of the experimental program, i.e.,

Condition 1: $M_\infty = 11.80$, $Re_{\infty/ft} = 1.50 \times 10^6$

Condition 2: $M_\infty = 12.25$, $Re_{\infty/ft} = 0.55 \times 10^6$

Condition 3: $M_\infty = 11.68$, $Re_{\infty/ft} = 0.11 \times 10^6$

Condition 4: $M_\infty = 15.70$, $Re_{\infty/ft} = 0.57 \times 10^6$

Condition 5: $M_\infty = 10.10$, $Re_{\infty/ft} = 0.50 \times 10^6$

Condition 6: $M_\infty = 18.59$, $Re_{\infty/ft} = 0.13 \times 10^6$

For the numerical solutions, the windward and the leeward sections were assumed to be isothermal, though not necessarily of equal temperature. A horizontal plane passing through the x-axis (waterline z338) of Fig. 8 divided the windward

section from the leeward section. Solutions were obtained with values for the ratio of T_{wwd}/T_t equal to:

a: $T_{wwd} = 0.90\ T_t$ b: $T_{wwd} = 0.176\ T_t$ c: $T_{wwd} = 0.307\ T_t$

and with values for the ratio for T_{lee}/T_t of

i: $T_{lee} = 0.090\ T_t$ ii: $T_{lee} = 0.114\ T_t$

A summary of the conditions for which solutions were computed assuming that the fluid at the edge of the boundary layer had accelerated isentropically from a stagnation point behind a normal shock (NSE) is presented in Table 4. Typical results from these solutions are presented in Figs. 9 through 14 as well as in Table 4. Solutions were also generated assuming the fluid at the edge of the boundary layer had accelerated isentropically after passing through an oblique shock (PSE). A summary of the conditions for the PSE solutions is presented in Table 5. Typical results are presented in Figs. 15-16.

Attention is called to three points along the streamline which are of special interest (refer to Fig. 8). Since the first, at s = 0.201L (or 0.216 ft.), is a station just upstream of the section interface, the boundary-layer has been subjected to a uniform temperature wall. Since the second, at s = 0.221L (or 0.237 ft.), is just downstream of the section interface, the solution at this location illustrates the effect of a sudden change in surface temperature. The third, at s = 0.326L (or 0.351 ft.), is just upstream of the "assumed" separation location. The term "assumed" is used since, downstream of this location, the surface of the vehicle is inclined away from the free-stream. However, as will be discussed subsequently, the data indicate that the actual flow remained attached downstream of this location.

The Lockheed-generated solutions (Ref. 14) for the Newtonian pressure distribution and the associated metric describing the streamline divergence are presented in Fig. 9. The fluid properties were calculated assuming the flow

accelerated isentropically from the stagnation point behind a normal shock wave (NSE) in accordance with the pressure distribution of Fig. 9. Making the small-cross-flow approximation, the heat-transfer rate along a surface streamline of the inviscid flow can be calculated using the metric scale-factor (or "equivalent radius") to represent an equivalent body of revolution at zero angle-of-attack. The metric coefficients were calculated using the relations described by DeJarnette (Ref. 15) and Rakich and Mateer (Ref. 16).

Also presented in Fig. 9 is an alternate representation for the pressure distribution. As can be seen in Fig. 9b, there were significant differences between the pressure measured on the leeward section of the model (Ref. 17) and the Newtonian value. However, for most of the windward section the Newtonian values provided a suitable representation of the actual pressures. This was evidenced by the satisfactory agreement between the heat transfer to the windward surface as calculated using the Newtonian flow field and the measured value at $s \approx 0.1$ ft (Ref. 17). Thus, an "empirical" pressure distribution was constructed which represents a fairing from the windward Newtonian values to the measured value.

The boundary-layer profiles of the nondimensionalized streamwise velocity and of the nondimensionalized static temperature are presented in Fig. 10 for flow condition 2. Solutions are presented for three values of the windward surface temperature, i.e., (a) $T_{wwd} = 0.090\ T_t$ for case 2aii, (b) $T_{wwd} = 0.176\ T_t$ for case 2bii, and (c) $T_{wwd} = 0.307\ T_t$ for case 2cii. For all three cases the leeward surface temperature was (ii) $0.114\ T_t$. The corresponding solutions for the surface heat-transfer distributions along the streamline are presented in Fig. 11.

At $s = 0.201L$, which is just upstream of the section interface, the boundary-layer thickness increased by 20% with temperature over the range of surface temperatures considered (see Fig. 10a and Table 4b). Furthermore, as the wall

temperature increased, the temperature gradient at the wall and, therefore, the heat transfer decreased dramatically. At s = 0.201L, the heat transfer for $T_{wwd} = 0.307\ T_t$ was approximately 45% of the heat transfer for $T_{wwd} = 0.090\ T_t$ (see Fig. 11a). The magnitude of the decrease was much greater than would be predicted using the relation:

$$\dot{q} = h(T_r - T_w), \tag{12}$$

where

$$T_r = \sqrt{Pr}\,(T_t - T_e) + T_e \quad . \tag{13}$$

Using this relation the recovery temperature was approximately $0.86\ T_t$ for all three cases. For this recovery temperature, $(T_r - T_w)$ for case 2cii was 72% of the value for $(T_r - T_w)$ for case 2aii. The decrease in $(T_r - T_w)$ for the two cases was much less than the decrease in the computed heat-transfer rate. Thus, either the local heat-transfer coefficient or the recovery temperature (or both) depend on the surface temperature for this highly accelerated flow. The computed displacement thickness at this location was small in magnitude and assumed both positive and negative values for these conditions. The values of the displacement thickness are, therefore, not presented in this report. The momentum thickness exhibits an inverse dependence on the surface temperature (see Table 4b).

The leeward surface temperature was the same for all three cases, i.e., $T_{lee} = 0.114\ T_t$. Thus, as the viscous flow passed from the windward section to the leeward section, it was subjected to an abrupt change in wall temperature. For cases 2bii and 2cii the wall temperature decreased from windward values of $0.176\ T_t$ and $0.307\ T_t$, respectively. However, for case 2aii, the surface temperature increased slightly from the windward value of $0.090\ T_t$, as the viscous layer moved onto the leeward section. As noted previously, with the wall temperature at s = 0.201L equal to $0.307\ T_t$ (i.e., case 2cii),

there was relatively little heat-transferred from the viscous layer to the surface. Thus, as the boundary layer passes onto the relatively cold, leeward section, there is a relative surplus of energy available for heat transfer. The temperature profile and the resultant increase in heat transfer are evident in Figs. 10b and 11a, respectively. A similar increase in heat transfer occurred for case 2bii. As would be expected, the heat transfer for case 2aii decreased abruptly as the boundary layer moved onto the leeward section. With all three viscous flows subjected to the same leeward surface temperature, the differences in the boundary-layer thicknesses for the three wall-temperature distributions quickly decreased. For example, note in Fig. 10b that the thickness of the boundary layer which had been subjected to the cold forebody (case 2aii) was 94% of that which had been subjected to the hot forebody. Substantial differences which continued to exist in the temperature profiles suggest the use of the enthalpy thickness to characterize the effect of the wall-temperature distribution on the boundary layer solutions. The enthalpy thickness is defined as (Ref. 18):

$$\theta_H = \int_0^{\delta} \frac{\rho u}{\rho_e u_e} \left(\frac{h}{h_e} - 1 \right) \, dy \quad , \tag{14}$$

which for a perfect gas is:

$$\theta_H = \int_0^{\delta} \frac{u}{u_e} \left(1 - \frac{T_e}{T} \right) \, dy \quad . \tag{15}$$

Values of the enthalpy thickness are presented in Table 4.

At the station just upstream of the separation location assumed for the theoretical solutions, i.e., s = 0.326L, the boundary-layer thickness was essentially the same for all three cases (refer to Fig. 10c and to Table 4). However, the average static temperature in the viscous layer was greatest for

the flow which has been exposed to the hottest windward surface (i.e., T_{wwd} = 0.307 T_t of case 2cii). This can be seen in the nondimensionalized temperature profiles of Fig. 10c. As a result, the enthalpy thickness and the heat transfer were greatest for case 2cii. At s = 0.326L, the computed heat-transfer for case 2cii was 1.13 times that for case 2bii and 1.23 times heat for case 2aii. Because the enthalpy thickness and the heat-transfer rate were greatest for the cases where the surface temperature of the windward section had been the greatest, one would expect the heat-transfer measurements for the downstream separated region to exhibit similar trends. Recall, however, that the wall-temperature distributions of the experimental program correspond to ratios of T_{wwd}/T_{lee} of (1) 0.090 T_t/0.090 T_t, which is combination ai, (2) 0.176 T_t/0.114 T_t, which is combination bii, and (3) 0.307 T_t/0.114 T_t, which is combination cii. Thus, the heat-transfer distribution for case 2ai (which is presented in Fig. 11b) would be more germaine to the analysis of the experimental data than that for case 2aii. For $0.206 \leq s \leq 0.326L$, the local heat-transfer rates computed for case 2ai were approximately equal to those computed for case 2bii. Thus, the difference in the theoretical heat-transfer at the last station before "separation" were of the order of 13% for the three most relevant cases.

The nondimensionalized streamwise velocity and the nondimensionalized temperature profiles for the boundary layer at s = 0.326L are presented in Fig. 12 for flow condition 4, M_∞ = 15.70, $Re_{\infty/ft} = 0.57 \times 10^6$. At this station, the difference in surface temperature of the windward section did not significantly affect the boundary-layer thickness. However, as was the case for flow condition 2, a significant difference remains in the average static temperature in the boundary layer, which is reflected in the enthalpy thickness.

The enthalpy thickness is presented in Fig. 13 as a function of the Reynolds number behind a normal shock wave. Note that, for these wind-tunnel

conditions, the enthalpy thickness can be correlated in terms of this single parameter, Re_{ns}, over the range of free-stream Reynolds numbers and free-stream Mach numbers considered. As has been discussed, the enthalpy thickness was greatest, i.e., least negative, for those cases where the windward surface temperature was greatest, i.e., $T_{wwd} = 0.307\ T_t$.

The momentum thickness

$$\theta = \int_0^{\delta} \frac{\rho u}{\rho_e u_e} \left(1 - \frac{u}{u_e} \right) dy, \tag{16}$$

which for a perfect gas is:

$$\theta = \int_0^{\delta} \frac{T_e\ u}{T\ u_e} \left(1 - \frac{u}{u_e} \right) dy \tag{17}$$

is presented as a function of the Reynolds number behind a normal shock wave in Fig. 14. As would be expected from a comparison of eqn. (15) with eqn. (17), the momentum thickness can also be correlated in terms of this single parameter, Re_{ns}, over the range of free-stream Reynolds number and of free-stream Mach numbers considered. The momentum thickness was the smallest for those cases where the windward surface temperature was greatest.

For the PSE solutions, the procedure used to calculate the fluid properties at the edge of the boundary layer was as follows. (1) The static pressure, the Mach number, and the isentropic stagnation pressure was calculated for the flow downstream of a shock wave which was inclined 30° to the free-stream. (2) The location on the streamline at which this value for the static pressure and the value predicted using the NSE distribution (presented in Fig. 9) were equal was determined. (3) Downstream of this location, the flow was assumed to acclerate isentropically in accordance with the pressure distribution (p/p_{te}) given by the product of the pressure distribution of Fig. 9 (p/p_{t2}) and the ratio p_{t2}/p_{te}. Numerical solutions for a nonsimilar, laminar boundary-layer were generated for

three of the test conditions:

$$\text{Condition II: } M_\infty = 12.25,\ Re_{\infty/ft} = 0.55 \times 10^6$$

$$\text{Condition IV: } M_\infty = 15.70,\ Re_{\infty/ft} = 0.47 \times 10^6$$

$$\text{Condition V: } M_\infty = 10.10,\ Re_{\infty/ft} = 0.50 \times 10^6$$

Note that these free-stream conditions are identical to those for condition 2, 4, and 5. However, the shock strengths and, therefore, the local flow conditions at the edge of the boundary-layer are markedly different. It was found that the local heat-transfer rate and the local Reynolds number integrated along the streamline for a given free-stream condition was much larger for the PSE solutions (see Table 5) than the corresponding values for the NSE solutions. As a result, the boundary layer is thinner. The effects of the surface temperature distribution on the PSE solutions for the boundary-layer thickness and for the momentum thickness (see Table 5), for the boundary-layer profiles of the nondimensionalized streamwise velocity and of the nondimensionalized static temperature (see Fig. 15) and for the heat-transfer distribution (see Fig. 16) were similar to those observed for the NSE solutions.

Recall that nonsimilar, laminar boundary-layer solutions have been generated for the modified Newtonian pressure-distribution and for the empirical pressure distribution using the NSE relations and the PSE relations. The theoretical heat-transfer thus computed for s = 0.326L (refer to Fig. 8) is presented in Fig. 17 as a function of Re_{ns}. The theoretical solutions for all four cases are correlated by:

$$St = A(Re_{ns})^{-0.5} \tag{18}$$

The specific value of A depends on the pressure distribution, the metric-coefficient distribution, and the assumed expansion process. (Although solutions are presented only for the metric distribution of Fig. 9, the heat transfer differed significantly for solutions generated for other distributions of the metric co-

efficient). Note that, for a given pressure distribution, the PSE heat-transfer is approximately 1.2 times the NSE value. Note, however, that the pressure distribution had a more pronounced effect on the heat-transfer rate. The heat transfer calculated using the empirical pressure distribution was approximately 2.7 times that calculated using the modified Newtonian pressure distribution. Although the empirical pressure distribution was only very approximate and although it was not possible to calculate a metric-coefficient distribution based on experimental pressures, the theoretical heat-transfer values based on the empirical pressure distributions, i.e., curves 3 and 4, will be used for the subsequent comparisons with the heat-transfer data from gages T18, T23, and T33.

B. The Experimental Data for an Angle-of-Attack of 30°

The heat-transfer measurements are presented in two forms:

(1) a dimensionless ratio of heat-transfer coefficients, $h/h_{t,ref}$, which involves the ratio of the measured, local heat-transfer rate to the theoretical heat-transfer rate to the stagnation point of a 0.01-ft. radius sphere as calculated using the theory of Fay and Riddell (Ref. 4). For purposes of data presentation, the recovery factor r has been set equal to unity. Although the definition for the heat-transfer coefficient employed by Calspan for data reduction (see eqn. 4) differs from that used in the theoretical section (see eqn. 12), the magnitude of the dimensionless ratio is the same for both definitions.

(2) a Stanton number where

$$St = \frac{\dot{q}_w}{\rho_\infty U_\infty (H_o - H_w)} = \frac{\dot{q}_w}{\rho_{ns} U_{ns} (H_o - H_w)}$$

Other parameters used in the data correlations include the free-stream Reynolds number based on model length, $Re_{\infty,L}$, where

$$Re_{\infty,L} = \frac{\rho_\infty U_\infty L}{\mu_\infty} \qquad (19)$$

(L is the model length, 1.075 ft.) and the Reynolds number behind a normal shock, Re_{ns}, where

$$Re_{ns} = \frac{\rho_{ns} U_{ns} r_{ref}}{\mu_{ns}} \qquad (20)$$

(r_{ref} = 0.01 ft.).

Heat-transfer distributions. - Typical heat-transfer distributions are presented in the isometric projections of Fig. 18 for the ϕ = 0° plane, which is the leeward pitch-plane or plane-of-symmetry, and for the ϕ = 90° plane, for which the boundary-layer was attached foreward of the wing. A viscous interaction between the vortex shed from the wing leading-edge and the attached boundary layer on the fuselage produced locally high heating rates at gage T33 (which is the fourth gage in the ϕ = 90° plane). This viscous interaction apparently also affected the heat transfer in the separated region. Note the relatively high heat-transfer rate recorded at the gage at x = 0.70L in the ϕ = 0° plane (i.e., the next-to-last gage in the leeward pitch-plane) for the higher Reynolds number flow. Heat-transfer data reported by Zakkay et al (Ref. 19) also exhibited locally high, leeward heating rates near the aft-end of the orbiter (at x ≈ 0.8L). The mechanism responsible for this heat-transfer perturbation is believed to be comparable to that of the present tests.

The heat-transfer distribution in the leeward plane of symmetry was similar to that observed during previous tests which were conducted in Tunnel B at AEDC (Ref. 20) of a model with a protuding cockpit. A shock-induced increase in the heating rate was recorded at the gages located on the canopy windshield. The shock-perturbed, nondimensionalized value for the heat transfer was greatest for the highest Reynolds number. Although the nose region geometry differed for the configurations tested in Tunnel B, the nondimensionalized heat-transfer coefficients for the windshield also increased with Reynolds number. The minimum heat-transfer occurred just downstream of the canopy.

At the lower Reynolds number (Fig. 18b) the downstream heat-transfer was essentially constant. However, at the higher Reynolds number, the heat-transfer increased markedly at $x \simeq 0.4L$ and remained high at the downstream gages. This Reynolds-number-dependent behavior indicates that the increase was due to transition of the shear layer. A similar increase was evident in the heat-transfer distributions for all three Reynolds numbers of Ref. 20 ($1.6 \times 10^6 \leq Re_{\infty,L} \leq 7.8 \times 10^6$). Increased heating to the leeward surface due to transition of the shear layer was also reported by Zakkay et al (Ref. 19) and by Whitehead et al (Ref. 21).

The heat-transfer measurements for those leeward pitch-plane gages downstream of the cockpit are presented in Fig. 19 for those runs where the free-stream Mach number was approximately 12. The data are presented for the highest windward-surface-temperature ($0.31\ T_t$) in Fig. 19a, for the intermediate windward-surface-temperature ($0.18\ T_t$) in Fig. 19b, and for the lowest windward-surface-temperature ($0.09\ T_t$) in Fig. 19c. For a given Reynolds number, the heat-transfer distributions were essentially the same for the two higher surface temperatures (Fig. 19a and Fig. 19b). The phrase "essentially the same" was chosen because, although the distributions were qualitatively similar for a given Reynolds number, the magnitude of the heat-transfer did depend on the windward surface-temperature (as will be discussed for subsequent figures). At the lowest Reynolds number, the heat-transfer distribution indicated that the shear layer was laminar. At the intermediate and at the highest Reynolds number, the heat-transfer distributions indicated the onset of transition. When the shear layer was turbulent, the dimensionless heat-transfer coefficient at a given station was Reynolds-number dependent. This Reynolds-number dependence resulted because the numerator contains the experimental value of the local heat-transfer which resulted from a turbulent shear-layer while the denominator contains the theoretical laminar value. Since the

Reynolds-number dependence for the numerator differs from that for the denominator, the dimensionless ratio would not be expected to be independent of Reynolds number.

Significant differences were observed at the highest Reynolds number for those runs where $T_{wwd} \approx 0.09\ T_t$ (see Fig. 19c). The shear layer apparently was laminar at the lowest Reynolds number. At the intermediate Reynolds number, the data indicated transition occurred, with the turbulent heat-transfer measurements exhibiting only a weak dependence on streamwise position. However, at the highest Reynolds number, there were marked streamwise variations in the heat-transfer measurements downstream of transition. This was the only run for which such locally severe heating rates were observed for the vortical, turbulent flow. Note that heat-transfer rates were measured only at finite number of points. It is possible that similar peaks occurred for other runs but were not measured.

Circumferential heat-transfer distributions for those runs where the free-stream Mach number was essentially 12 are presented in Fig. 20. Distributions are presented for two axial-stations: $x = 0.335L$ and $x = 0.420L$ for each of the three surface-temperature combinations. Recall that $\phi = 0°$ (0.0 radians) corresponds to the leeward pitch-plane and that $\phi = 90°$ (1.571 radians) is the tangency point for the leeward arc. Based on the heat-transfer data, the boundary-layer separation occurred between 40° and 56° from the leeward plane-of-symmetry (at these two stations). At the forward station, i.e., $x = 0.335L$, the heat-transfer data indicated that both the attached boundary-layer and the shear layer were laminar. At the downstream station, i.e., $x = 0.420L$, the heat-transfer measurements reflect the complexity of the local flow. The Reynolds-number dependence of the heat-transfer measurments for gage T33 (at $\phi = 90°$) was due to the viscous interaction between the boundary layer and the vortical flow generated by the wing leading-edge. The onset of shear-layer

transition affected the heat-transfer measurements for the gage located in the leeward plane-of-symmetry at x = 0.420L (which was gage T29). As noted when discussing the data of Fig. 19, the shear layer was laminar at the lowest Reynolds number, turbulent at the two higher Reynolds numbers. However, the heat-transfer measurements from the gages between $\phi = 90°$ and $\phi = 0°$ were independent of Reynolds number, indicating that the attached boundary-layer and the separated shear-layer were laminar.

The heat-transfer distributions for those leeward pitch-plane gages downstream of the canopy are presented in Fig. 21 for those runs where the free-stream Reynolds number based on model length, $Re_{\infty,L}$, was nominally 0.6×10^6. The controlled test-parameter which was varied for these runs was the free-stream Mach number. However, because the free-stream Mach number varied, the Reynolds number behind a normal shock wave,

$$Re_{ns} = \frac{\rho_{ns} U_{ns} r_{ref}}{\mu_{ns}} ,$$

(r_{ref} = 0.01 ft) also varied. Specifically, the values were as follows:

Run	M_∞	$Re_{\infty,L}$	Re_{ns}
15	10.05	0.525×10^6	704.9
10	12.26	0.566×10^6	528.9
13	15.71	0.613×10^6	354.0
38	10.16	0.610×10^6	770.1
34	12.28	0.600×10^6	557.9
37	15.70	0.619×10^6	357.5

Over the Mach number range of the present test program, Re_{ns} varied by a factor of two, although $Re_{\infty,L}$ was approximately constant.

Note that, if one considers the leeward viscous flow as characterized more by the Reynolds number behind a normal shock wave than by the free-

stream Reynolds number, the nondimensionalized values of the heat-transfer coefficient increased with Re_{ns}. As noted previously, this is not unexpected since the numerator would exhibit the Reynolds-number dependence of turbulent data, while the denominator would exhibit that for laminar theory. Thus, it is suggested that the data of Fig. 21 not be interpreted in terms of a Mach number effect but in terms of a Reynolds number effect. Further, the parameters used in correlations of the data should be evaluated using properties downstream of the shock wave rather than the free-stream conditions. The use of local flow conditions to correlate the separated-flow parameters is certainly not innovative (e.g., ref. 22).

Circumferential heat-transfer distributions are presented in Fig. 22 for those runs where the free-stream Reynolds number, $Re_{\infty,L}$, was nominally 0.6×10^6. The variation in heat transfer near the leeward plane-of-symmetry at $x = 0.420L$ was due to the turbulent character of the shear layer. Thus, these data are believed to exhibit a Reynolds-number dependence (characterized for the present report by the parameter Re_{ns}) rather than a Mach-number dependence.

Data for individual gages. - So that the relation between the local flow characteristics and the local heat transfer can be better seen, the experimental Stanton numbers (St) for a particular gage are presented as a function of Re_{ns}. The sketches of Fig. 23 illustrate the locations of the gages for which heat-transfer data are presented. Similarly, experimental pressures for specific orifices are presented as a function either of $Re_{\infty,L}$ or Re_{ns}. The nondimensionalized pressure parameter is the local static-pressure measurements divided by either the calculated free-stream static-pressure (p/p_∞) or divided by the calculated stagnation pressure behind a normal shock wave (p/p_{t2}).

For the correlations of the measurements for a given gage (both pressure data and heat-transfer data), the symbols used are consistent from one figure

to another. Since the data are presented as a function of the Reynolds number, the symbols are used to identify the nominal values for the two remaining test parameters (Recall that $\alpha = 30°$ for this section). For the free-stream Mach numbers:

○ $M_\infty \simeq 10$; □ $M_\infty \simeq 12$; ◇ $M_\infty \simeq 16$; ▽ $M_\infty \simeq 18$

For the temperature combinations:

open: $T_{wwd} \simeq 0.31\ T_t$, $T_{lee} \simeq 0.11\ T_t$

half-filled: $T_{wwd} \simeq 0.18\ T_t$, $T_{lee} \simeq 0.11\ T_t$

filled: $T_{wwd} \simeq 0.09\ T_t$, $T_{lee} \simeq 0.09\ T_t$

This symbol logic was not used in figures where the experimental measurements are presented as a distribution rather than data for a particular gage, e.g., Fig. 26.

(a) Gages located on the lateral surface of the fuselage where the boundary layer is attached. - The experimentally-determined Stanton numbers for gages T18, T23, and T33 are compared with the theoretical values in Fig. 24a, 24b, and 24c, respectively. The theoretical values are those for s = 0.326L (see Fig. 8) as calculated using the "empirical" pressure distribution and the Newtonian metric coefficient distribution of Fig. 9. Thus, the theoretical values correspond to correlations 3 and 4 of Fig. 17. Note that for these flow-field assumptions, the theoretical values did not provide even rough estimates for the experimental values. Based on a telephone conversation with Dr. W. D. Goodrich of NASA/JSC, it is believed that the correlation between theory and data would be significantly improved if a metric coefficient distribution based on the actual pressures were to be used.

However, a comparison between the measurements and the laminar, theoretical values indicates that the boundary layer was laminar for gages T18 and T23. For gage T33 (see Fig. 24c), the experimentally-determined Stanton numbers indicated the flow was laminar for some runs. However, for other runs the

data were correlated by the turbulent correlation

$$St = B(Re_{ns})^{-0.2} \tag{21}$$

This turbulent behavior is attributed to the interaction between the vortical flow generated by the wing leading-edge and the boundary layer. With the exception of these turbulent data, the experimental heat-transfer values for gages T18, T23, and T33 were usually highest for those runs where $T_{wwd} = 0.31\ T_t$. This is consistent with the correlation between wall-temperature distributions and the theoretical, laminar heat-transfer calculations presented in Figs. 11 and 16.

(b) Gages located on the nose upstream of the cockpit. - The static-pressure data for P2, a pressure orifice located in the leeward pitch-plane upstream of the cockpit, is shown in Fig. 25. Oil-flow patterns from other investigations (e.g., Ref. 20) indicate that the nose-region separation pattern was of the free-vortex-layer type. At $x \simeq 0.12L$, the data from Ref. 20 shows that the circumferential component of the flow which was initially directed toward the leeward plane of symmetry reversed direction. At the separation line, oil accumulated and proceeded to travel down the separation line toward the rear of the orbiter. The oil near the leeward plane-of-symmetry continued to flow from the attached region into the vortex region indicating that the longitudinal component of the skin friction was always finite. Thus, it can be assumed that P2 for this test was located in a region of attached flow.

The dimensionless pressure parameter p/p_∞ is presented as a function of Re_{ns} in Fig. 25a. Note that, for a given Mach number, this parameter was approximately constant. Thus, the experimental value of p/p_∞ was a function of the free-stream Mach number rather than the Reynolds number. As would now be expected, the pressure ratio p/p_{t2} for the orifice in this attached flow region was essentially constant, independent both of Mach number and of Reynolds number. The pressure measurements for P2, thus nondimensionalized, are presented in Fig. 25b.

The pressure distribution for the leeward plane-of-symmetry is presented in Fig. 26. Included are data from the present tests and from the Ames Research Center (Ref. 17). The streamwise pressure decrease in the Ames data indicates the rapid acceleration of the flow over the nose. Note that the measured pressure was a minimum at x = 0.10L then increased for the next orifice, which was upstream of the canopy. Bertin, et al (Ref. 20) found that 30^{o} was the lowest angle-of-attack at which the cockpit-generated flow-field perturbation caused the heat transfer to increase at locations upstream of the cockpit. The cockpit-generated shock-wave produced the sharp increase in the pressure measurements for those orifices located on the cockpit windshield. Upstream of the cockpit, the nondimensionalized pressures from the Ames tests were independent of the test conditions. However, downstream of the cockpit, the pressure data were not independent of the test conditions.

Theoretical solutions for the nose-region boundary-layer in the leeward plane-of-symmetry were generated using the code of Ref. 13. The local fluid properties at the edge of the boundary layer were evaluated assuming the inviscid flow expanded isentropically from the stagnation point behind a normal shock wave (NSE) in accordance with the pressures measured at the Ames Research Center (Fig. 26). Solutions were generated for a two-dimensional boundary-layer and for a three-dimensional boundary-layer with small cross-flow. For the three-dimensional solutions, the Newtonian values for the metric-coefficient distribution provided by Houston (Ref. 14) were used.

The theoretical values for the nose-region heat-transfer are compared with the experimental values for T4 (x = 0.100L) and for T8 (x = 0.125L) in Fig. 27. The theoretical solutions for three-dimensional flow underpredicted the heat transfer by (typically) one-third. Thus, the data indicate that, although the free-vortex separation of the boundary layer has occurred in this region away

from the plane of symmetry, there was a strong axial flow component near the plane of symmetry. The resultant shearing force can be seen in oil-flow photographs (Ref. 20) and in the heat-transfer data of Fig. 27. Improved correlation between data and theory would be expected if the effect of the entropy gradients on the fluid properties at the edge of the boundary layer were to be included and if a metric-coefficient distribution based on the actual flow field were to be used. Nevertheless, the similarity between the Reynolds number dependence of the data and of the theoretical, laminar values indicates that the flow was laminar at both stations for all conditions. Note also that the experimental heat-transfer rates were greatest for those runs where the windward surface-temperature was greatest ($T_{wwd} \simeq 0.31\ T_t$). Thus, as noted in the theoretical section, since there was less heat transferred from the boundary layer to the relatively hot wall, there was a "surplus" of energy available for heat transfer to the leeward section.

(c) A gage located on the cockpit windshield. - A shock wave was generated as the supersonic flow of the nose region encountered the cockpit windshield. The interaction between the viscous layer and the shock wave, which was evident in the schlieren photographs (see Appendix B), significantly perturbed the flow field. The experimentally-determined Stanton numbers for a gage on the cockpit windshield are presented in Fig. 28 as a function of the Reynolds number behind a normal shock wave. For relatively low values of Re_{ns} (i.e., $Re_{ns} < 130$), the $St:Re_{ns}$ relationship was that for a laminar flow. For $Re_{ns} > 300$, the shock-induced perturbation apparently promoted premature transition of the boundary layer. The Stanton number, however, did not vary as $(Re_{ns})^{-0.2}$ as one might expect for a turbulent shear-layer but was essentially constant.

(d) Gages located in the separated region downstream of the cockpit in the separated region where the shear layer was laminar. - The heat-transfer measurements for T19 and for T21 are presented in Fig. 29. These gages were located

in the separated region downstream of the cockpit at x = 0.279L. For a given test condition, the heat-transfer rates were essentially equal for these two gages and were approximately one-sixth the heat-transfer rates measured at T23, which was subjected to the attached, laminar boundary-layer at this station. Note that, for gages T19 and T21, the experimentally-determined Stanton numbers varied as $(Re_{ns})^{-0.5}$, as did the data for T23. Thus, it is concluded that the shear layer was laminar for all test conditions at this station. Note that the heat transfer was usually greatest for those runs where the windward surface-temperature was greatest, i.e., $T_{wwd} \approx 0.31\ T_t$.

(e) Gages located in the separated region downstream of the cockpit where the shear layer was transitional. - The heat-transfer measurements for T29 and for T31 are presented in Fig. 30. These gages were located in the separated region downstream of the cockpit at x = 0.420L. Note, however, that the relation between the experimentally-determined Stanton number and the Reynolds number differed significantly for these two gages. For gage T29, the measurements followed a laminar correlation, $(Re_{ns})^{-0.5}$, for $Re_{ns} < 130$. For $Re_{ns} > 300$, the data for gage T29 followed a turbulent correlation, $(Re_{ns})^{-0.2}$. Over the entire Reynolds number range, the experimentally-determined Stanton number for gage T31 varied roughly as $(Re_{ns})^{-0.5}$. For $Re_{ns} < 130$, i.e., where the shear layer was laminar for both locations, the heat-transfer rates were approximately equal for the two gages and were roughly one-sixth of the values measured at T33. Referring to Fig. 24c, the boundary layer for T33 was laminar and attached. For $Re_{ns} > 300$, the heat-transfer rates for gage T29 were significantly greater than those for gage T31 but significantly less than the attached values for gage T33.

The static-pressure measurements for PS4 are presented in Fig. 31. The static pressures which have been divided either by the free-stream value (p/p_∞) or by the stagnation pressure behind a normal shock wave (p/p_{t2}) are presented

as a function either of Re_{ns} or of $Re_{\infty,L}$. The presentation of the data in terms of the parameter p/p_{t2} as a function of Re_{ns} appears to provide the best correlation. The static pressure at this location in the separated region decreased as the Reynolds number increased. The Reynolds-number dependence of these data corresponded to the second of the four regions described by Crocco and Lees (Ref. 23) to characterize the correlation between base pressure and Reynolds number. The decrease in base pressure as the Reynolds number increased occurred because transition in the shear layer moved upstream from the throat (with a corresponding order-of-magnitude increase in the local mixing rate). The increased mixing rate was more important than the accompanying increase in the thickness of the mixing layer which, by itself, would have caused the base pressure ratio to decrease.

(f) Gages located in the separated region downstream of the cockpit where the shear layer was turbulent. - Heat-transfer measurements for gages T37, T39, and T41 are presented in Fig. 32. For all three gages, the experimentally determined Stanton number varied as $(Re_{ns})^{-0.2}$, the correlation for a turbulent shear layer. Note, however, that the measurements for gage T41 exhibited significant scatter. Recall that this gage was located in the region affected by the flow-field perturbation created by the interaction between the viscous flow and the vortex shed from the wing leading-edge.

The highest heat-transfer rates recorded at T37 were those runs where $T_{wwd} \approx 0.31\ T_t$. (Unfortunately, the gage was inoperative for the runs where $T_{wwd} \approx 0.09\ T_t$). Thus, although the shear layer was turbulent, the correlation between the local heating rate and the windward surface temperature is similar to that observed for gages where the shear layer was laminar. For gages T39 and T41, there was no clear correlation between the local heat-transfer rate and the windward surface-temperature. The mixing due to the interaction with the vortical flow apparently eliminated the effect of the windward surface-temperature.

VI. DISCUSSION OF RESULTS - FUSELAGE MODEL

A. Theoretical Calculations

A primary motivation for the inclusion of a series of fuselage tests (at $\alpha = 90^{o}$) was the expectation that direct comparison of test data with planar theoretical models would be facilitated. The theoretical computation procedure did not attempt to predict the complete flow field and resulting convective heat transfer distributions but, instead, utilized measured base pressures and an assumed location of boundary layer separation to predict the average level of heat transfer to the leeward surface. The general features of the computation technique are outlined in the following paragraphs.

The integral model of laminar wake heat transfer developed by Lamb and Hsieh Reference (24), which is summarized in Appendix A, requires as an input the boundary layer thickness at the separation location. This parameter naturally requires a boundary layer prediction for the attached flow upstream of separation. The laminar boundary calculation method is also described in Appendix A; a primary requirement in this computation is the wall pressure distribution. A limited number of data channels prevented extensive measurement of pressures in the current test program. Hence it was necessary to estimate the wall pressure variation using previous measurements reported in Reference (25). These data were obtained on a 1.5-inch wide model (designated C-3), the cross-section of which was similar to the fuselage model. Test data were obtained at $\alpha = 90^{o}$ in the Vought Aeronautics Hypervelocity Tunnel under flow conditions similar to those of the present test program.

Figure 33 depicts the measured pressures on the C-3 model; the length scale begins just aft of the chine. Using a measured base pressure value one can construct the approximate pressure distribution shown as a solid line. A similar estimation technique was employed for the fuselage boundary layer

calculations. By juxtaposing the C-3 pressure distribution to the same relative location on the fuselage cross section and employing measured base pressures, one can obtain approximate pressure distributions of the form shown in Figure 33 with the broken lines. For the $\alpha = 90^{\circ}$ runs all base pressures were between the values indicated whereas, for both $\alpha = 30^{\circ}$ runs, the base pressure values were approximately 0.009. The foregoing procedure assumes that the small chine radius effectively extinguishes the stagnation region boundary layer.

The separation location ($\phi = 60^{\circ}$) shown in Figure 33 was based on the surface heat transfer distributions to be discussed subsequently. In addition, the wall temperature distribution employed in the boundary layer computation was based on values of T_{wwd} and T_{lee} presented in Table 3; the temperature across the insulation strip between windward and leeward fuselage sections was assumed to vary linearly between the two theoretical temperatures. Effects of this approximation will also be discussed subsequently.

Initial calculations of wake heat transfer using the foregoing boundary layer prediction method yielded results which were lower than experiment by approximately 50%. Investigation of possible causes of the discrepancy ruled out either the boundary layer or wake calculations but, rather, suggested that the boundary layer separation process itself was not being modeled in sufficient detail. This portion of the flow field is of crucial importance for it serves as the primary connection between the attached layer and the wake region. Additional insight was obtained from a parallel study of supersonic turbulent boundary layer separation which suggested that the pressure rise associated with separation causes the lower part of the viscous layer to be lifted away from the wall while the outer region of the layer is virtually unaffected; this is a result primarily of the inclination of Mach waves within the layer. The resulting distortion of the incoming velocity profile is depicted schematically in Figure 34.

A simple relation between the two thickness values, δ_1 and δ_s, was obtained using a result from the turbulent flow study which showed that the sonic line remains nearly parallel to the wall for a short distance downstream of the onset of the pressure rise. Using the velocity profile associated with δ_1 and the corresponding Karman-Polhausen separation profile, Reference (18), along with the compressibility transformation summarized in Appendix A, it is possible to compute the ratio δ_s/δ_1 under the assumption that y^* is constant. Values of δ_s/δ_1 ranged from 0.43 to 0.56 and thus the nominal value of 0.5 was employed in all subsequent wake heat transfer calculations. Despite its simplicity the model suggests the existence of an important influence in predicting heat transfer to smooth leeward surfaces; namely, that heat transfer depends strongly on the inner part of the boundary layer and, hence, a length scale based on δ_1 is inappropriate.

The wake heat transfer solutions were generated with the theoretical model outlined in Appendix A. Using as inputs the measured base pressure and computed boundary layer thickness, δ_s, along with the local unit Reynolds number determined from Re_{ns} and the pressure distribution of Figure 33, the wake calculation iterated on the shear layer inclination angle ψ (Figure A-1) until the flow field was uniquely determined; the thermal energy balance then provided a prediction of the leeward surface heat transfer rate. No special procedure was employed for Runs 1 and 32 in which $\alpha = 30^\circ$. The predictions are thus representative of a hypothetical flow at $\alpha = 90^\circ$. A summary of input parameters and predictions is tabulated in Table 6.

B. Experimental Results

Figures 35a through 35j present the measured circumferential distributions of heat transfer for the eight longitudinal stations downstream of the nose and canopy region; for these stations the leeward surface contour was constant. Identified on each plot is the average of the leeward heat transfer measurements ($\phi \leq 60^{\circ}$) which is denoted by "A". Also identified is the corresponding theoretical prediction, denoted by "T", as well as the assumed location of separation, denoted by "S", at $\phi = 60^{\circ}$. It is observed that only for Run 31 did the average measured value fall above the prediction; in all other cases the theory was either above or equal to the measured average. However, in all cases (including the two $\alpha = 30^{\circ}$ runs) the predictions are within the scatter of the data.

It is also noted that, within the separated region, the highest values of heat transfer fall on the leeward pitch-plane ($\phi = 0^{\circ}$). Moreover, the lowest values tend to occur just downstream of separation. Both of these trends can be explained with the flow field depicted in Figure A-1 which suggests that the leeward pitch-plane receives a stagnation line flow whereas the upward flow along the leeward surface develops a boundary layer which tends to provide greater insulation than the stagnation layer.

More detail on the longitudinal distributions, which is not evident in the circumferential plots, is presented in Figures 36a through 36e. The two $\alpha = 30^{\circ}$ runs are shown in Figure 36a and it is again observed that the predictions, which did not include any angle of attack influence, are within the experimental variation. With respect to the eight distributions for the $\alpha = 90^{\circ}$ runs there are large excursions in heat transfer in most cases which suggest either a lack of two-dimensionality or possible near wake transition.

One can observe the effect of a high T_{wwd} value by comparing the distributions for Runs 26 and 28 (Figures 36b and d). As Table 3 shows, the primary difference between these runs was the higher value of T_{wwd} in Run 28. It is clear from the two distributions that the heated windward section resulted in a substantially larger leeward heat transfer level. Note also that the theoretical predictions do not exhibit any affect of T_{wwd} because, as was noted earlier, the attached boundary layer computation was based on an idealized wall temperature variation which, for large values of T_{wwd}, is clearly inappropriate. Thus future analytical treatments of the boundary layer should include a simultaneous solution of the energy equation with the momentum equation.

The foregoing effect of T_{wwd}, as well as the influences of α and M_∞, can be illucidated more clearly by employing the average measured heat transfer levels shown in Figure 35 as characteristic parameters for leeward heat transfer. After conversion to Stanton number with equation (3) the average heat transfer values have been plotted in Figure 37 versus the Reynolds number Re_{ns} defined in equation (20). This plot displays the very obvious differences due to angle of attack and also indicates that the high Mach number run (No. 30) is easily correlated. The effect of T_{wwd}/T_{lee} is observable for Runs 26, 28, Runs 1, 32, and Runs 3, 27, 31. It is now seen that the heat transfer difference attributable to the high value of T_{wwd} is much less pronounced at the high Reynold numbers. The broken line shown in Figure 37 was added to assist in the visual correlation of the data; its slope was calculated subsequently as -0.42. The theoretical laminar value of -0.5 from equation (18) could be obtained by connecting the two data points for Runs 29 and 31. Thus it is concluded that there were no significant transition effects present in the fuselage tests.

Recalling that wake heat transfer is proportional to the base pressure level, one can correlate the $\alpha = 30^o$ data merely by dividing the Stanton number by the

ratio $P_b/P_{t,2}$ tabulated in Table 6. This correlation is illustrated in Figure 38 where it is observed that the only remaining uncorrelated influence is that of T_{wwd}/T_{lee}. Two approaches toward clarification of this effect are presented. For Runs 26, 28 and Runs 1, 32 it was found that, after dividing the foregoing Stanton number-base pressure parameter by $(T_{wwd}/T_{lee})^{1/2}$, the heat transfer data were brought into congruence as shown in Figure 39. However, since the effect of T_{wwd} is Reynolds number dependent this new correlation parameter fails to be effective for Runs 3, 27, 31.

A more promising approach is shown in Figure 40 in which the Re_{ns} parameter has been modified with a T_{wwd} parameter based on the following rationale. The effect of T_{wwd} downstream of the insulation should decrease as $Re^{-1/2}$ so that T_w at the separation is proportional to T_{wwd}. Thus one can define a parameter $TF = (T_{wwd}/T_{lee})(Re_{ns})^{-1/2}$ which, when divided into Re_{ns}, tends to separate horizontally the data for Runs 26, 28, Runs 1, 32, and Runs 3, 27, 31 in the desired manner. Although such a correlation is by no means complete it does suggest a direction in which further correlation efforts should proceed.

REFERENCES

1. Bertin, J.J.: "A Study of Parameters Which Influence Surface Pressure and Heat-Transfer In Separated Regions - A Literature Review", Aerospace Engineering Report 74004, September 1974, The University of Texas at Austin.

2. Bogdan, L.: "Instrumentation Techniques for Short-Duration Test Facilities", CAL Report No. WTH-030, March 1967, Cornell Aeronautical Laboratory.

3. Vidal, R.J.: "Transient Surface Temperature Measurements", CAL Report No. 114, March 1962, Cornell University Laboratory.

4. Fay, J.A. and Riddell, F.R.: "Theory of Stagnation Point Heat Transfer in Dissociated Air", Journal of the Aeronautical Sciences, Vol. 25, No. 2, February 1958, pp. 73-85, 121.

5. Reece, J.W.: "Shock Tube Theory for Real Air with Applications to Wind Tunnel Testing and to Flight Simulation", CAL Experimental Facilities Division, WTH-003, October 1958 (Revised August 1959).

6. Wittliff, C.: Unpublished Normal Shock Calculations Using Duff's Computing Procedure, Aerodynamics Research Department, CAL about 1963.

7. Lewis, Clark H. and Burgess, E.G.: "Charts of Normal Shock Wave Properties in Imperfect Air", AEDC-TDR-64-43, March 1964.

8. Hilsenrath, J.; Beckett, C.W.; et al.: "Tables of Thermal Properties of Gases", National Bureau of Standards Circular 564, November 1965.

9. Reece, J.W.: "Test Section Conditions Generated in the Supersonic Expansion of Real Air", Reader's Forum, Journal of Aerospace Sciences, Vol. 29, No. 5, May 1962, pp. 617-618.

10. Neel, C.A. and Lewis, Clark H.: "Interpolations of Imperfect Air Thermodynamic Data, II, at Constant Pressure", AEDC-TDR-64-184, September 1964.

11. Hirschfelder, J.O.; Curtis, C.F.; and Bird, R.G.: Molecular Theory of Gases and Liquids, J. Wiley and Sons, 1954.

12. Hansen, C.F.: "Approximations for Thermodynamic and Transport Properties of High Temperature Air", NACA-TN-4150, March 1958 (Revised NASA TR-50, 1959).

13. Bertin, J.J., and Byrd, O.E., Jr.: "The Analysis of a Nonsimilar Boundary Layer - A Computer Code (NONSIMBL)" Aerospace Engineering Report 70002, August 1970, The University of Texas at Austin.

14. Houston, K.: Private transmittal, Dec. 23, 1974.

15. DeJarnette, F.R.: "Calculation of Inviscid Surface Streamlines and Heat Transfer on Shuttle Type Configurations", CR-11921, August 1971, NASA (prepared by North Carolina State University).

16. Rakich, J.V., and Mateer, G.G.: "Calculation of Metric Coefficients for Streamline Coordinates", AIAA Journal, Vol. 10, No. 11, November 1972, pp. 1538-1540.

17. Goodrich, W.D.: Data from tests conducted at the Ames Research Center, as transmitted on February 6, 1975.

18. Schlichting, H., Boundary-Layer Theory, Chapter 15, McGraw-Hill Book Company, 1960, New York.

19. Zakkay, V., Miyazawa, M., and Wang, C.R.: "Lee Surface Flow Phenomena Over Space Shuttle at Large Angles of Attack at M_∞ = 6", AIAA Paper 75-148, presented at AIAA 13th Aerospace Sciences Meeting, Pasadena, Calif., January 1975 (Also NASA CR-132501 from New York University).

20. Bertin, J.J., Faria, H.T., Goodrich, W.D., and Martindale, W.R.: "Effect of Nose Geometry on the Aerothermodynamic Environment of Shuttle Entry Configurations", Journal of Spacecraft and Rockets, May 1974, Vol. 11, No. 5, pp. 275-281.

21. Whitehead, A.H., Jr., Hefner, J.N., and Rao, D.M., "Lee-Surface Vortex Effects Over Configurations in Hypersonic Flow", AIAA Paper No. 72-77, Presented at the AIAA 10th Aerospace Sciences Meeting, San Diego, Calif., January 1972.

22. Cassanto, J.M.: "A Base Pressure Experiment for Determining the Atmospheric Pressure Profile of Planets", Journal of Spacecraft and Rockets, April 1973, Vol. 10, No. 4, pp. 253-261.

23. Crocco, L. and Lees, L.: "A Mixing Theory for the Interaction Between Dissipative Flows and Nearly Isentropic Streams", Journal of the Aeronautical Sciences, October 1952, Vol. 19, No. 10, pp. 649-676.

24. Lamb, J. P. and Hsieh, S. - J., "An Integral Model of Supersonic Laminar Near Wakes Including Convective Heat Transfer," Aerospace Engineering Report 74001, January 1974, The University of Texas at Austin.

25. Bertin, J. J., Lamb, J. P., Zickler, J. L., and Goodrich, W. D., "Flow Field Measurements for Space Shuttle-Related Cylindrical Configurations in Hypersonic Streams," AIAA Paper 72-294, April 1972.

VIII. TABLE INDEX

Table No.

Table 1. - Location of heat-transfer gages

Gage No.	Model Station (in/cm)	x (in/cm)	$\frac{x}{L}$	ϕ (°)
1	2.767/7.028	0.387/0.983	0.030	0
2	3.154/8.011	0.774/1.966	0.060	0
3	3.541/8.994	1.161/2.282	0.090	0
4	3.670/9.322	1.290/3.277	0.100	0
5	3.670/9.322	1.290/3.277	0.100	41
6	3.670/9.322	1.290/3.277	0.100	69
7	3.670/9.322	1.290/3.277	0.100	90
8	3.993/10.142	1.613/4.097	0.125	0
9	4.315/10.960	1.935/4.915	0.150	0
10	4.445/11.290	2.065/5.245	0.160	0
11	4.574/11.617	2.194/5.573	0.170	0
12	4.703/11.945	2.323/5.900	0.180	0
13	5.130/13.030	2.750/6.985	0.213	0
14	5.130/13.030	2.750/6.985	0.213	17.5
15	5.130/13.030	2.750/6.985	0.213	35
16	5.130/13.030	2.750/6.985	0.213	52.5
17	5.130/13.030	2.750/6.985	0.213	70
18	5.130/13.030	2.750/6.985	0.213	90
19	5.980/15.189	3.600/9.144	0.279	0
20	5.980/15.189	3.600/9.144	0.279	22
21	5.980/15.189	3.600/9.144	0.279	44
22	5.980/15.189	3.600/9.144	0.279	66
23	5.980/15.189	3.600/9.144	0.279	90
24	6.700/17.018	4.320/10.973	0.335	0
25	6.700/17.018	4.320/10.973	0.335	20
26	6.700/17.018	4.320/10.973	0.335	40
27	6.700/17.018	4.320/10.973	0.335	56
28	6.700/17.018	4.320/10.973	0.335	90
29	7.799/19.809	5.419/13.764	0.420	0
30	7.799/19.809	5.419/13.764	0.420	20
31	7.799/19.809	5.419/13.764	0.420	40
32	7.799/19.809	5.419/13.764	0.420	56
33	7.799/19.809	5.419/13.764	0.420	90

Table 1. - Continued

Gage No.	Model Station (in/cm)	x (in/cm)	$\frac{x}{L}$	ϕ (°)
34	8.832/22.433	6.452/16.388	0.500	0
35	8.832/22.433	6.452/16.388	0.500	30
36	8.832/22.433	6.452/16.388	0.500	56
37	10.122/25.709	7.742/19.665	0.600	0
38	10.122/25.709	7.742/19.665	0.600	30
39	10.122/25.709	7.742/19.665	0.600	56
40	10.122/25.709	7.742/19.665	0.600	90
41	11.412/28.986	9.032/22.941	0.700	0
42	11.412/28.986	9.032/22.941	0.700	90
43	12.702/32.263	10.322/26.218	0.800	0
44	2.380/6.045	0.000/0.000	0.000	180
45	3.670/9.321	1.290/3.277	0.100	180
46	5.130/13.030	2.750/6.985	0.213	180
47	6.700/17.018	4.320/10.973	0.335	180
48	12.702/32.263	10.322/26.218	0.800	180

Table 2. - Location of static-pressure orifices

Gage No.	Model Station (in/cm)	x (in/cm)	$\frac{x}{L}$	ϕ (°)
1	3.348/8.503	0.968/2.459	0.075	0
2	3.799/9.649	1.419/3.604	0.110	0
3	5.468/13.888	3.088/7.8435	0.239	0
4	8.056/20.462	5.676/14.417	0.440	0
5	11.692/29.697	9.312/23.652	0.722	0

Table 3. - Run schedule

(a) English units

(i) Fuselage Only

Run	α (°)	M_∞	Re_∞/ft_6 (x 10^{-6})	p_{t2} (psia)	T_t (°R)	T_{wwd} (°R)	T_{lee} (°R)
1	30	12.26	0.5648	4.311	4626	420	420
2	90	12.26	0.5643	4.307	4626	420	420
3	90	11.87	1.629	13.24	4644	420	420
26	90	12.32	0.5389	3.639	4336	860	530
27	90	11.81	1.589	13.61	4758	1430	530
28	90	12.24	0.5103	3.872	4605	1440	530
29	90	11.66	0.1091	0.898	4564	1440	530
30	90	15.70	0.5790	2.786	4643	1440	530
31	90	11.83	1.613	13.94	4792	860	530
32	30	12.26	0.5737	4.305	4578	1460	530

(ii) Orbiter

Run	α (°)	M_∞	Re_∞/ft_6 (x 10^{-6})	p_{t2} (psia)	T_t (°R)	T_{wwd} (°R)	T_{lee} (°R)
4	30	11.80	1.516	12.98	4751	833	530
5	30	12.24	0.5272	4.103	4675	820	530
6	30	11.67	0.1155	0.983	4658	820	530
7	30	15.71	0.5722	2.772	4670	830	530
8	30	11.81	1.559	13.24	4734	1460	530
9	30	11.61	1.045	9.139	4729	1420	530
10	30	12.26	0.5263	4.003	4623	1410	530
11	30	11.64	0.1078	0.905	4603	1420	530
12	30	16.01	0.8793	4.094	4657	1440	530
13	30	15.71	0.5701	2.721	4631	1420	530
14	30	10.16	0.9917	1.092	4717	1430	530
15	30	10.05	0.4883	5.340	4641	1430	530
16	30	15.81	0.1123	0.681	5299	1430	530
17	40	12.24	0.5476	4.219	4640	830	530
18	40	11.82	1.578	13.57	4776	1440	530
19	40	12.23	0.5530	4.288	4763	1430	530
20	40	11.68	0.1069	0.884	4714	1440	530
21	40	15.70	0.5789	2.767	4770	1430	530

Table 3. - Continued.

(a) English units

(ii) Orbiter

Run	α (°)	M_∞	Re_∞/ft (x 10^{-6})	p_{t2} (psia)	T_t (°R)	T_{wwd} (°R)	T_{lee} (°R)
22	40	10.01	0.4808	5.545	4821	1440	530
23	30	18.26	0.1349	0.442	4423	1430	530
24	30	18.59	0.2210	0.790	4727	1420	530
33	30	11.80	1.560	13.39	4758	430	430
34	30	12.28	0.5577	4.206	4607	430	430
35	30	11.70	0.1074	0.886	4597	420	420
36	30	16.09	0.9186	4.038	4539	420	420
37	30	15.70	0.5759	2.736	4613	420	420
38	30	10.16	0.5678	5.433	4342	420	420
39	40	12.23	0.5622	4.262	4590	425	425
40	40	15.70	0.5859	2.825	4651	430	430

Table 3. - Run schedule

(b) Metric units

(i) Fuselage Only

Run	α (°)	M_∞	Re_∞/m ($\times 10^{-6}$)	P_{t2} ($N/m^2 \times 10^{-4}$)	T_t (°K)	T_{wwd} (°K)	T_{lee} (°K)
1	30	12.26	1.853	2.972	2570	233.4	233.4
2	90	12.25	1.851	2.970	2570	233.4	233.4
3	90	11.87	5.345	9.129	2580	233.4	233.4
26	90	12.32	1.768	2.509	2409	477.8	294.5
27	90	11.81	5.213	9.384	2643	794.5	294.5
28	90	12.24	1.674	2.670	2558	800.0	294.5
29	90	11.66	0.358	0.619	2536	800.0	294.5
30	90	15.70	1.900	1.920	2579	800.0	294.5
31	90	11.83	5.292	9.734	2662	477.8	294.5
32	30	12.26	1.882	2.968	2543	811.1	294.5

(ii) Orbiter

Run	α (°)	M_∞	Re_∞/m ($\times 10^{-6}$)	P_{t2} ($N/m^2 \times 10^{-4}$)	T_t (°K)	T_{wwd} (°K)	T_{lee} (°K)
4	30	11.80	4.974	8.950	2639	462.8	294.5
5	30	12.23	1.730	2.830	2597	455.6	294.5
6	30	11.67	0.379	0.678	2588	455.6	294.5
7	30	15.71	1.877	1.911	2594	461.1	294.5
8	30	11.81	5.115	9.129	2630	811.1	294.5
9	30	11.61	3.428	6.301	2627	788.9	294.5
10	30	12.26	1.727	2.760	2568	783.3	294.5
11	30	11.64	0.354	0.624	2557	788.9	294.5
12	30	16.01	2.885	2.823	2587	800.0	294.5
13	30	15.71	1.870	1.876	2573	788.9	294.5
14	30	10.16	3.254	0.753	2621	794.5	294.5
15	30	10.05	1.602	3.682	2578	794.5	294.5
16	30	15.81	0.368	0.469	2944	794.5	294.5
17	40	12.24	1.797	2.909	2578	461.1	294.5
18	40	11.82	5.177	9.357	2653	800.0	294.5
19	40	12.23	1.814	2.957	2646	794.5	294.5
20	40	11.68	0.351	0.610	2619	800.0	294.5
21	40	15.70	1.899	1.908	2650	794.5	294.5
22	40	10.01	1.577	3.823	2678	800.0	294.5

Table 3. - Continued

(b) Metric units

(ii) Orbiter

Run	α (°)	M_∞	Re_∞/m ($\times 10^{-6}$)	p_{t_2} ($N/m^2 \times 10^{-4}$)	T_t (°K)	T_{wwd} (°K)	T_{lee} (°K)
22	40	10.01	1.577	3.823	2678	800.0	294.5
23	30	18.26	0.443	0.305	2457	794.5	294.5
24	30	18.59	0.725	0.545	2626	788.9	294.5
33	30	11.80	5.118	9.232	2643	238.9	238.9
34	30	12.28	1.830	2.900	2559	238.9	238.9
35	30	11.70	0.352	0.611	2554	233.4	233.4
36	30	16.09	3.014	2.784	2522	233.4	233.4
37	30	15.70	1.889	1.886	2563	233.4	233.4
38	30	10.16	1.863	3.746	2412	233.4	233.4
39	40	12.23	1.845	2.939	2550	236.1	236.1
40	40	15.70	1.922	1.948	2584	238.9	238.9

Table 4. - Theoretical solution for a nonsimilar, laminar boundary-layer assuming the air at the edge of the boundary layer has accelerated isentropically from the stagnation point (NSE).

(a) Identification of cases

Case I.D.	M_∞	Re_∞/ft ($\times 10^6$)	P_{t2} (psia)	T_t (°R)	$\frac{T_{wwd}}{T_t}$	$\frac{T_{lee}}{T_t}$
1ai	11.80	1.50	13.0	4750	0.090	0.090
1aii	↓	↓	↓	↓	↓	0.114
1bii	↓	↓	↓	↓	0.176	↓
1cii	↓	↓	↓	↓	0.307	↓
2ai	12.25	0.55	4.1	4650	0.090	0.090
2aii	↓	↓	↓	↓	↓	0.114
2bii	↓	↓	↓	↓	0.176	↓
2cii	↓	↓	↓	↓	0.307	↓
3ai	11.68	0.11	0.9	4650	0.090	0.090
3aii	↓	↓	↓	↓	↓	0.114
3bii	↓	↓	↓	↓	0.176	↓
3cii	↓	↓	↓	↓	0.307	↓
4ai	15.70	0.57	2.8	4650	0.090	0.090
4aii	↓	↓	↓	↓	↓	0.114
4cii	↓	↓	↓	↓	0.307	↓
5ai	10.10	0.50	5.3	4650	0.090	0.090
5aii	↓	↓	↓	↓	↓	0.114
5cii	↓	↓	↓	↓	0.307	↓
6ai	18.59	0.13	0.4	4400	0.090	0.090
6aii	↓	↓	↓	↓	|	0.114
6cii	↓	↓	↓	↓	0.307	↓

Table 4. - Continued.

(b) Boundary-layer parameters

Case I.D.	At s = 0.216 ft (which is just upstream of the section interface)				At s = 0.351 ft (which is just upstream of the "assumed" separation)			
	δ $(ft)_2$ $\times 10^2$	θ $(ft)_3$ $\times 10^3$	θ_H $(ft)_2$ $\times 10^2$	Re_s $\times 10^{-4}$	δ $(ft)_2$ $\times 10^2$	θ $(ft)_3$ $\times 10^3$	θ_H $(ft)_2$ $\times 10^2$	Re_s $\times 10^{-4}$
1ai	.436	.911	—	6.933	1.597	3.506	—	8.190
1aii	.436	.911	-.200	↓	1.648	3.496	-.863	↓
1bii	.470	.876	-.185		1.634	3.385	-.831	
1cii	.520	.824	-.163	↓	1.633	3.246	-.796	↓
2ai	.769	1.604	—	2.186	2.810	6.178	—	2.593
2aii	.769	1.604	-.354	↓	2.900	6.160	-1.527	↓
2bii	.828	1.544	-.327		2.877	5.965	-1.468	
2cii	.916	1.451	-.288	↓	2.875	5.721	-1.406	↓
3ai	1.642	3.424	—	0.480	5.948	13.19	—	0.569
3aii	1.642	3.424	-.755	↓	6.189	13.15	-3.257	↓
3bii	1.767	3.296	-.715		6.140	12.73	-3.132	
3cii	1.954	3.098	-.613	↓	6.136	12.21	-3.001	↓
4ai	.931	1.941	—	1.493	3.400	7.476	—	1.771
4aii	.931	1.941	-.428	↓	3.509	7.454	-1.847	↓
4cii	1.108	1.756	-.348	↓	3.479	6.923	-1.701	↓
5ai	.677	1.411	—	2.826	2.471	5.434	—	3.351
5aii	.677	1.411	-.311	↓	2.550	5.418	-1.342	↓
5cii	.805	1.277	-.253	↓	2.528	5.032	-1.237	↓
6ai	2.396	4.988	—	.218	8.722	19.22	—	.260
6aii	2.396	4.988	-1.106	↓	9.000	19.17	-4.767	↓
6cii	2.848	4.518	-.899	↓	8.929	17.80	-4.668	↓

Table 5. - Theoretical solution for a nonsimilar, laminar boundary-layer assuming the air of the edge of the boundary layer accelerates isentropically after passing through a shock wave parallel to the surface (PSE).

(a) Identification of cases

Case I.D.	M_∞	Re_{∞}/ft ($\times 10^{-6}$)	p_{te} (psia)	T_t (°R)	$\frac{T_{wwd}}{T_t}$	$\frac{T_w}{T_t}$
II ai	12.25	0.55	95.505	4650	0.090	0.090
II bi	12.25	0.55	95.505	4650	0.176	0.090
II ci	12.25	0.55	95.505	4650	0.307	0.090
IV ai	15.70	0.57	70.692	4650	0.090	0.090
IV bi	15.70	0.57	70.692	4650	0.176	0.090
IV ci	15.70	0.57	70.692	4650	0.307	0.090
V ai	10.10	0.50	110.208	4650	0.090	0.090
V bi	10.10	0.50	110.208	4650	0.176	0.090
V ci	10.10	0.50	110.208	4650	0.307	0.090
II aii	12.25	0.55	95.505	4650	0.090	0.114
II bii	12.25	0.55	95.505	4650	0.176	0.114
II cii	12.25	0.55	95.505	4650	0.307	0.114
IV aii	15.70	0.57	70.692	4650	0.090	0.114
IV bii	15.70	0.57	70.692	4650	0.176	0.114
IV cii	15.70	0.57	70.692	4650	0.307	0.114
V aii	10.10	0.50	110.208	4650	0.090	0.114
V bii	10.10	0.50	110.208	4650	0.176	0.114
V cii	10.10	0.50	110.208	4650	0.307	0.114

Table 5. - Continued

(b) Boundary-layer parameters

	At s = 0.216 ft (which is just upstream of the section interface)			At s = 0.351 ft (which is just upstream of the "assumed" separation)		
Case I.D.	δ (ft) $\times 10^2$	θ (ft) $\times 10^3$	$Re_s \times 10^{-5}$	δ (ft) $\times 10^2$	θ (ft) $\times 10^3$	$Re_s \times 10^{-5}$
II ai	0.563	0.636	1.1481	2.046	2.439	1.3541
II bi	0.616	0.603	1.1481	2.052	2.339	1.3541
II ci	0.714	0.561	1.1481	2.140	2.237	1.3541
IV ai	0.679	0.746	0.8173	2.488	2.858	0.9641
IV bi	0.743	0.707	0.8173	2.498	2.741	0.9641
IV ci	0.862	0.657	0.8173	2.602	2.610	0.9641
V ai	0.497	0.588	1.3994	1.824	2.240	1.6507
V bi	0.544	0.554	1.3994	1.831	2.149	1.6507
V ci	0.630	0.517	1.3994	1.906	2.053	1.6507
II aii	0.563	0.636	1.1481	2.152	2.417	1.3541
II bii	0.616	0.603	1.1481	2.165	2.313	1.3541
II cii	0.714	0.561	1.1481	2.210	2.225	1.3541
IV aii	0.679	0.746	0.8173	2.582	2.842	0.9641
IV bii	0.743	0.707	0.8173	2.585	2.723	0.9641
IV cii	0.862	0.657	0.8173	2.686	2.596	0.9641
V aii	0.497	0.588	1.3994	1.893	2.227	1.6507
V bii	0.544	0.554	1.3994	1.895	2.135	1.6507
V cii	0.630	0.517	1.3994	1.967	2.043	1.6507

Table 6. - Selected input data and results from wake heat transfer calculations for fuselage test conditions.

Run No.	$P_b/P_{t,2}$	$Re_H \times 10^{-4}$ (See Note)	δ_s/w	$\frac{\dot{q}_{lee}}{\dot{q}_{t,ref}} \times 10^3$	$St_{lee} \times 10^4$
1	.0090	2.42	.0965	4.54	3.70
2	.0175	3.66	.0790	7.92	6.46
3	.0175	11.0	.0452	7.76	3.63
26	.0185	2.97	.0807	6.44	5.45
27	.0210	10.4	.0390	9.66	4.46
28	.0185	3.0	.0797	6.62	5.55
29	.0215	0.737	.146	7.37	12.93
30	.0150	1.90	.120	6.17	6.24
31	.0175	9.51	.0451	6.57	3.01
32	.0090	2.45	.106	4.71	3.75

NOTE: Re_H is based on free stream properties just prior to separation and the local distance H depicted in Fig. A-1.

IX. FIGURE INDEX

Figure No.

Figure No.

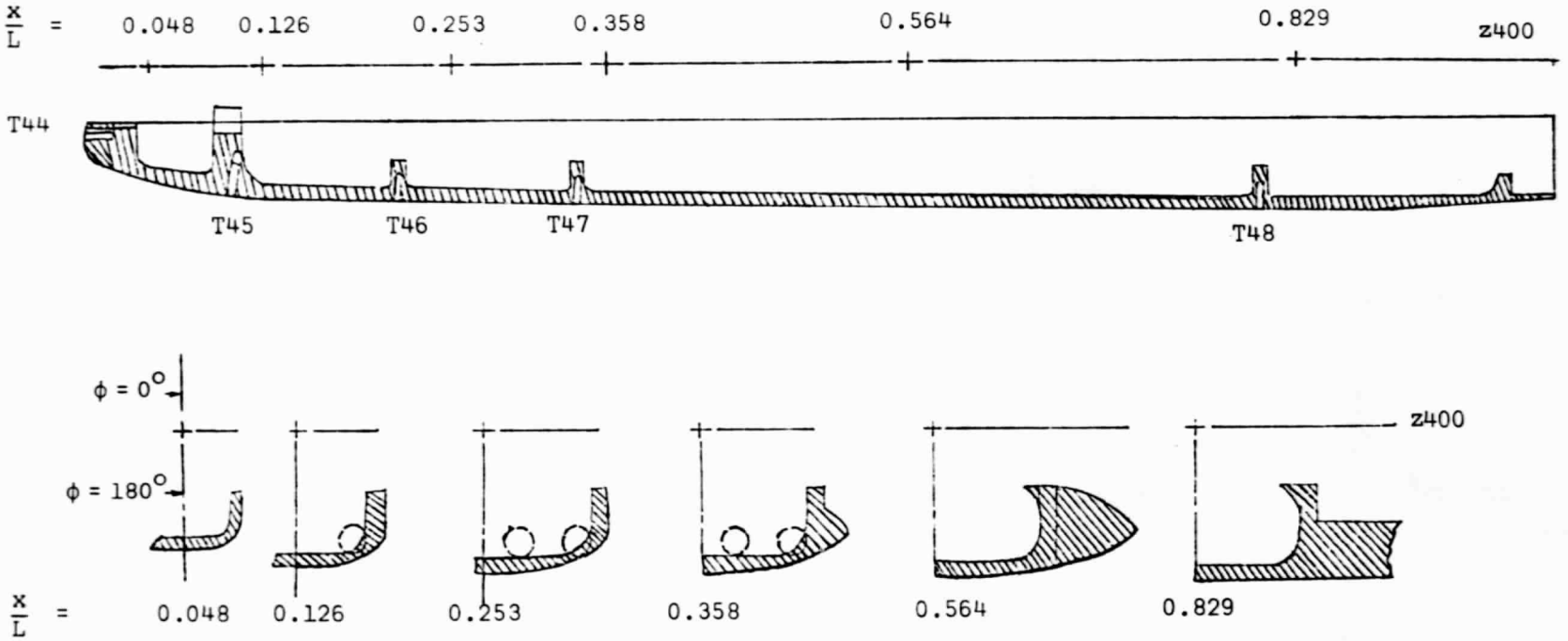

(a) Windward Sections for orbiter model.

Figure 1. - Sketch of the 0.01-scale 139 shuttle orbiter model.

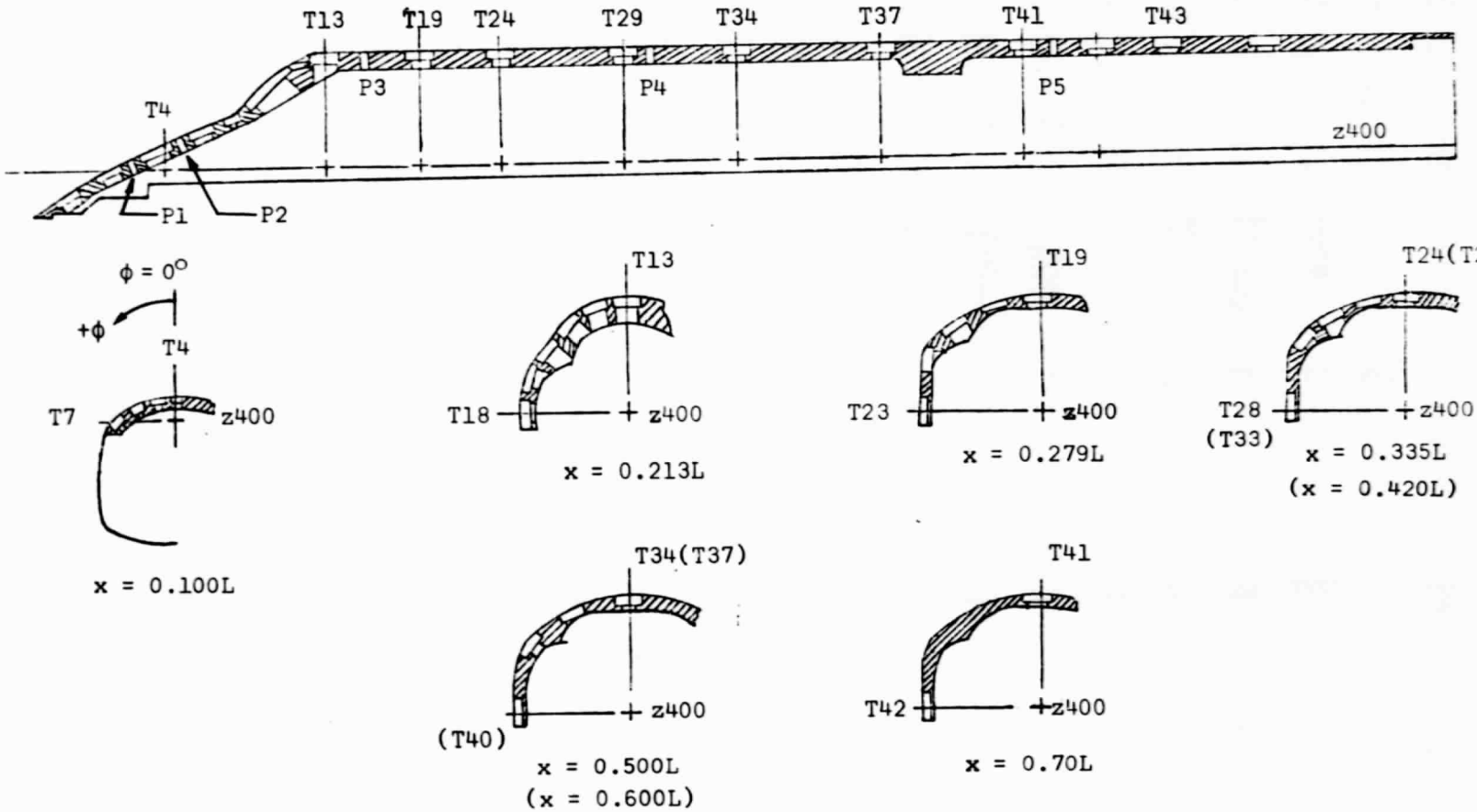

(b) Leeward sections of orbiter model (looking forward)

Figure 1. - Continued

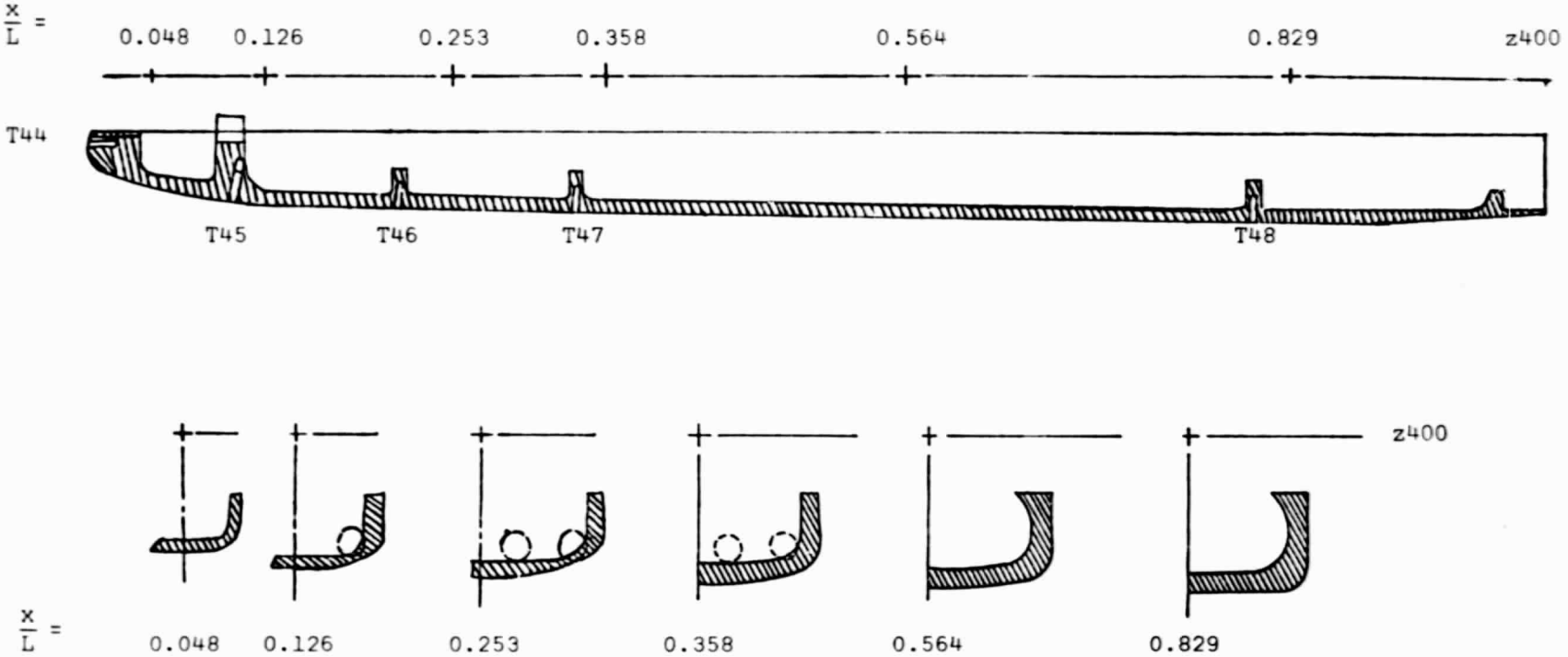

(c) Windward Sections of fuselage model

Figure 1. - Concluded.

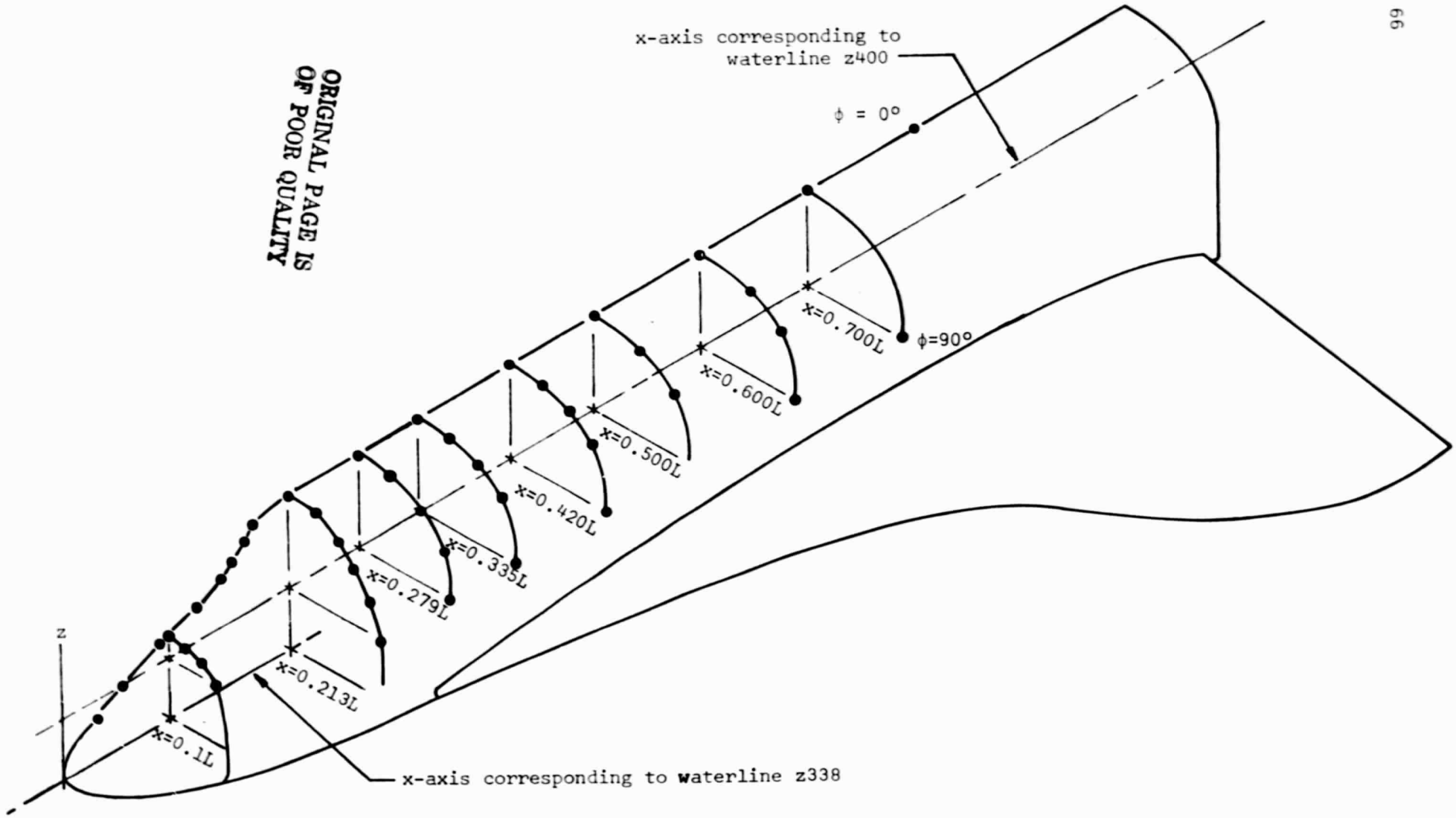

Figure 2. - An isometric sketch of the shuttle orbiter model illustrating the locations of the leeward heat-transfer gages.

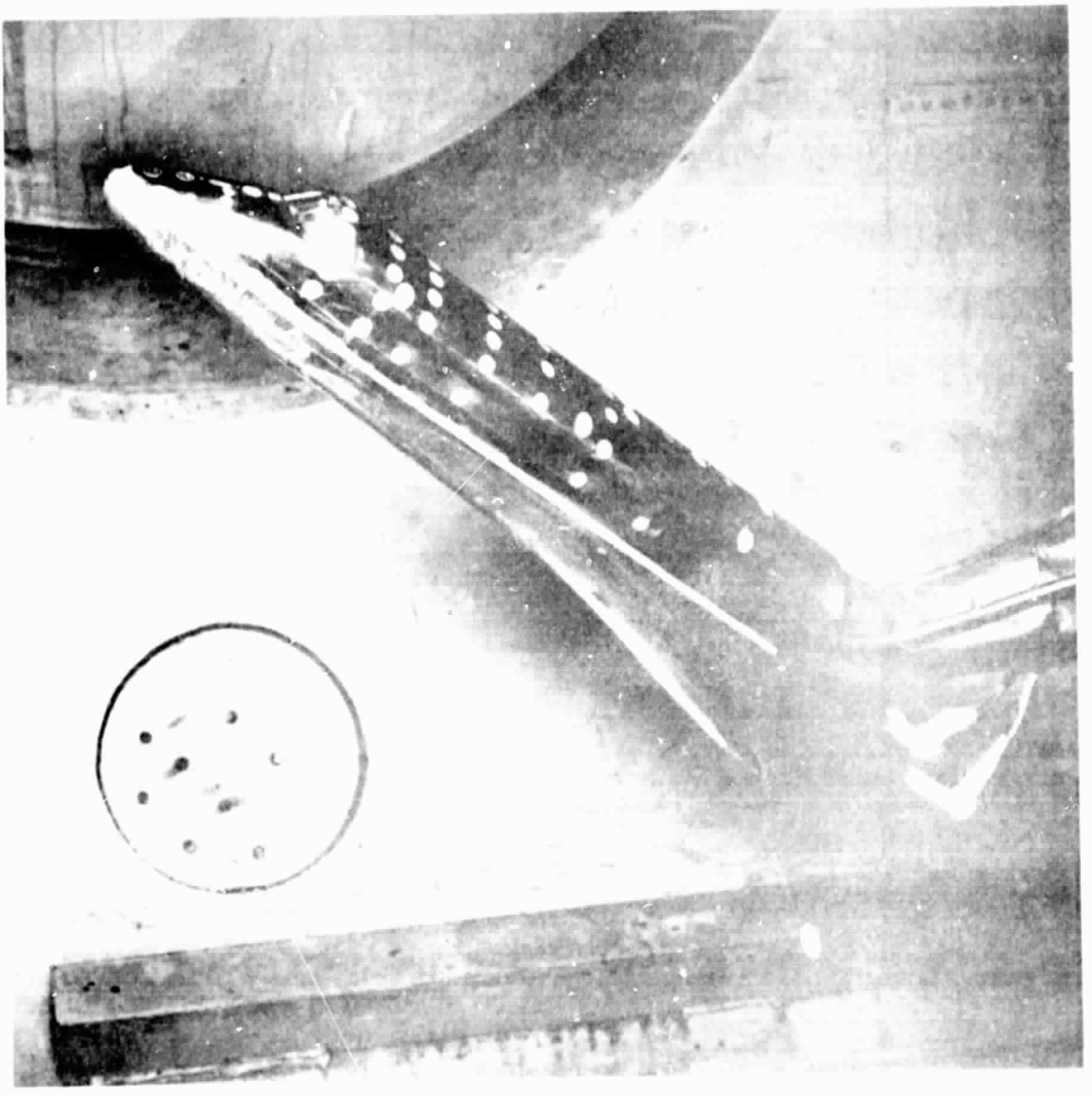

Figure 3. - Photograph of the [illegible]
Calspan [illegible]

(b) View of leeward surface

Figure 3. - Concluded.

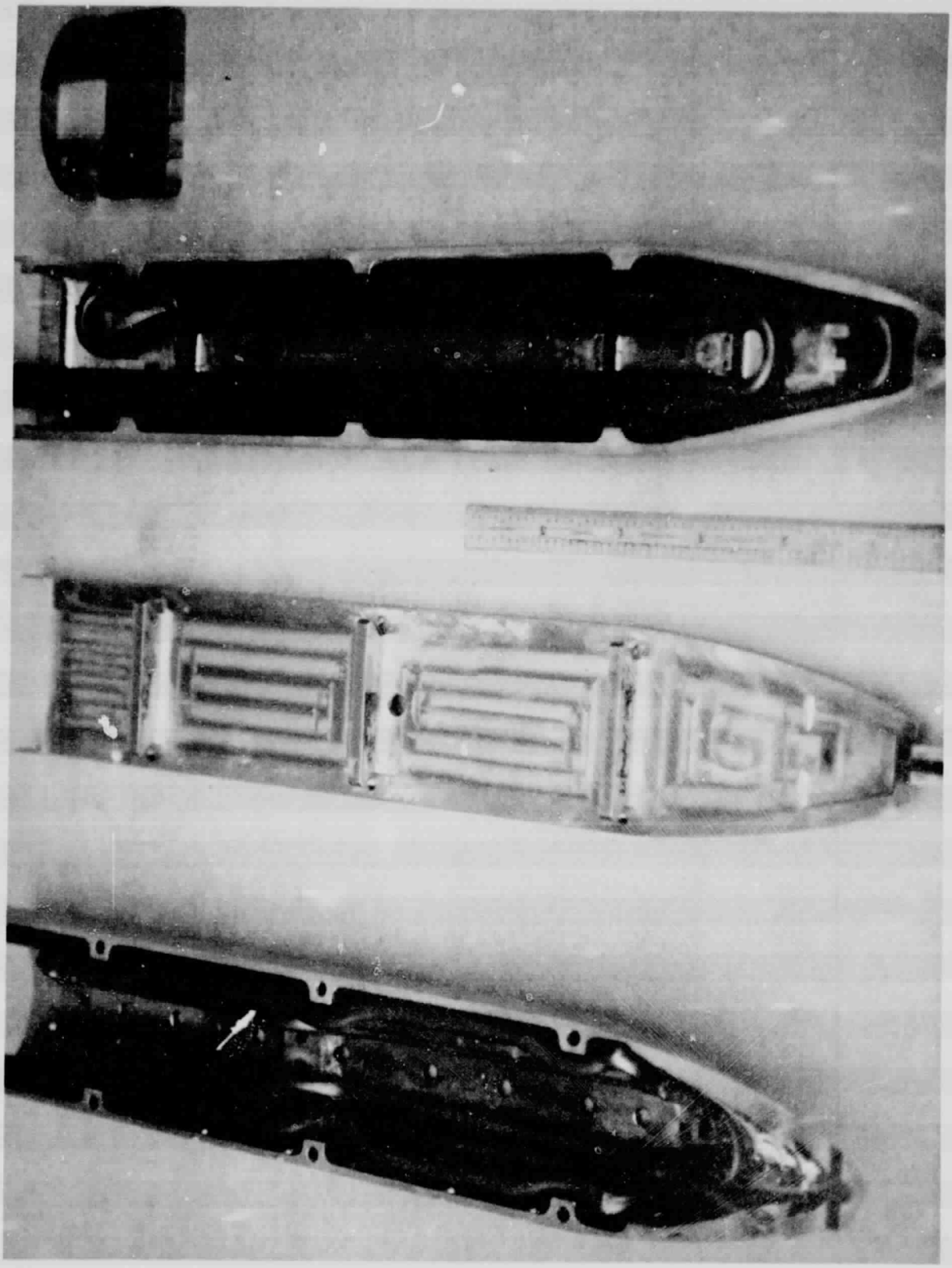

Figure 4. - Photograph of the fuselage only configuration disassembled to illustrate the windward section, leeward section, insulation sheet, and cooling coils.

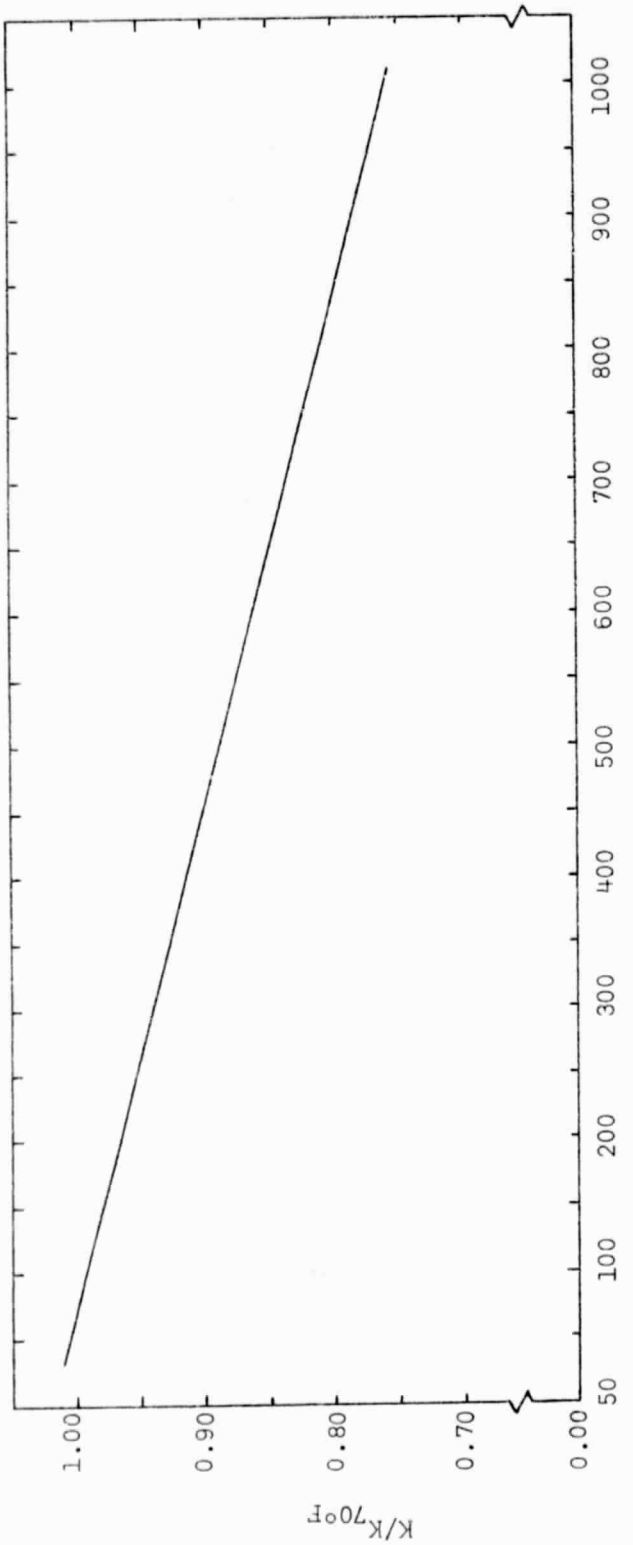

Figure 5. - Variation of heat transfer gage sensitivity with temperature.

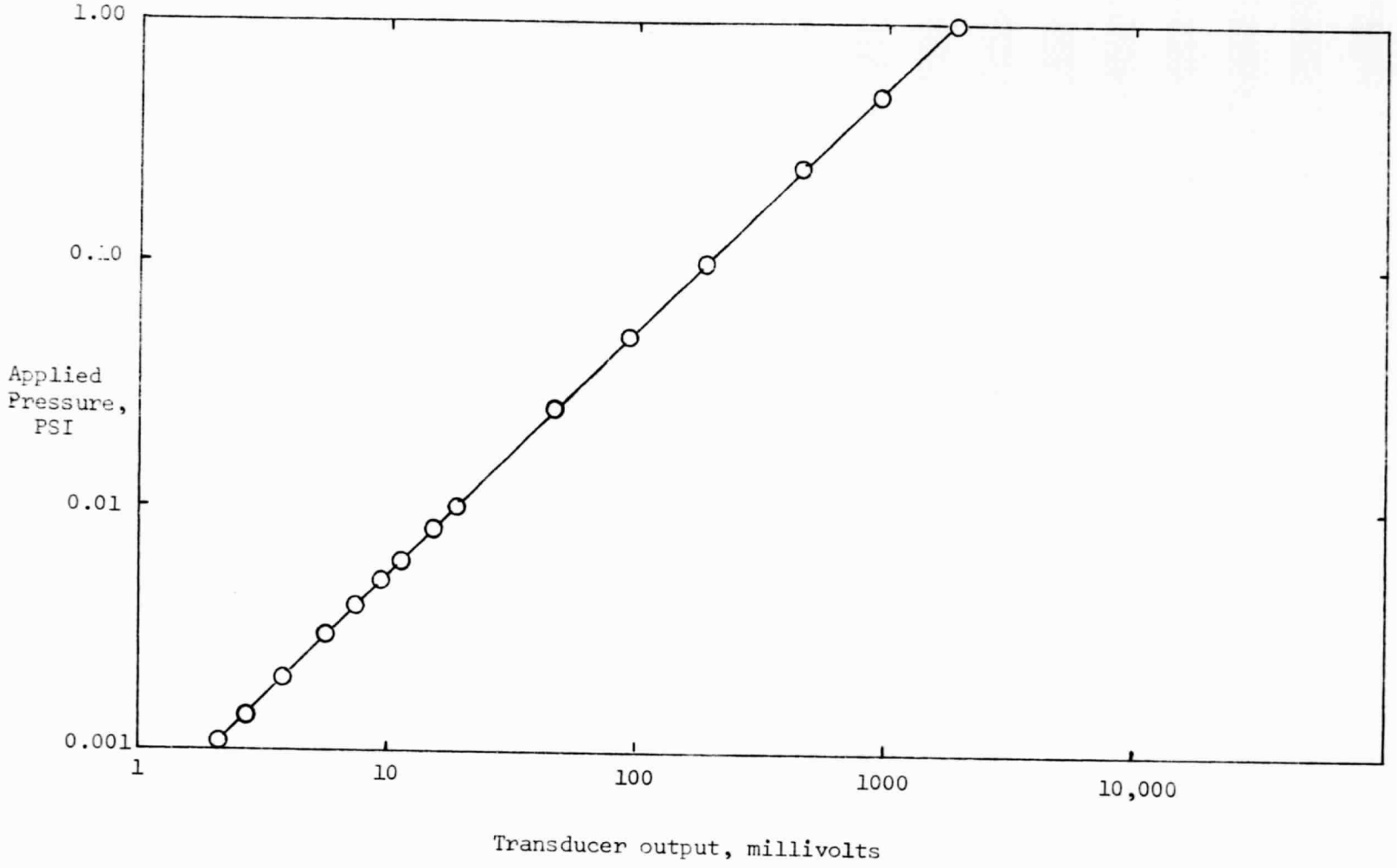

Figure 6. - Transducer calibration curve.

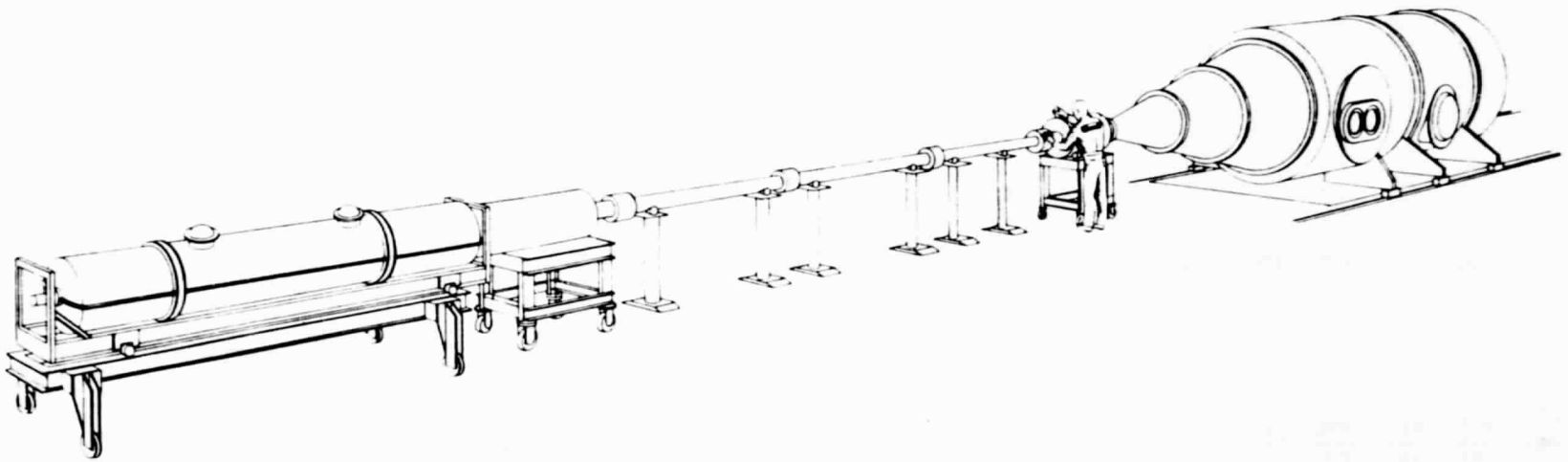

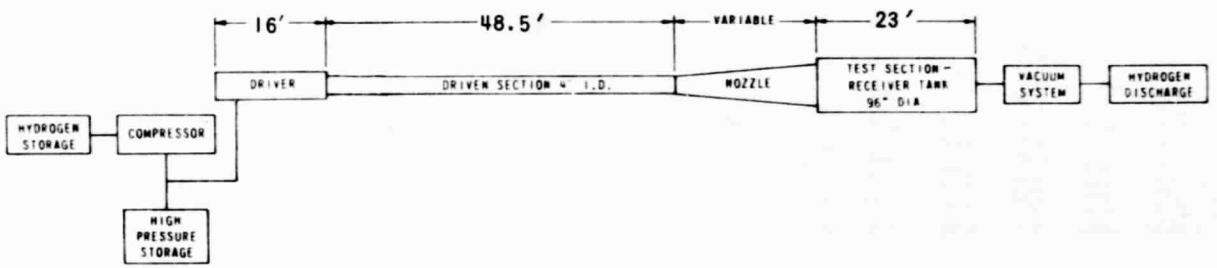

Figure 7. - Basic components of the Calspan 96" Hypersonic Shock Tunnel

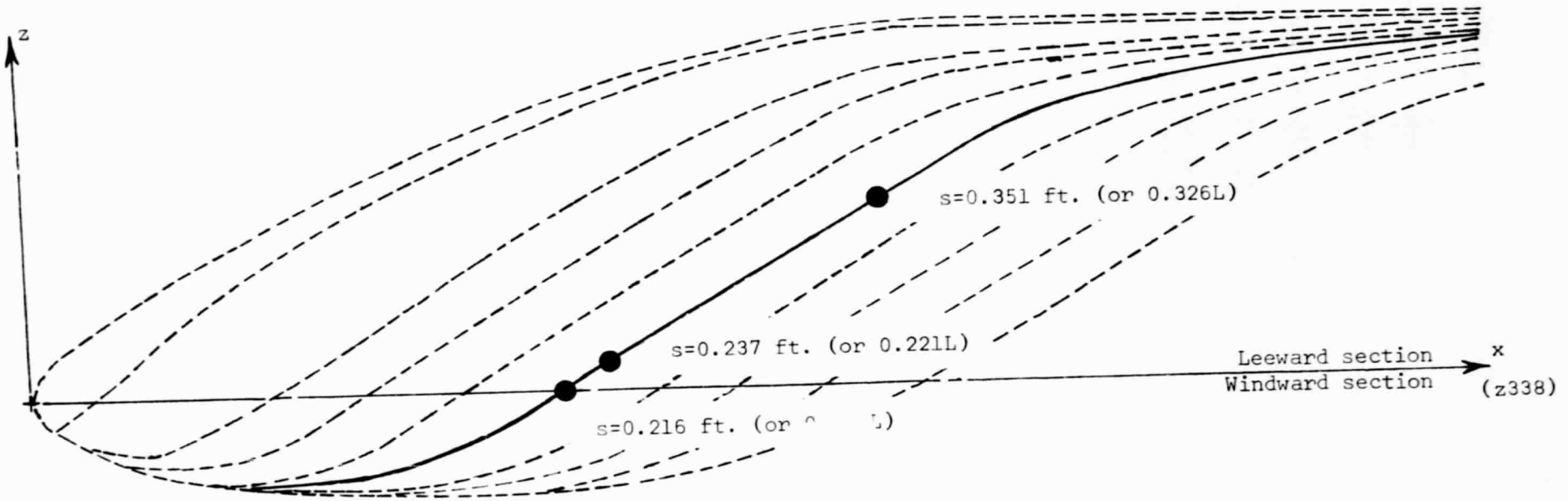

Figure 8. - A sideview sketch of the Newtonian streamlines calculated for a representative orbiter geometry (without a canopy), $\alpha = 30°$.

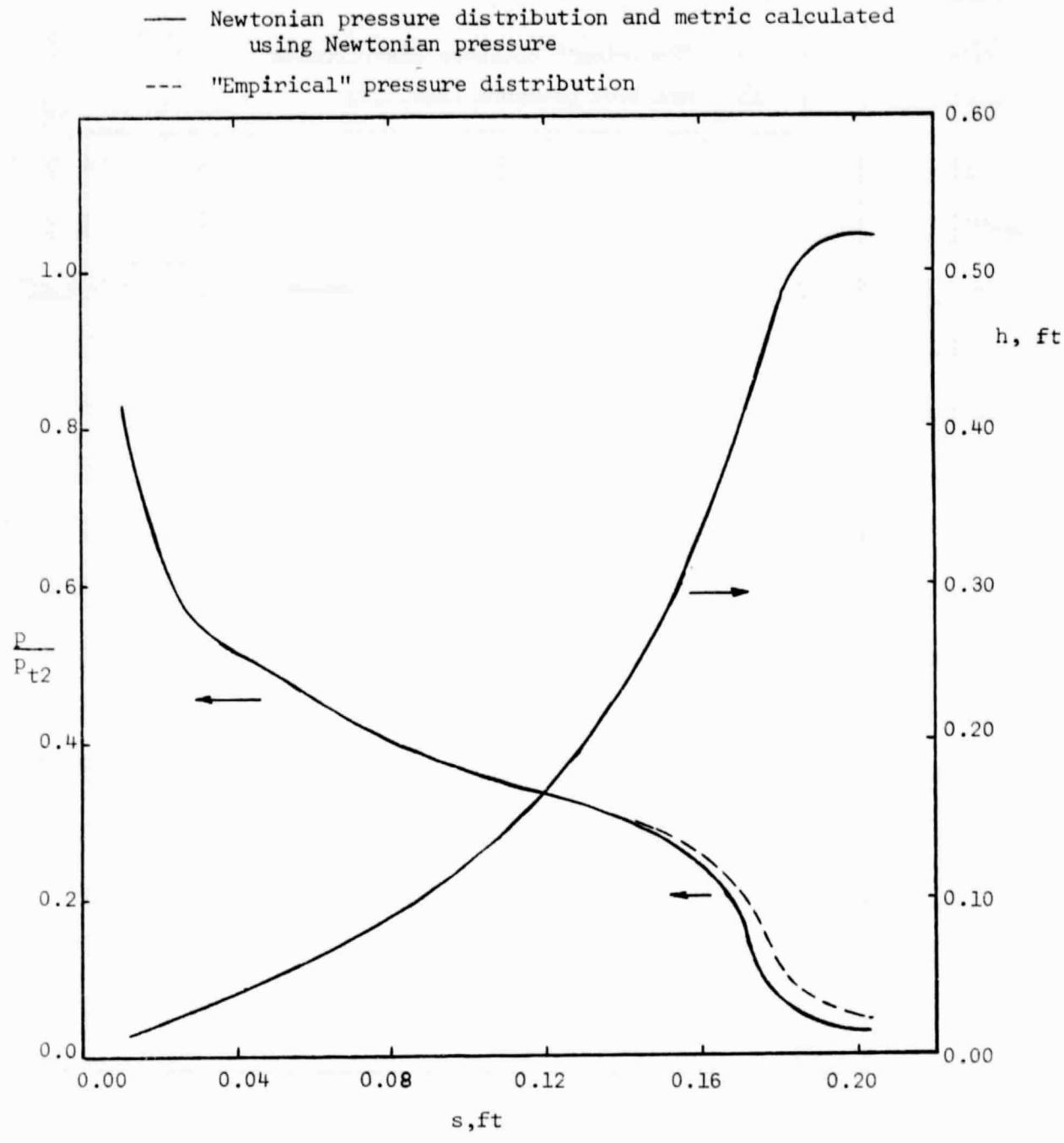

(a) Windward section

Figure 9. - The theoretical flow-characteristics along a streamline as determined for a Newtonian pressure distribution using the Lockheed program (NSE, $\alpha = 30°$).

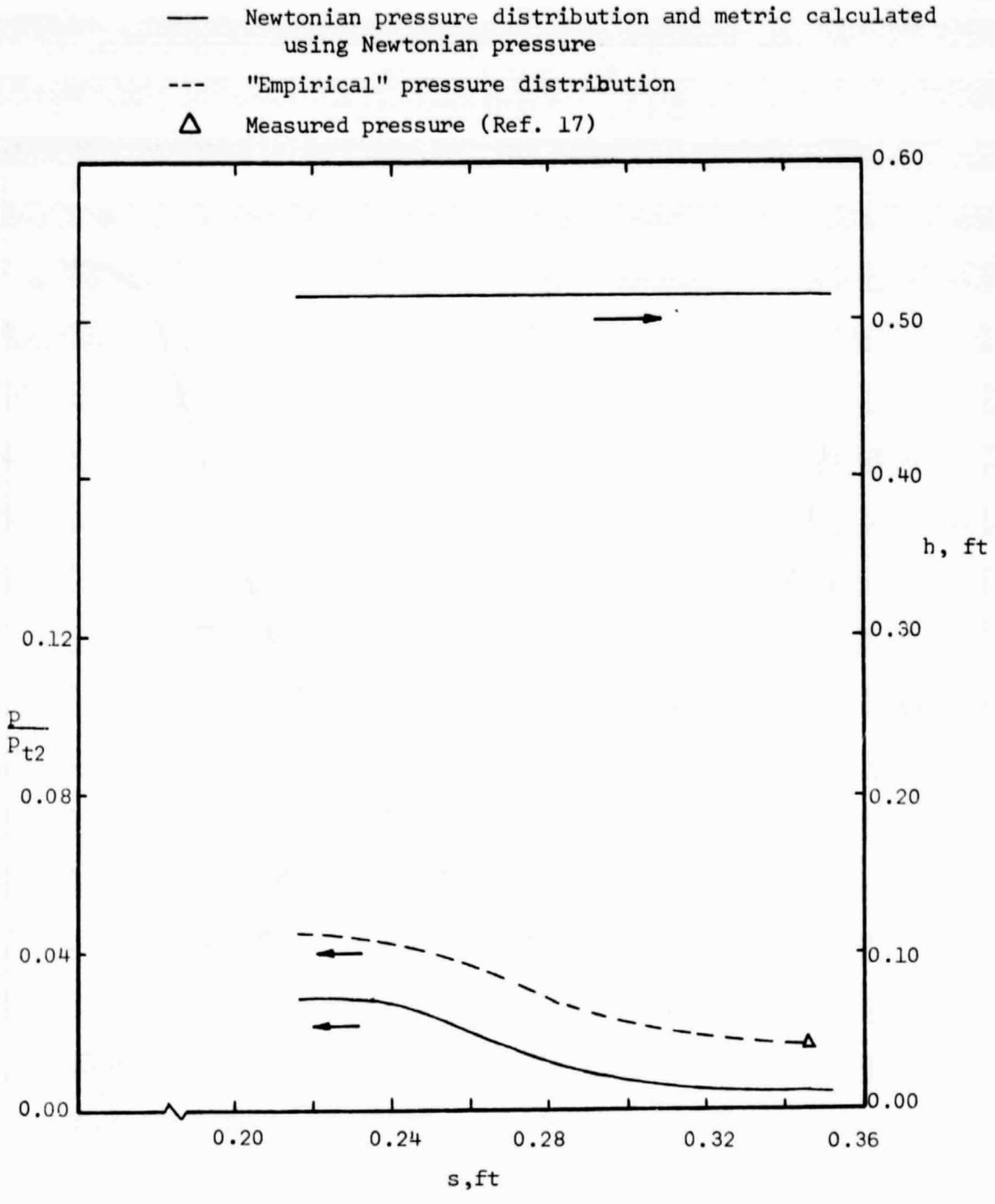

(b) Leeward section

Figure 9. - Concluded.

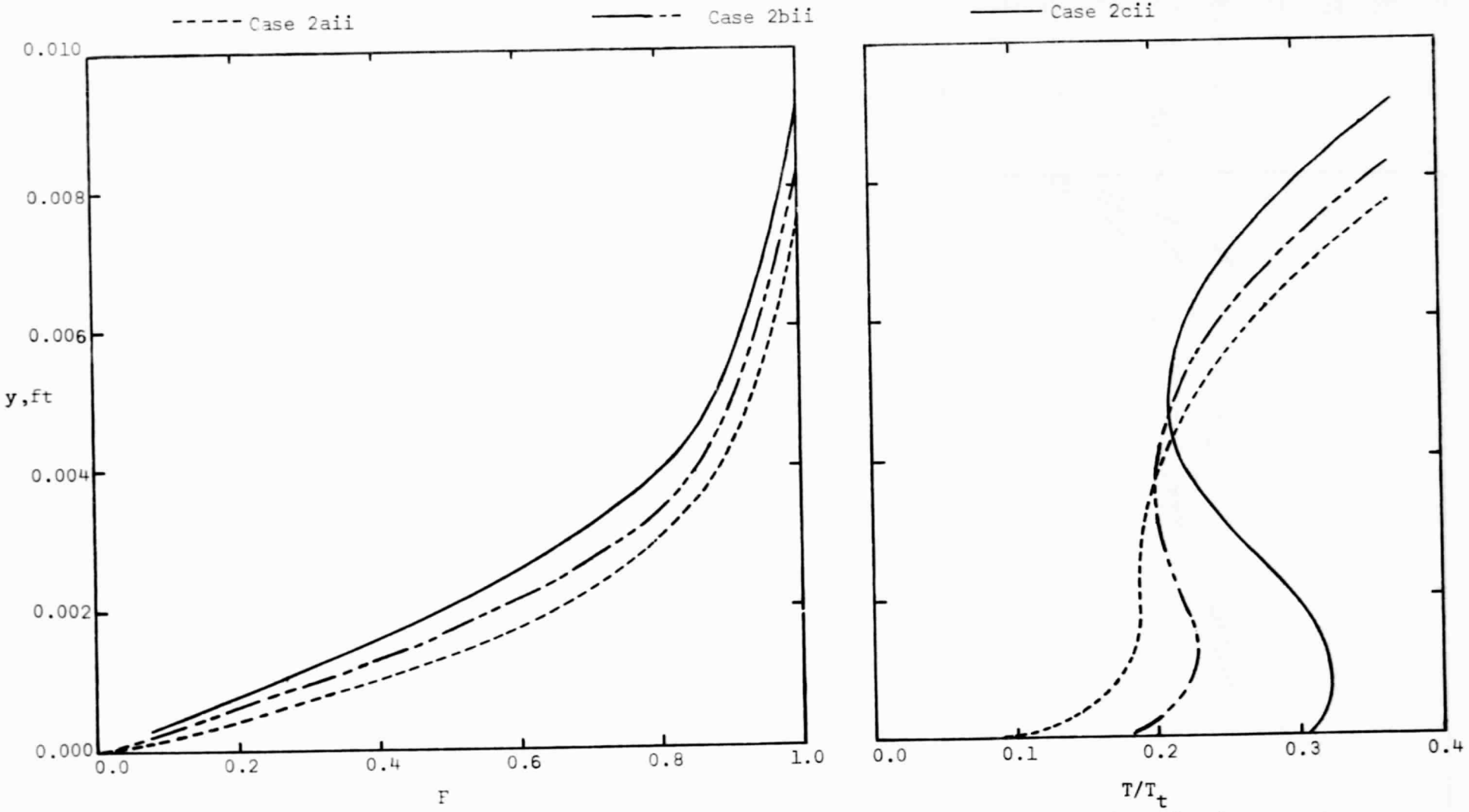

(a) s = .216 ft (i.e., s = 0.201 L, which is just upstream of the section interface)

Figure 10. - The effect of surface temperature on the theoretical, laminar boundary-layer (NSE for $\alpha = 30°$), $M_\infty = 12.25$, $Re_{\infty,L} = 0.59 \times 10^6$.

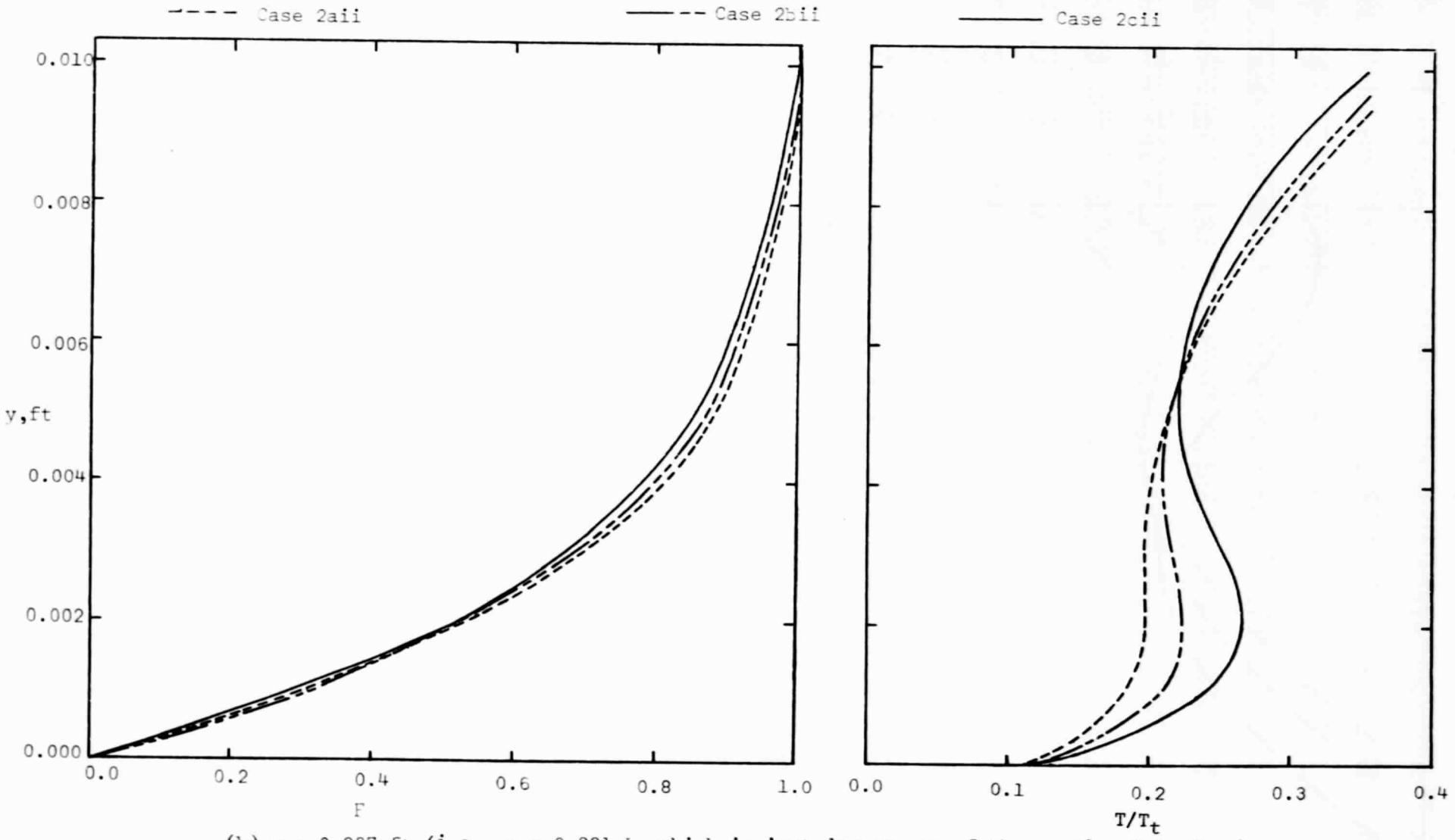

(b) s = 0.237 ft (i.e., s = 0.221 L, which is just downstream of the section interface)

Figure 10. - Continued.

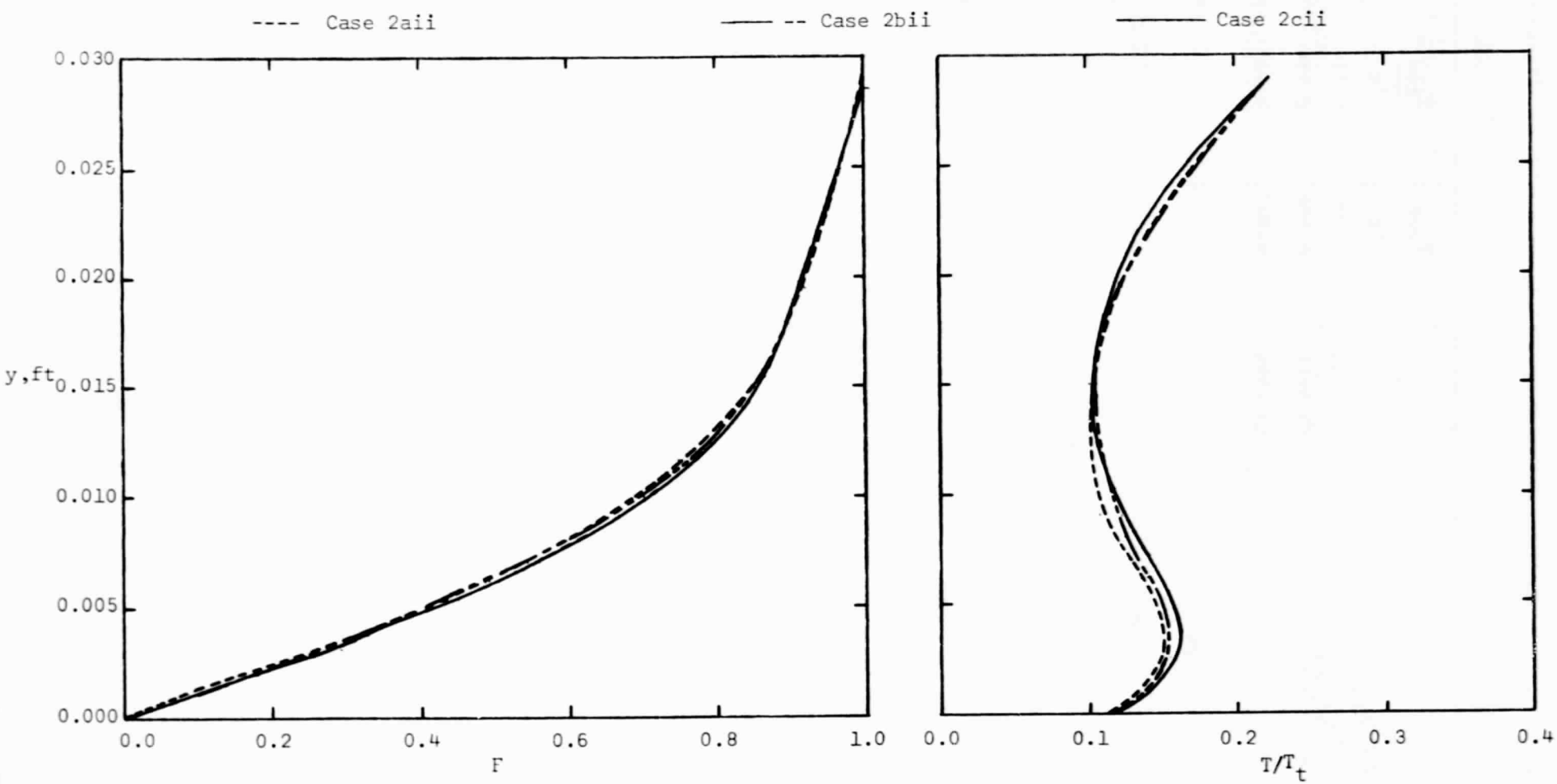

(c) s = 0.351 ft (i.e., s = 0.326L, which is just upstream of the "assumed" separation).

Figure 10. - Concluded.

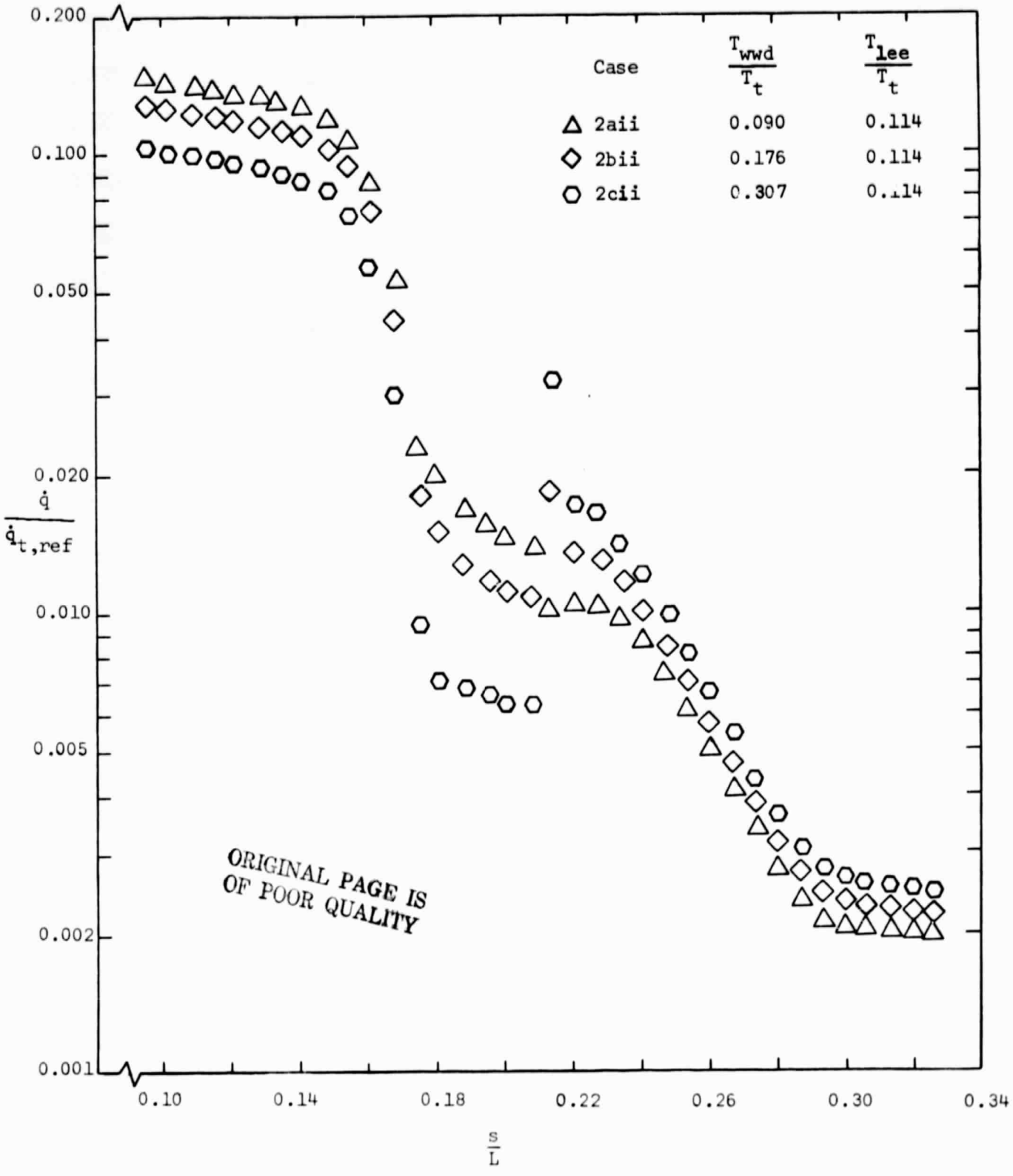

(a) The effect of the windward-section temperature.

Figure 11. - The effect of the surface temperature distribution on the streamwise heat-transfer distribution for flow condition 2, M_∞ = 12.25, $Re_{\infty/ft}$ = 0.55 x 10^6 (NSE for $\alpha = 30^\circ$).

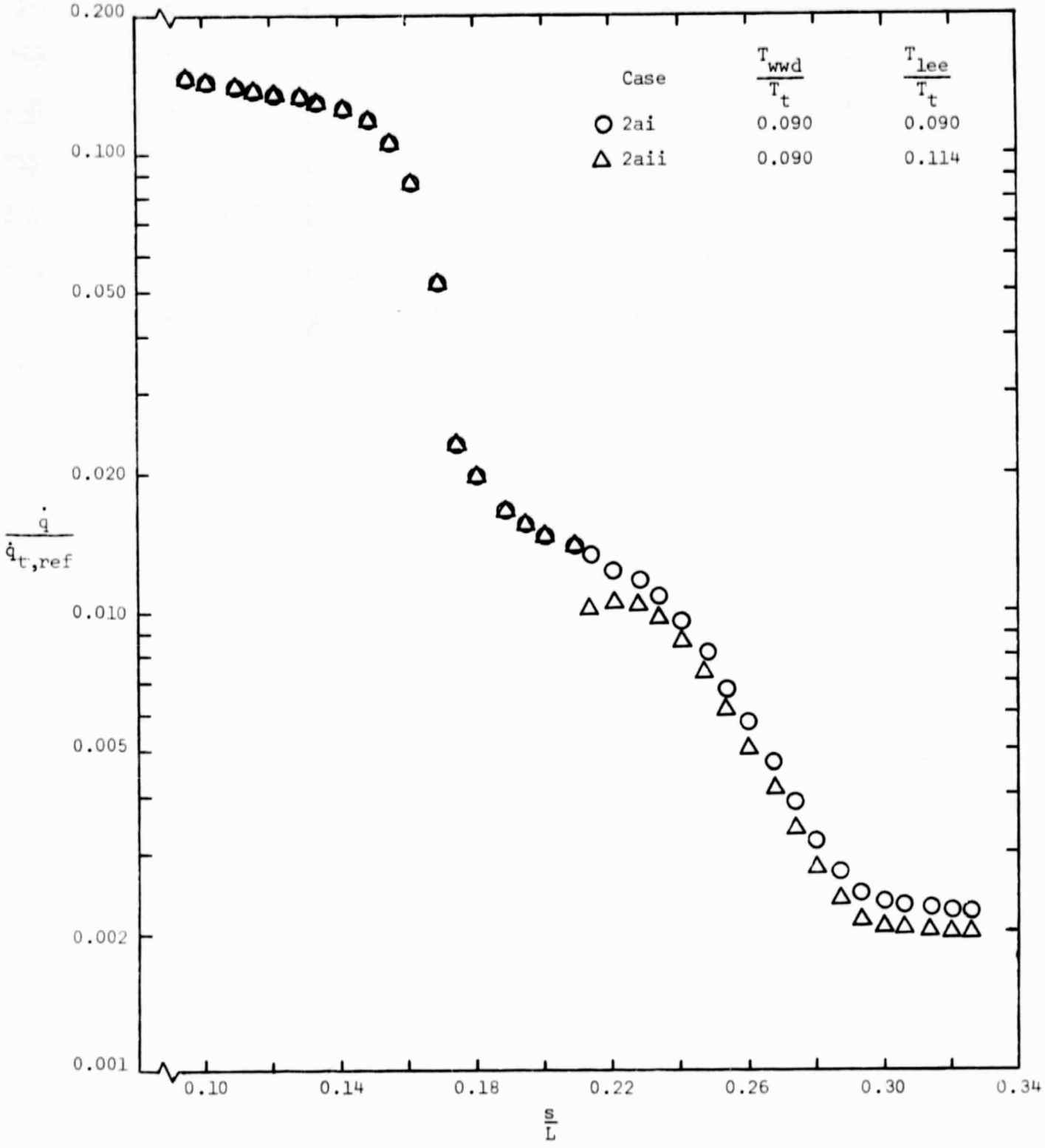

(b) The effect of the leeward-section temperature

Figure 11. - Concluded.

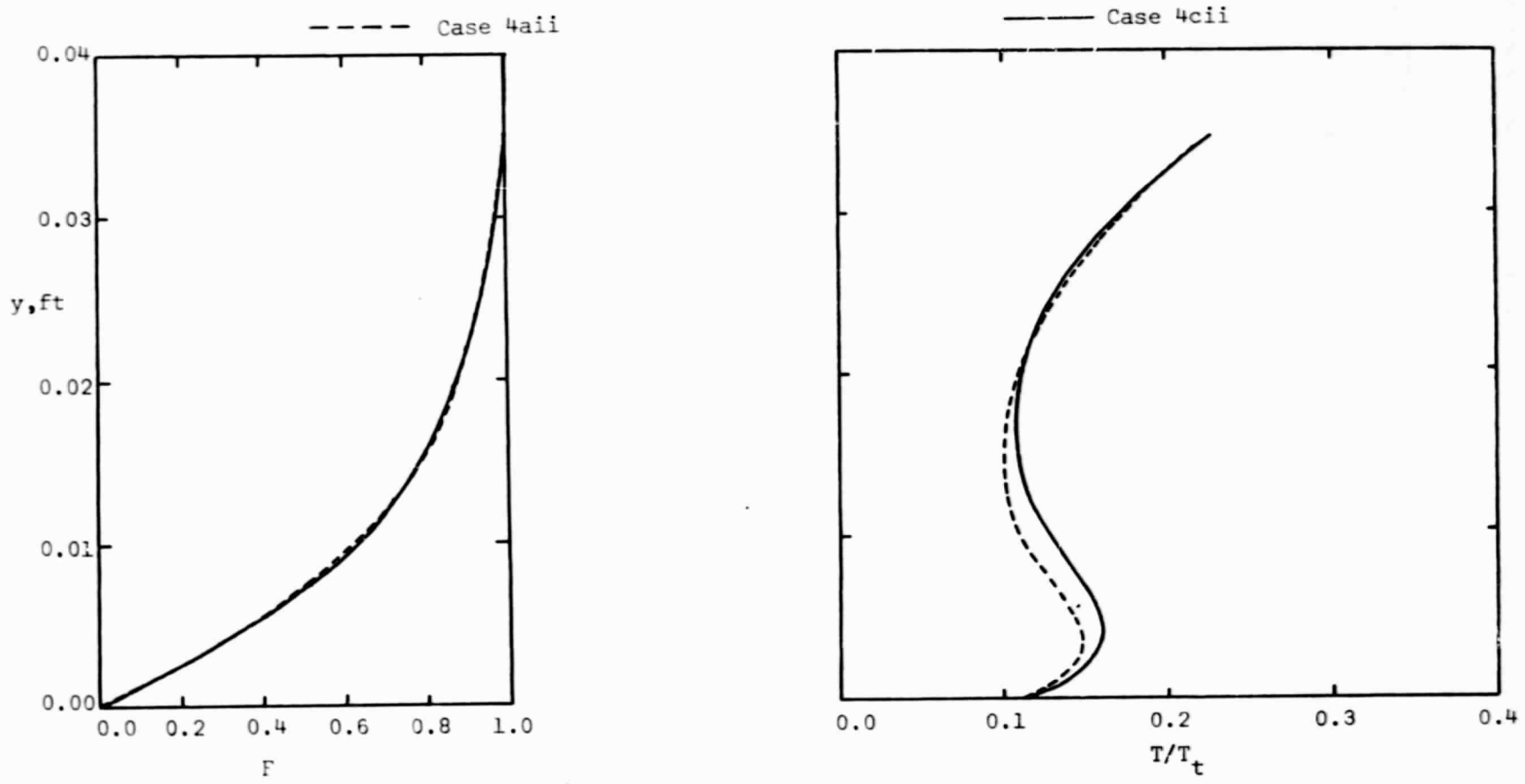

s = 0.351 ft (i.e., s = 0.326 L, which is just upstream of the "assumed"separation)

Figure 12. - The effect of surface temperature on the theoretical, laminar boundary-layer (NSE for $\alpha = 30°$), $M_\infty = 15.70$, $Re_{\infty,L} = 0.61 \times 10^6$.

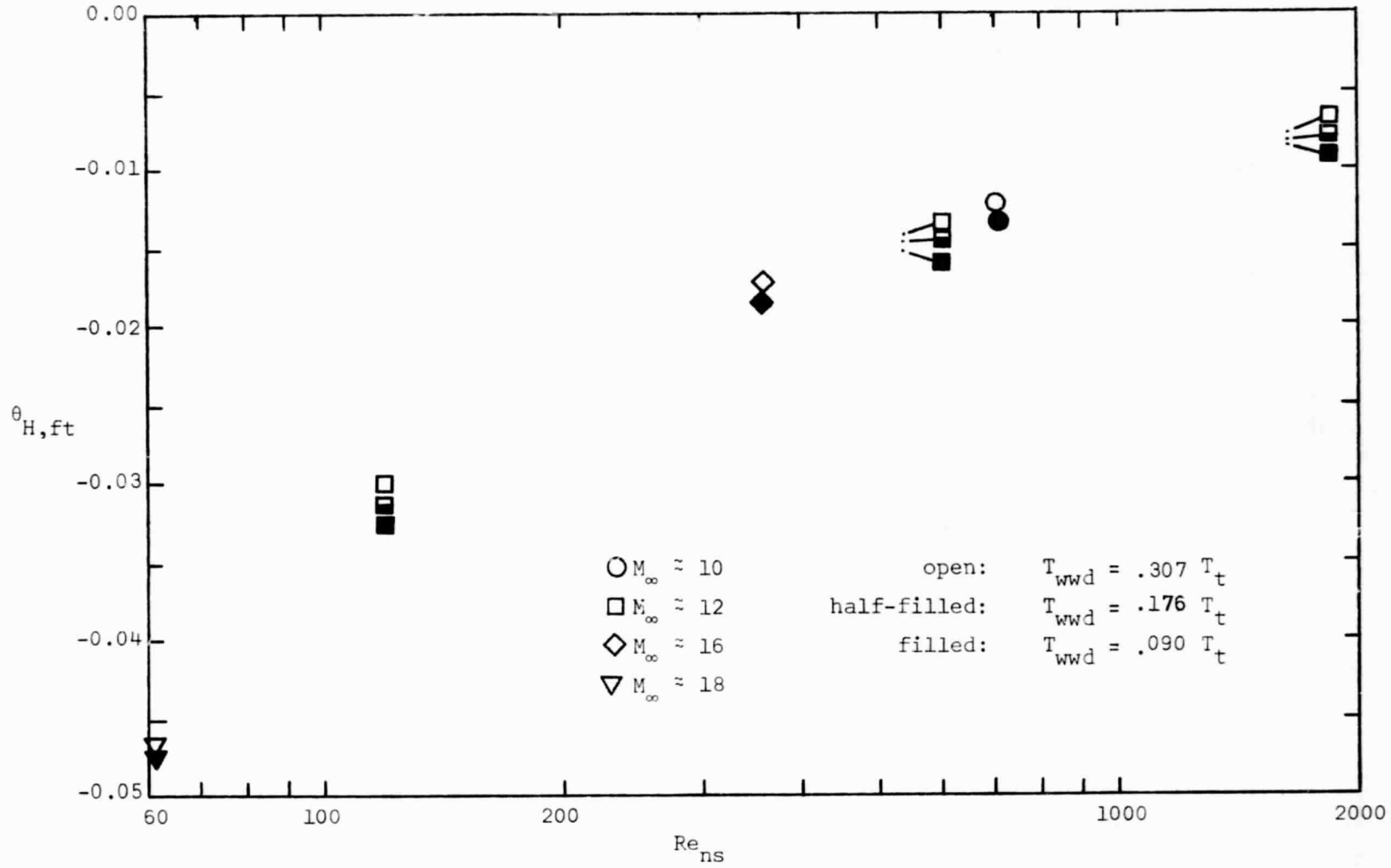

Figure 13. - The computed enthalpy thickness at the "assumed" separation location as a function of the Reynolds number behind a normal shock wave (NSE for $\alpha = 30°$).

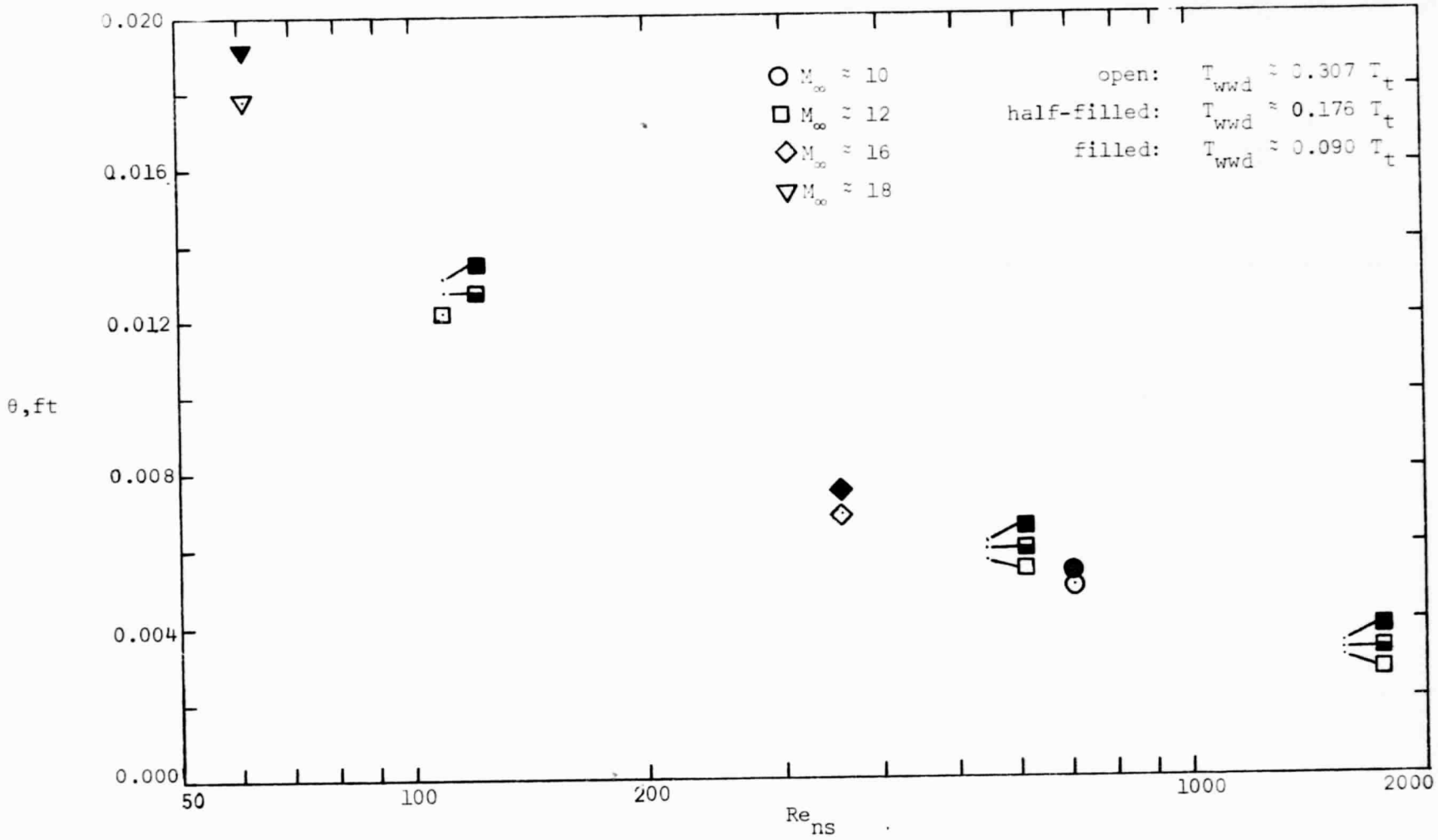

Figure 14. - The computed momentum thickness at the "assumed" separation location as a function of the Reynolds number behind a normal shock wave (NSE for $\alpha = 30°$).

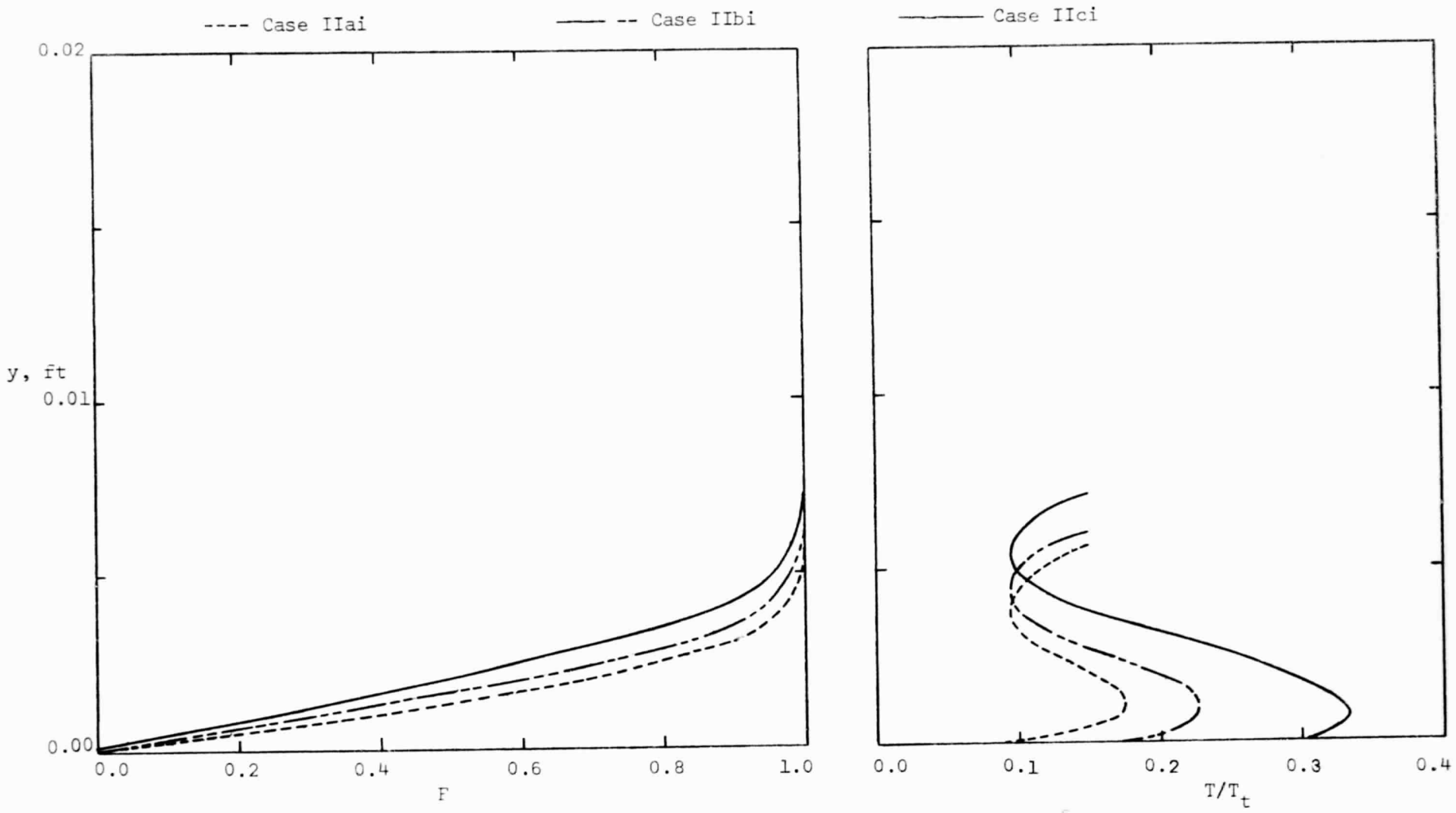

(a) s = 0.216 ft (i.e., s = 0.201L, which is just upstream of the section interface)

Figure 15. - The effect of surface temperature on the theoretical, laminar boundary-layer (PSE for $\alpha = 30°$) M = 12.25, $Re_{\infty,L} = 0.59 \times 10^6$.

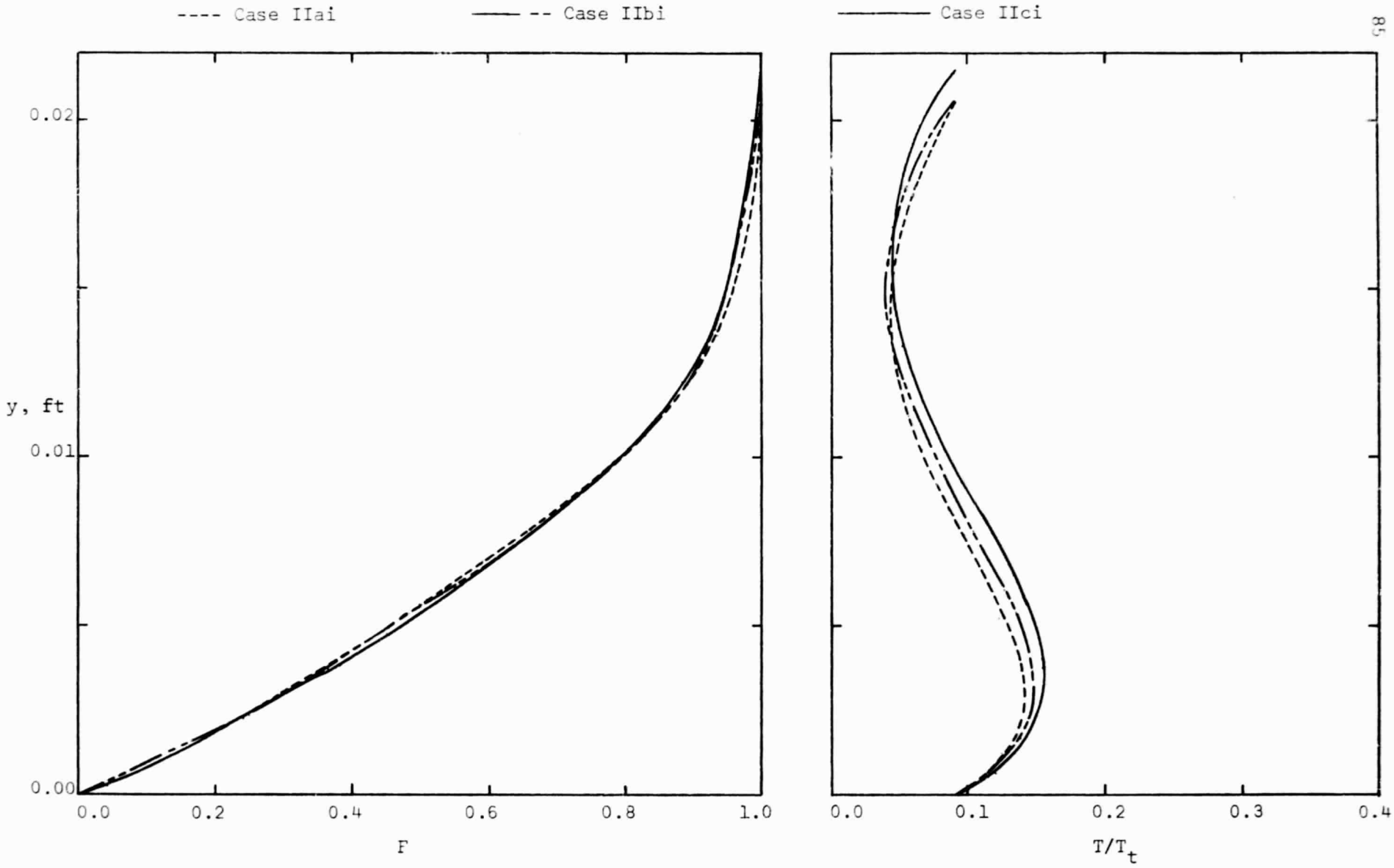

(b) s = 0.351 ft (i.e., s = 0.326L, which is just upstream of the "assumed" separation)

Figure 15. - Concluded.

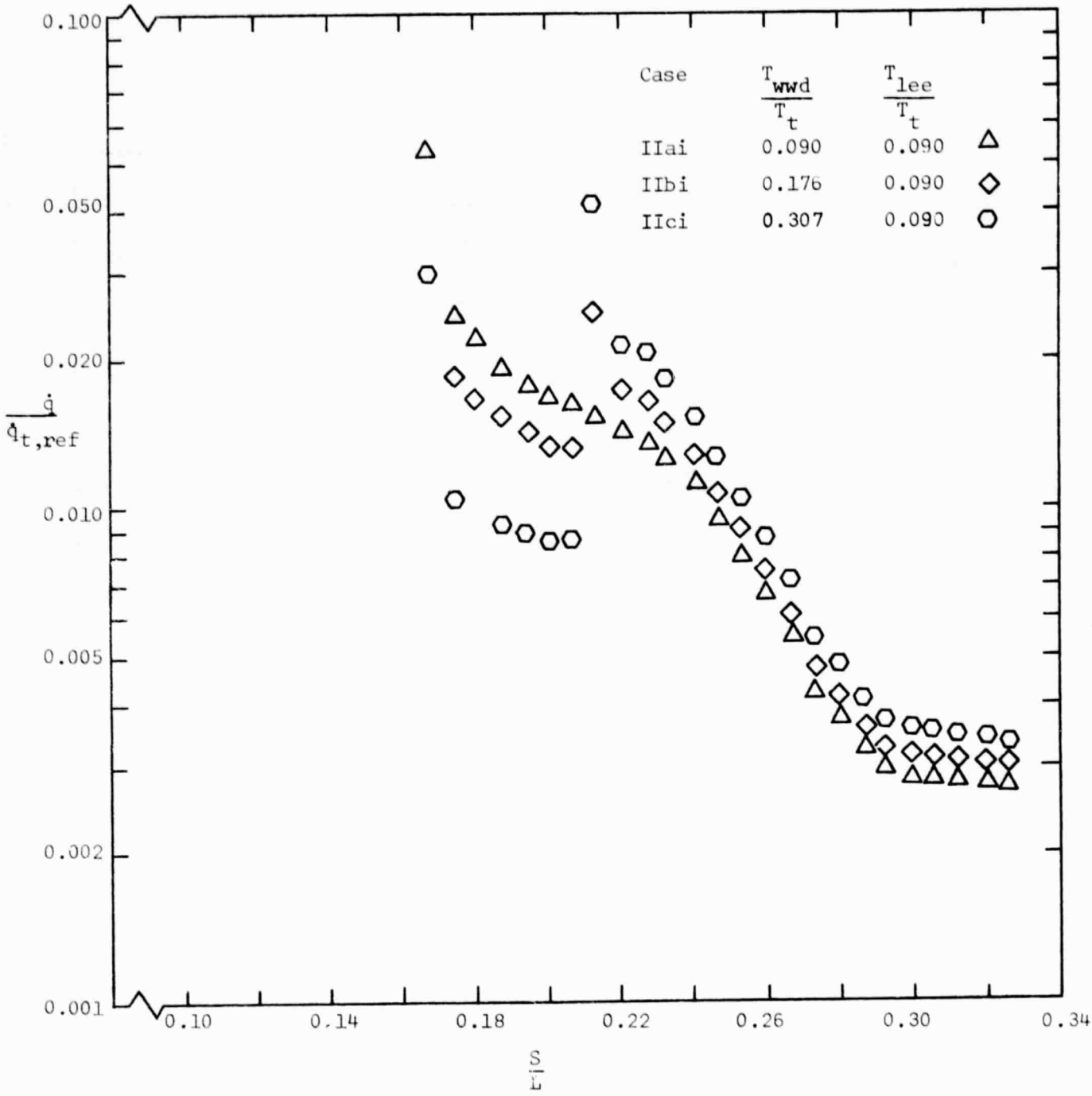

Figure 16. - The effect of the windward-section surface temperature distribution on the streamwise heat-transfer distribution for flow condition II, M_∞ = 12.25, $Re_{\infty,L}$ = 0.59 x 10^6 (PSE for α = 30°).

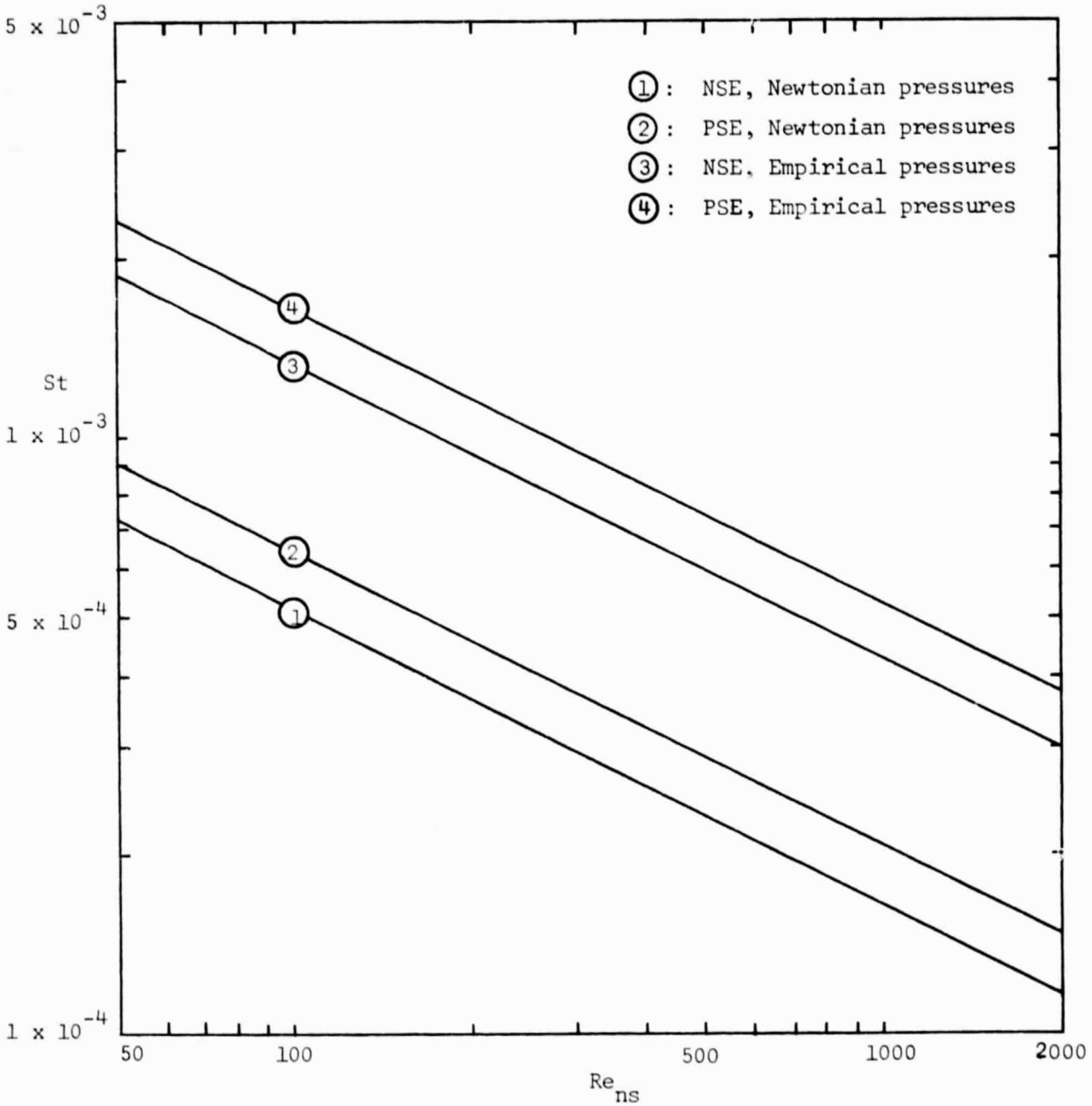

Figure 17. - The effect of inviscid flow model on the theoretical heat-transfer at s = 0.351 ft (s = 0.326L), α = 30°.

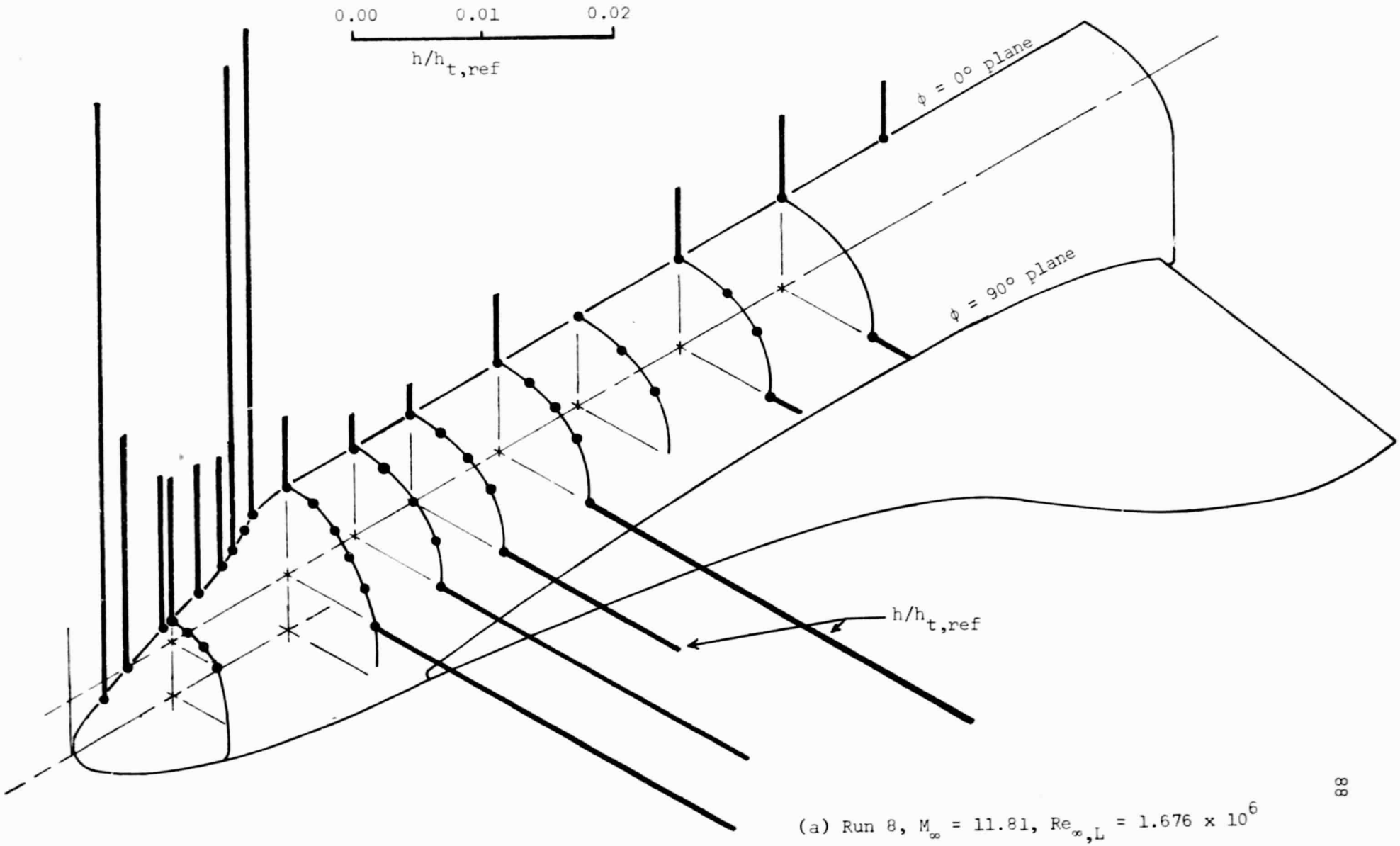

(a) Run 8, M_∞ = 11.81, $Re_{\infty,L}$ = 1.676 x 10^6

Figure 18. - Typical heat-transfer distributions in the ϕ = 0° plane and in the ϕ = 90° plane, α = 30°.

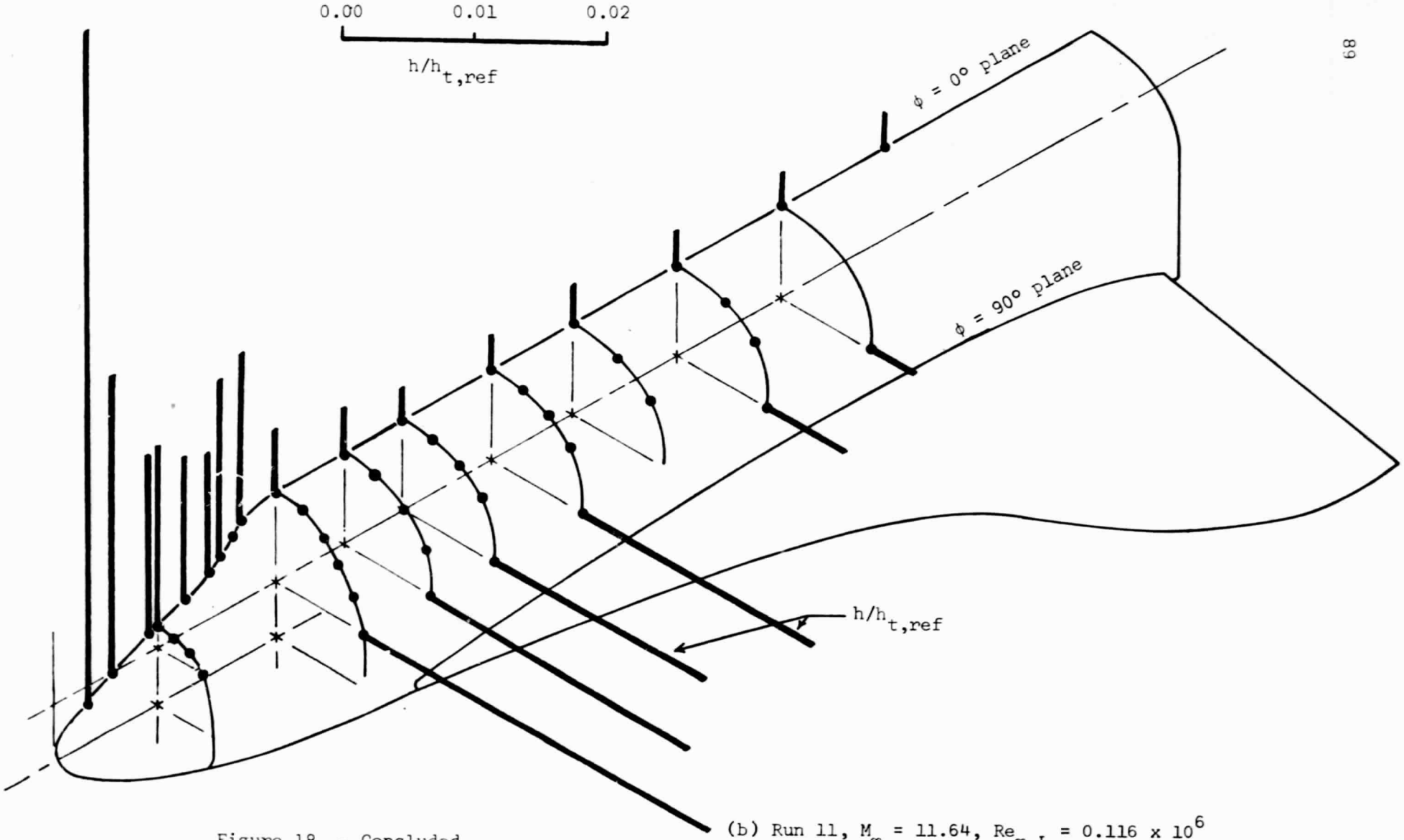

(b) Run 11, M_∞ = 11.64, $Re_{\infty,L}$ = 0.116 x 10^6

Figure 18. - Concluded.

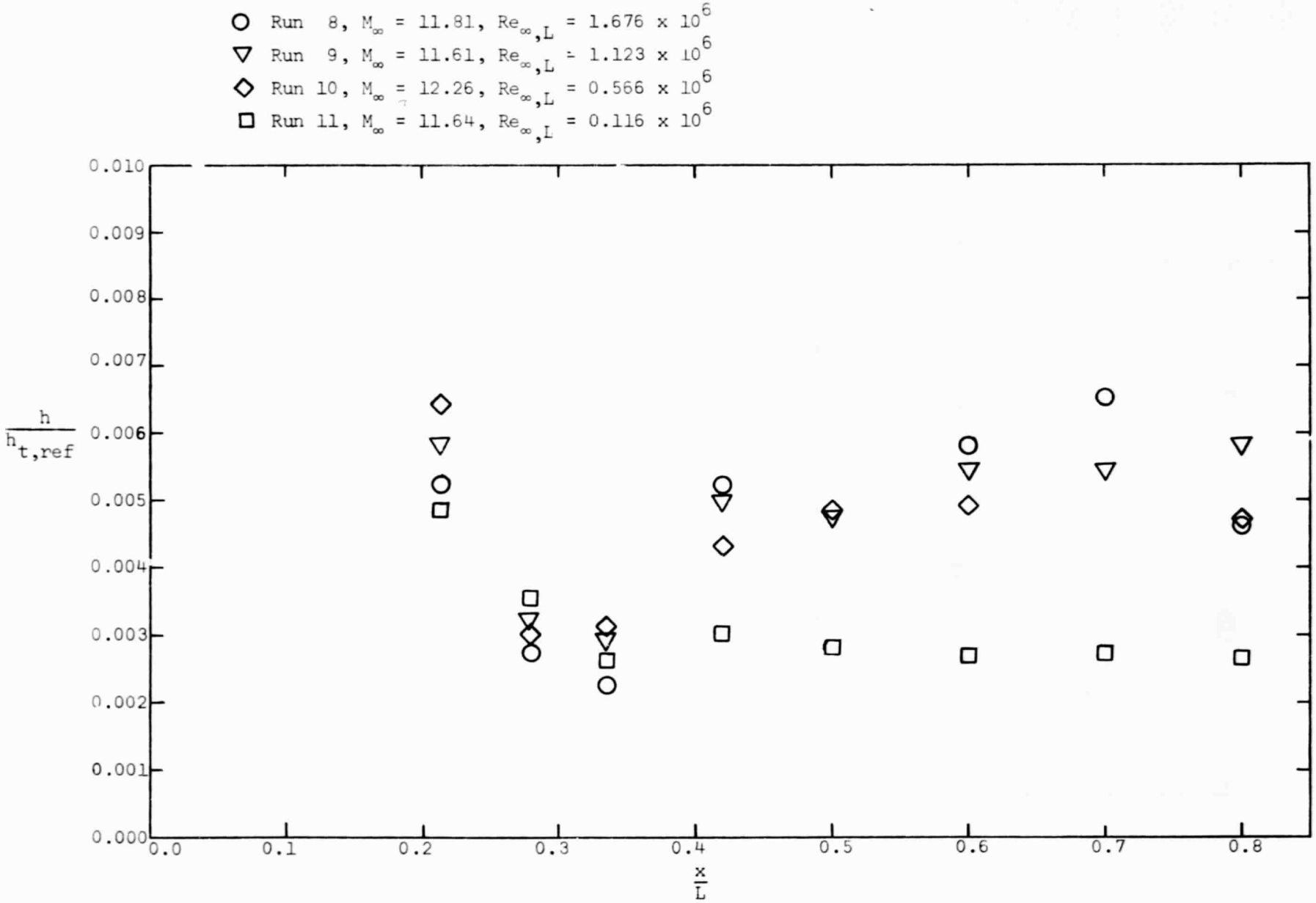

(a) $T_{wwd} \approx 0.31\ T_t$, $T_{lee} \approx 0.11\ T_t$

Figure 19. - The effect of Reynolds number on the heat-transfer distribution in the leeward pitch plane for the nominal Mach 12 flows, $\alpha = 30°$.

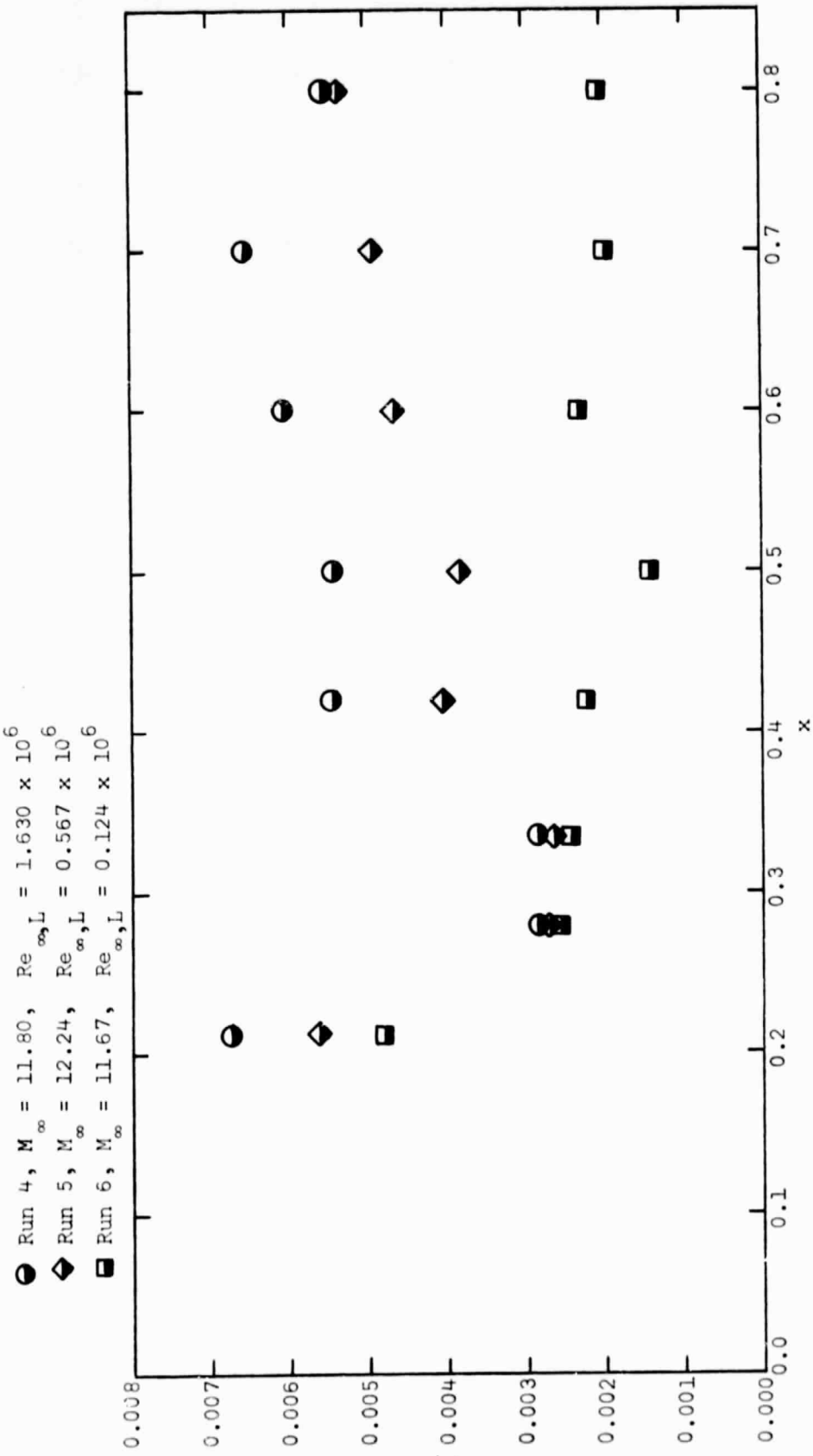

(b) $T_{wwd} \approx 0.18\ T_t$, $T_{lee} \approx 0.11\ T_t$

Figure 19. - Continued.

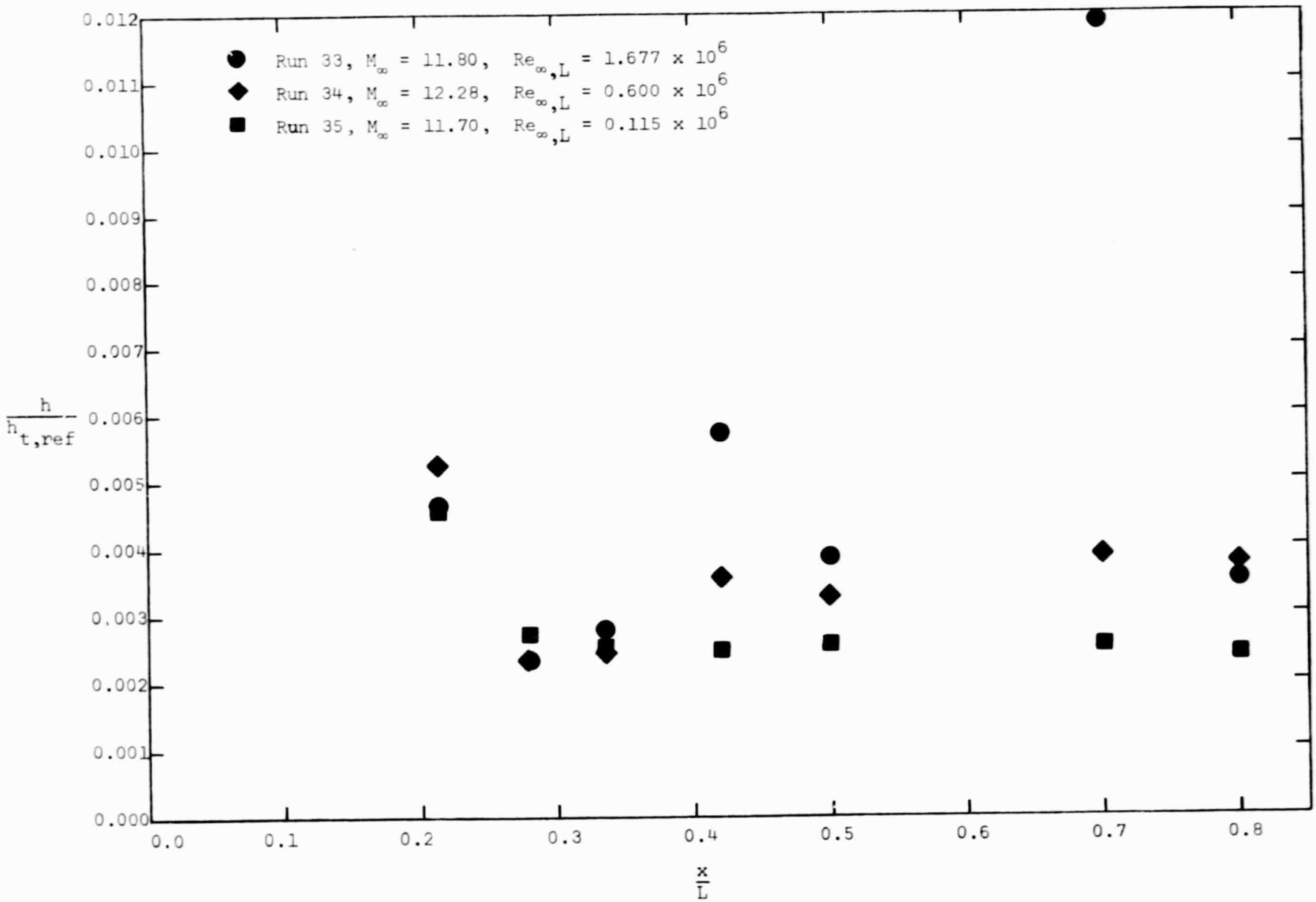

(c) $T_{wwd} \approx 0.09\ T_t$, $T_{jee} \approx 0.09\ T_t$

Figure 19. - Concluded.

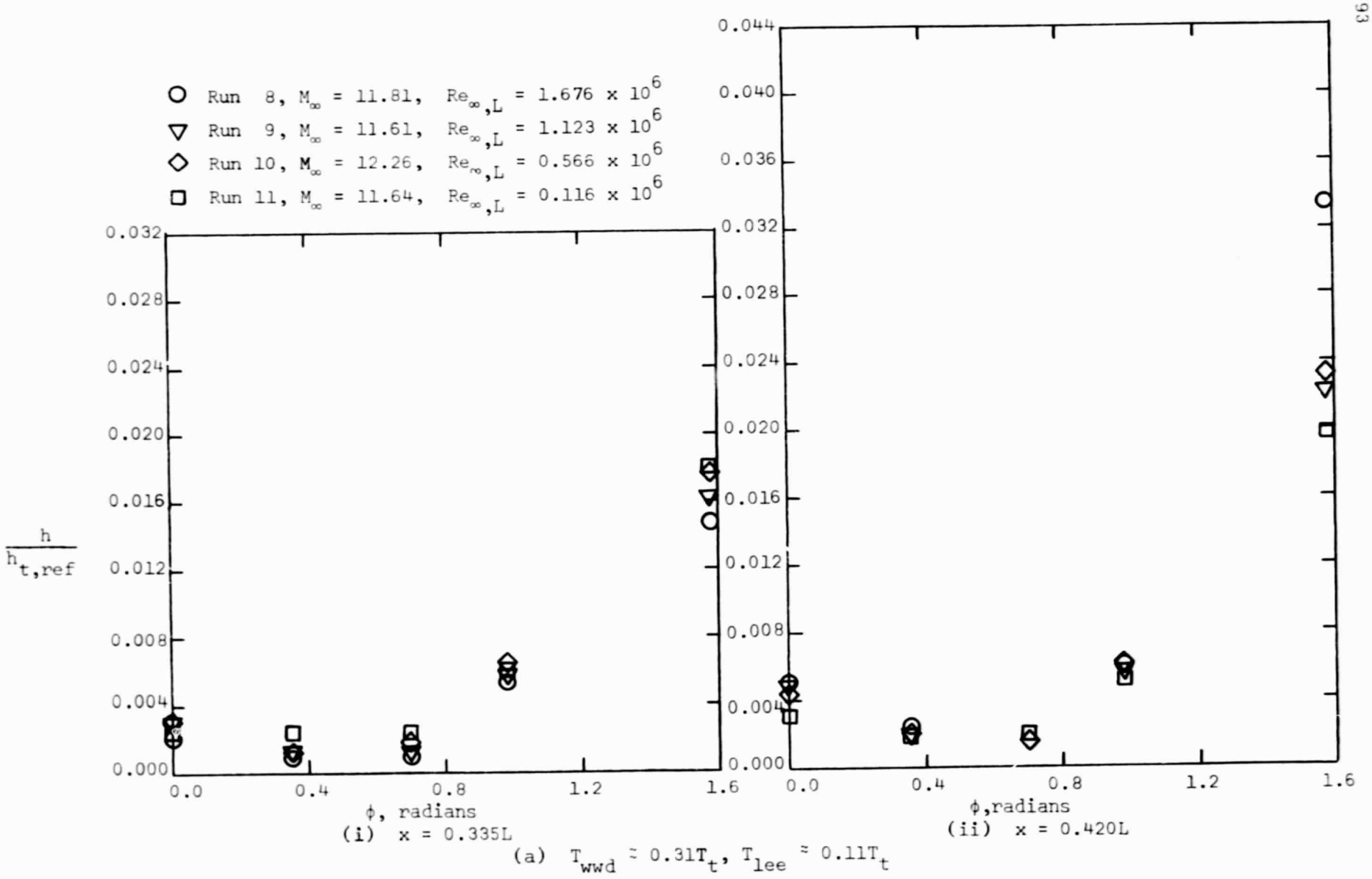

Figure 20. - The effect of Reynolds number on the circumferential heat-transfer distribution for the nominal Mach 12 flow, $\alpha = 30°$.

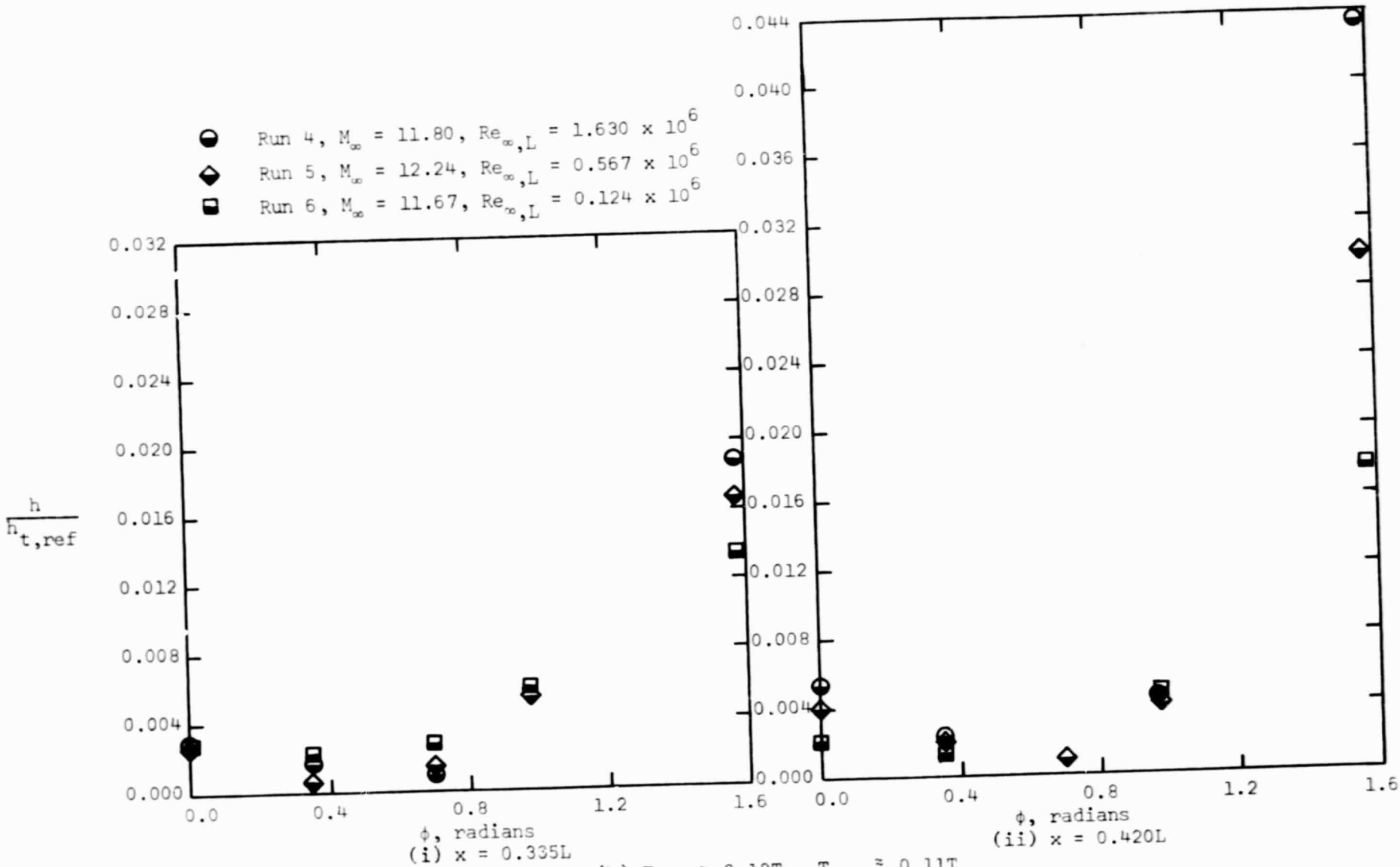

(b) $T_{wwd} \approx 0.18T_t$, $T_{lee} \approx 0.11T_t$

Figure 20. - Continued.

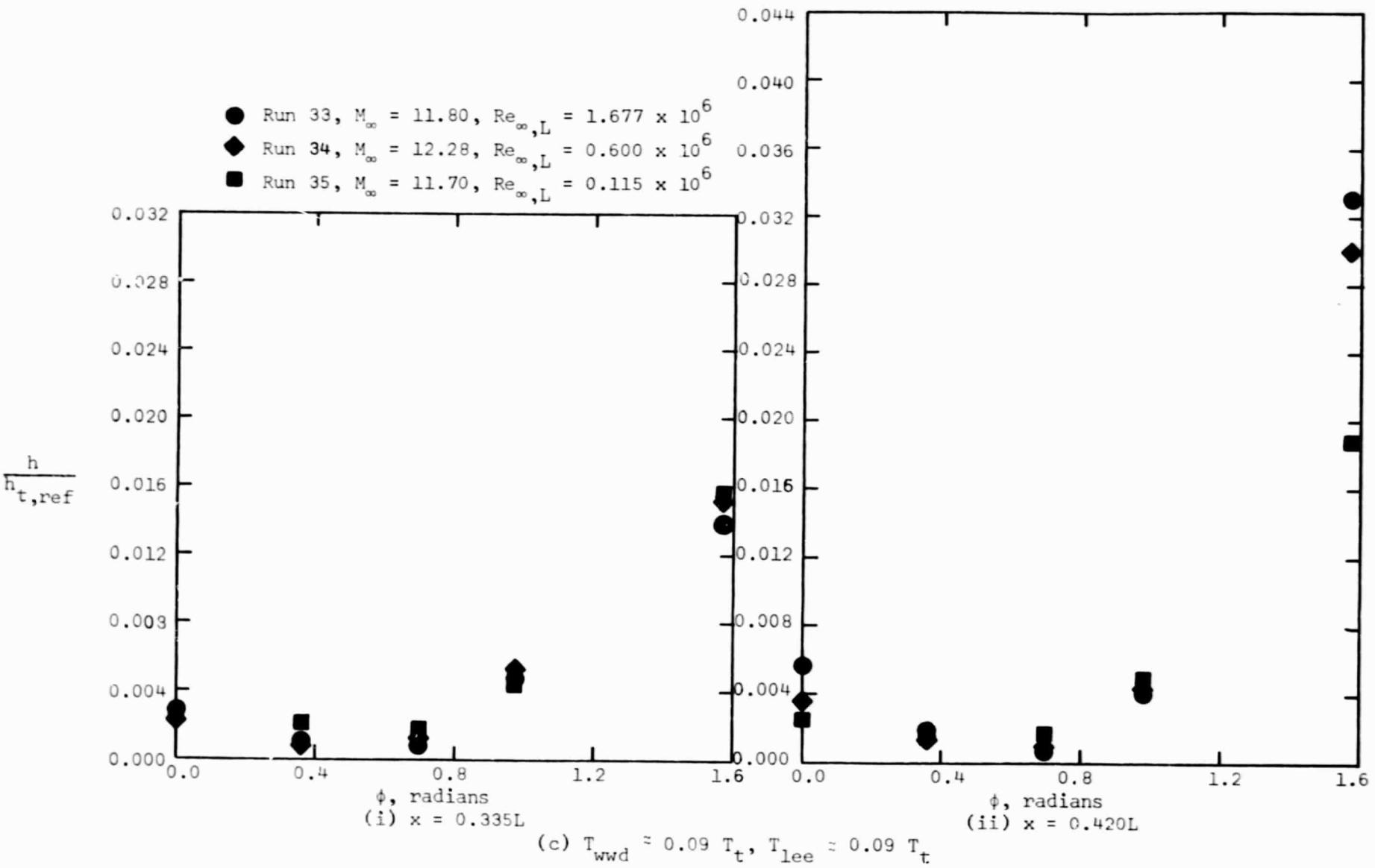

(c) $T_{wwd} \approx 0.09\ T_t$, $T_{lee} \approx 0.09\ T_t$

Figure 20. - Concluded.

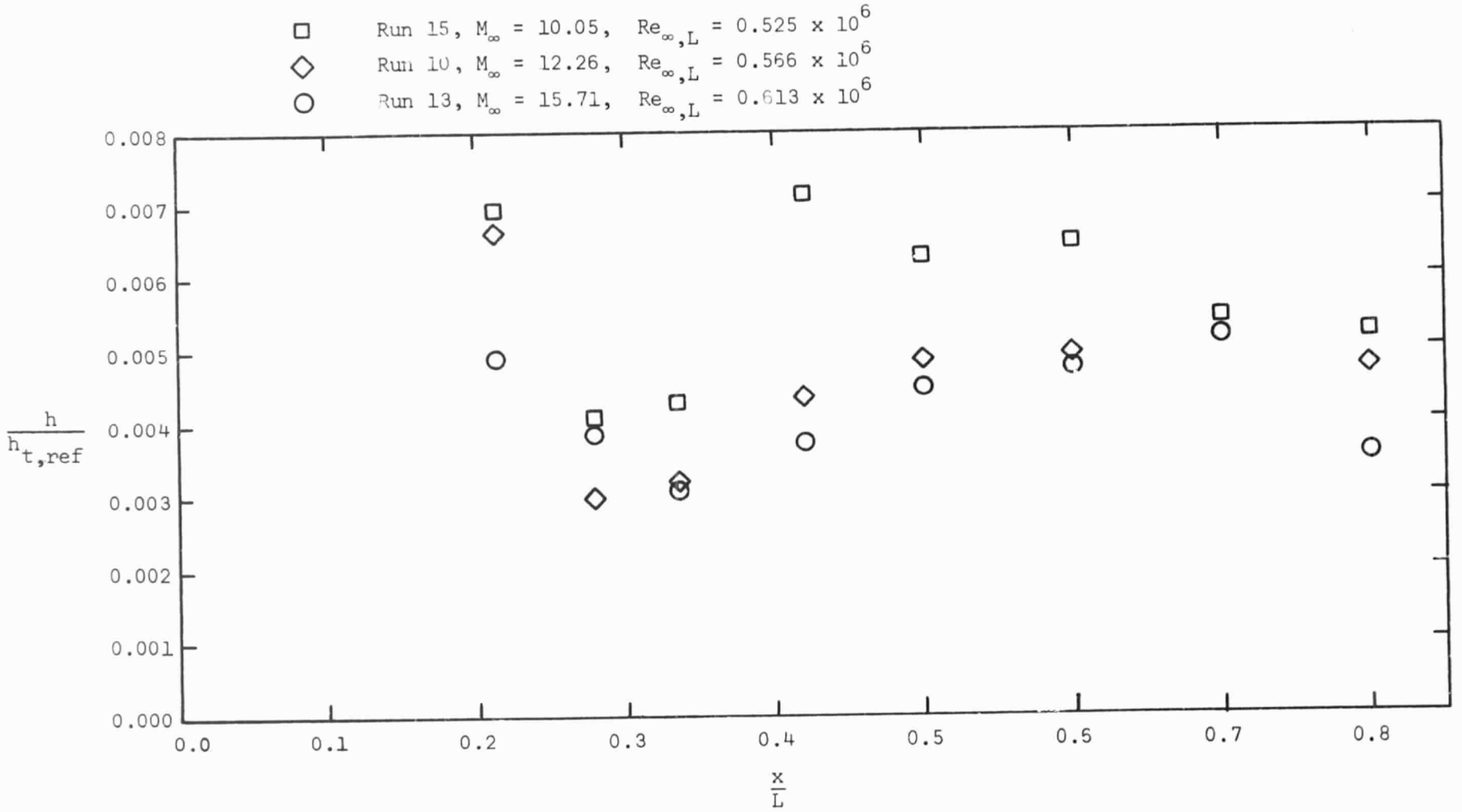

(a) $T_{wwd} \approx 0.31\ T_t$, $T_{lee} \approx 0.11\ T_t$

Figure 21. - The heat-transfer distribution in the leeward pitch plane for those runs with the nominal $Re_{\infty,L}$ of 0.6 x 10^6, $\alpha = 30°$.

(b) $T_{wwd} \approx 0.09\ T_t, T_{lee} \approx 0.09\ T_t$

Figure 21. - Concluded.

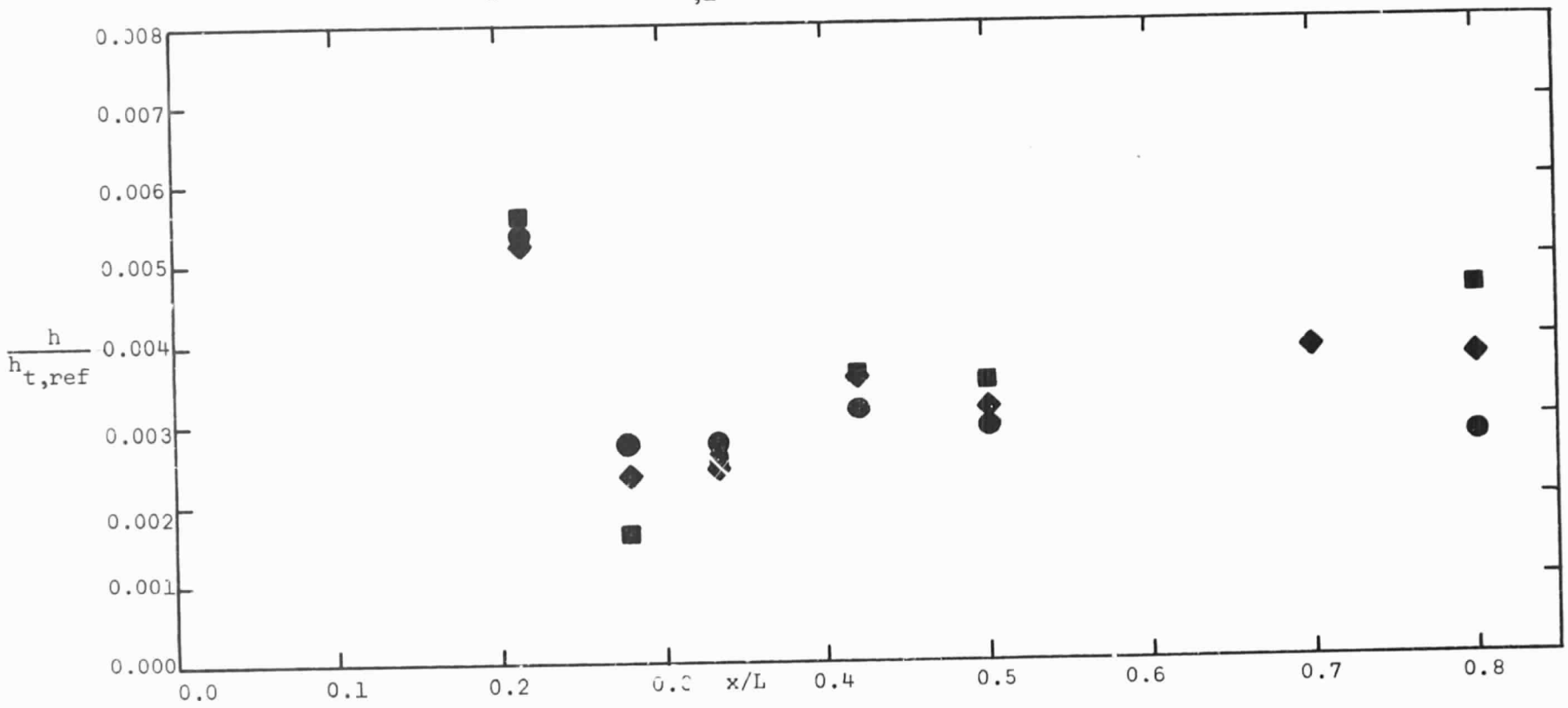

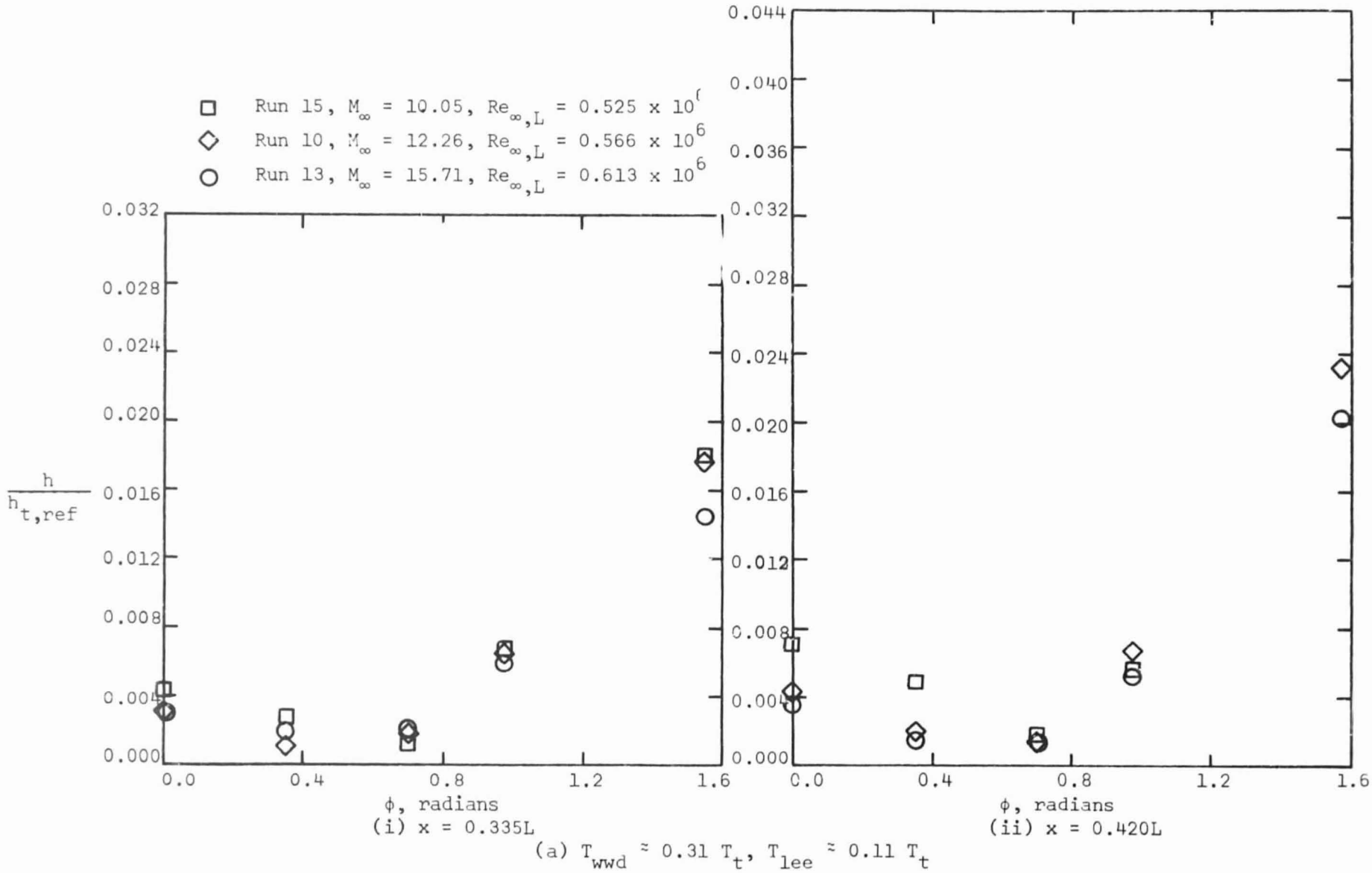

Figure 22. - The circumferential heat-transfer distribution in the leeward pitch plane for those runs with the nominal $Re_{\infty,L}$ of 0.6 x 10^6, α = 30°.

(b) $T_{wwd} \approx 0.09\ T_t$, $T_{lee} \approx 0.09\ T_t$

Figure 22. - Concluded.

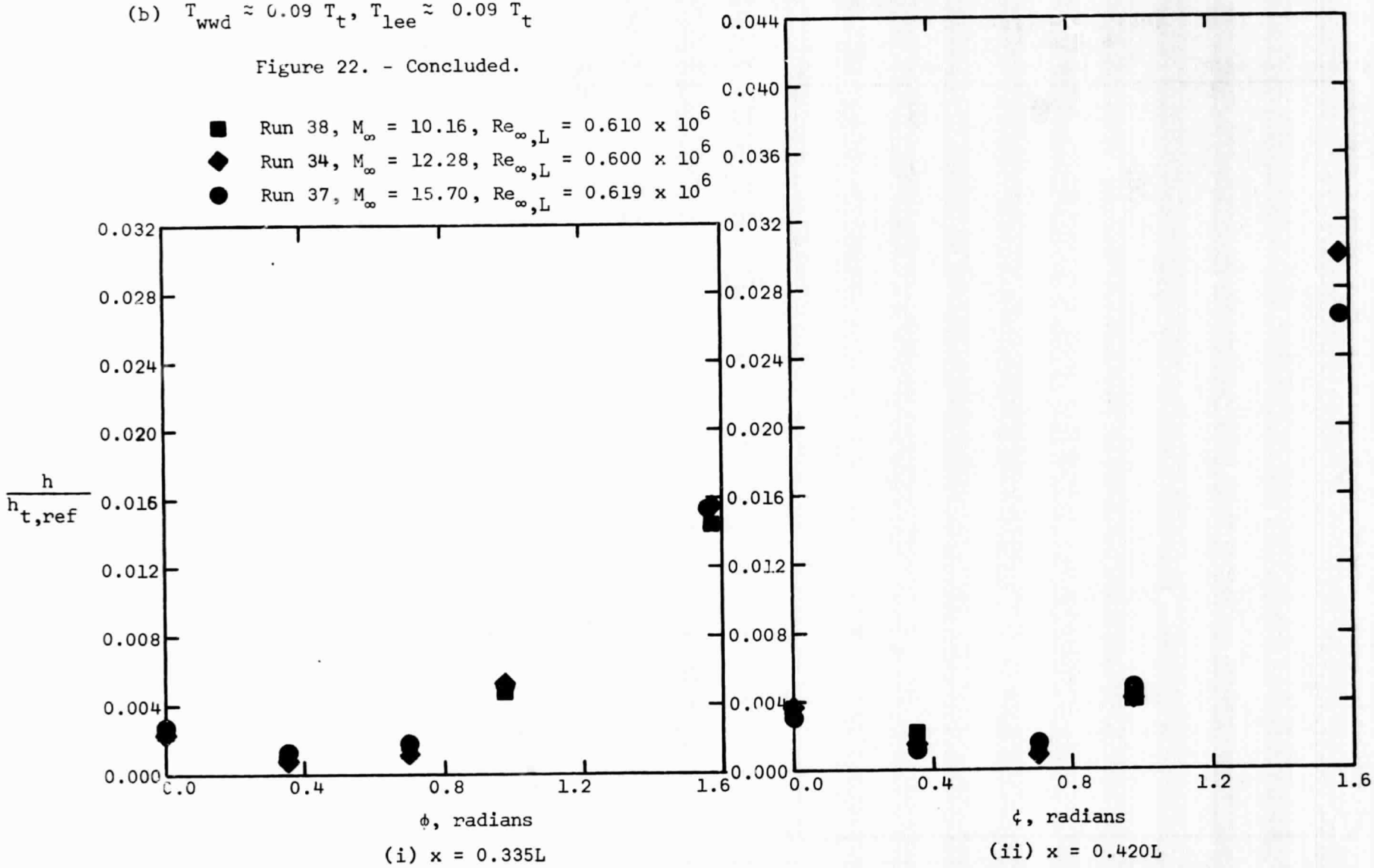

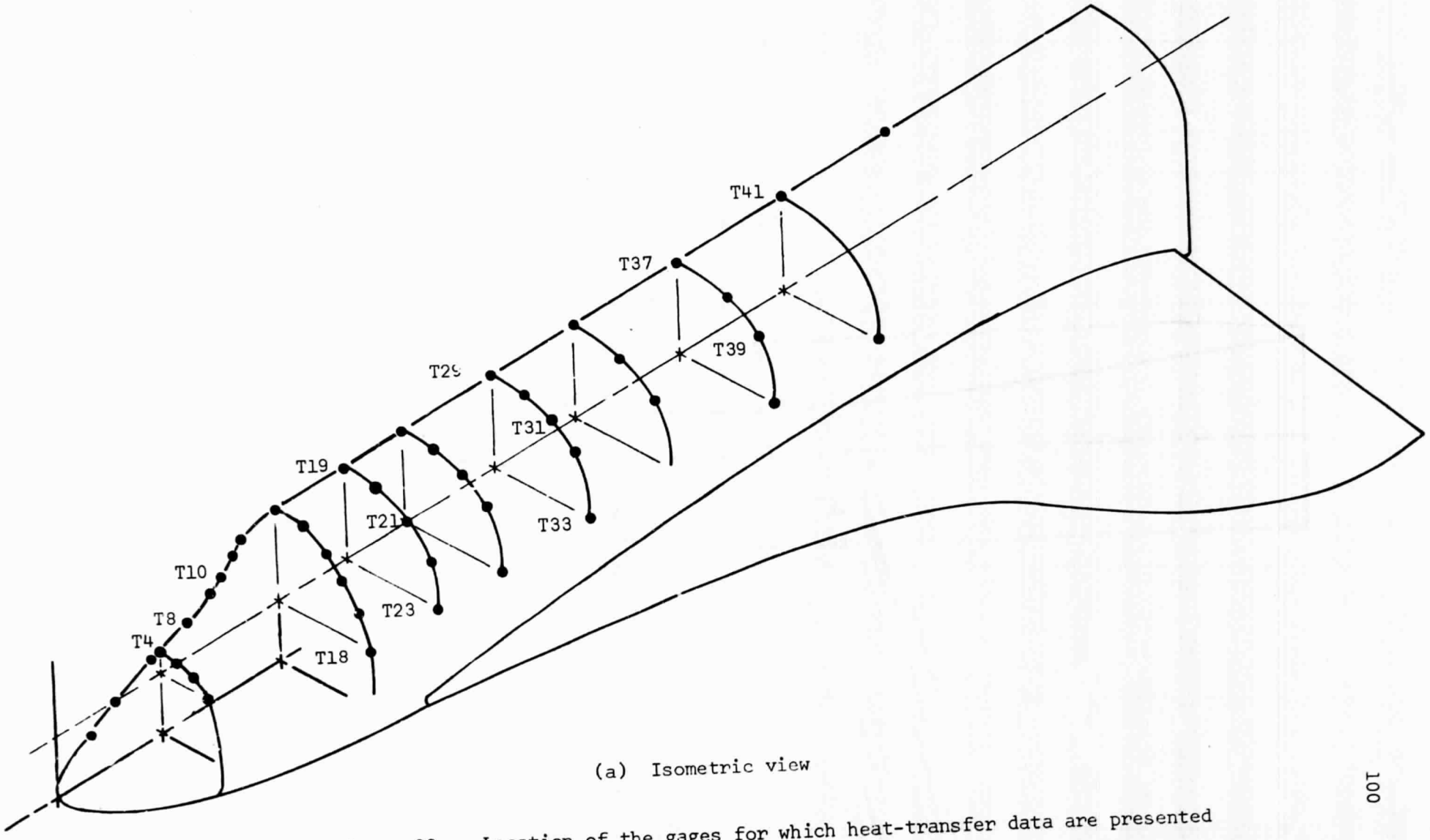

(a) Isometric view

Figure 23. - Location of the gages for which heat-transfer data are presented as a function of Re_{ns}.

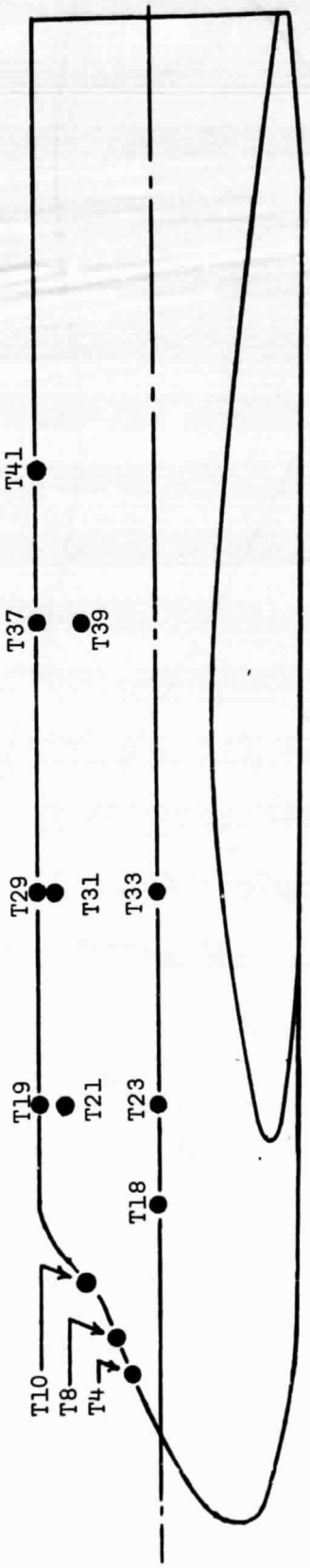

(b) Side view

Figure 23. - Concluded.

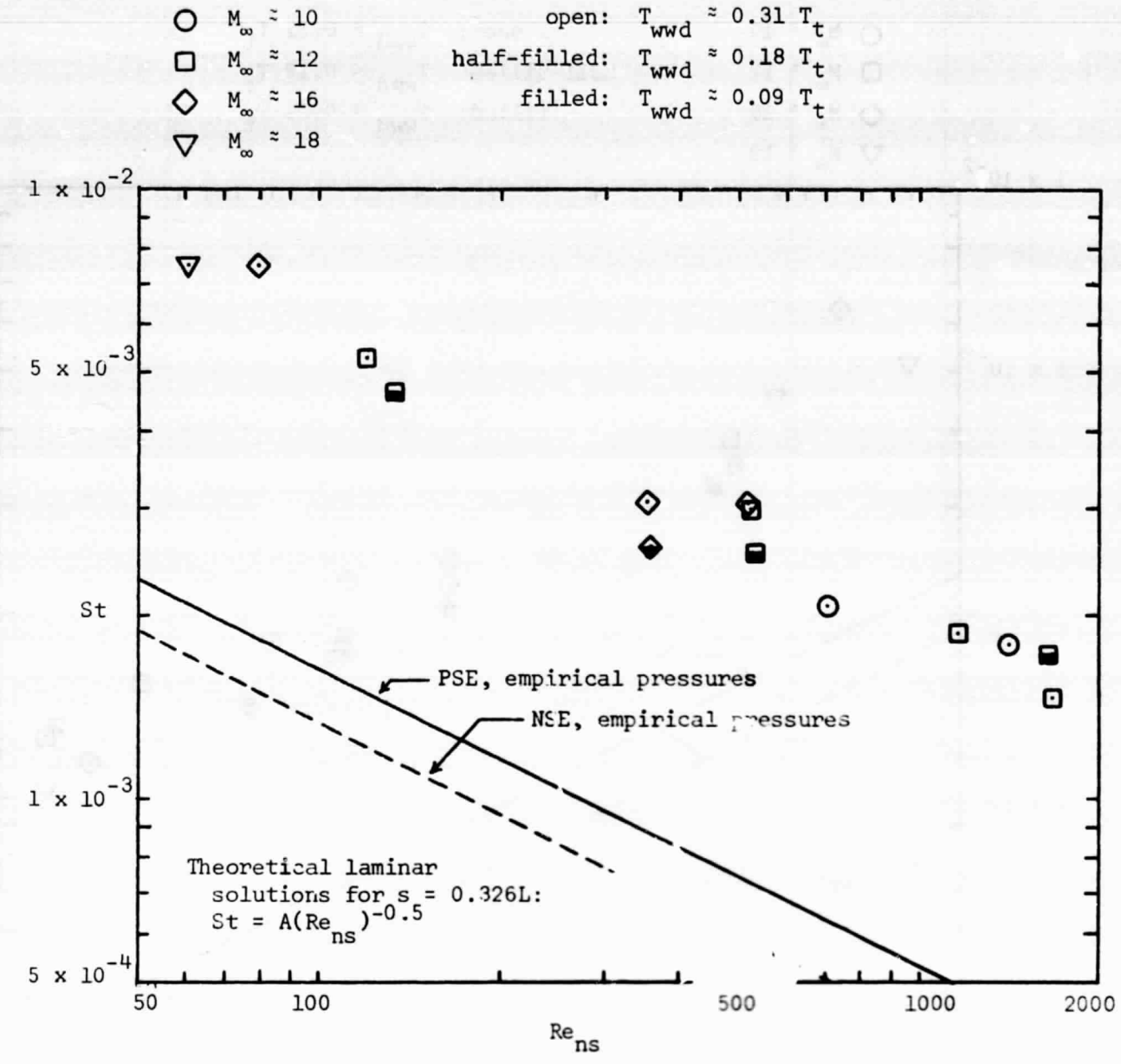

(a) Gage T18, x = 0.213L, ϕ = 90°

Figure 24. - The Stanton number as a function of the Reynolds number behind a normal shock wave for gages on the lateral surface of the fuselage (where the boundary-layer is attached), α = 30°.

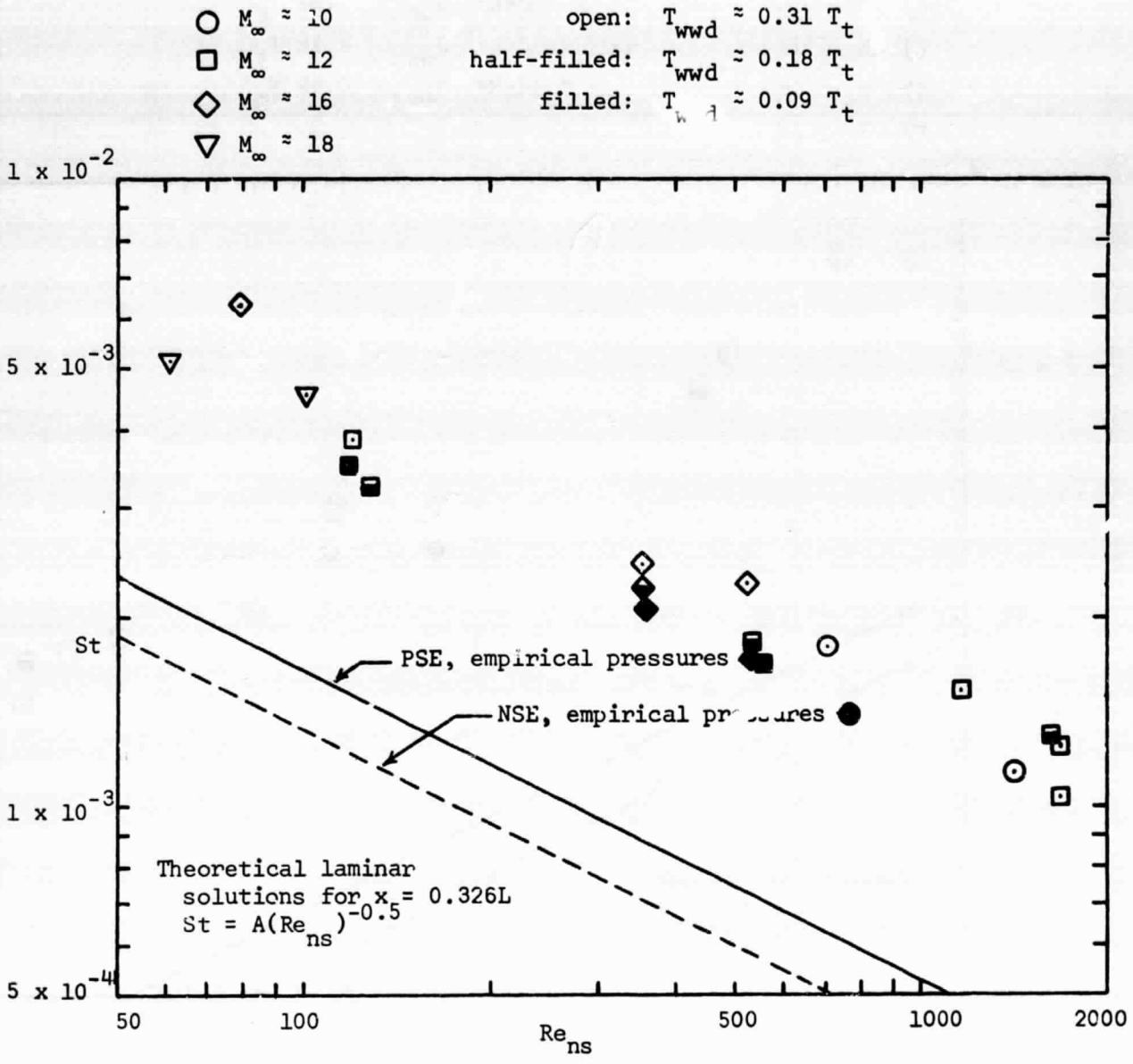

(b) Gage T23, x = 0.279L, ϕ = 90°

Figure 24. - Continued.

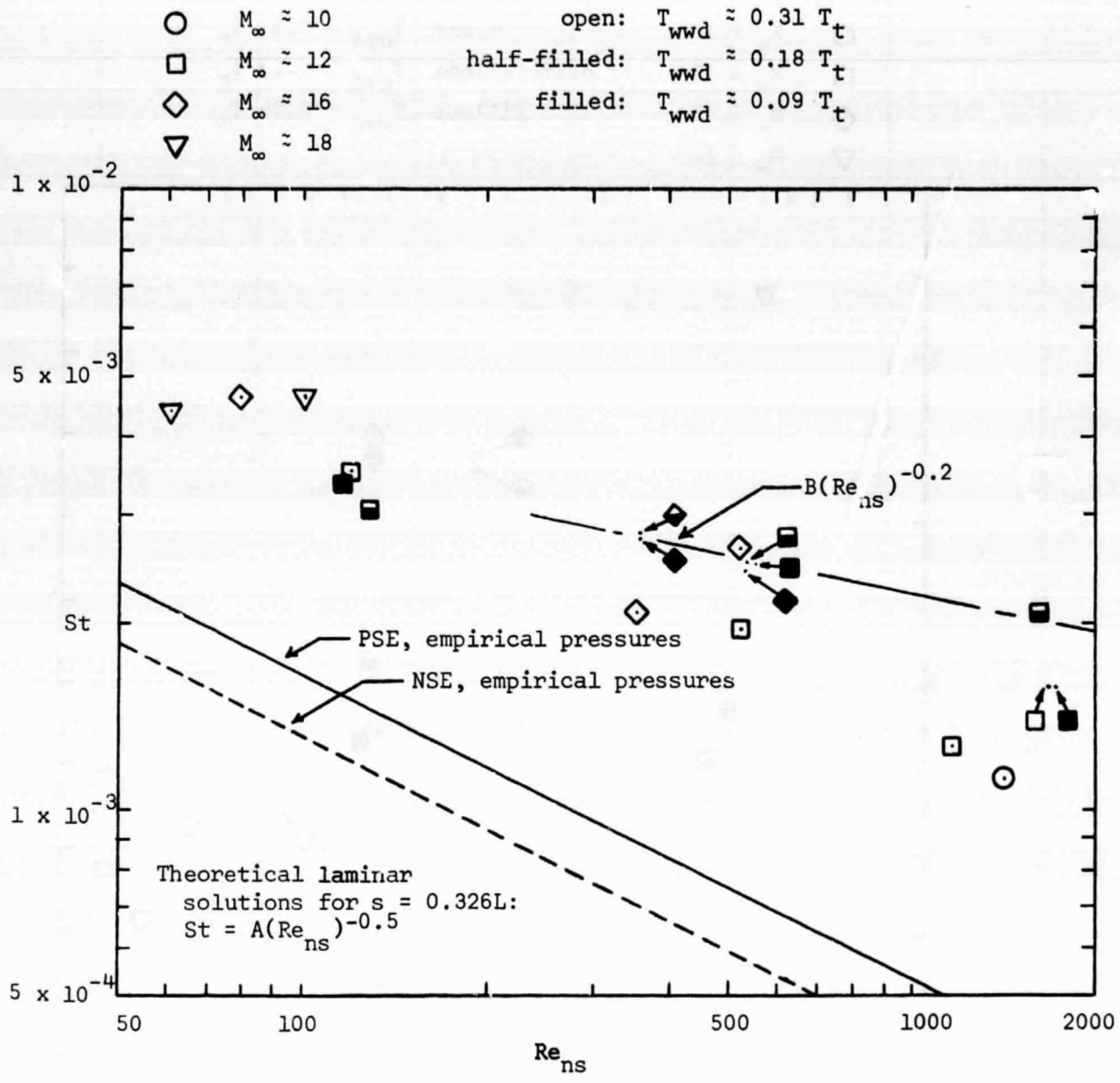

(c) Gage T33, $x = 0.420L$, $\phi = 90°$.

Figure 24. - Concluded.

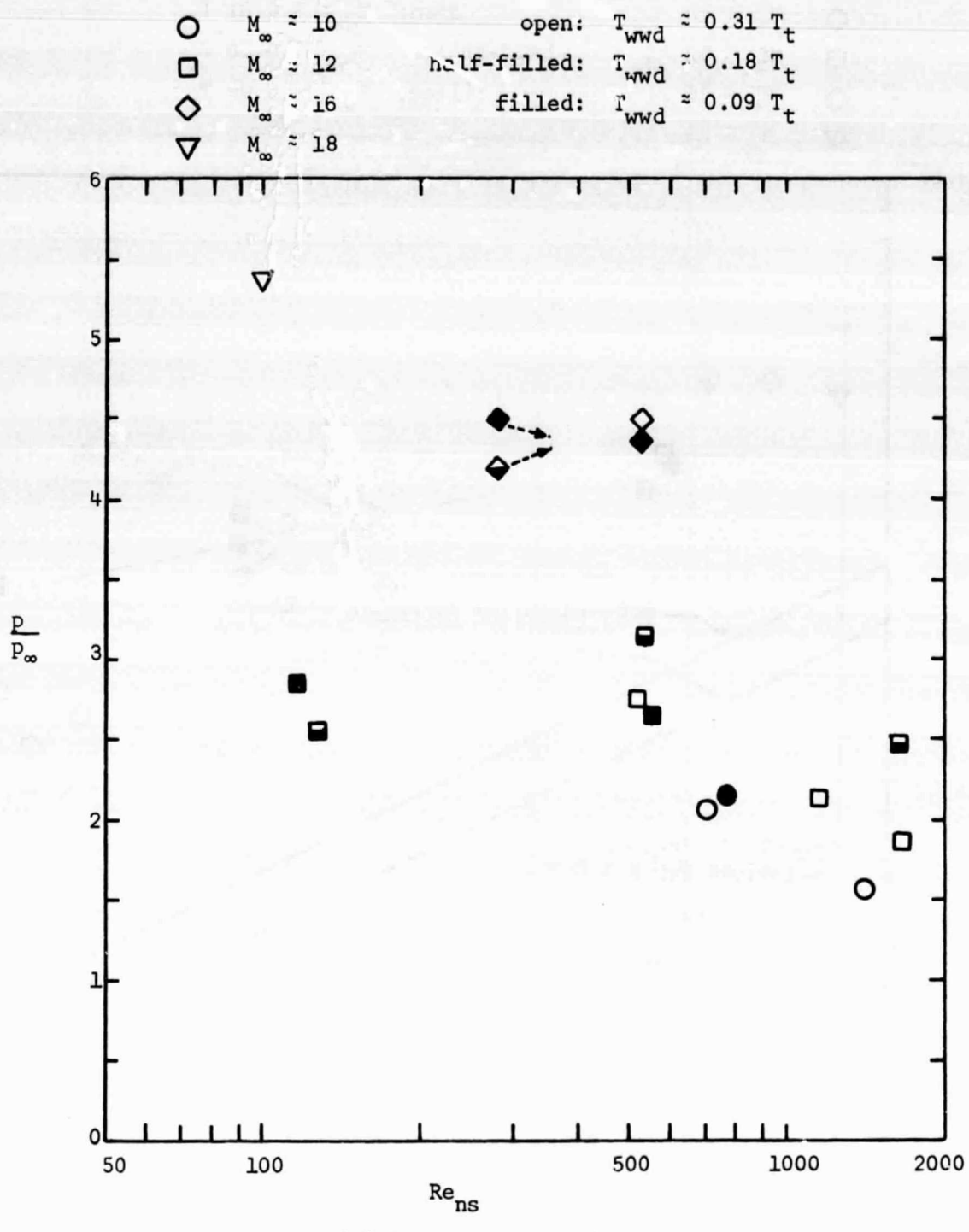

(a) The parameter p/p_∞

Figure 25. - The pressure measurements as a function of Reynolds number for an orifice on the nose upstream of the cockpit ($x = 0.110L$, $\phi = 0^o$).

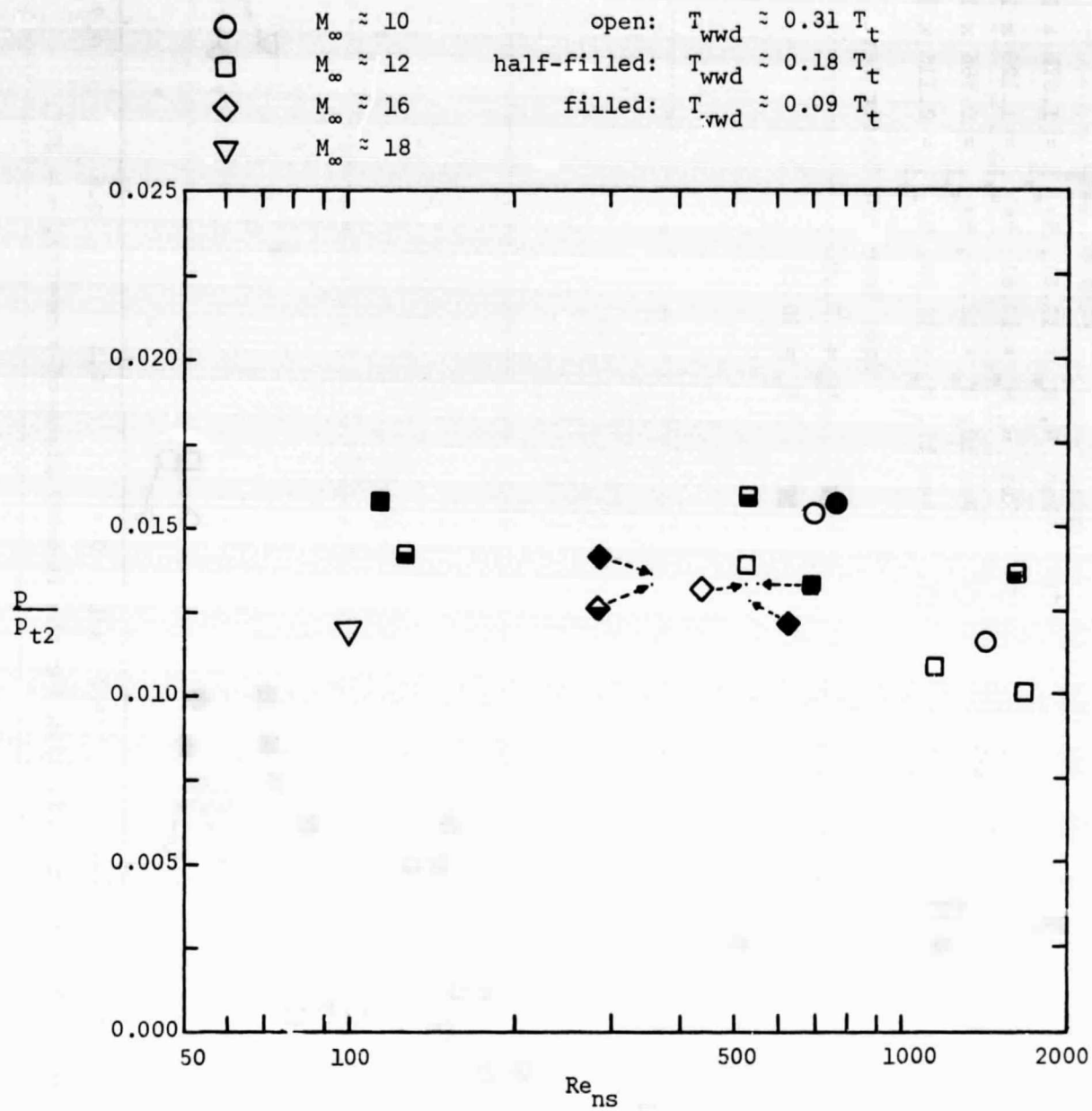

(b) The parameter p/p_{t2}

Figure 25. - Concluded.

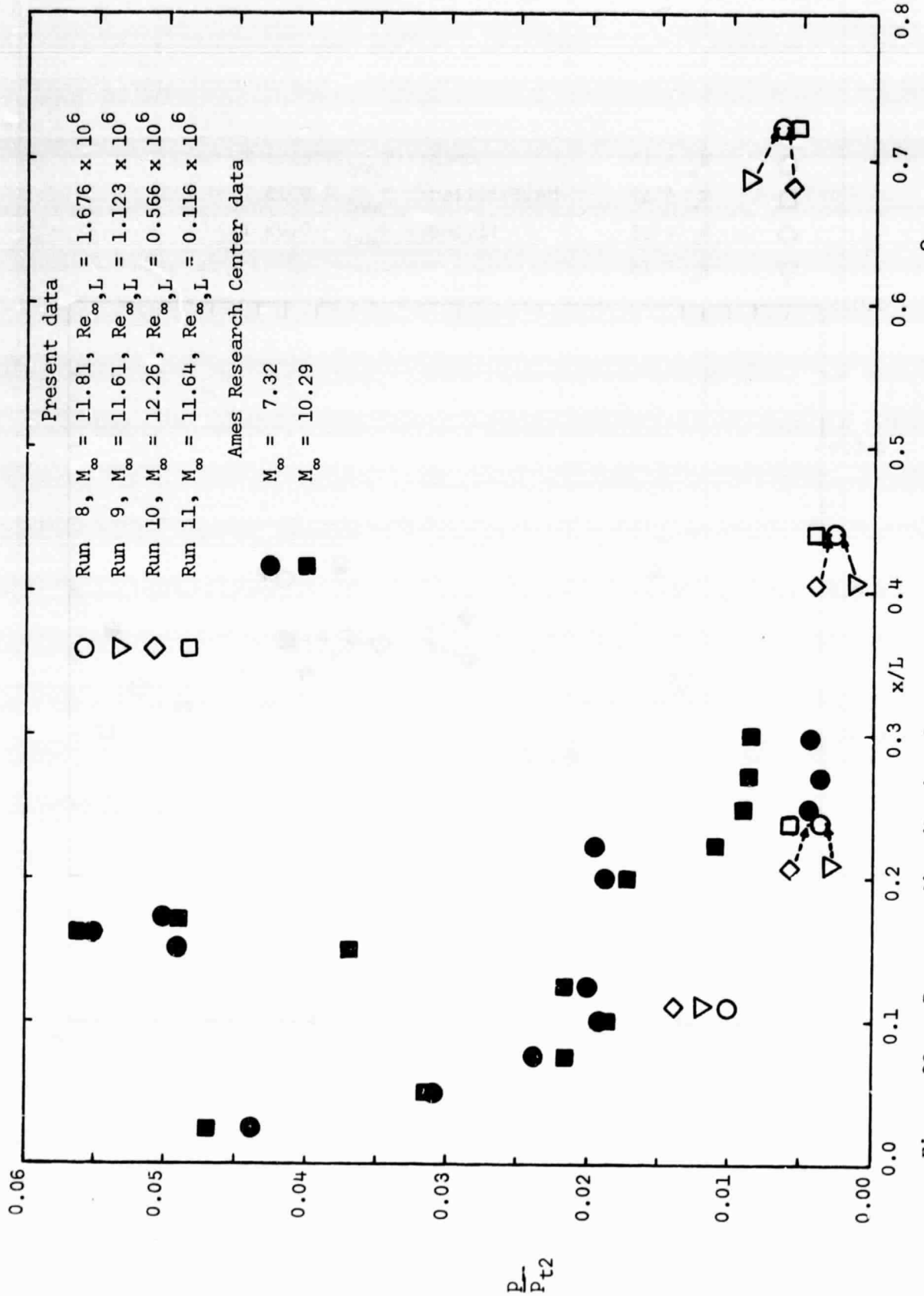

Figure 26. - Pressure distribution for the leeward plane-of-symmetry, $\alpha = 30^\circ$.

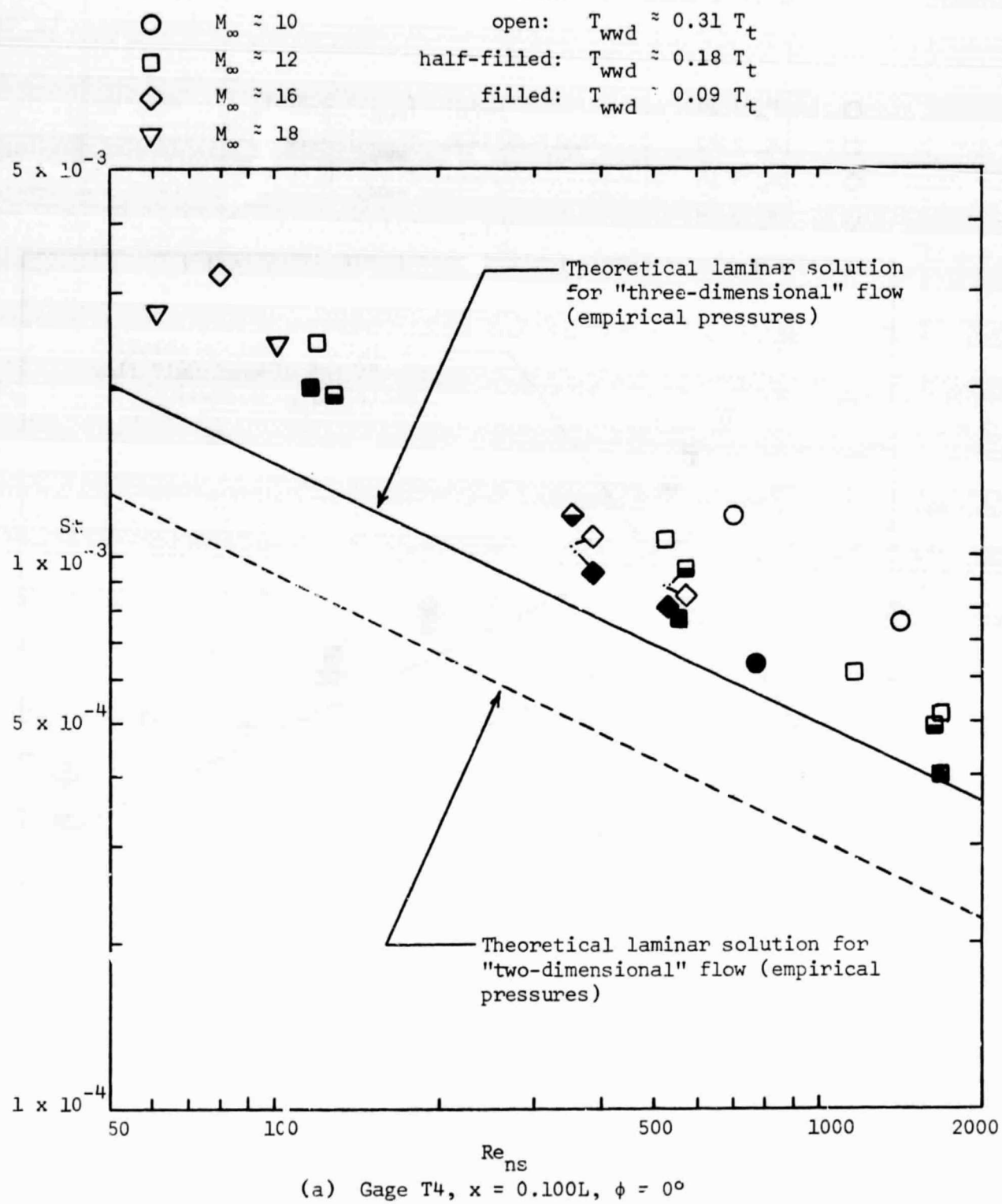

(a) Gage T4, x = 0.100L, ϕ = 0°

Figure 27. - The Stanton number as a function of the Reynolds number behind a normal shock wave for gages on the nose-region (upstream of the cockpit), α = 30°.

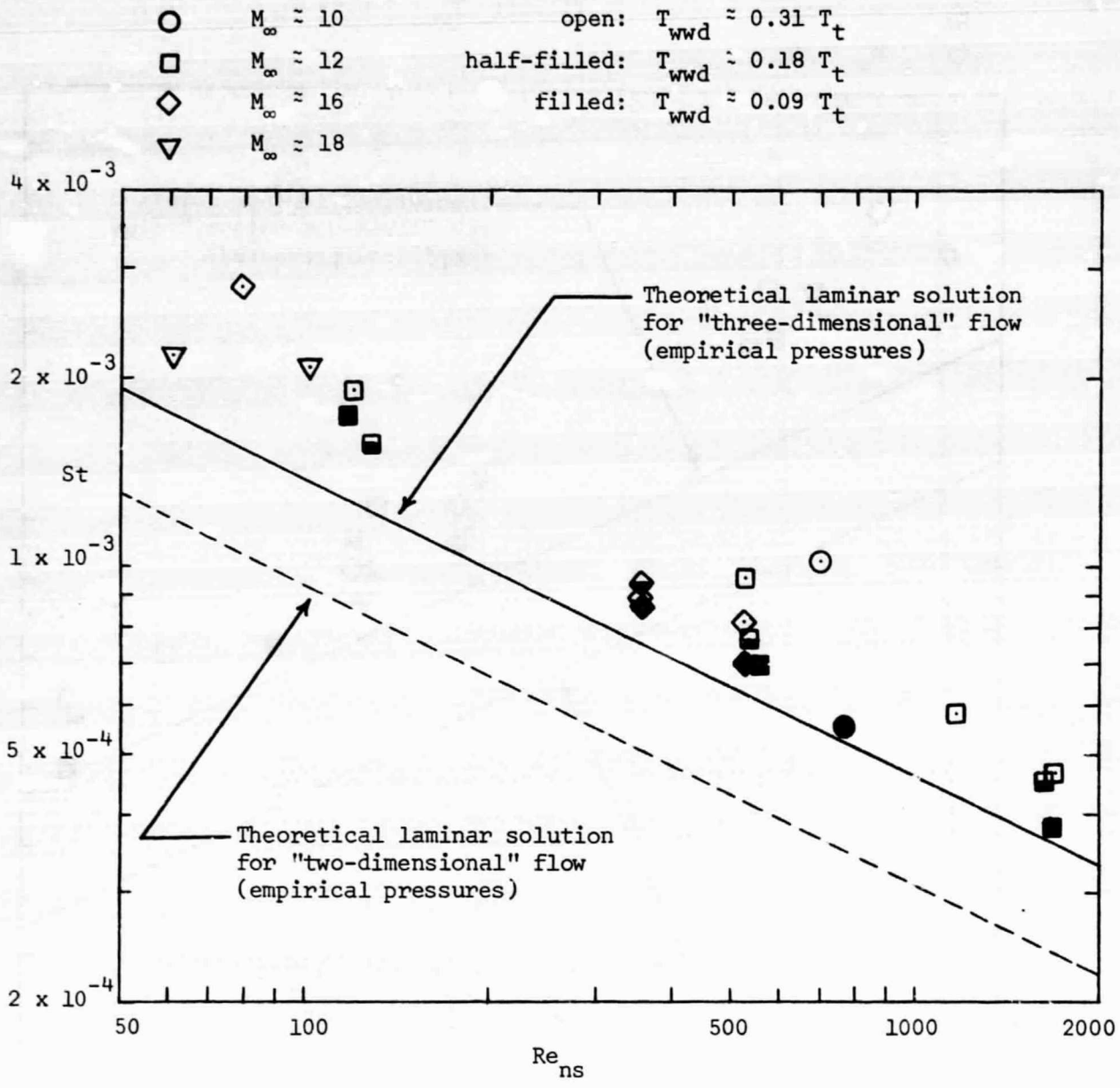

(b) Gage T8, x = 0.125L, ϕ = 0°.

Figure 27. - Concluded.

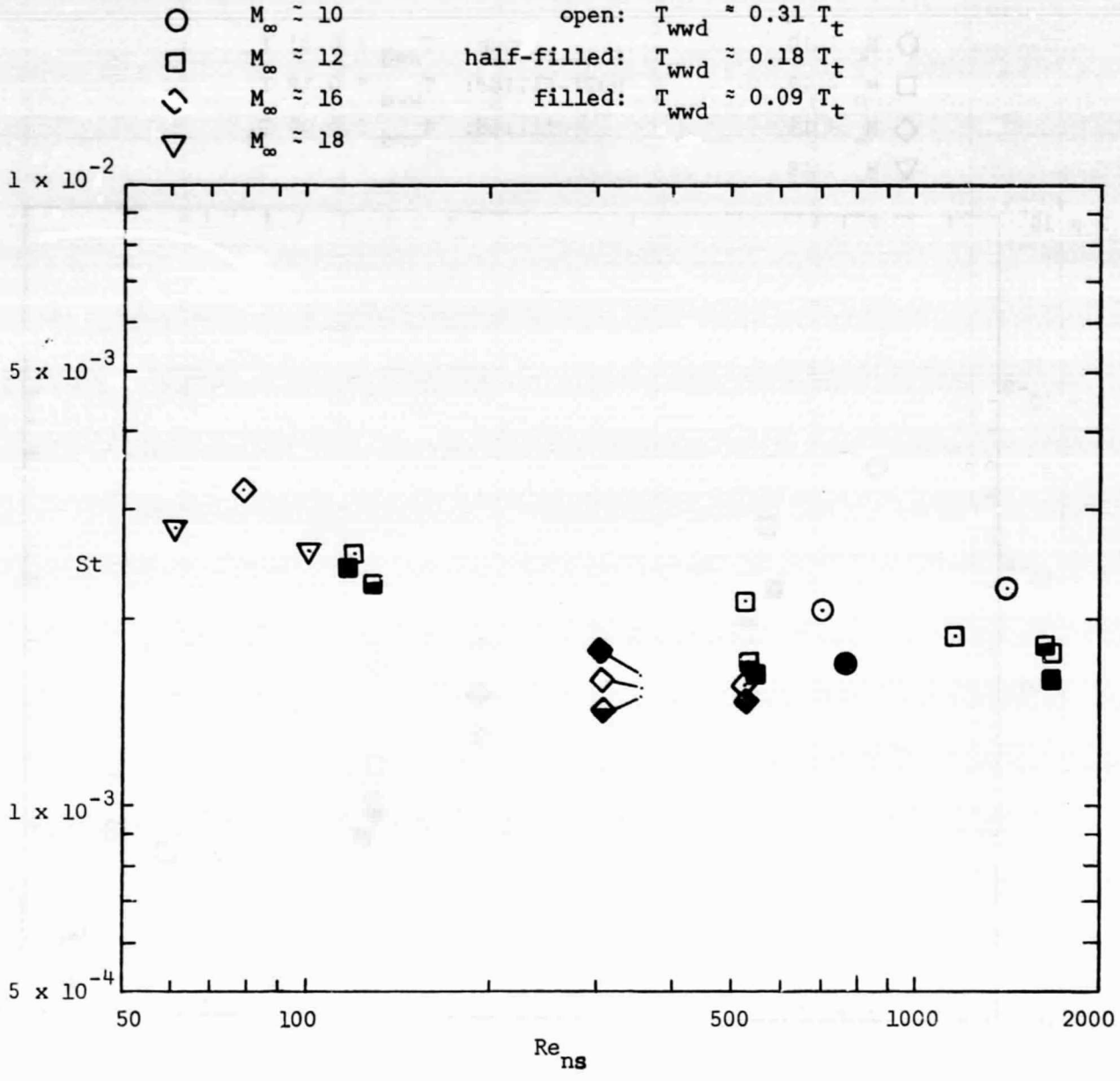

Gage T10, $x \simeq 0.160L$, $\phi = 0°$.

Figure 28. - The Stanton number as a function of the Reynolds number behind a normal shock wave for a gage on the cockpit windshield, $\alpha = 30°$.

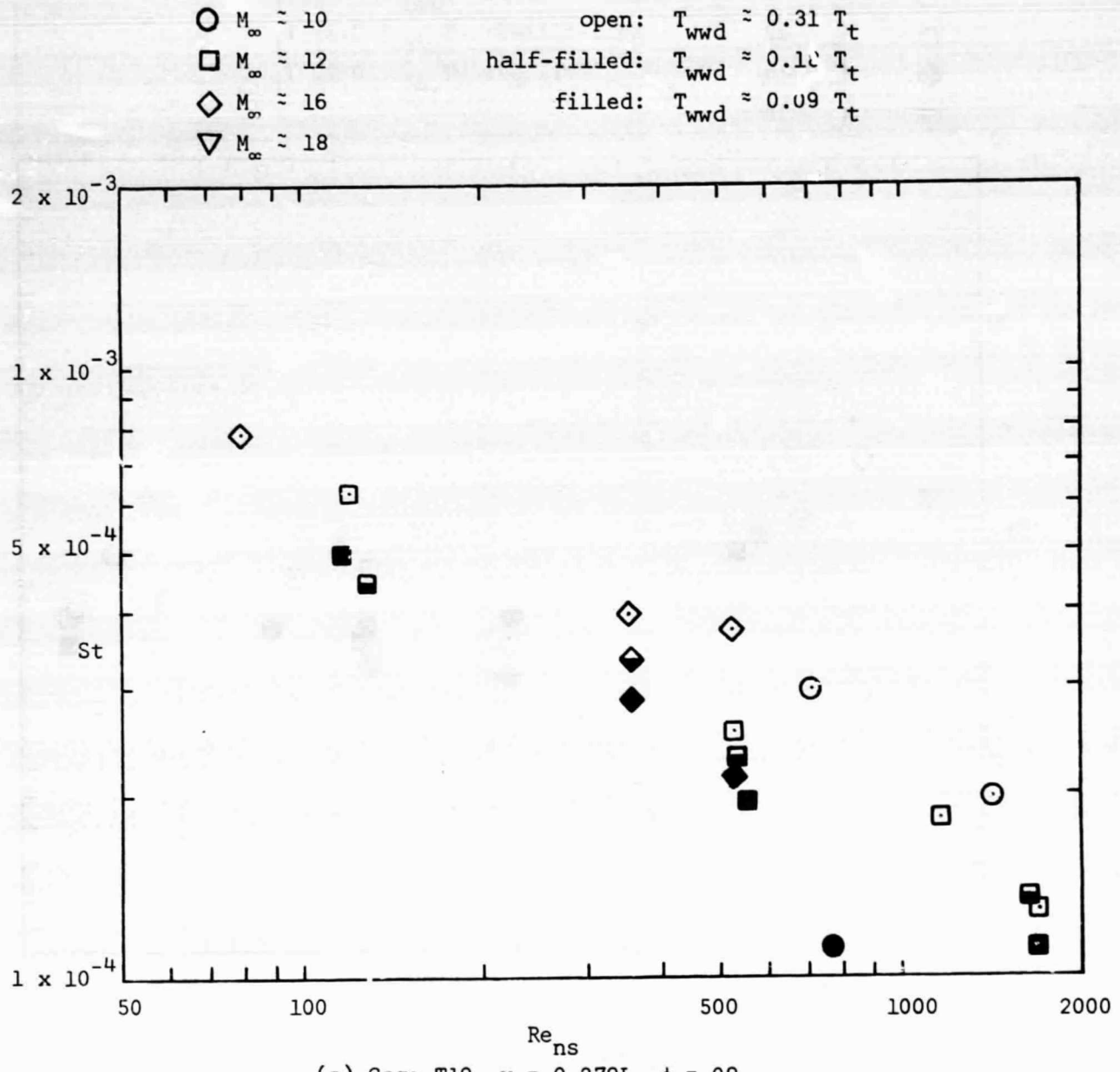

(a) Gage T19, x = 0.279L, $\phi = 0°$

Figure 29. - The Stanton number as a function of the Reynolds number behind a normal shock wave for gages aft of the cockpit where the shear layer was laminar, $\alpha = 30°$.

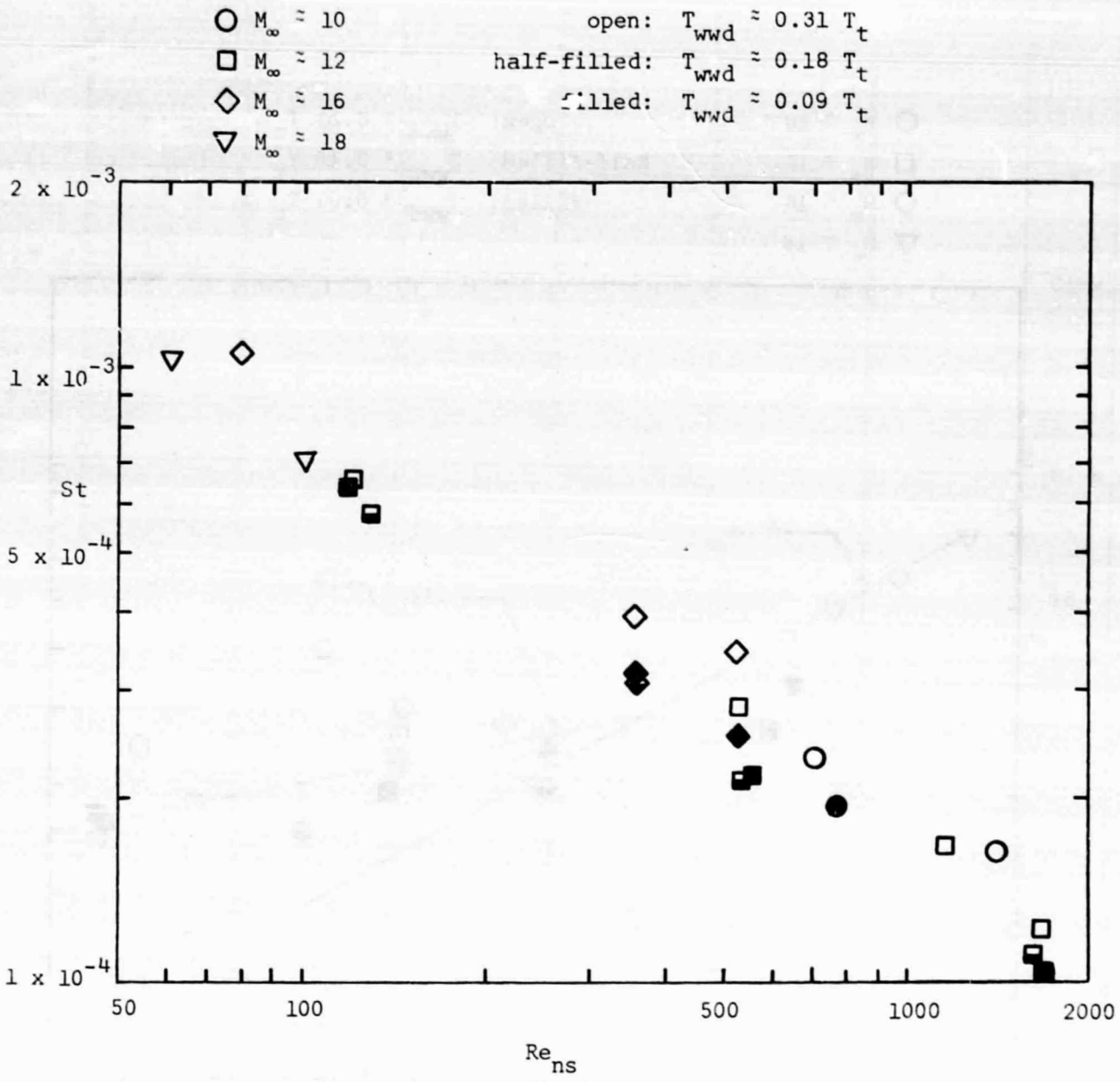

(b) Gage T21, x = 0.279L, ϕ = 44°.

Figure 29. - Concluded.

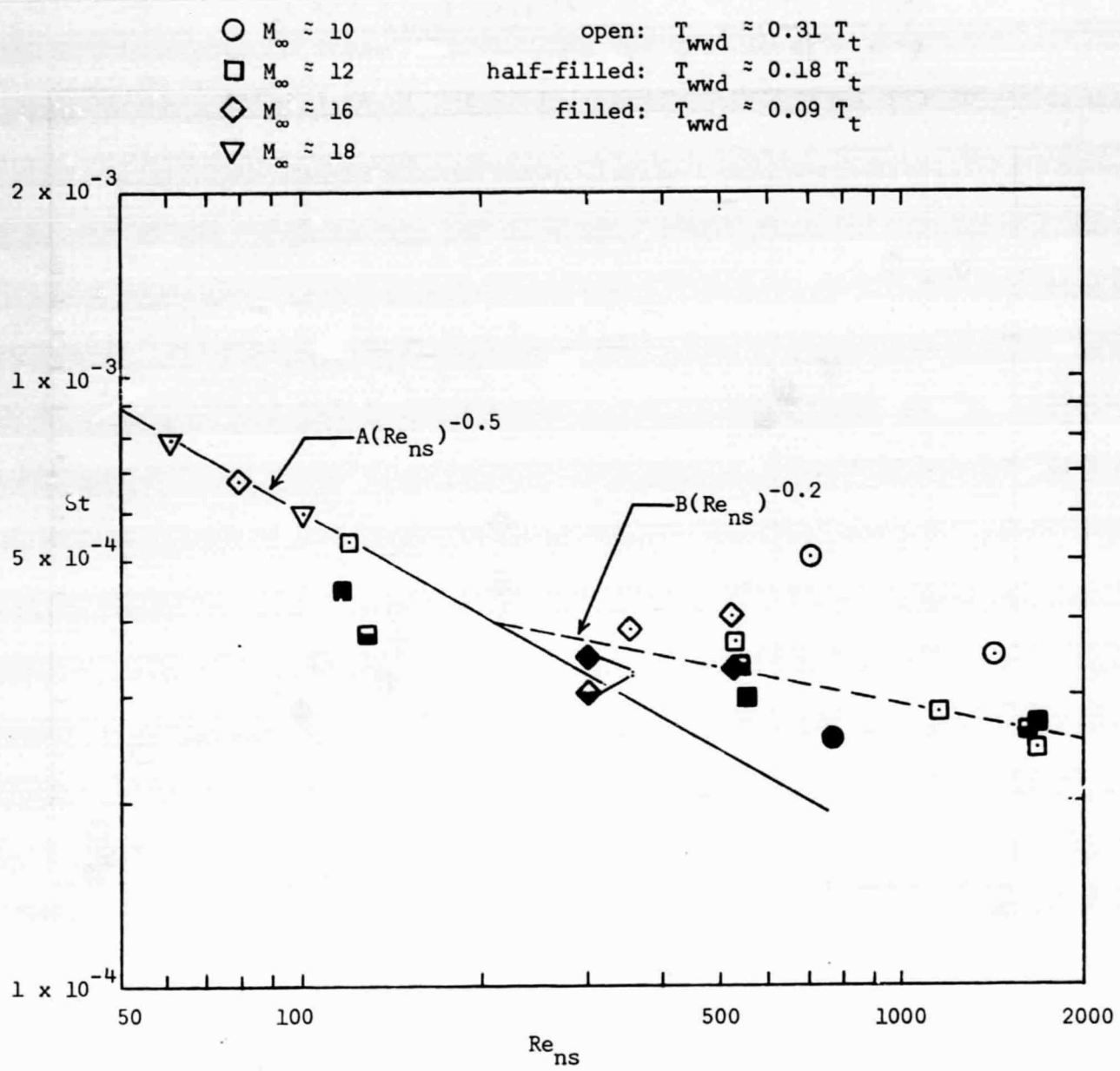

(a) Gage T29, $x = 0.420L$, $\phi = 0°$

Figure 30. - The Stanton number as a function of the Reynolds number behind a normal shock wave for gages aft of the cockpit where the shear layer was transitional, $\alpha = 30°$.

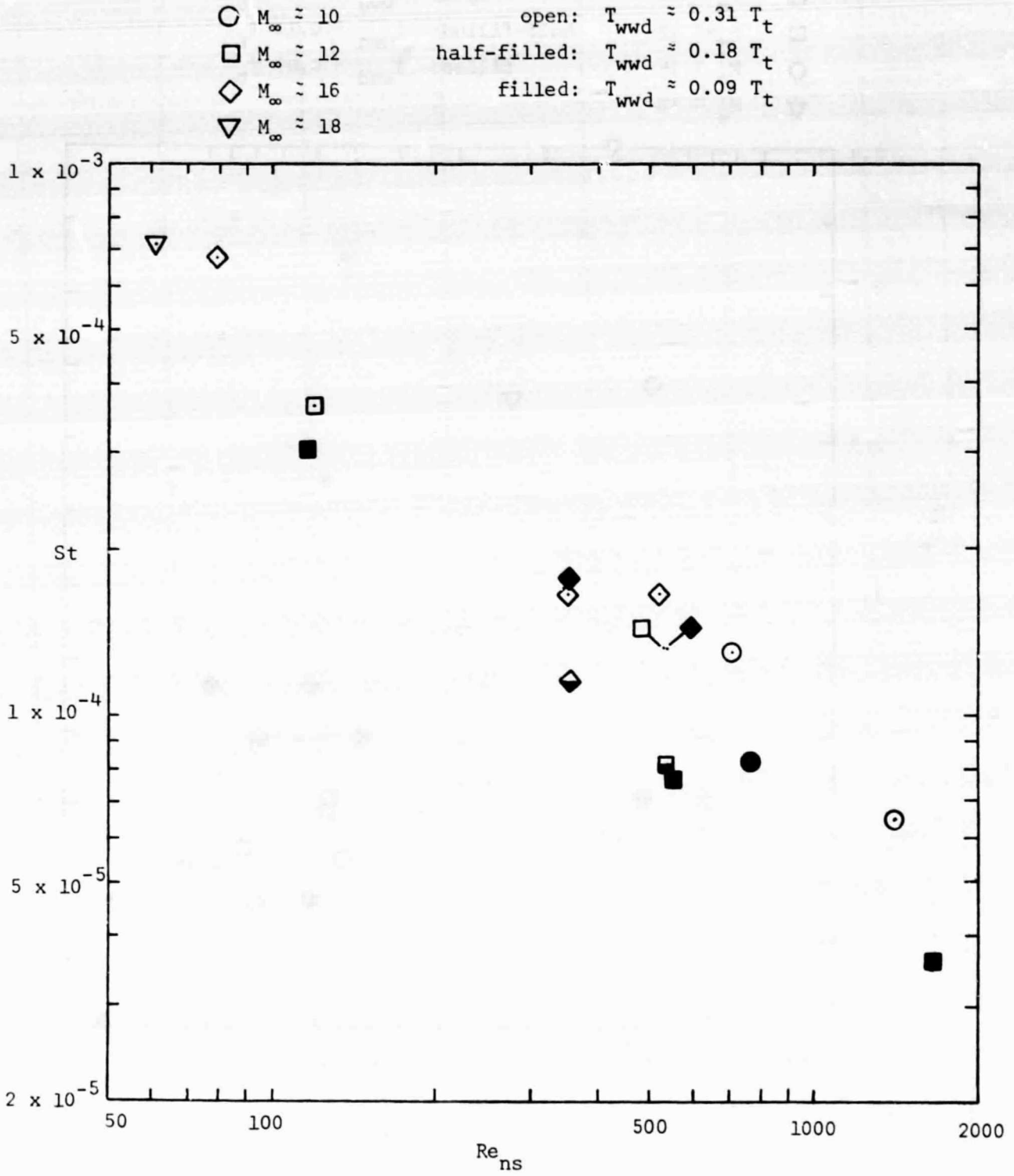

(b) Gage T31, x = 0.420L, ϕ = 40°

Figure 30. - Concluded.

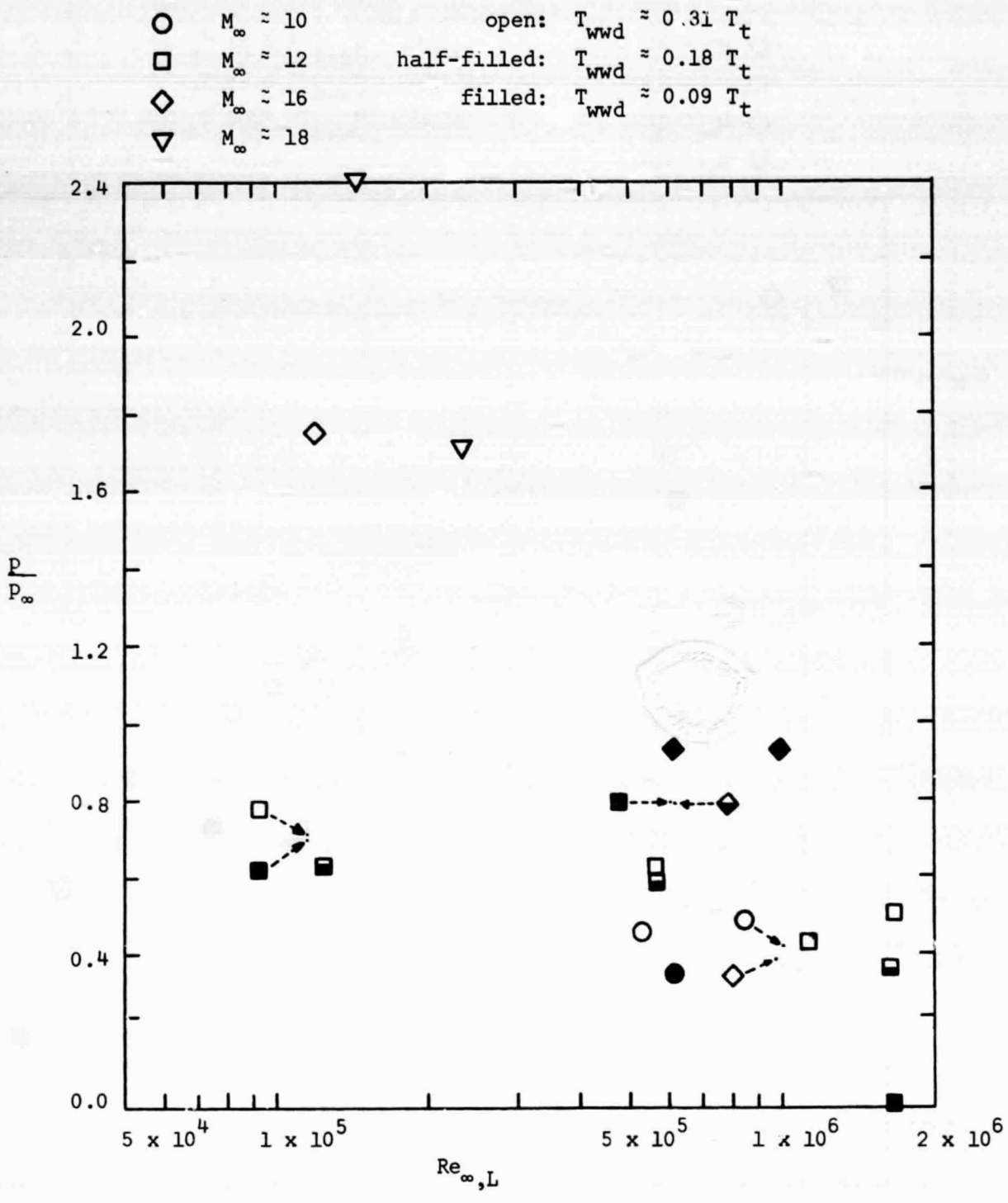

(a) p/p_∞ as a function of $Re_{\infty,L}$

Figure 31. - The pressure measurements as a function of Reynolds number for PS4, x = 0.440L, ϕ = 0°, α = 30°.

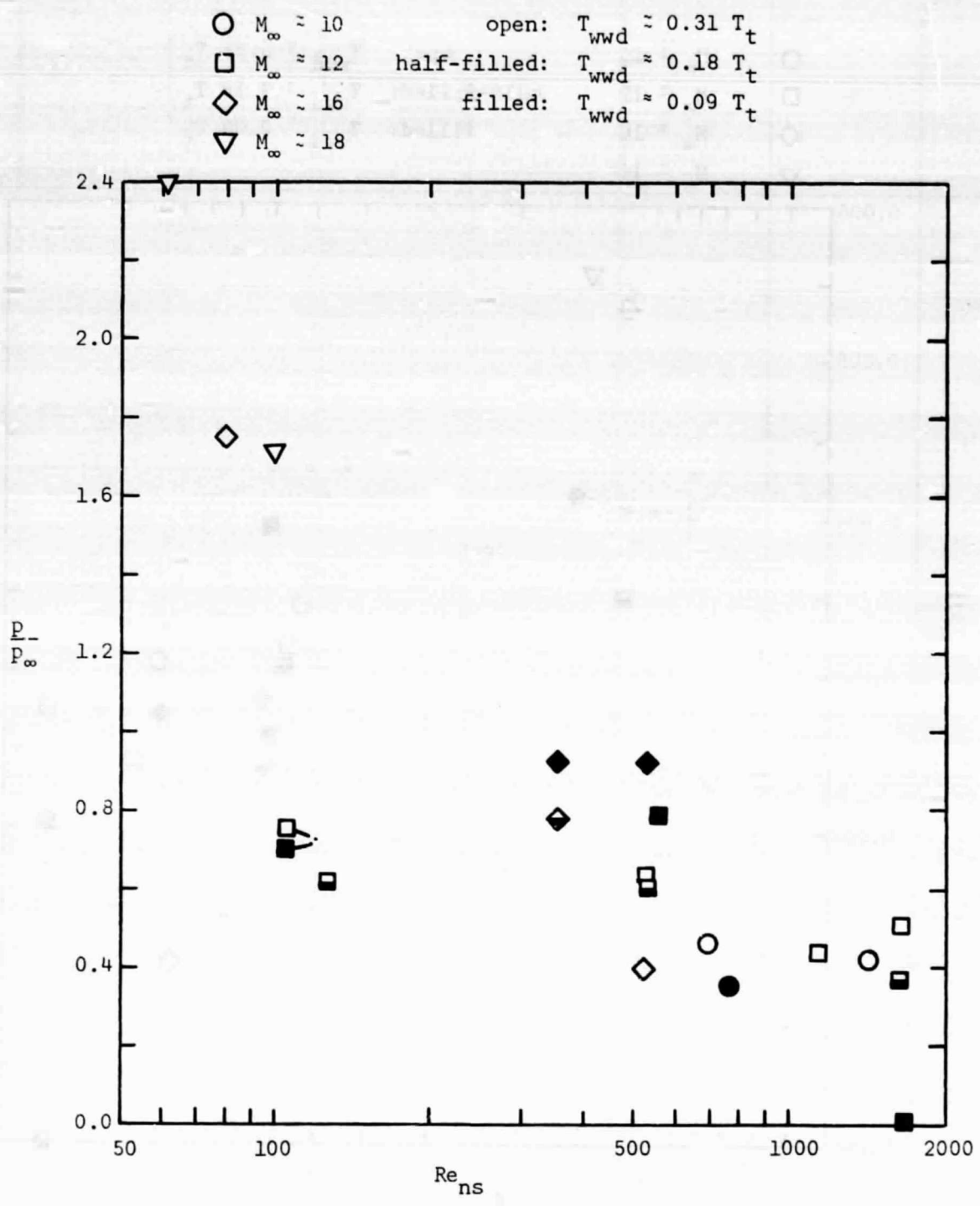

(b) p/p_∞ as a function of Re_{ns}

Figure 31. - Continued

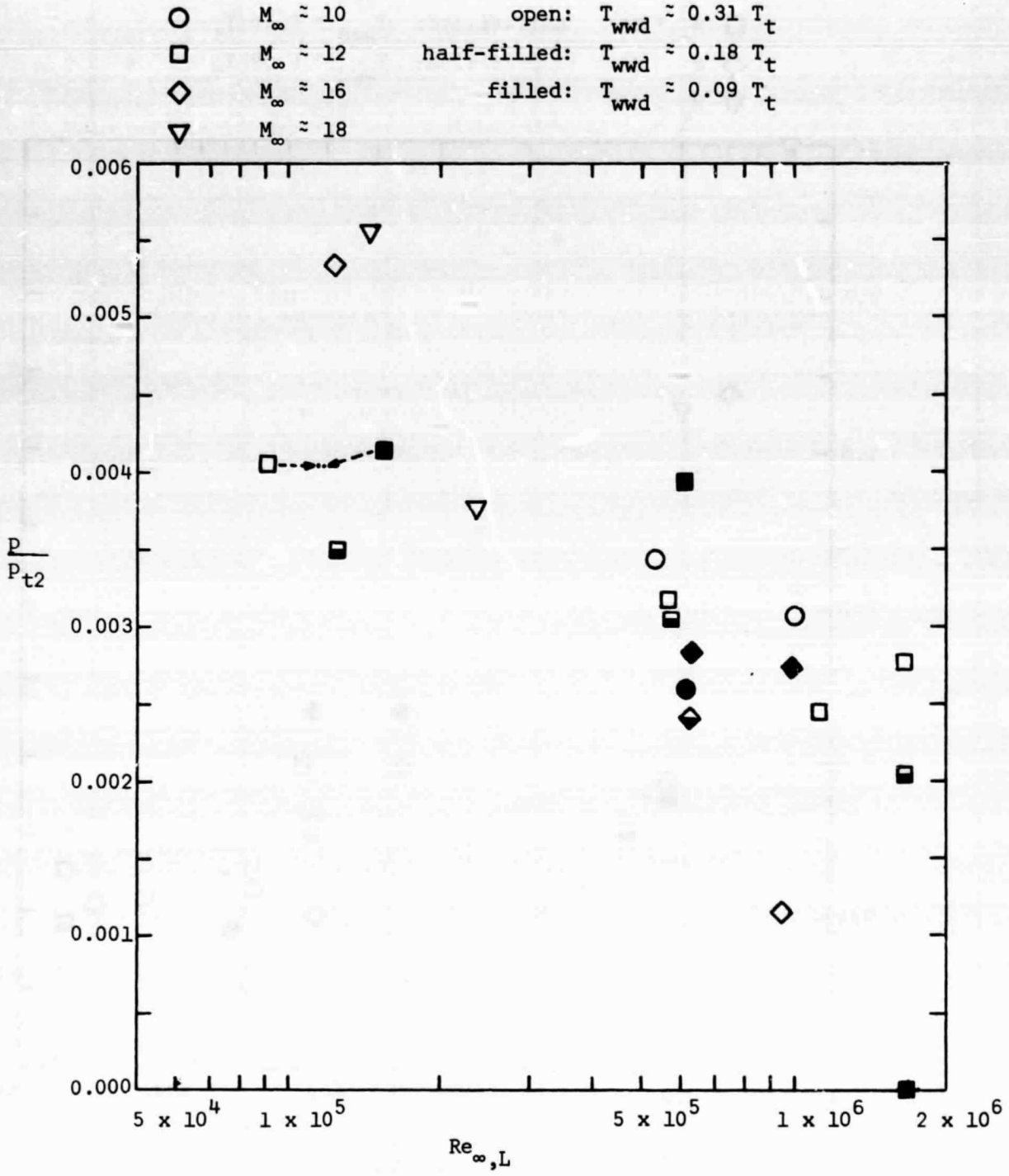

(c) p/p_{t2} as a function of $Re_{\infty,L}$

Figure 31. - Continued.

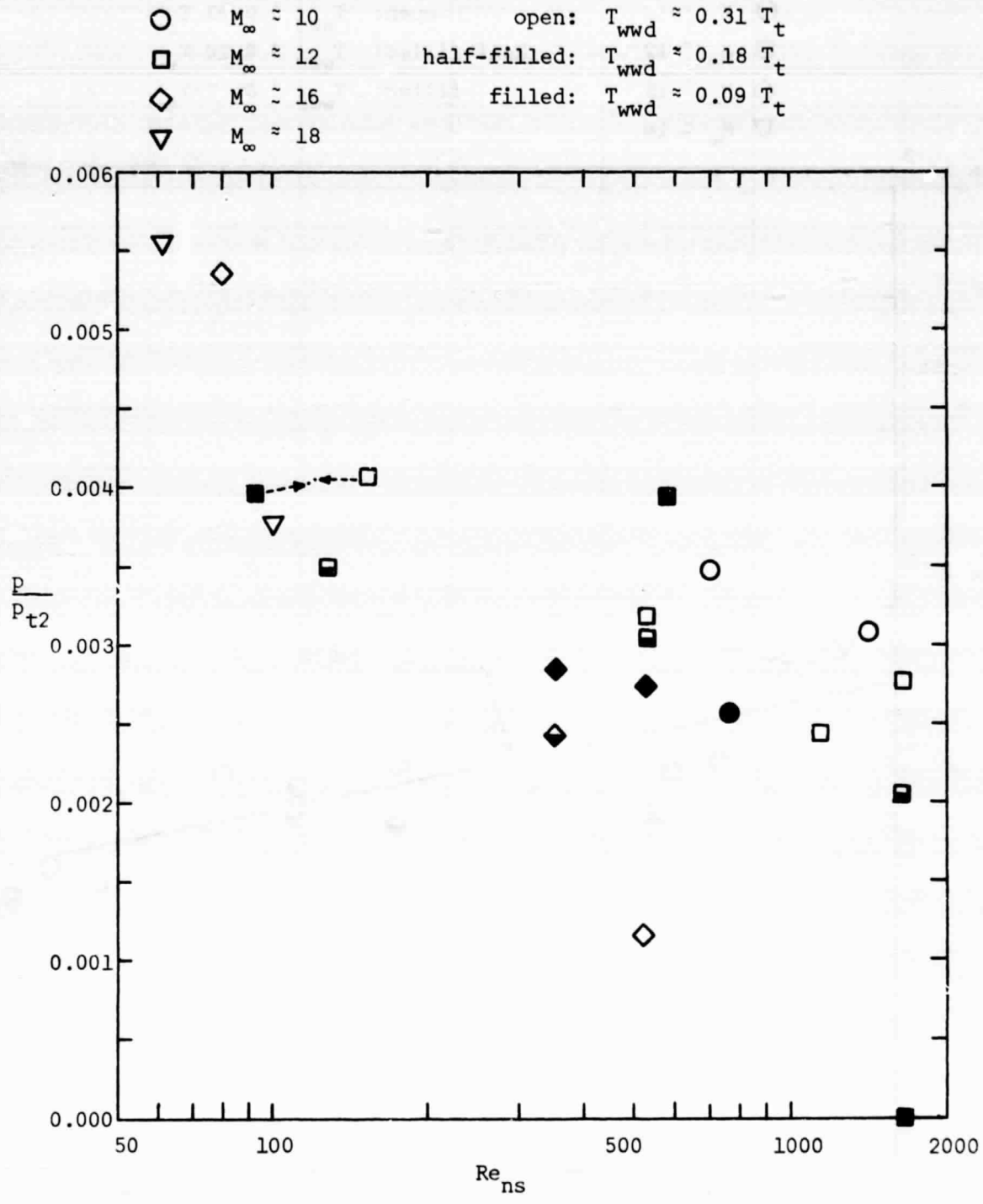

(d) p/p_{t2} as a function of Re_{ns}

Figure 31. - Concluded.

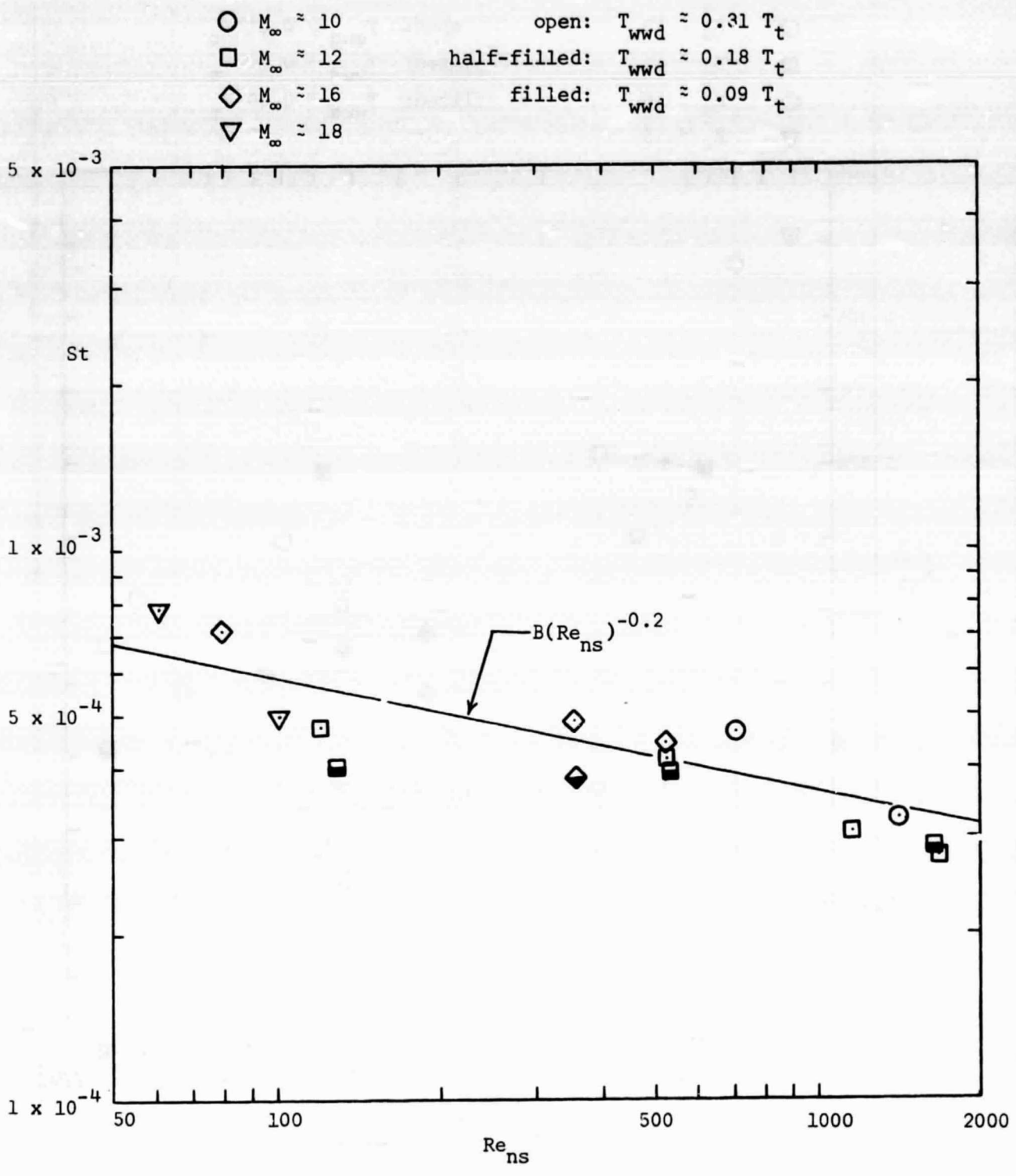

(a) Gage T37, x = 0.600L, ϕ = 0°

Figure 32. - The Stanton number as a function of the Reynolds number behind a normal shock wave for gages aft of the cockpit where the shear layer was turbulent, α = 30°.

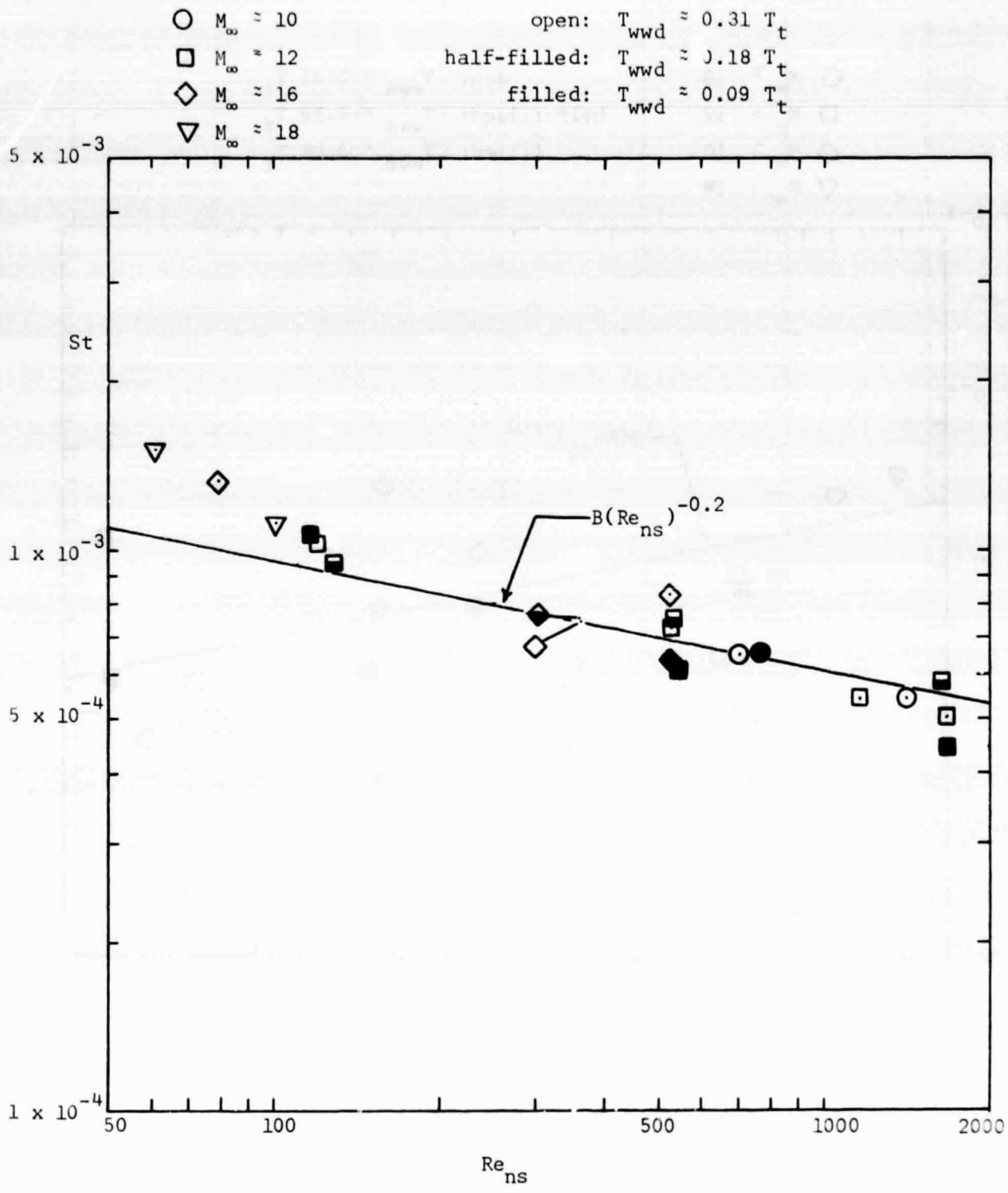

(b) Gage T39, x = 0.600L, ϕ = 56°

Figure 32. - Continued.

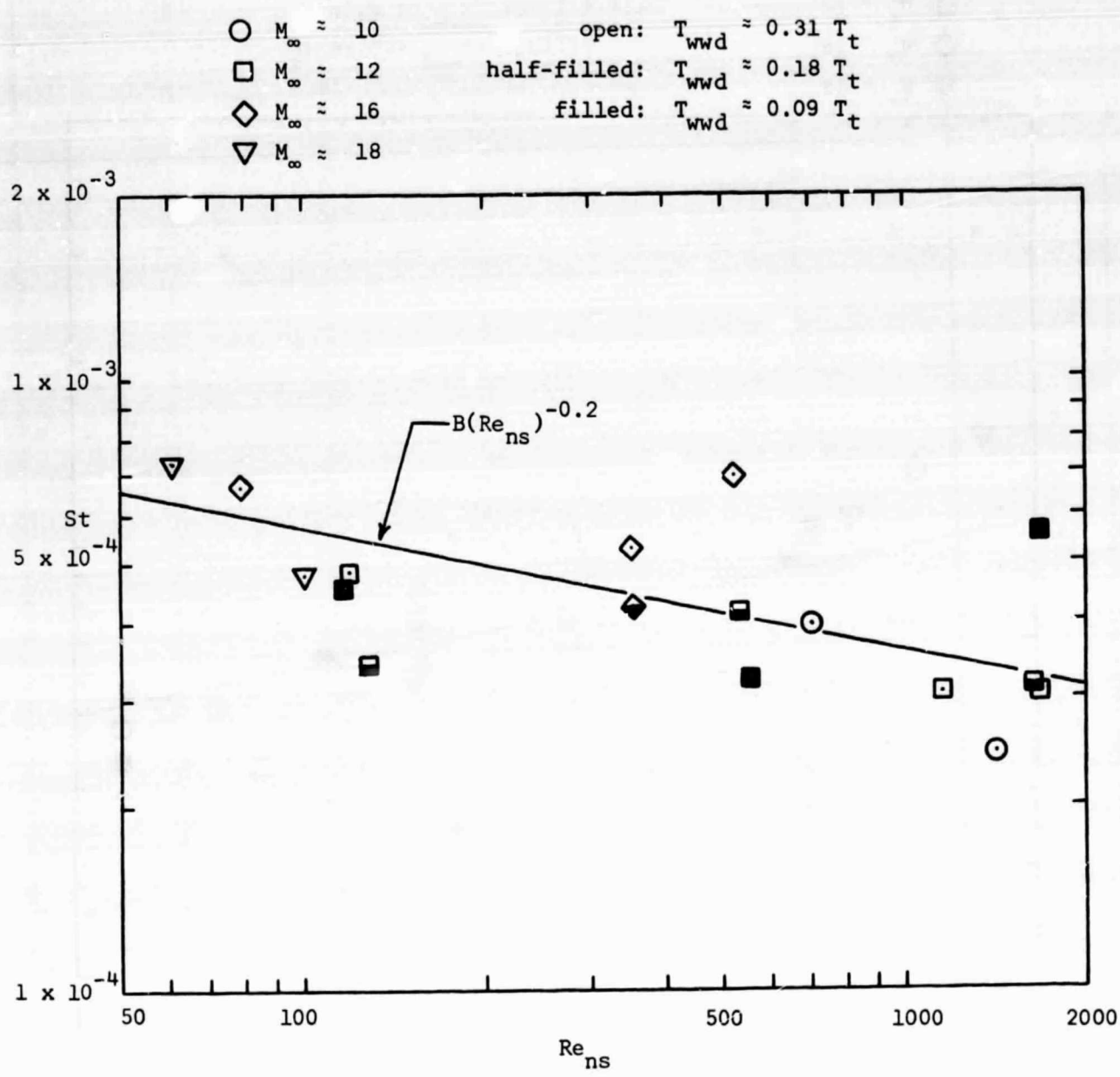

(c) Gage T41, x = 0.700L, ϕ = 0°

Figure 32. - Concluded.

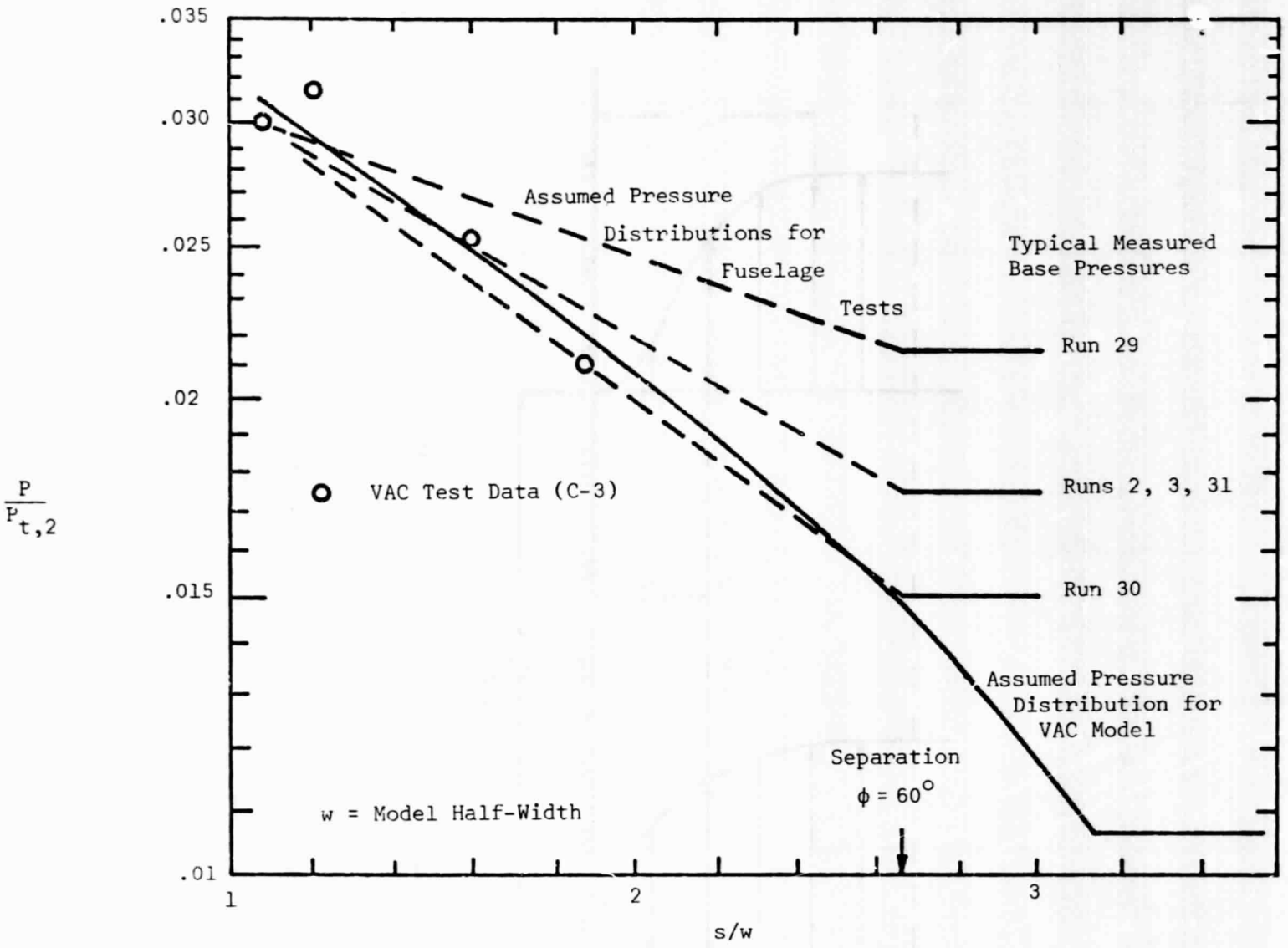

Figure 33. - Surface pressure distributions utilized in laminar boundary layer calculation for fuselage tests.

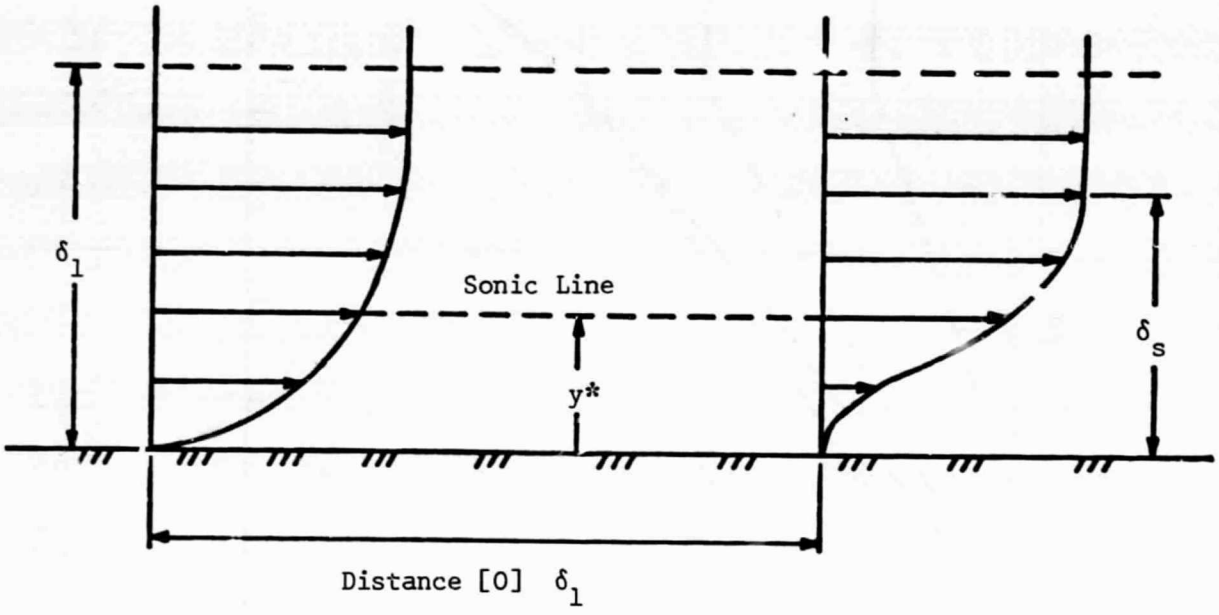

Figure 34. - Schematic representation of boundary layer separation illustrating the change in effective thickness of the layer.

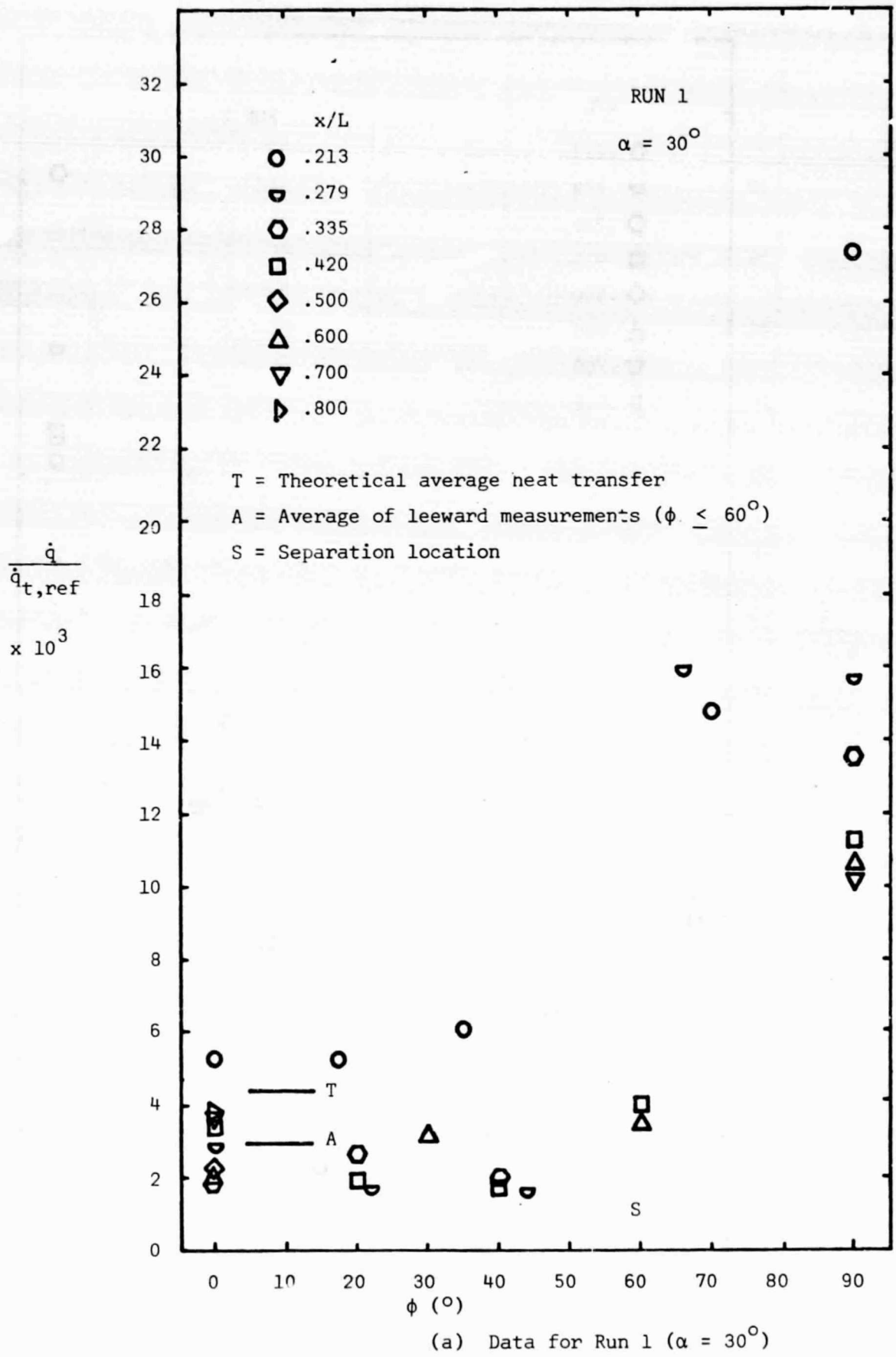

(a) Data for Run 1 (α = 30°)

Figure 35. - Circumferential distributions of heat transfer for fuselage tests and comparison with theoretical predictions.

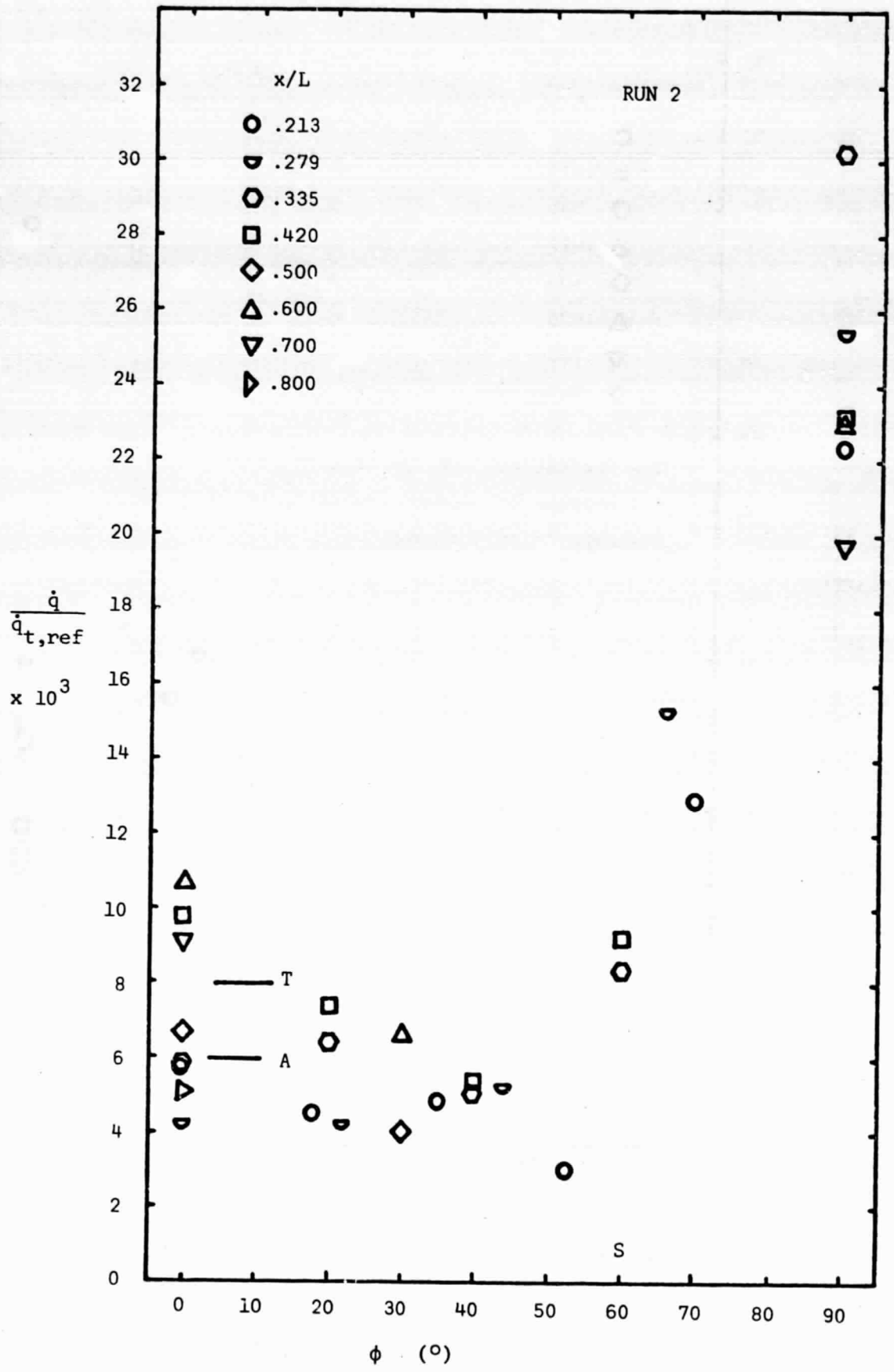

(b) Data for Run 2 ($\alpha = 90^{\circ}$)

Figure 35. - Continued.

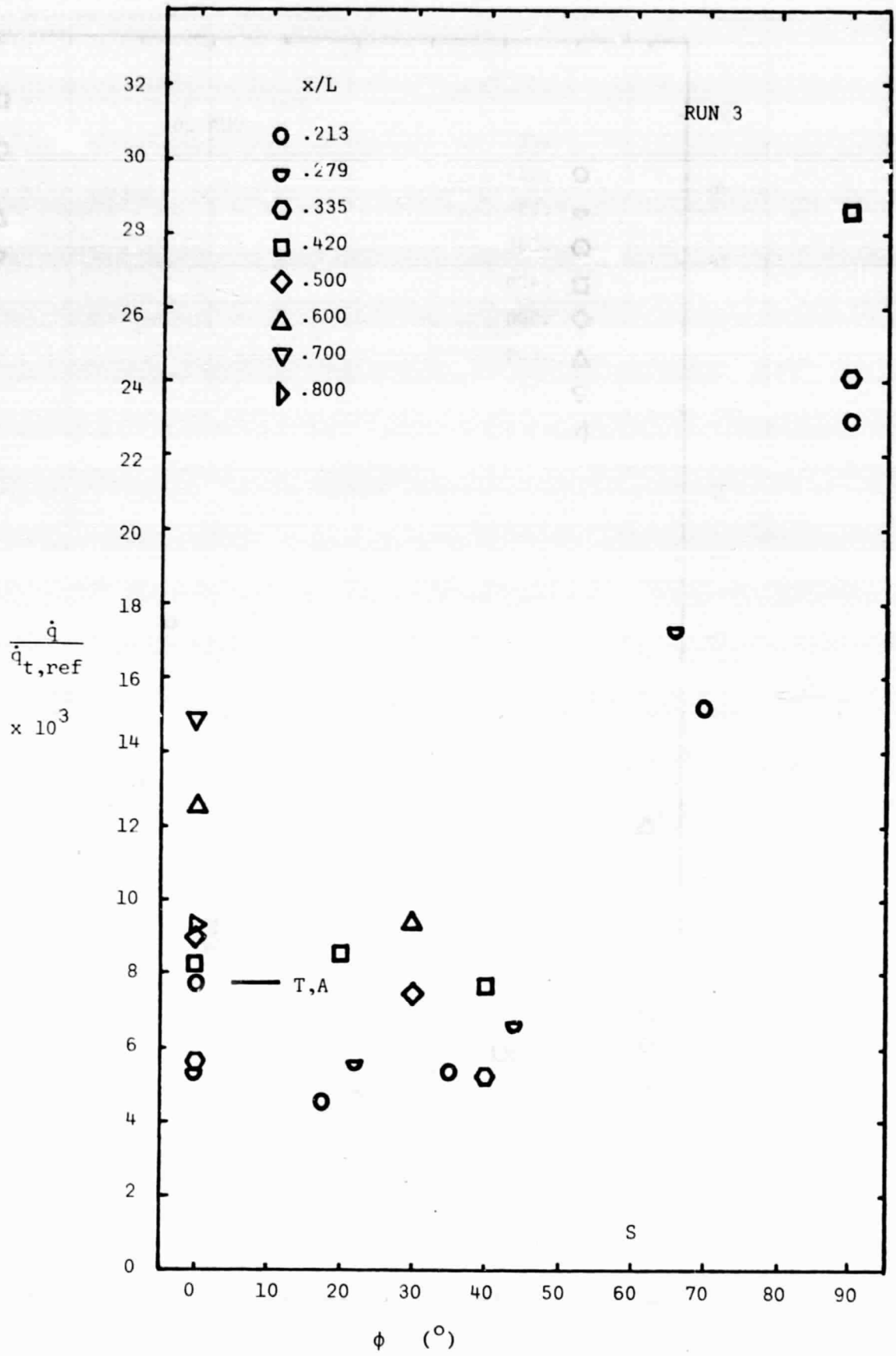

(c) Data for Run 3 ($\alpha = 90^\circ$)

Figure 35. - Continued

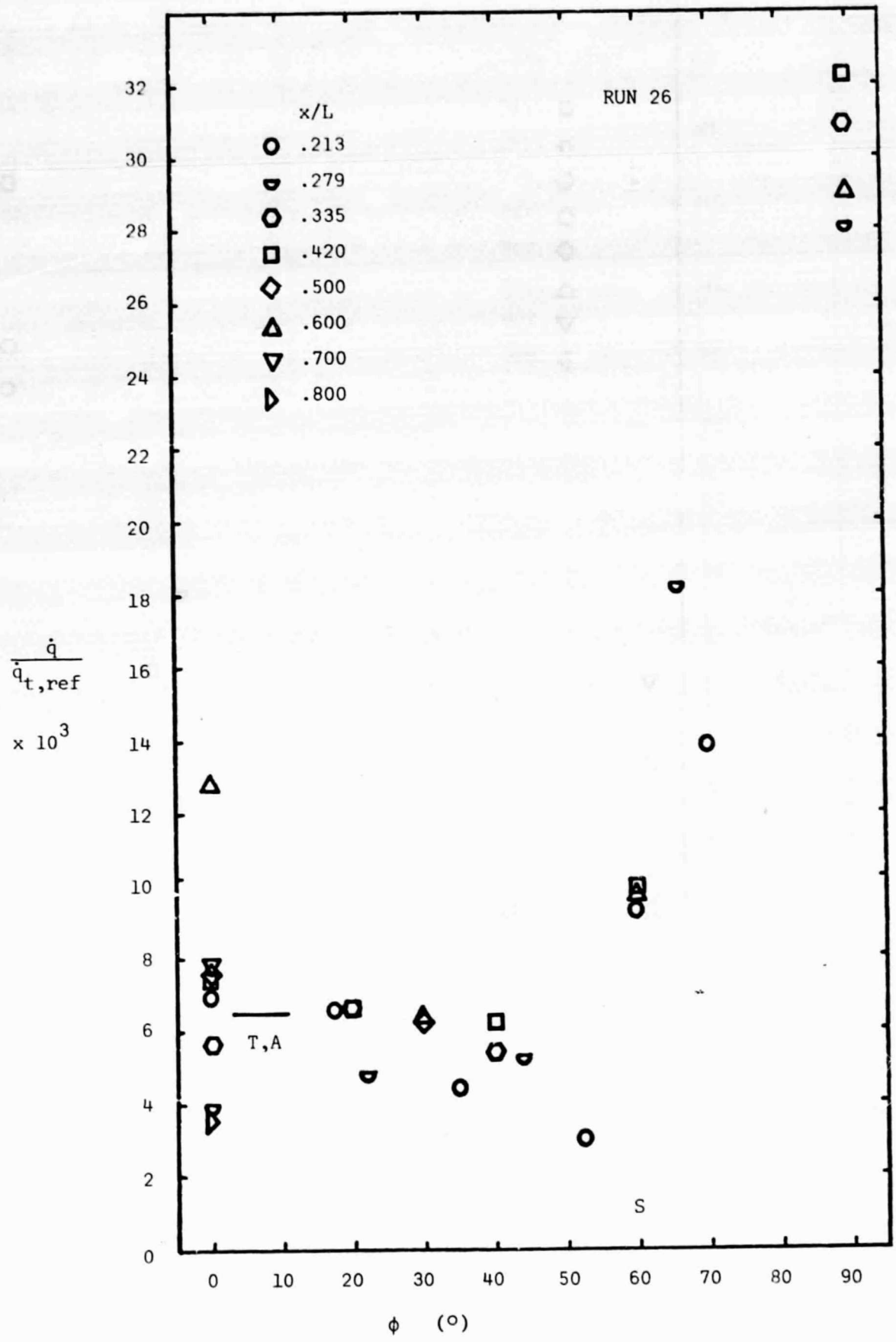

(d) Data for Run 26 ($\alpha = 90^{\circ}$)

Figure 35. - Continued.

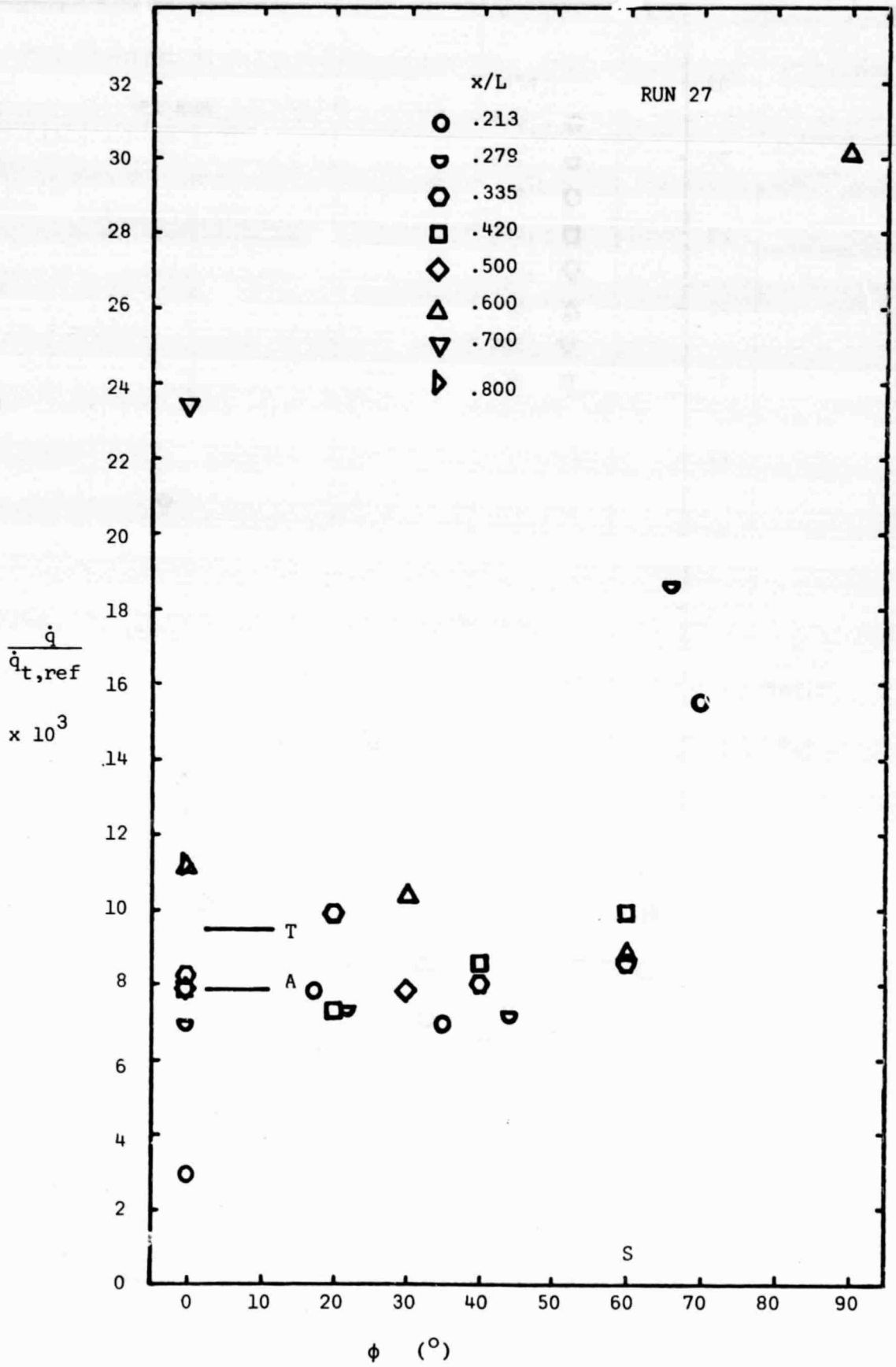

(e) Data for Run 27 ($\alpha = 90^{\circ}$)

Figure 35. - Continued

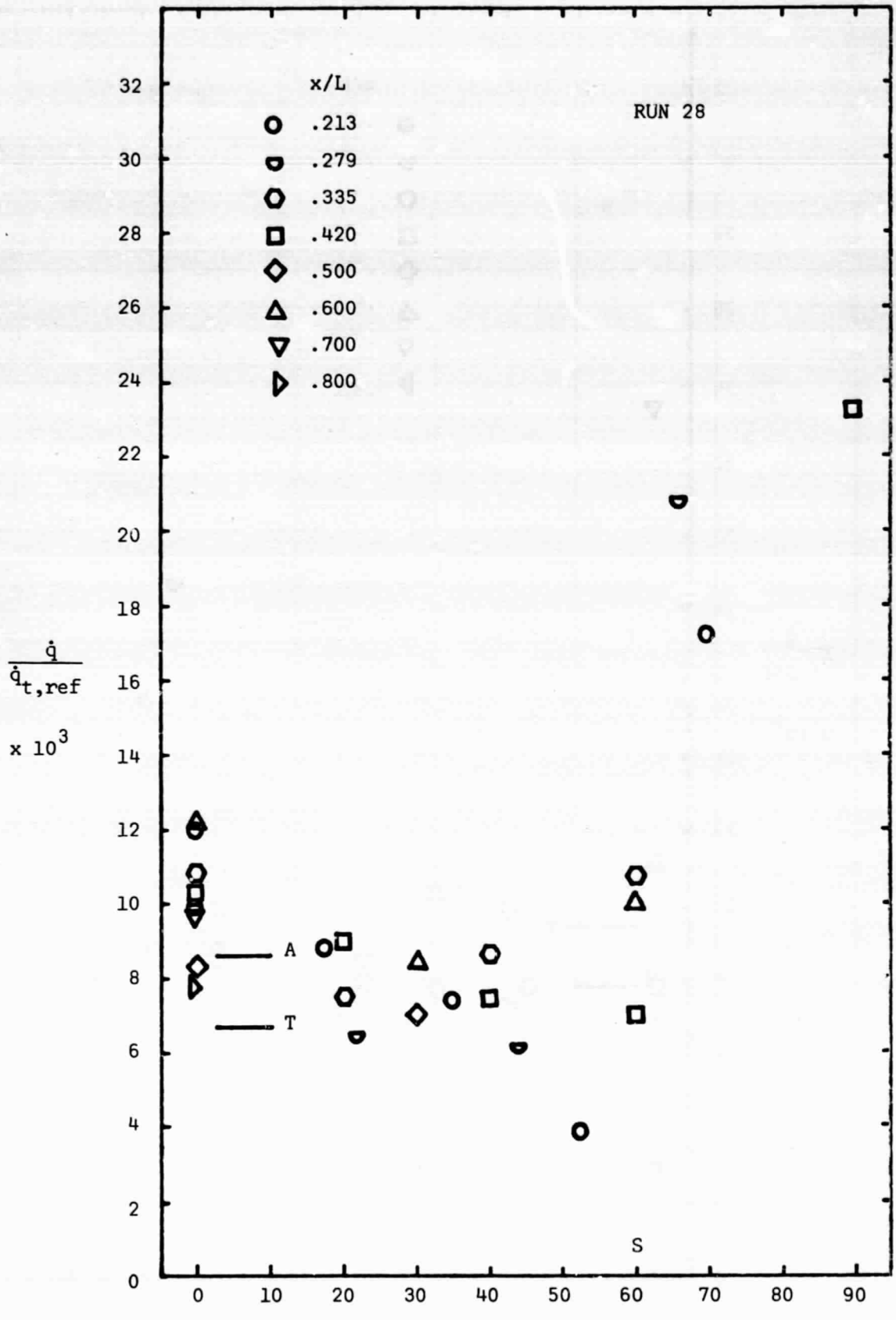

(f) Data for Run 28 ($\alpha = 90^\circ$)

Figure 35. - Continued.

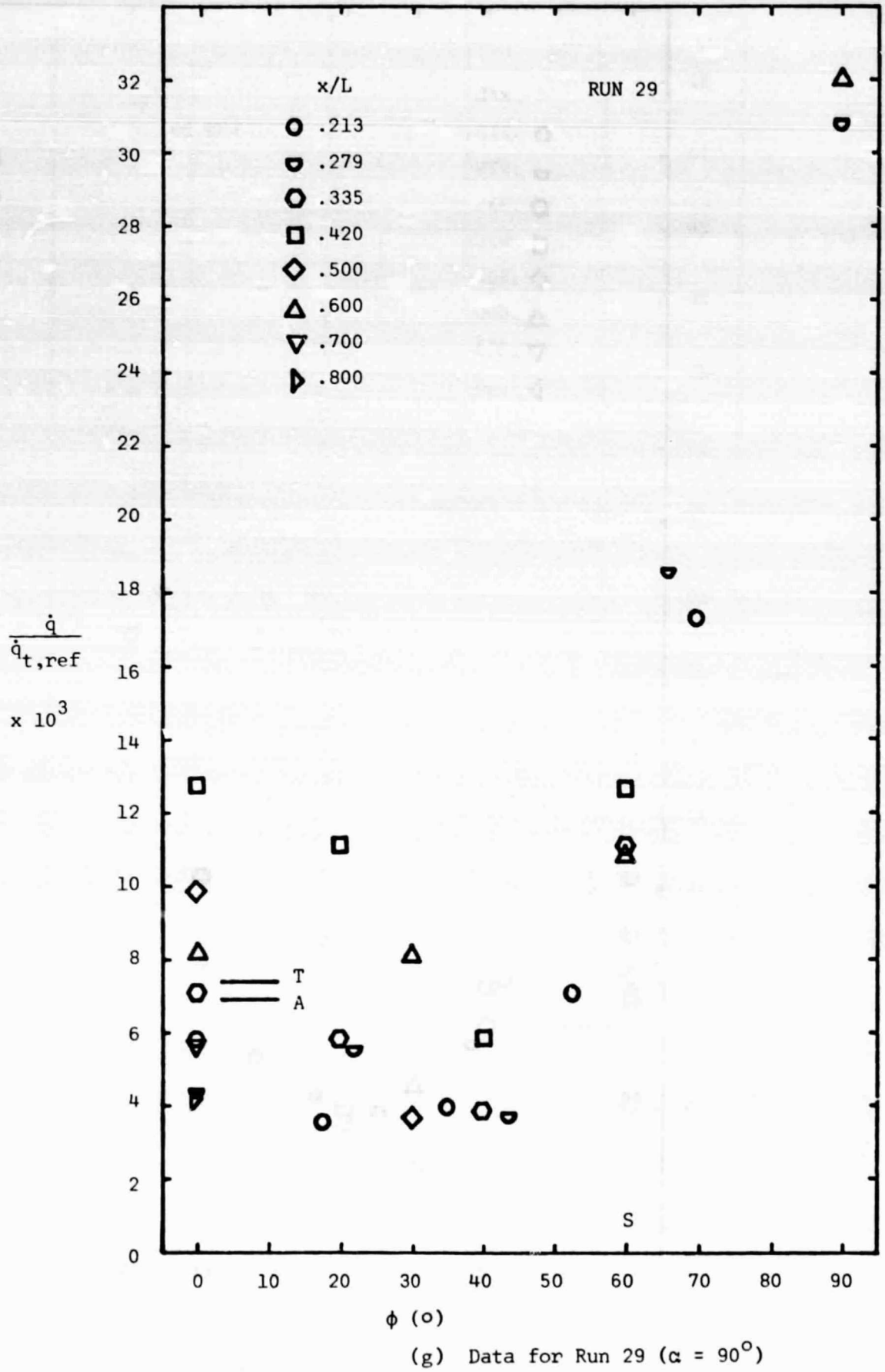

(g) Data for Run 29 ($\alpha = 90^o$)

Figure 35. - Continued.

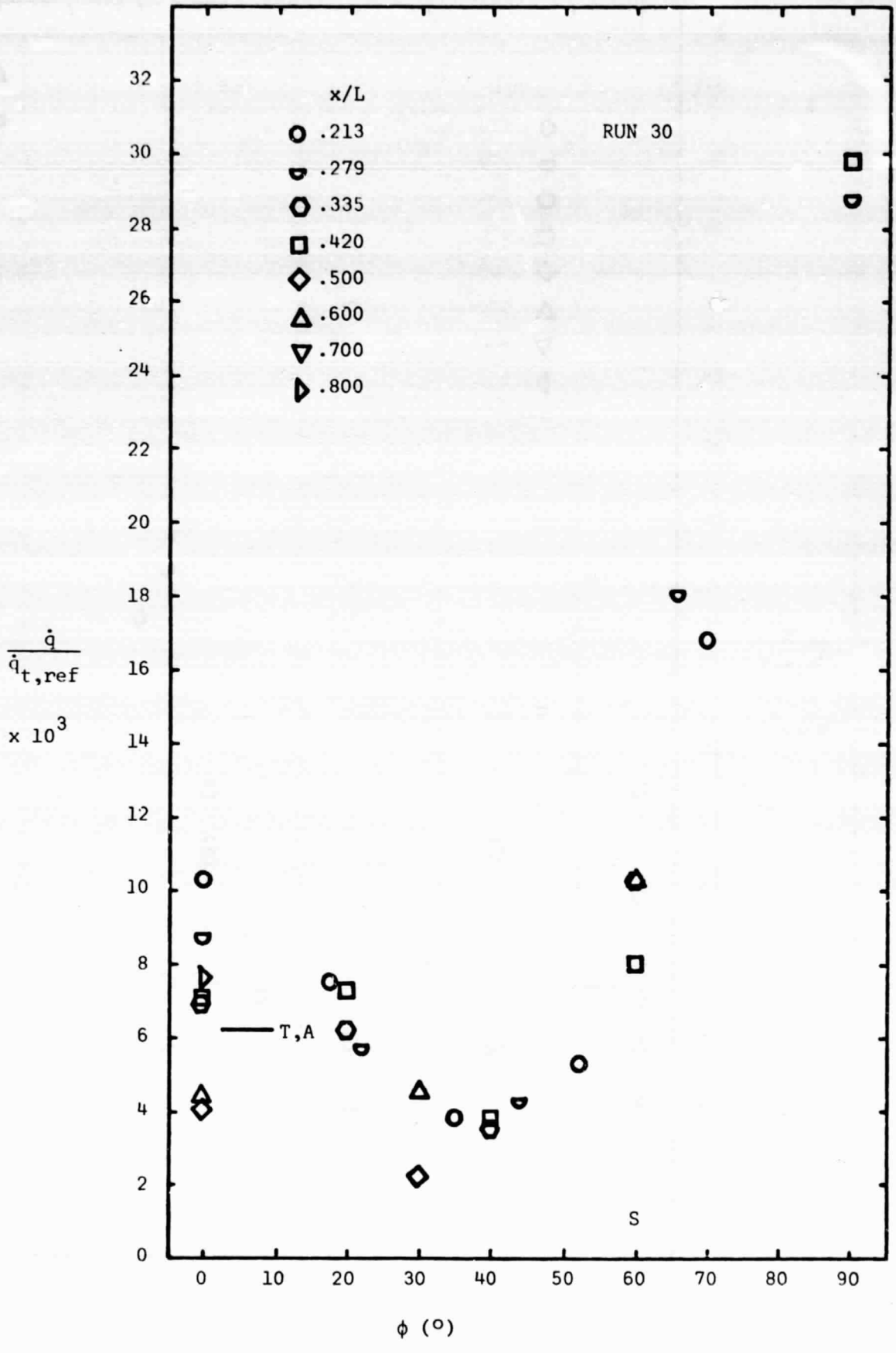

(h) Data for Run 30 ($\alpha = 90^\circ$)

Figure 35. - Continued.

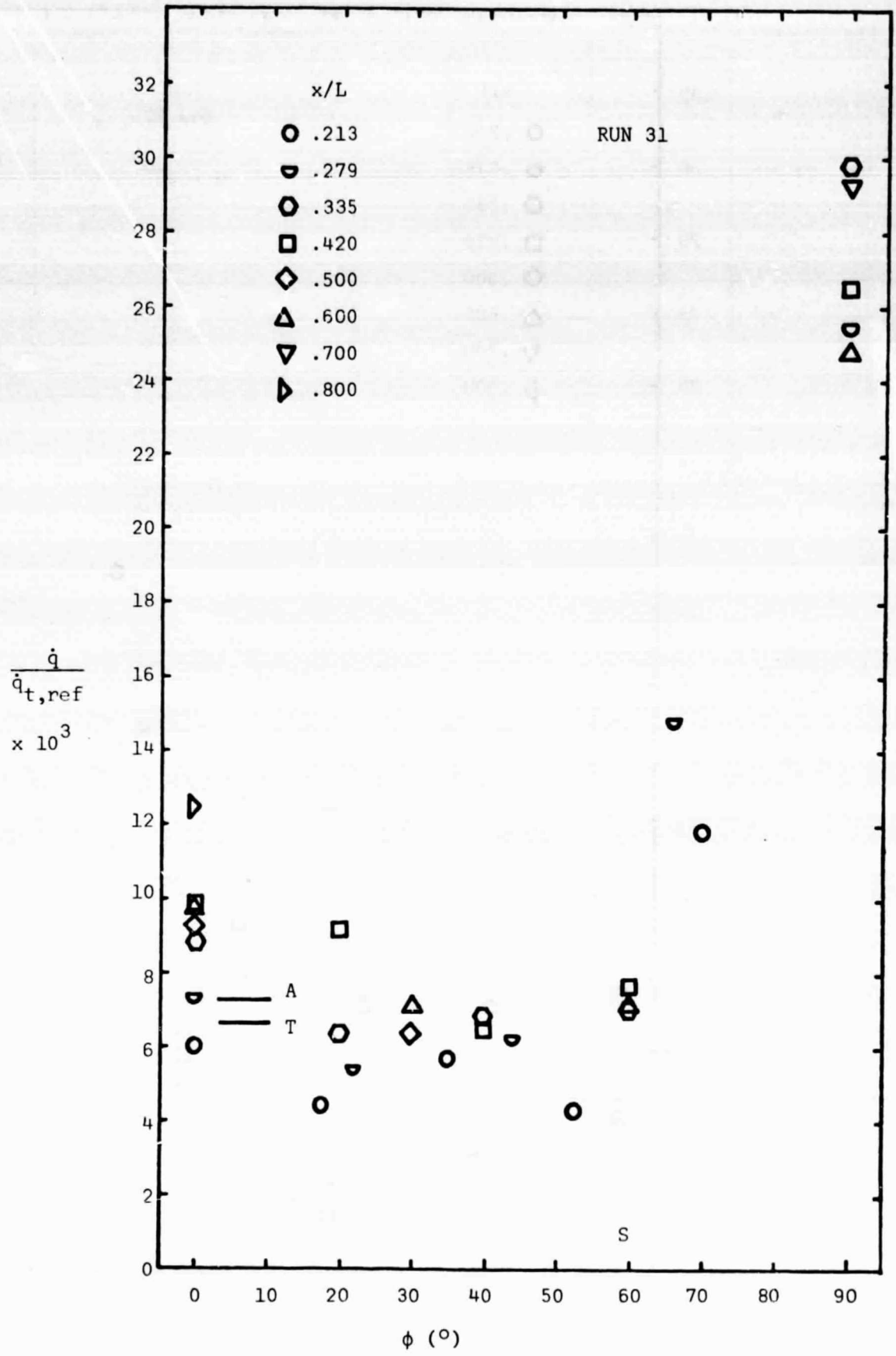

(i) Data for Run 31 ($\alpha = 90^{\circ}$)

Figure 35. - Continued.

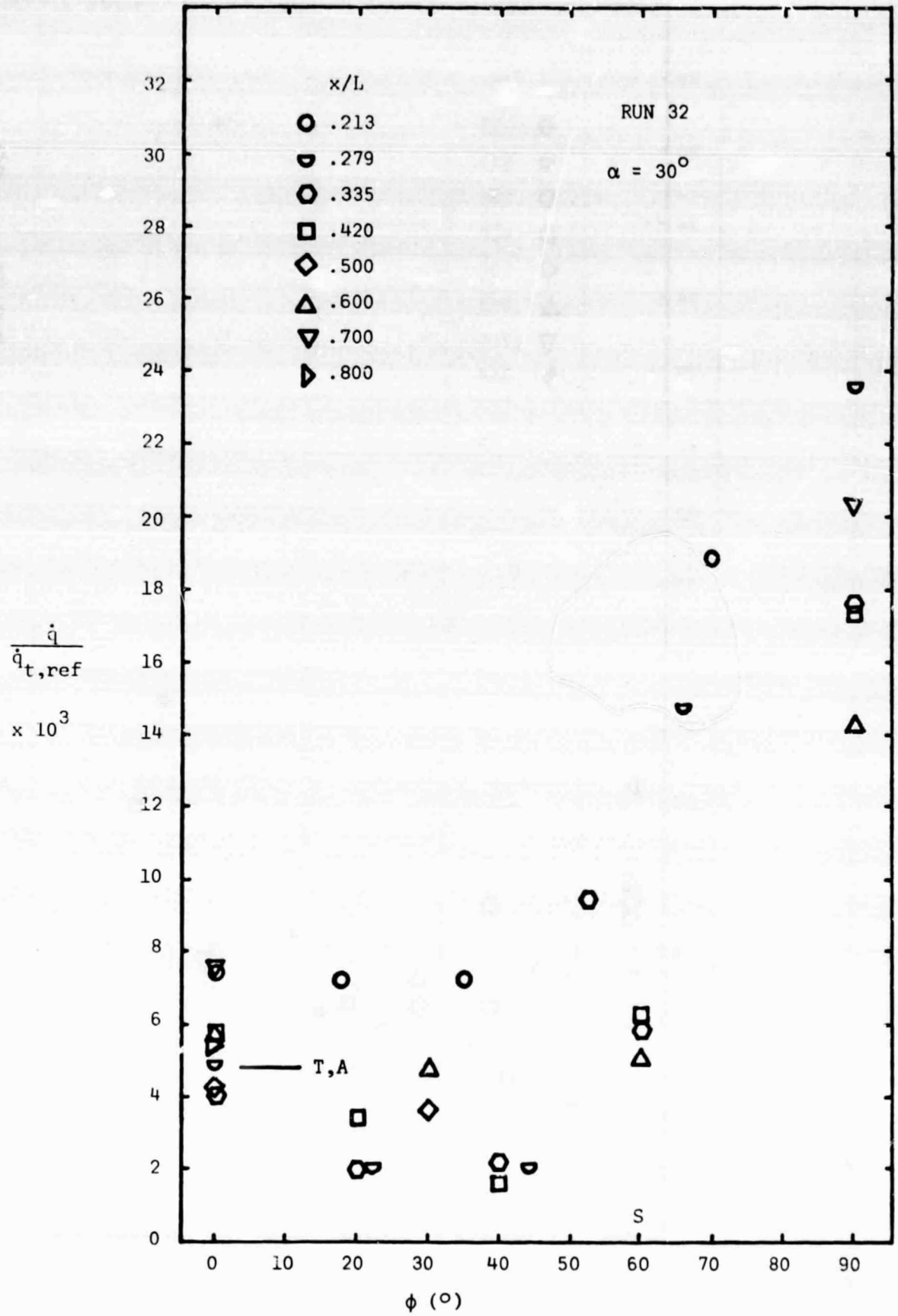

(j) Data for Run 32 ($\alpha = 30^\circ$)

Figure 35. - Concluded.

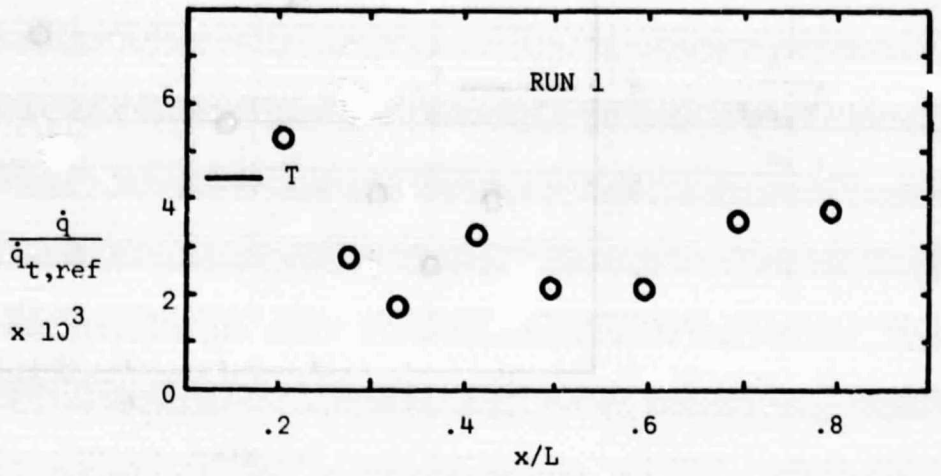

T = Theoretical average heat transfer

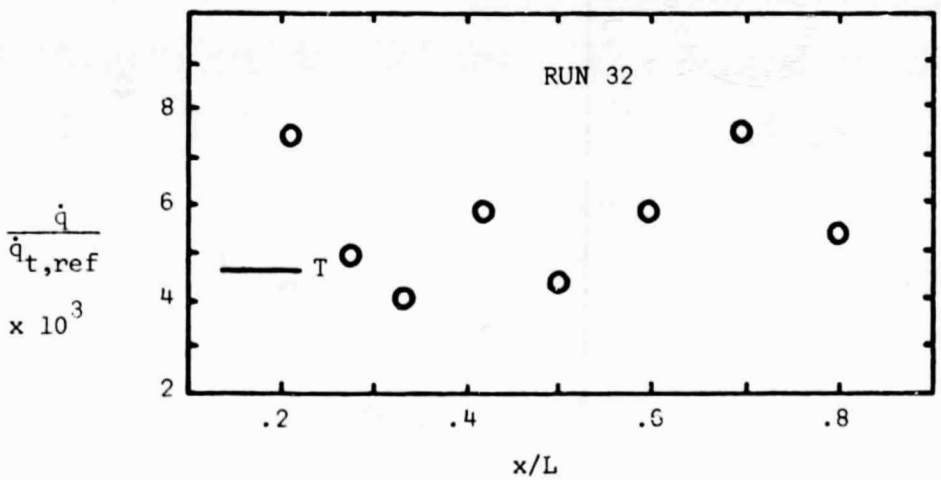

(a) Data for Runs 1 and 32 ($\alpha = 30^\circ$)

Figure 36. - Longitudinal distribution of heat transfer for leeward pitch plane ($\phi = 0^\circ$).

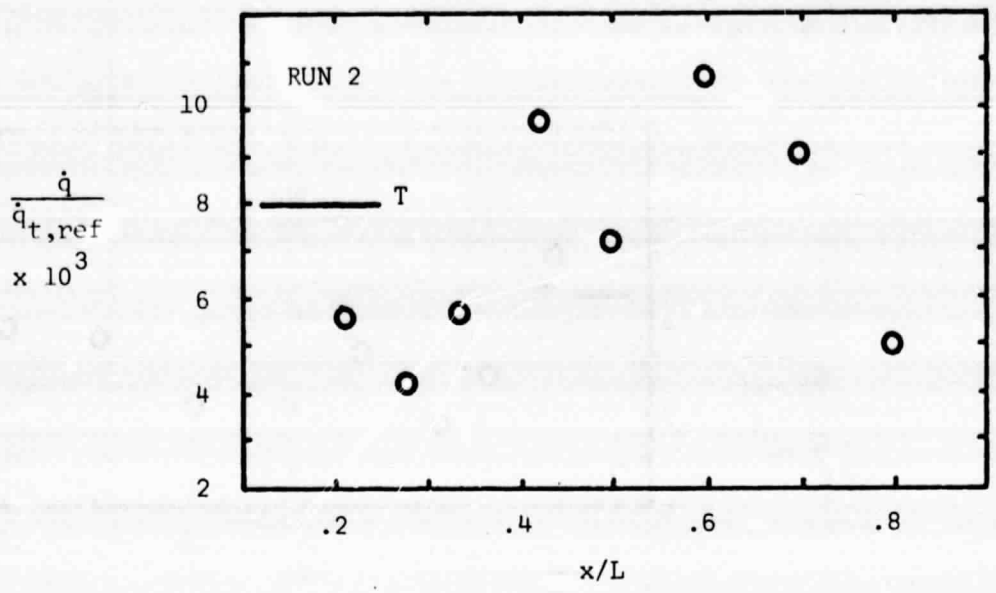

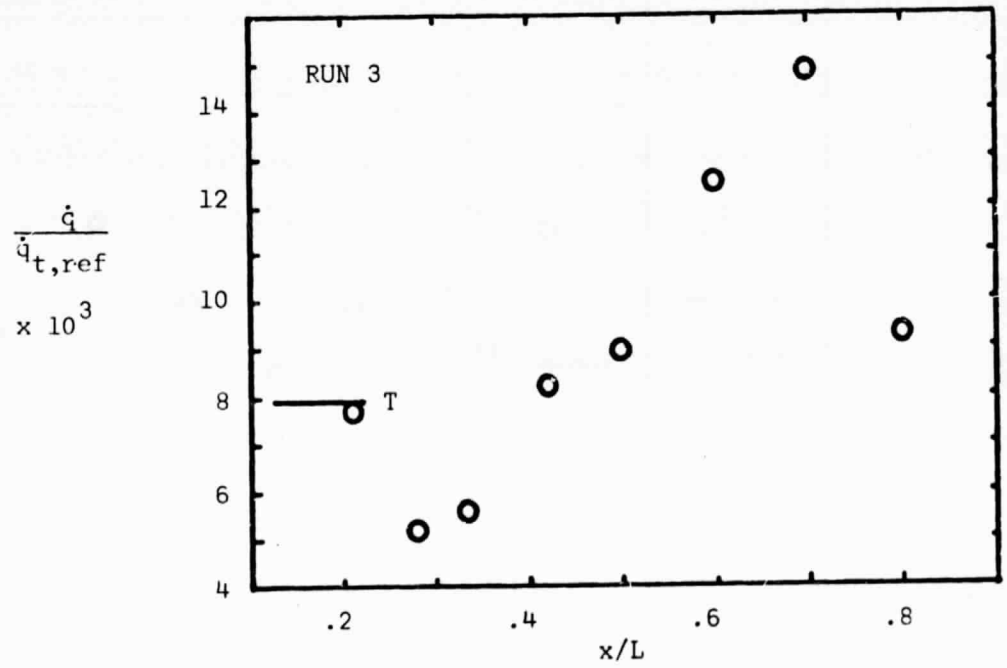

(b) Data for Runs 2 and 3 ($\alpha = 90^{\circ}$)

Figure 36. - Continued.

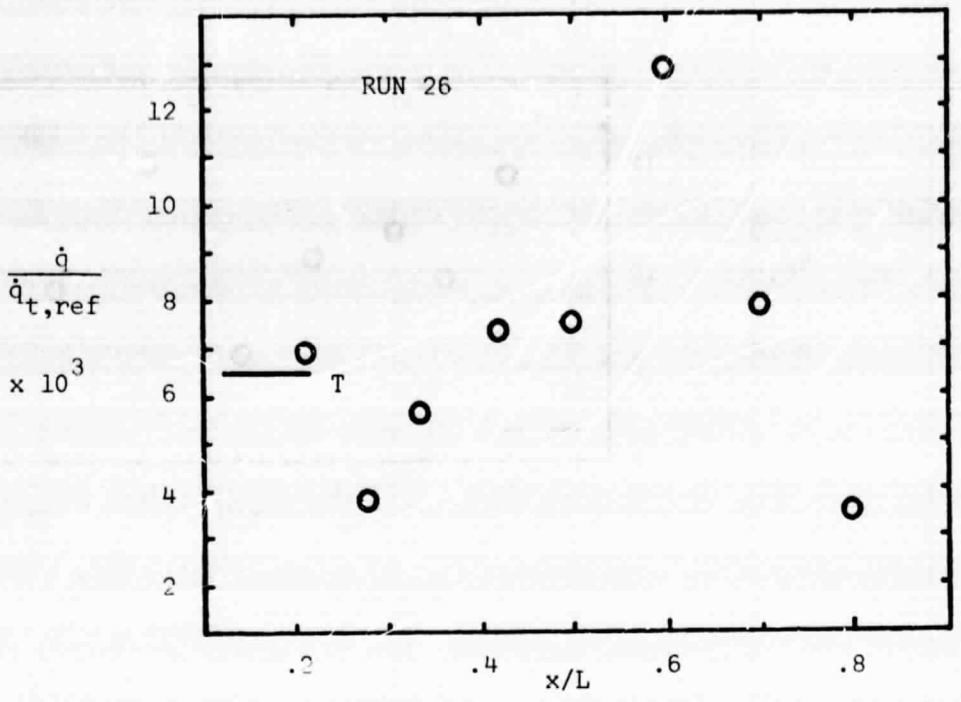

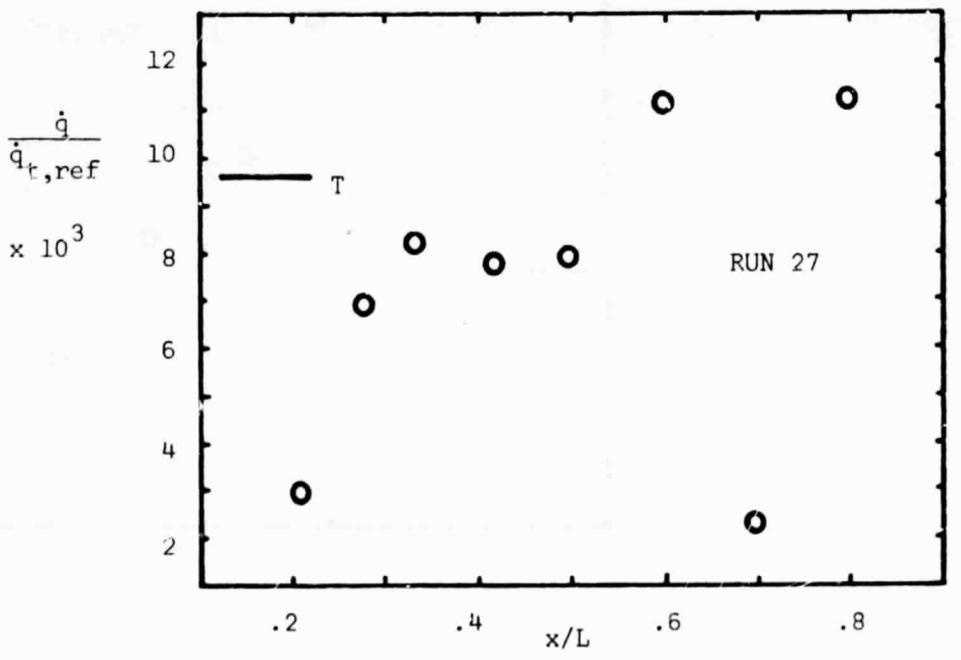

(c) Data for Runs 26 and 27 ($\alpha = 90^{\circ}$)

Figure 36. - Continued.

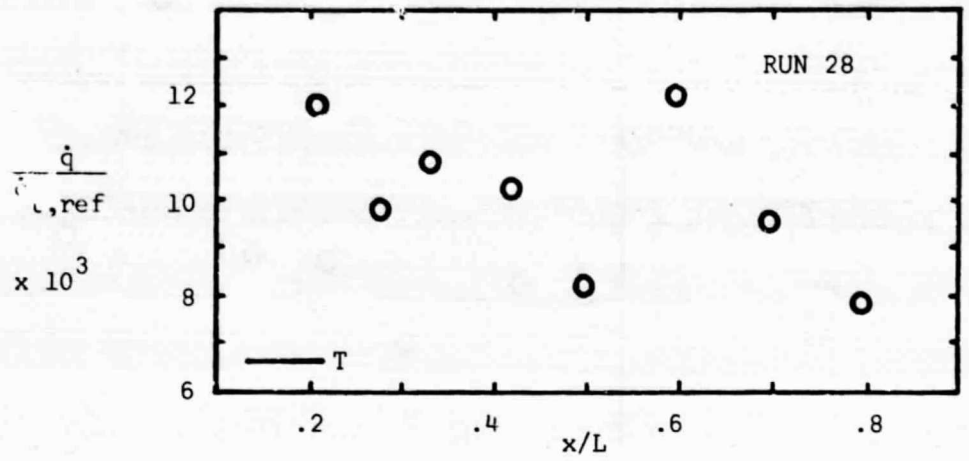

$\frac{\dot{q}}{\dot{q}_{t,ref}} \times 10^3$

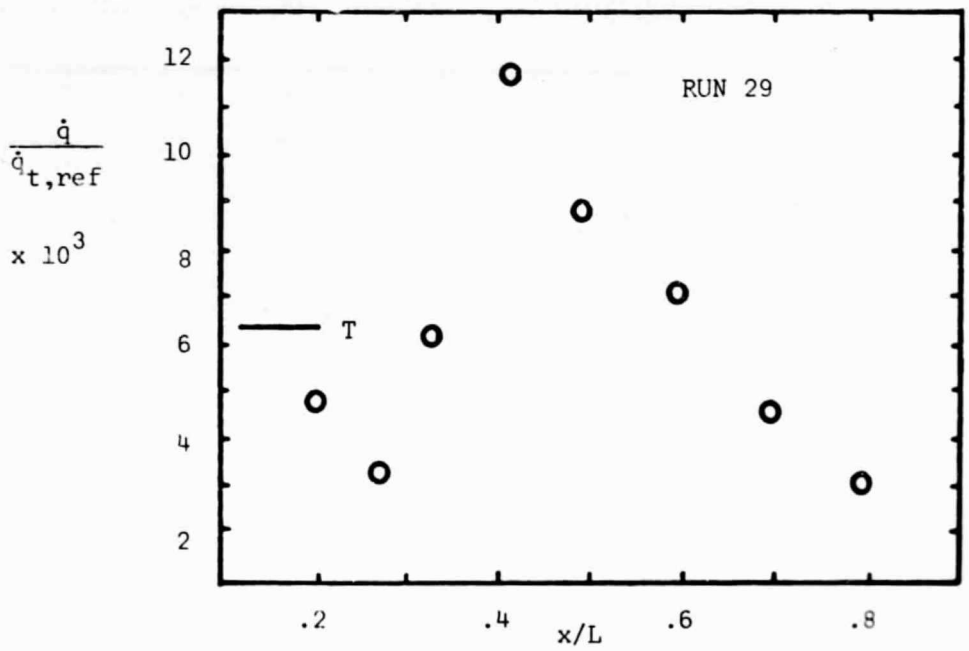

$\frac{\dot{q}}{\dot{q}_{t,ref}} \times 10^3$

(d) Data for Runs 28 and 29 ($\alpha = 90^\circ$,

Figure 36. - Continued.

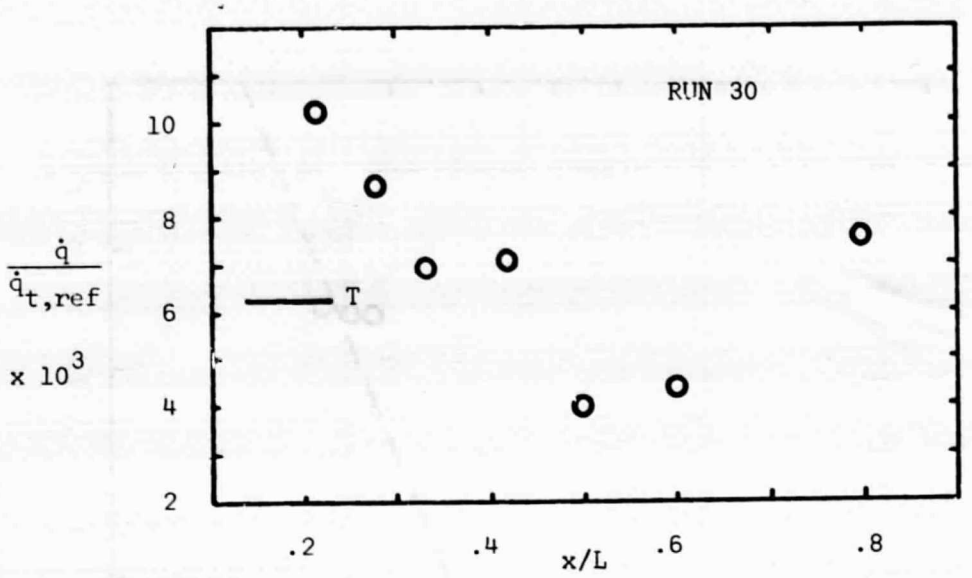

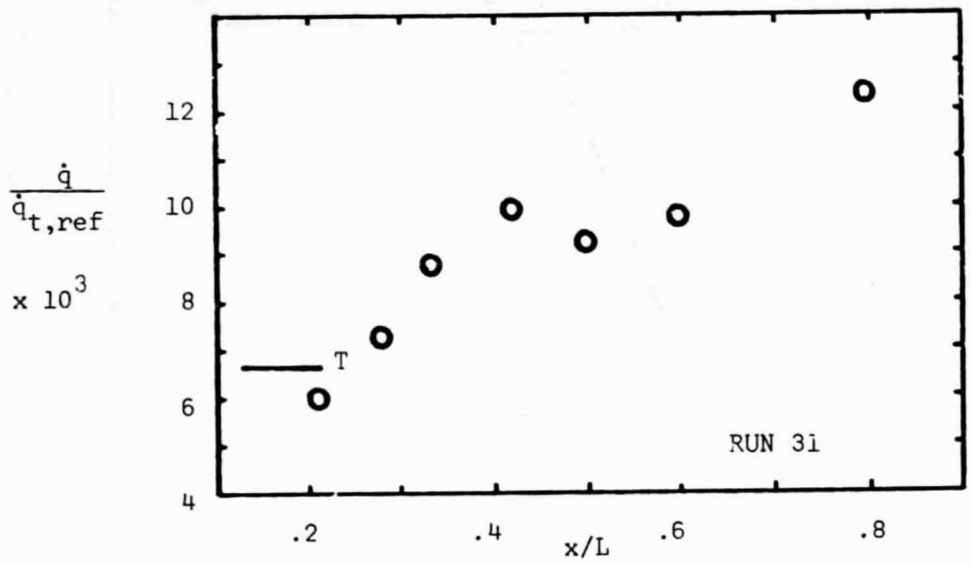

(e) Data for Runs 30 and 31 ($\alpha = 90^{\circ}$)

Figure 36. - Concluded.

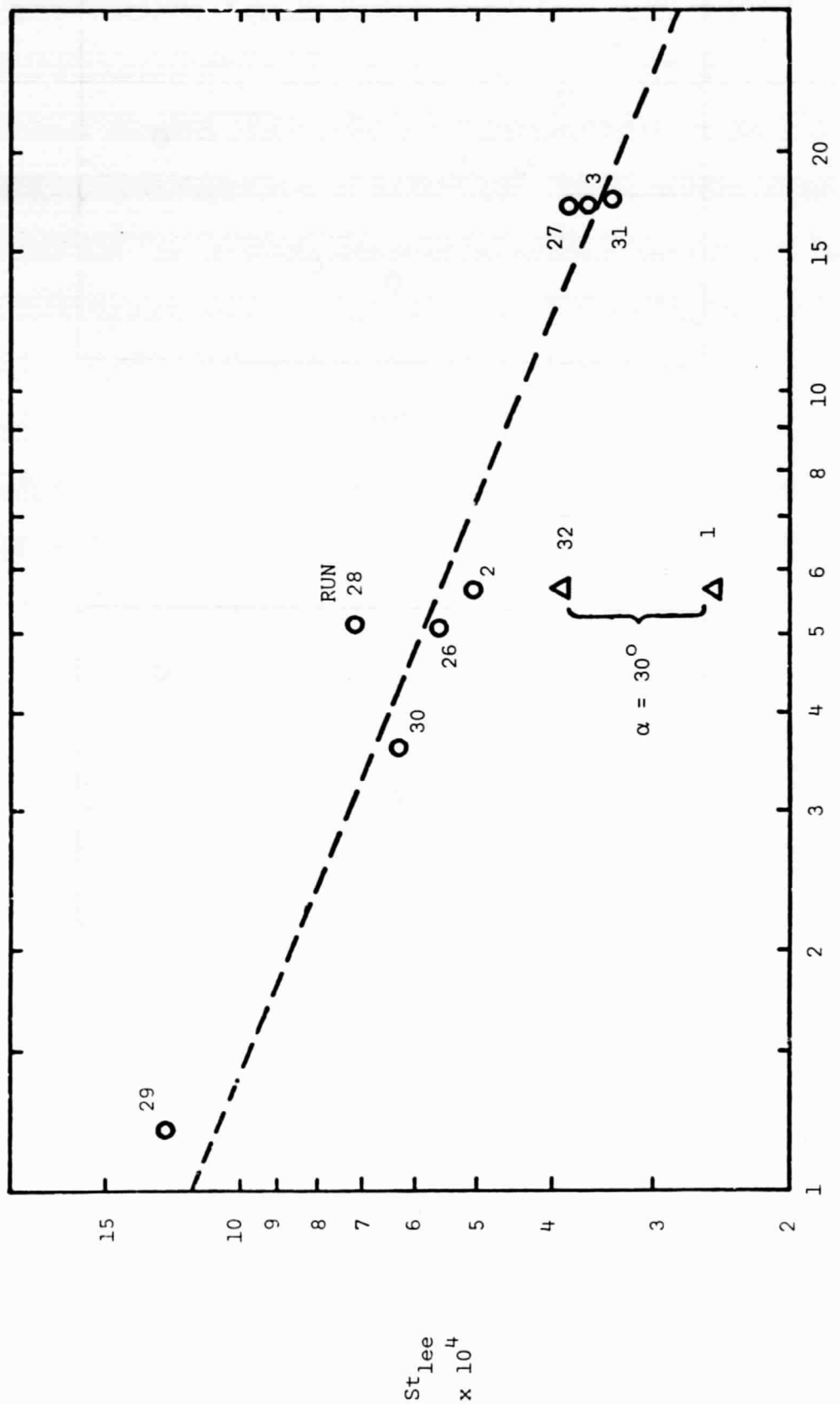

Figure 37. - Summary of fuselage heat transfer data.

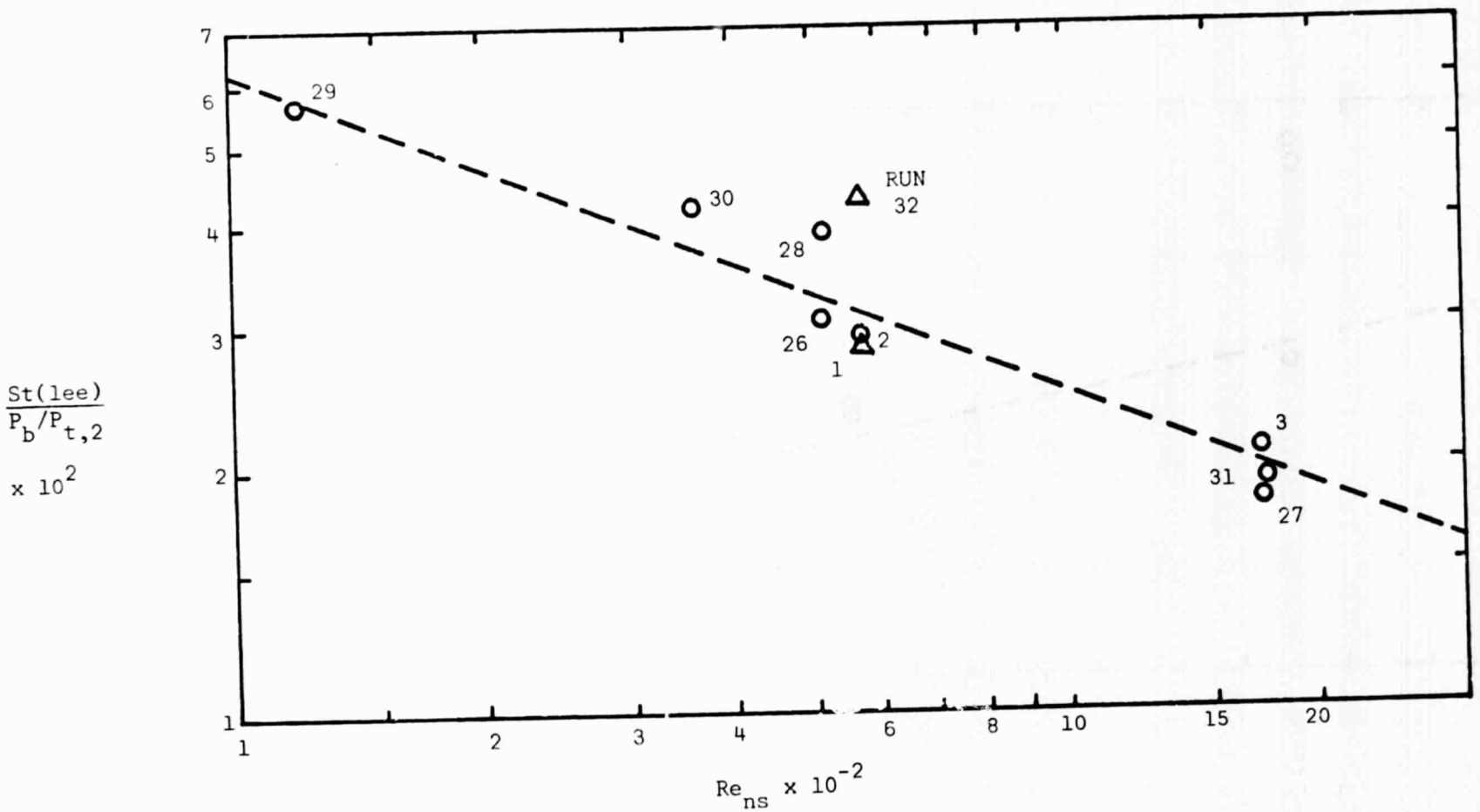

Figure 38. - Correlation of fuselage heat transfer data.

$$STT = \frac{St(lee)}{P_b/P_{t,2}} \left(\frac{T_{lee}}{T_{wwd}} \right)^{1/2} \times 10^2$$

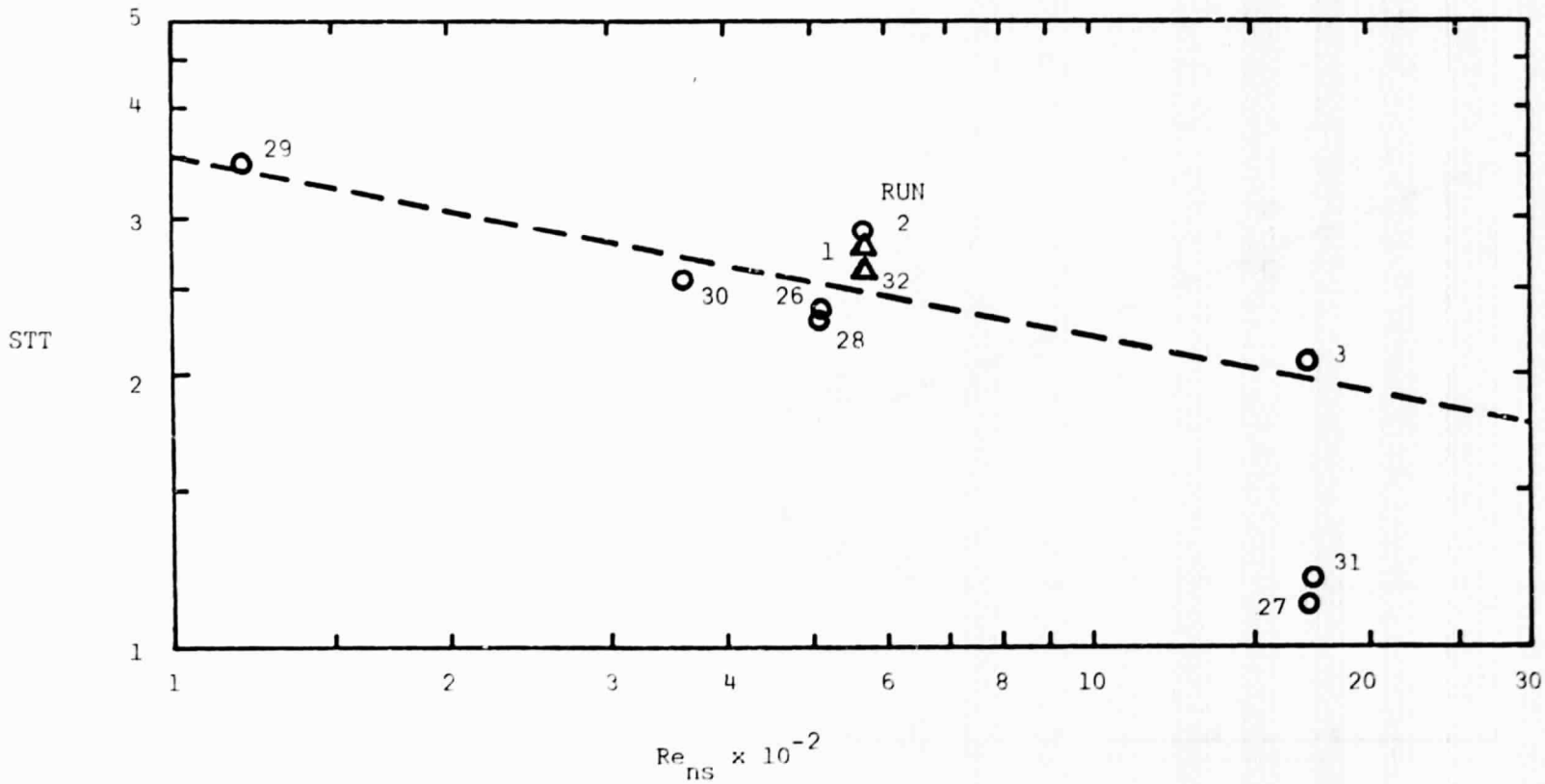

Figure 39. - Correlation of fuselage heat transfer data.

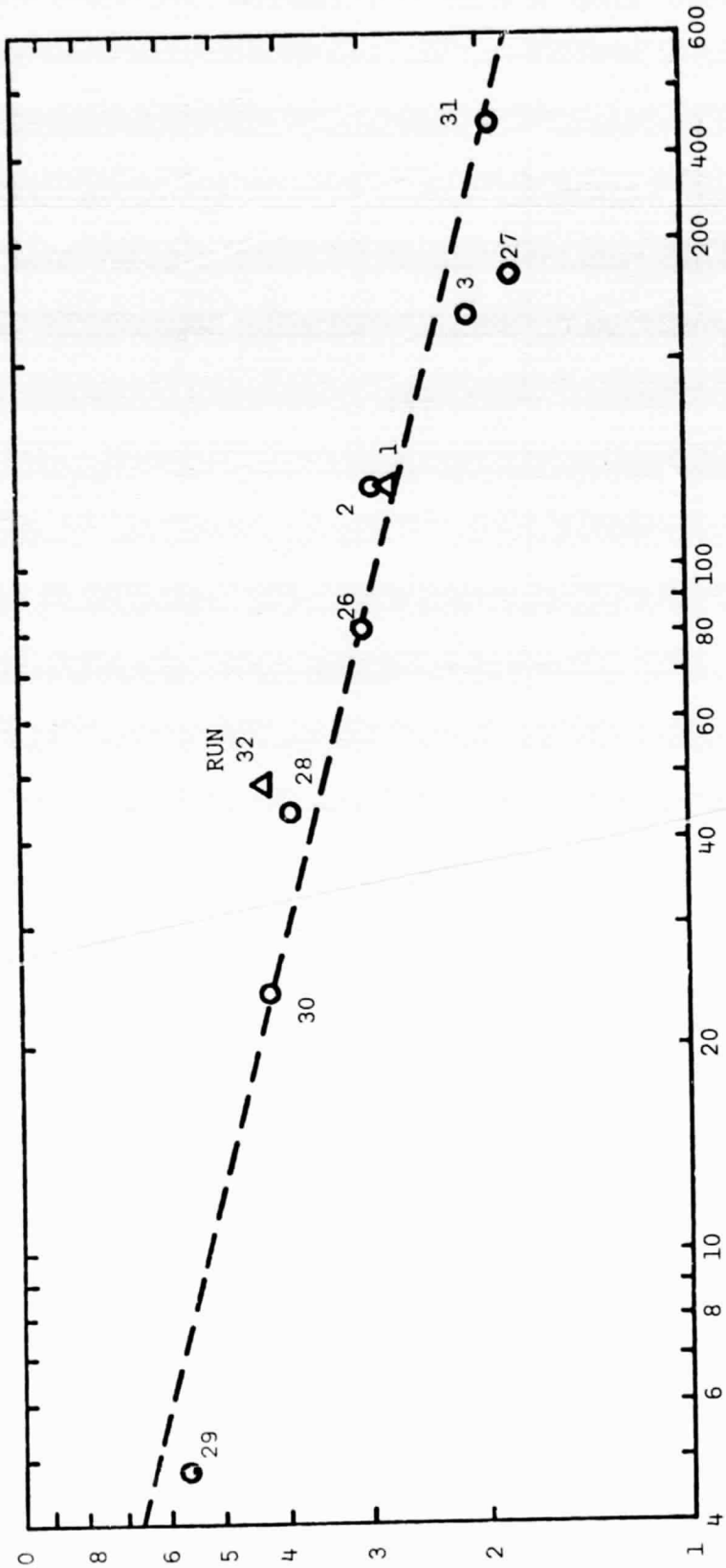

Figure 40. - Correlation of fuselage heat transfer data.

APPENDIX A

SUMMARY OF THEORETICAL MODELS FOR FUSELAGE TESTS

I. Wake Heat Transfer Analysis

The planar integral model of Lamb and Hsieh [24] has been employed to provide theoretical comparison with the present fuselage-only experimental data. This theory estimates laminar convective heat transfer from the simultaneous satisfaction of various governing equations for the geometry shown schematically in Fig. A-1 which divides the near wake region into two parts: a nearly isobaric zone (Control Volume I) adjacent to the leeward surface of the body and a zone of increasing pressure in which the external flow is turned back toward the axial direction. A portion of near wake flow cannot negotiate the rising pressure and is reversed into the isobaric zone; this flow reversal region is identified in Fig. A-1 as Control Volume II.

Both control volumes are bounded by the dividing streamline, so-called because it separates the primary external flow which continues downstream from the low speed fluid which is continually circulated from the free shear layer to Control Volume II and then back toward the body surface from whence it reenters the shear layer. A primary feature of the present theoretical model is the treatment of transport rates across the dividing streamline in the isobaric zone. Velocity and temperature profiles in the shear layer are considered to be nonsimilar which results in local transverse derivatives, and hence shear stresses and heat conduction rates, being highly dependent on the shape and thickness of the upstream boundary layer just prior to separation. This feature thus permits the theoretical model to reflect the strong influence of Reynolds number which is characteristic of laminar wakes.

Governing integral equations for Control Volume I include continuity and mechanical energy, which is obtained by multiplying the motion equation by the

local velocity prior to integration. To simplify numerical computation all governing equations are converted to an incompressible plane with the usual Howarth-Levy density transformation. In general, one must determine the base pressure (which is related to the angle ψ in Fig. A-1 as well as the associated free stream Mach number), the length L of the isobaric region and the wake stagnation pressure P_w. After assuming a base pressure P_b, one varies the value of L until both continuity and mechanical energy are satisfied for CV-I. Two values of P_w are then found, one from the hypothetical inviscid flow using Prandtl-Meyer relations and the other using an isentropic stagnation of the dividing streamline velocity along a parabolic trajectory which forms the upper boundary of CV-II.

Since, for arbitrary values of P_b, the two values of P_w will not be equal, one can repeat the foregoing search procedure until a single value of P_w is obtained for an assumed value of P_b; this provides uniqueness of the flow field and allows one to return to CV-I and compute an overall energy balance. Treating the reverse flow of CV-I as a jet impinging on a planar wall, one can then estimate both the average and peak convective heat transfer on the body surface which bounds Control Volume I.

II. Laminar Boundary Layer Computation

The boundary layer thickness prior to separation is required as an input to the wake heat transfer analysis. To obtain this parameter the present computations have employed a simple integral procedure using a variant of the Howarth-Levy compressibility transformation along with the classical Karman-Pohlhausen velocity profile family. As outlined in Schlichting [18] one can

define two coordinates $(\tilde{x}, \tilde{y})$ for a hypothetical incompressible flow in the form*

$$\tilde{x} = \int_0^x \frac{P_e}{P_t} \frac{c_e}{c_t} \left(\frac{T_e}{T_t} \right)^{1/2} dx$$

and

$$\tilde{y} = \frac{c_e}{c_t} \int_0^x \frac{P}{P_t} \frac{T_t}{T} dy$$

where the subscript e refers to conditions in the external flow and t refers to the corresponding stagnation conditions. In addition, S is the reference temperature of the Sutherland viscosity law, and c is the sonic velocity, $(\gamma RT)^{1/2}$.

It is shown in [18] that the foregoing transformation allows the compressible boundary layer equations to be written as

$$u \frac{\partial u}{\partial x} + v \frac{\partial u}{\partial y} = u_e \frac{du_e}{dx} \frac{T_w}{T_t} + \nu_t \frac{\partial^2 u}{\partial y^2}$$

where T_w is the local wall temperature and ν is the kinematic viscosity. All velocity components and spatial coordinates in the foregoing expression are those of the hypothetical incompressible flow even though the symbol $(\sim)$ has been omitted for simplicity. The motion equation can be integrated across the boundary layer to produce the integral momentum expression

$$\frac{d\theta}{dx} + \frac{1}{u_e} \frac{du_e}{dx} \left(2\theta + \delta^* \frac{T_w}{T_t} \right) = \frac{\tau_w}{\rho u_e^2}$$

---

*The parameter "b" defined in [18] was found to be incorrect. The correct value can be found from the foregoing expression for $\tilde{x}$.

which differs from the usual incompressible expression only by the inclusion of the wall temperature factor.

The Karman-Polhausen velocity profile family allows all viscous layer parameters to be expressed as functions of the pressure gradient parameter $G = (\delta^2/\nu_t)\, du_e/dx$. That is

$$\frac{\theta}{\delta} = f_1(G), \quad \frac{\delta^*}{\delta} = f_2(G) \text{ and } \frac{\tau_w}{\rho u_e^2} = \frac{\nu_t}{\delta u_e} f_3(G)$$

where, in general, the f's are of the form $A_1 + A_2G + A_3G^2$.

In the present computation the pressure distribution P(x) of the actual flow is transformed to the incompressible plane as $\tilde{u}_e(\tilde{x})$ which then allows one to solve the momentum equation and obtain the incompressible layer thickness $\tilde{\delta}(\tilde{x})$. After applying the inverse transformation one obtains the actual layer thickness $\delta(x)$. The present computations employed a simple, modified Euler technique for marching out the solution numerically.

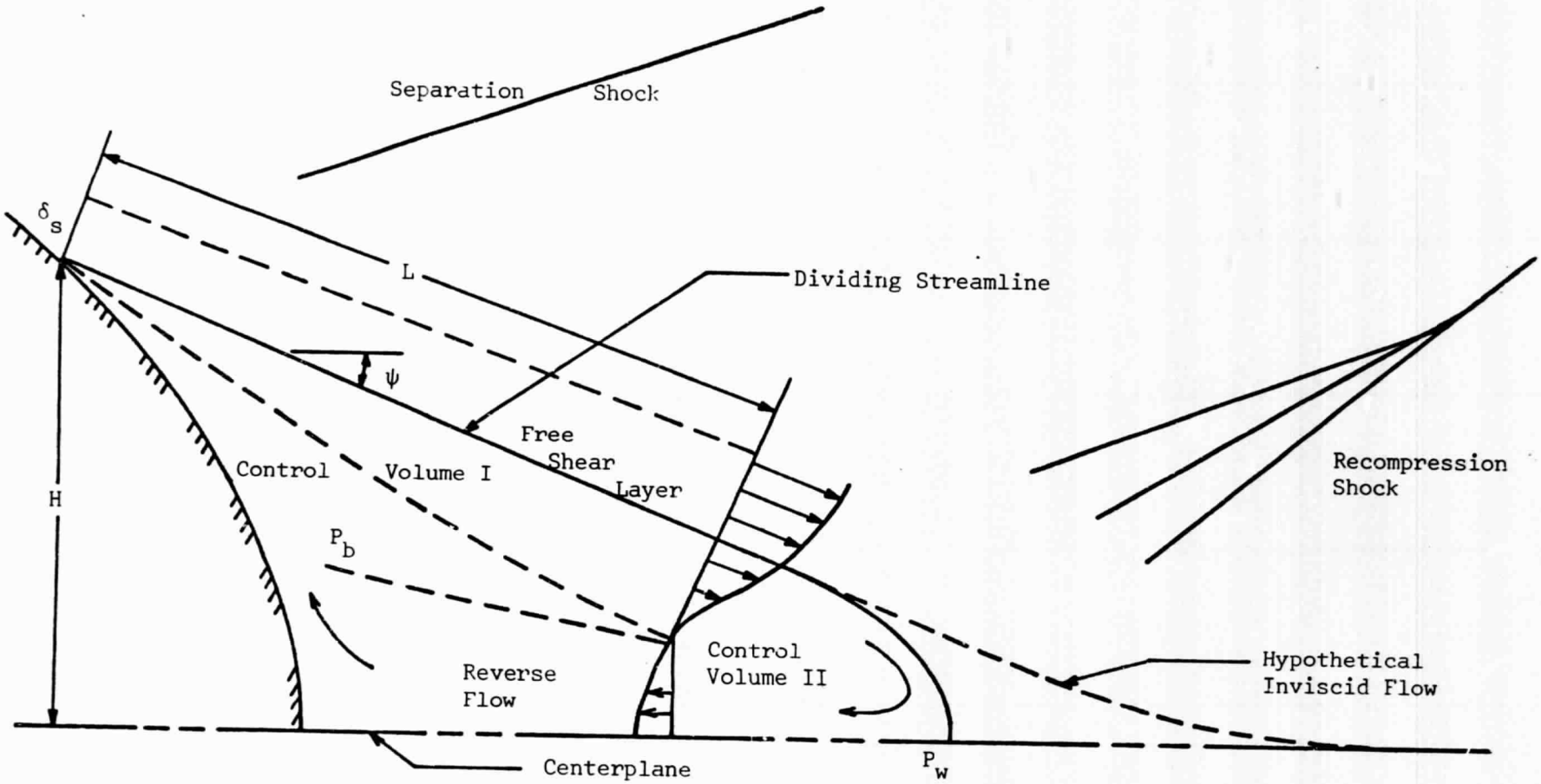

Figure A-1. - Schematic representation of laminar near wake flow field.

APPENDIX B

Selected Schlieren Photographs

(a) Run 4, α = 30°, M_∞ = 11.80, $Re_{\infty,L}$ = 1.630 x 10^6

Figure B-1. - Schlieren photographs for the orbiter configuration.

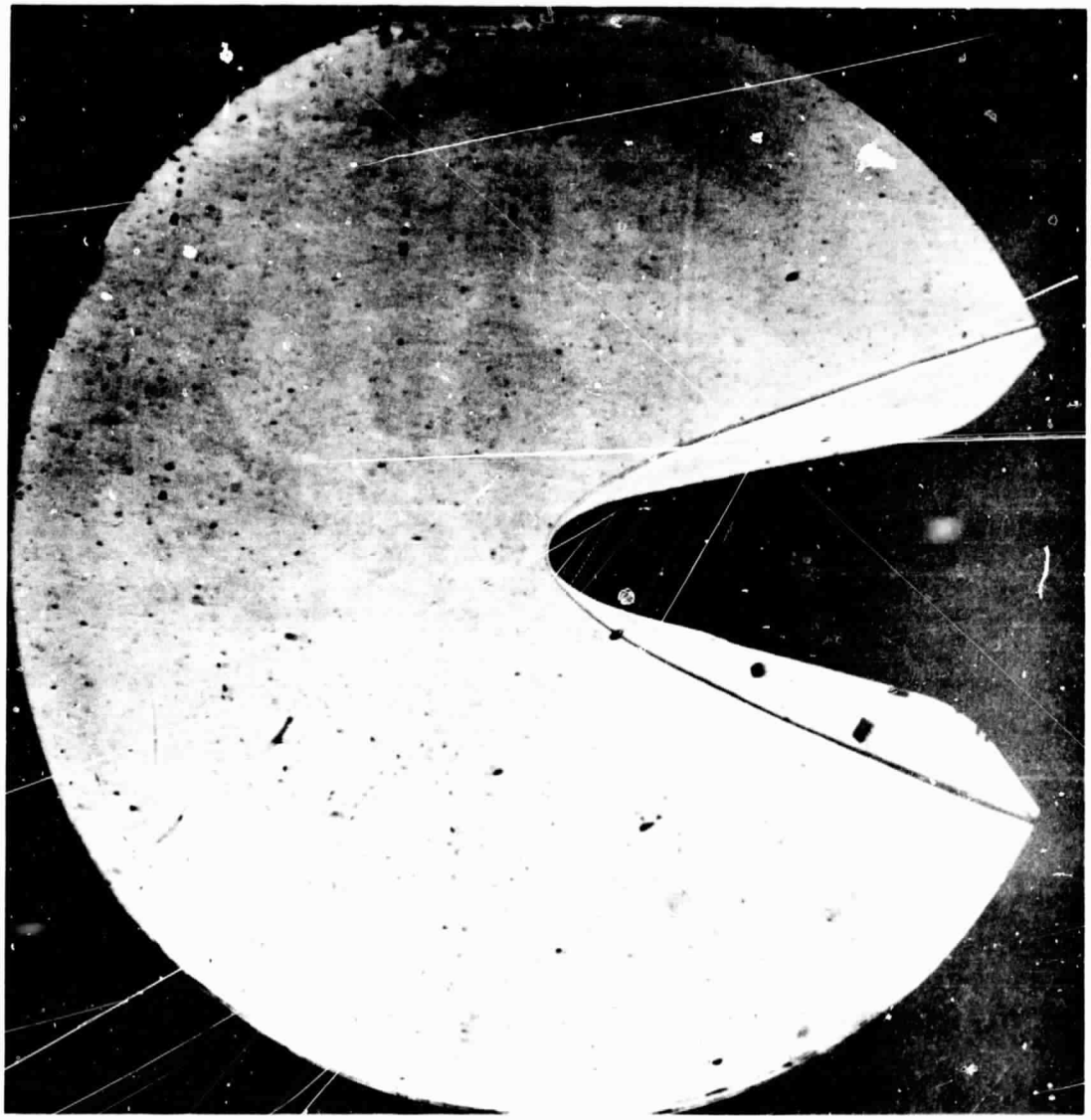

(b) Run 22, $\alpha = 40°$, $M_\infty = 10.01$, $Re_{\infty,L} = 0.517 \times 10^6$

Figure B-1. - Continued.

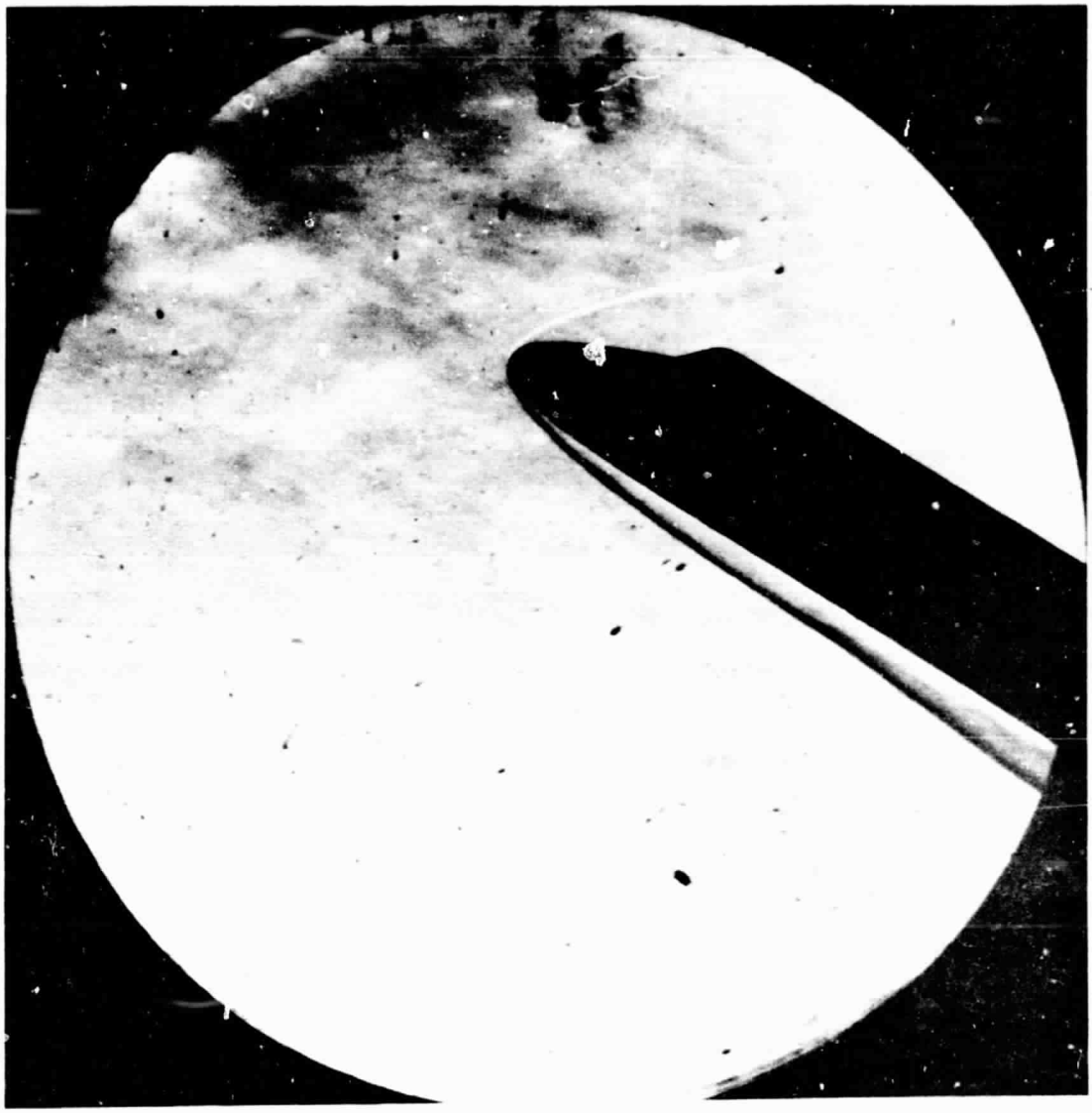

(c) Run 38, $\alpha = 30°$, $M_\infty = 10.16$, $Re_{\infty,L} = 0.610 \times 10^6$

Figure B-1. - Concluded.

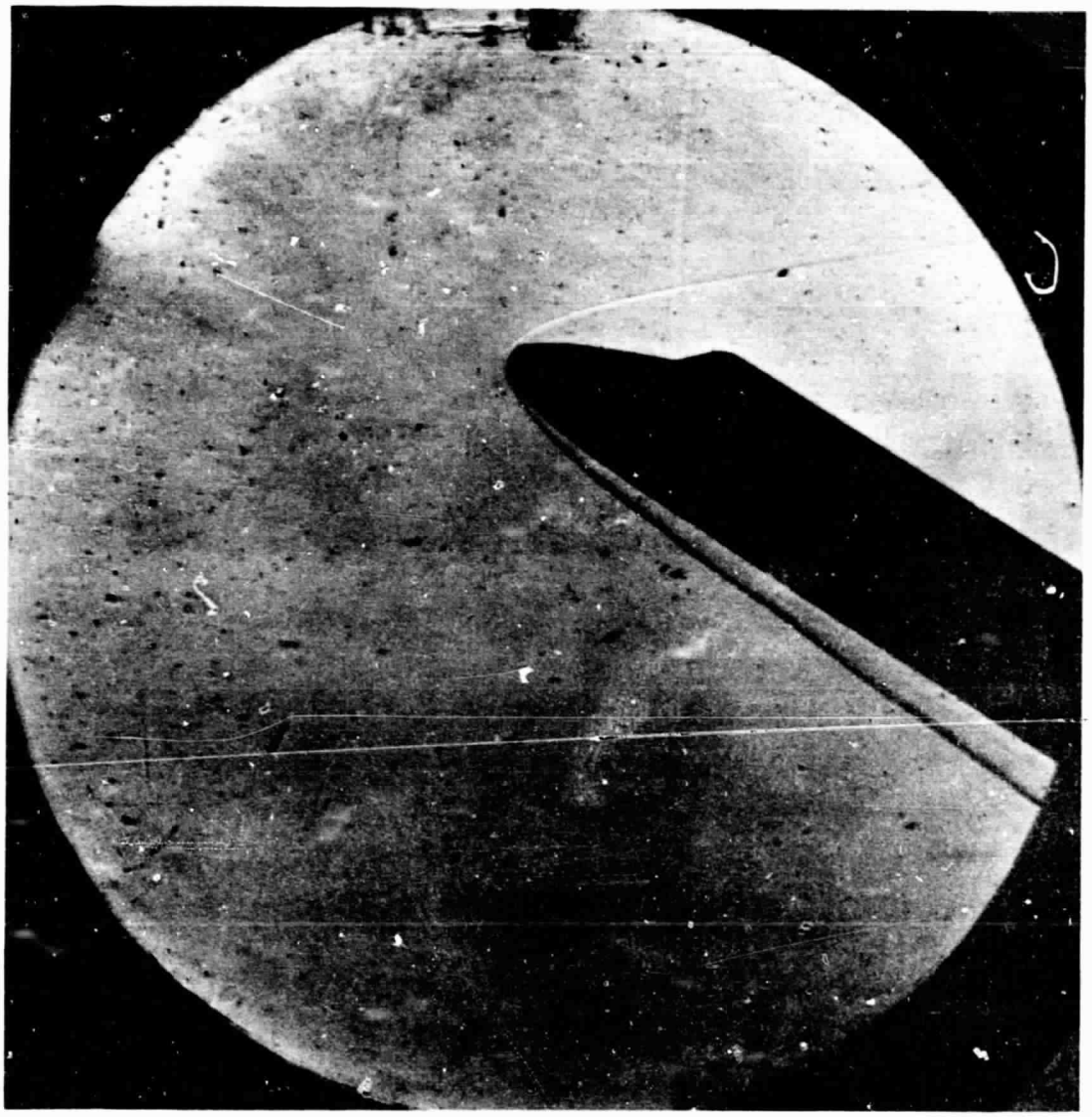

(a) Run 1, $\alpha = 30^{\circ}$, $M_{\infty} = 12.26$, $Re_{\infty,L} = .608 \times 10^{6}$

Figure B-2. - Schlieren photographs for the fuselage configuration.

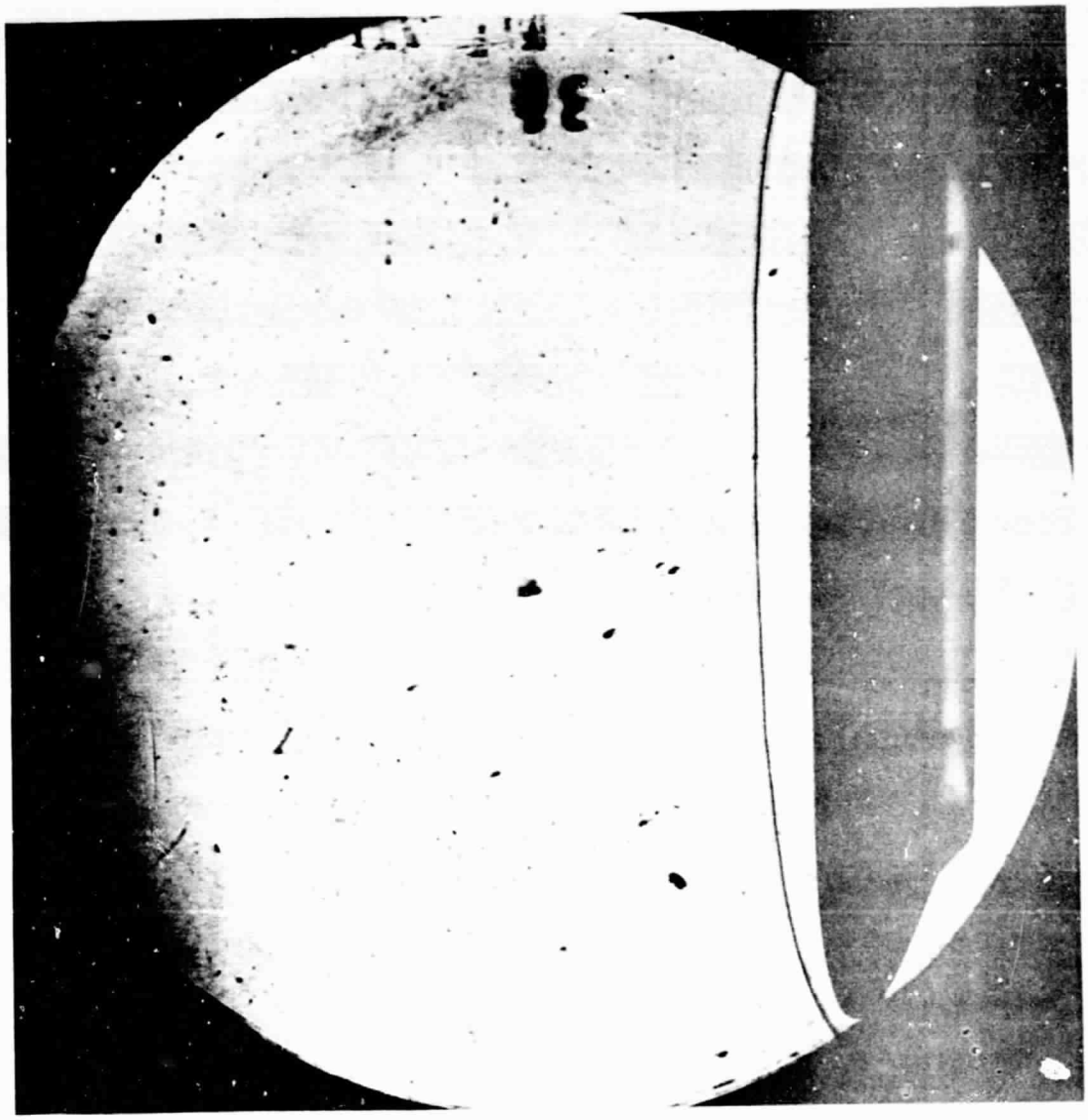

(b) Run 31, $\alpha = 90^{\circ}$, $M_{\infty} = 13.94$, $Re_{\infty,L} = 1.735 \times 10^{6}$

Figure B-2. Concluded.

APPENDIX C

Tabulation of Experimental Data

RUN NO.	1	2	3	4	5	6	7	8
ATTACK	3.000E+01	9.000E+01	9.000E+01	3.000E+01	3.000E+01	3.000E+01	3.000E+01	3.000E+01
YAW	0.0	0.0	0.0	0.0	0.0	0.0	0.0	0.0
ROLL	0.0	0.0	0.0	0.0	0.0	0.0	0.0	0.0
M(I)	4.733E+00	4.733E+00	4.749E+00	4.821E+00	4.735E+00	4.767E+00	4.767E+00	4.821E+00
P(O)	5.210E+03	5.205E+03	1.288E+04	1.253E+04	4.985E+03	9.968E+02	1.054E+04	1.279E+04
H(O)	3.285E+07	3.285E+07	3.293E+07	3.385E+07	3.323E+07	3.326E+07	3.317E+07	3.372E+07
T(O)	4.626E+03	4.626E+03	4.644E+03	4.751E+03	4.675E+03	4.658E+03	4.670E+03	4.734E+03
M	1.226E+01	1.226E+01	1.187E+01	1.180E+01	1.224E+01	1.167E+01	1.571E+01	1.181E+01
U	7.978E+03	7.977E+03	7.980E+03	8.088E+03	8.023E+03	8.015E+03	8.068E+03	8.073E+03
T	1.761E+02	1.761E+02	1.878E+02	1.955E+02	1.785E+02	1.962E+02	1.096E+02	1.943E+02
P	2.184E-02	2.182E-02	7.148E-02	7.097E-02	2.083E-02	5.496E-03	8.546E-03	7.227E-02
Q	2.300E+00	2.298E+00	7.063E+00	6.922E+00	2.189E+00	5.244E-01	1.478E+00	7.062E+00
RHO	1.041E-05	1.040E-05	3.194E-05	3.047E-05	9.791E-06	2.351E-06	6.540E-06	3.121E-05
MU	1.470E-07	1.470E-07	1.565E-07	1.626E-07	1.490E-07	1.631E-07	9.223E-08	1.616E-07
RE/FT.	5.648E+05	5.643E+05	1.629E+06	1.516E+06	5.272E+05	1.155E+05	5.722E+05	1.559E+06
PITOT	4.311E+00	4.307E+00	1.324E+01	1.298E+01	4.103E+00	9.832E-01	2.772E+00	1.324E+01
T*	1.285E+03	1.285E+03	1.291E+03	1.372E+03	1.349E+03	1.355E+03	1.327E+03	1.368E+03
MU*	7.048E-07	7.048E-07	7.069E-07	7.345E-07	7.267E-07	7.287E-07	7.193E-07	7.331E-07
SQRT.C*	8.105E-01	8.105E-01	8.107E-01	8.023E-01	8.035E-01	8.042E-01	8.027E-01	8.027E-01
H(W)	2.523E+06	2.523E+06	2.523E+06	3.183E+06	3.183E+06	3.183E+06	3.183E+06	3.183E+06
T(W)	4.200E+02	4.200E+02	4.200E+02	5.300E+02	5.300E+02	5.300E+02	5.300E+02	5.300E+02
P(TS)	3.868E-05	5.802E-05	5.802E-05	5.802E-05	7.736E-04	5.802E-05	3.868E-05	5.802E-05
RE(STAG)	5.700E+02	5.695E+02	1.717E+03	1.644E+03	5.362E+02	1.289E+02	3.573E+02	1.684E+03
POP4TH	9.795E-01	9.785E-01	9.337E-01	8.738E-01	9.363E-01	1.069E+00	9.845E-01	8.921E-01
Q(O)	2.643E+02	2.642E+02	4.655E+02	4.619E+02	2.537E+02	1.243E+02	2.085E+02	4.645E+02
HQ(O)	2.181E-01	2.180E-01	3.831E-01	3.770E-01	2.114E-01	1.034E-01	1.740E-01	3.807E-01
CHQ(O)	8.166E-02	8.170E-02	4.672E-02	4.755E-02	8.363E-02	1.706E-01	1.025E-01	4.697E-02

RUN NO.	9	10	11	12	13	14	15	16
ATTACK	3.000E+01	3.000E+01	3.000E+01	3.000E+01	3.000E+01	3.000E+01	3.000E+01	3.000E+01
YAW	0.0	0.0	0.0	0.0	0.0	0.0	0.0	0.0
ROLL	0.0	0.0	0.0	0.0	0.0	0.0	0.0	0.0
M(I)	4.784E+00	4.700E+00	4.777E+00	4.812E+00	4.751E+00	4.785E+00	4.750E+00	5.166E+00
P(O)	8.378E+03	4.863E+03	8.994E+02	1.634E+04	1.029E+04	5.511E+03	2.611E+03	3.219E+03
H(O)	3.366E+07	3.278E+07	3.285E+07	3.309E+07	3.285E+07	3.360E+07	3.302E+07	3.877E+07
T(O)	4.729E+03	4.623E+03	4.603E+03	4.657E+03	4.631E+03	4.717E+03	4.641E+03	5.299E+03
M	1.161E+01	1.226E+01	1.164E+01	1.601E+01	1.571E+01	1.016E+01	1.005E+01	1.581E+01
U	8.061E+03	7.970E+03	7.964E+03	8.062E+03	8.029E+03	8.010E+03	7.936E+03	8.724E+03
T	2.005E+02	1.756E+02	1.948E+02	1.055E+02	1.086E+02	2.585E+02	2.592E+02	1.266E+02
P	5.160E-02	2.026E-02	5.091E-03	1.216E-02	8.392E-03	8.051E-02	4.024E-02	2.067E-03
Q	4.873E+00	2.136E+00	4.830E-01	2.184E+00	1.452E+00	5.824E+00	2.849E+00	3.619E-01
RHO	2.160E-05	9.684E-06	2.193E-06	9.677E-06	6.485E-06	2.614E-05	1.303E-05	1.369E-06
MU	1.666E-07	1.466E-07	1.620E-07	8.872E-08	9.134E-08	2.112E-07	2.117E-07	1.064E-07
RE/FT.	1.045E+06	5.263E+05	1.078E+05	8.793E+05	5.701E+05	9.917E+05	4.883E+05	1.123E+05
PITOT	9.139E+00	4.003E+00	9.053E-01	4.094E+00	2.721E+00	1.092E+01	5.340E+00	6.808E-01
T*	1.368E+03	1.335E+03	1.342E+03	1.324E+03	1.317E+03	1.383E+03	1.366E+03	1.497E+03
MU*	7.332E-07	7.218E-07	7.245E-07	7.181E-07	7.159E-07	7.381E-07	7.324E-07	7.754E-07
SQRT.C*	8.032E-01	8.048E-01	8.055E-01	8.031E-01	8.038E-01	8.083E-01	8.103E-01	7.851E-01
H(W)	3.183E+06	3.183E+06	3.183E+06	3.183E+06	3.183E+06	3.183E+06	3.183E+06	3.183E+06
T(W)	5.300E+02	5.300E+02	5.300E+02	5.300E+02	5.300E+02	5.300E+02	5.300E+02	5.300E+02
P(TS)	3.868E-05	5.802E-05	5.802E-05	5.802E-05	1.547E-04	3.868E-05	5.802E-05	3.868E-05
RE(STAG)	1.162E+03	5.289E+02	1.203E+02	5.237E+02	3.540E+02	1.418E+03	7.049E+02	7.990E+01
POP4TH	9.375E-01	9.311E-01	9.589E-01	9.512E-01	9.693E-01	8.939E-01	8.790E-01	9.953E-01
Q(O)	3.851E+02	2.467E+02	1.175E+02	2.529E+02	2.042E+02	4.193E+02	2.873E+02	1.228E+02
HO(O)	3.162E-01	2.087E-01	9.915E-02	2.117E-01	1.723E-01	3.450E-01	2.410E-01	8.635E-02
CHQ(O)	5.647E-02	8.404E-02	1.765E-01	8.434E-02	1.029E-01	5.121E-02	7.246E-02	2.247E-01

RUN NO.	17	18	19	20	21	22	23	24
ATTACK	4.000E+01	4.000E+01	4.000E+01	4.000E+01	4.000E+01	4.000E+01	3.000E+01	3.000E+01
YAW	0.0	0.0	0.0	0.0	0.0	0.0	0.0	0.0
ROLL	0.0	0.0	9.000E+01	9.000E+01	9.000E+01	9.000E+01	1.800E+02	1.800E+02
M(I)	4.753E+00	4.827E+00	4.763E+00	4.714E+00	4.770E+00	4.821E+00	4.583E+00	4.824E+00
P(0)	5.075E+03	1.326E+04	5.159E+03	8.919E+02	1.042E+04	2.715E+03	3.592E+03	7.095E+03
H(0)	3.297E+07	3.405E+07	3.310E+07	3.266E+07	3.385E+07	3.410E+07	3.112E+07	3.372E+07
T(0)	4.640E+03	4.776E+03	4.655E+03	4.589E+03	4.688E+03	4.769E+03	4.423E+03	4.727E+03
M	1.224E+01	1.182E+01	1.223E+01	1.168E+01	1.570E+01	1.001E+01	1.826E+01	1.859E+01
U	7.993E+03	8.113E+03	8.008E+03	7.942E+03	8.029E+03	8.064E+03	7.835E+03	8.157E+03
T	1.774E+02	1.958E+02	1.782E+02	1.921E+02	1.088E+02	2.699E+02	7.652E+01	8.006E+01
P	2.145E-02	7.386E-02	2.181E-02	4.928E-03	8.546E-03	4.210E-02	1.011E-03	1.740E-03
Q	2.251E+00	7.236E+00	2.287E+00	4.715E-01	1.476E+00	2.956E+00	2.363E-01	4.214E-01
RHO	1.015E-05	3.166E-05	1.027E-05	2.153E-06	6.595E-06	1.309E-05	1.108E-06	1.824E-06
MU	1.481E-07	1.628E-07	1.487E-07	1.599E-07	9.147E-08	2.196E-07	6.435E-08	6.733E-08
RE/FT.	5.476E+05	1.578E+06	5.530E+05	1.069E+05	5.789E+05	4.808E+05	1.349E+05	2.210E+05
PITOT	4.219E+00	1.357E+01	4.288E+00	8.636E-01	2.767E+00	5.545E+00	4.423E-01	7.903E-01
T*	1.341E+03	1.378E+03	1.345E+03	1.336E+03	1.317E+03	1.401E+03	1.256E+03	1.335E+03
MU*	7.240E-07	7.365E-07	7.254E-07	7.223E-07	7.160E-07	7.441E-07	6.948E-07	7.219E-07
SQRT.C*	8.042E-01	8.017E-01	8.039E-01	8.060E-01	8.038E-01	8.080E-01	8.109E-01	8.019E-01
H(W)	3.183E+06	3.183E+06	3.183E+06	3.183E+06	3.183E+06	3.183E+06	3.183E+06	3.183E+06
T(W)	5.300E+02	5.300E+02	5.300E+02	5.300E+02	5.300E+02	5.300E+02	5.300E+02	5.300E+02
P(TS)	5.602E-05	7.736E-05	5.802E-05	5.802E-05	7.736E-05	7.736E-05	5.802E-05	5.802E-05
RE(STAG)	5.565E+02	1.709E+03	5.638E+02	1.176E+02	3.604E+02	7.114E+02	6.097E+01	1.010E+02
P0P4TH	9.439E-01	9.211E-01	9.543E-01	9.839E-01	9.715E-01	8.800E-01	9.761E-01	1.007E+00
Q(0)	2.549E+02	4.756E+02	2.581E+02	1.154E+02	2.059E+02	3.038E+02	7.726E+01	1.133E+02
HQ(0)	2.142E-01	3.856E-01	2.159E-01	9.798E-02	1.737E-01	2.459E-01	6.920E-02	9.289E-02
CHQ(0)	8.209E-02	4.666E-02	8.161E-02	1.781E-01	1.020E-01	7.241E-02	2.477E-01	1.941E-01

RUN NO.	26	27	28	29	30	31	32	33
ATTACK	9.000E+01	9.000E+01	9.000E+01	9.000E+01	9.000E+01	9.000E+01	3.000E+01	3.000E+01
YAW	0.0	0.0	0.0	0.0	0.0	0.0	0.0	0.0
ROLL	0.0	0.0	0.0	0.0	0.0	0.0	1.800E+02	1.800E+02
M(I)	4.576E+00	4.837E+00	4.709E+00	4.744E+00	4.780E+00	4.838E+00	4.732E+00	4.837E+00
P(0)	4.327E+03	1.321E+04	4.666E+03	8.953E+02	1.050E+04	1.368E+04	5.162E+03	1.295E+04
H(0)	3.044E+07	3.392E+07	3.265E+07	3.251E+07	3.298E+07	3.419E+07	3.247E+07	3.392E+07
T(0)	4.336E+03	4.758E+03	4.605E+03	4.564E+03	4.643E+03	4.792E+03	4.578E+03	4.758E+03
M	1.232E+01	1.181E+01	1.224E+01	1.166E+01	1.570E+01	1.183E+01	1.226E+01	1.180E+01
U	7.681E+03	8.097E+03	7.954E+03	7.923E+03	8.045E+03	8.129E+03	7.931E+03	8.097E+03
T	1.617E+02	1.953E+02	1.756E+02	1.919E+02	1.092E+02	1.962E+02	1.741E+02	1.957E+02
P	1.829E-02	7.421E-02	1.968E-02	5.029E-03	8.608E-03	7.572E-02	2.182E-02	7.313E-02
Q	1.945E+00	7.258E+00	2.066E+00	4.793E-01	1.486E+00	7.430E+00	2.297E+00	7.139E+00
RHO	9.494E-06	3.189E-05	9.406E-06	2.199E-06	6.613E-06	3.238E-05	1.052E-05	3.136E-05
MU	1.353E-07	1.625E-07	1.466E-07	1.598E-07	9.188E-08	1.632E-07	1.454E-07	1.627E-07
RE/FT.	5.389E+05	1.589E+06	5.103E+05	1.091E+05	5.790E+05	1.613E+06	5.737E+05	1.560E+06
PITOT	3.639E+00	1.361E+01	3.872E+00	8.981E-01	2.786E+00	1.394E+01	4.305E+00	1.339E+01
T*	1.261E+03	1.374E+03	1.331E+03	1.331E+03	1.321E+03	1.382E+03	1.325E+03	1.327E+03
MU*	6.963E-07	7.352E-07	7.206E-07	7.207E-07	7.173E-07	7.379E-07	7.185E-07	7.194E-07
SQRT.C*	8.123E-01	8.021E-01	8.052E-01	8.065E-01	8.034E-01	8.013E-01	8.058E-01	8.073E-01
H(W)	3.183E+06	3.183E+06	3.183E+06	3.183E+06	3.183E+06	3.183E+06	3.183E+06	2.583E+06
T(W)	5.300E+02	5.300E+02	5.300E+02	5.300E+02	5.300E+02	5.300E+02	5.300E+02	4.300E+02
P(TS)	5.802E-05	9.670E-05	5.802E-05	7.736E-05	3.868E-05	3.868E-05	3.868E-05	3.868E-05
RE(STAG)	5.133E+02	1.722E+03	5.140E+02	1.204E+02	3.616E+02	1.749E+03	5.759E+02	1.693E+03
POP4TH	8.878E-01	9.132E-01	8.890E-01	9.716E-01	9.734E-01	9.451E-01	9.713E-01	8.953E-01
Q(0)	2.159E+02	4.741E+02	2.416E+02	1.157E+02	2.075E+02	4.841E+02	2.529E+02	4.827E+02
MQ(0)	1.983E-01	3.861E-01	2.052E-01	9.872E-02	1.743E-01	3.908E-01	2.162E-01	3.855E-01
CMQ(0)	8.453E-02	4.648E-02	8.524E-02	1.761E-01	1.019E-01	4.615E-02	8.056E-02	4.719E-02

RUN NO.	34	35	36	37	38	39	40
ATTACK	3.000E+01	3.000E+01	3.000E+01	3.000E+01	3.000E+01	4.000E+01	4.000E+01
YAW	0.0	0.0	0.0	0.0	0.0	0.0	0.0
ROLL	1.800E+02	1.800E+02	1.800E+02	1.800E+02	1.800E+02	2.700E+02	2.700E+02
M(I)	4.699E+00	4.693E+00	4.720E+00	4.760E+00	4.587E+00	4.761E+00	4.785E+00
P(0)	5.112E+03	9.019E+02	1.618E+04	1.029E+04	2.664E+03	5.073E+03	1.067E+04
H(0)	3.265E+07	3.269E+07	3.208E+07	3.272E+07	3.053E+07	3.259E+07	3.305E+07
T(0)	4.607E+03	4.597E+03	4.539E+03	4.613E+03	4.342E+03	4.590E+03	4.651E+03
M	1.228E+01	1.170E+01	1.609E+01	1.570E+01	1.016E+01	1.223E+01	1.570E+01
U	7.955E+03	7.946E+03	7.938E+03	8.013E+03	7.636E+03	7.946E+03	8.053E+03
T	1.745E+02	1.917E+02	1.012E+02	1.083E+02	2.347E+02	1.756E+02	1.094E+02
P	2.124E-02	4.926E-03	1.188E-02	8.449E-03	4.018E-02	2.170E-02	8.723E-03
Q	2.244E+00	4.728E-01	2.155E+00	1.460E+00	2.909E+00	2.274E+00	1.507E+00
RHO	1.022E-05	2.156E-06	9.852E-06	6.547E-06	1.437E-05	1.037E-05	6.693E-06
MU	1.457E-07	1.596E-07	8.513E-08	9.110E-08	1.932E-07	1.466E-07	9.199E-08
RE/FT.	5.577E+05	1.074E+05	9.186E+05	5.759E+05	5.678E+05	5.622E+05	5.859E+05
PITOT	4.206E+00	8.661E-01	4.038E+00	2.736E+00	5.443E+00	4.262E+00	2.825E+00
T*	1.284E+03	1.285E+03	1.240E+03	1.262E+03	1.233E+03	1.280E+03	1.276E+03
MU*	7.043E-07	7.046E-07	6.891E-07	6.966E-07	6.865E-07	7.029E-07	7.017E-07
SQRT.C*	8.105E-01	8.118E-01	8.127E-01	8.102E-01	8.224E-01	8.111E-01	8.085E-01
H(W)	2.583E+06	2.523E+06	2.523E+06	2.523E+06	2.523E+06	2.553E+06	2.583E+06
T(W)	4.300E+02	4.200E+02	4.200E+02	4.200E+02	4.200E+02	4.250E+02	4.300E+02
P(TS)	3.868E-05	5.802E-05	1.354E-04	7.736E-05	1.160E-04	7.736E-05	7.736E-05
RE(STAG)	5.579E+02	1.176E+02	5.304E+02	3.575E+02	7.701E+02	5.692E+02	3.661E+02
POP4TH	9.791E-01	1.006E+00	9.890E-01	9.644E-01	9.815E-01	9.395E-01	9.866E-01
Q(0)	2.587E+02	1.192E+02	2.498E+02	2.100E+02	2.734E+02	2.600E+02	2.152E+02
HQ(0)	2.153E-01	9.889E-02	2.115E-01	1.740E-01	2.443E-01	2.166E-01	1.768E-01
CHQ(0)	8.237E-02	1.794E-01	8.409E-02	1.031E-01	6.922E-02	8.171E-02	1.020E-01

RUN	GAGE	Q(CW)	Q(AV)/Q(O)	H(A)	H(B)	H(A)/H(O)	C(H)	Q(O)	C(H(O))
1	1	1.105E+01	4.183E-02	9.184E-03	1.098E-02	4.210E-02	3.438E-03	2.643E+02	8.166E-02
1	2	4.847E+00	1.834E-02	4.019E-03	4.803E-03	1.842E-02	1.504E-03	2.643E+02	8.166E-02
1	3	2.885E+00	1.092E-02	2.396E-03	2.855E-03	1.095E-02	8.946E-04	2.643E+02	8.166E-02
1	4	2.730E+00	1.033E-02	2.261E-03	2.701E-03	1.036E-02	8.464E-04	2.643E+02	8.166E-02
1	5	2.462E+00	9.316E-03	2.039E-03	2.436E-03	9.347E-03	7.633E-04	2.643E+02	8.166E-02
1	6	3.858E+00	1.460E-02	3.195E-03	3.818E-03	1.465E-02	1.196E-03	2.643E+02	8.166E-02
1	7	5.668E+00	2.145E-02	4.695E-03	5.610E-03	2.152E-02	1.758E-03	2.643E+02	8.166E-02
1	8	2.279E+00	8.623E-03	1.886E-03	2.252E-03	8.644E-03	7.059E-04	2.643E+02	8.166E-02
1	10	5.615E+00	2.125E-02	4.651E-03	5.557E-03	2.132E-02	1.741E-03	2.643E+02	8.166E-02
1	11	8.395E+00	3.176E-02	6.950E-03	8.303E-03	3.186E-02	2.602E-03	2.643E+02	8.166E-02
1	12	7.027E+00	2.659E-02	5.811E-03	6.941E-03	2.664E-02	2.176E-03	2.643E+02	8.166E-02
1	13	1.394E+00	5.274E-03	1.152E-03	1.376E-03	5.283E-03	4.314E-04	2.643E+02	8.166E-02
1	14	1.394E+00	5.275E-03	1.153E-03	1.377E-03	5.285E-03	4.316E-04	2.643E+02	8.166E-02
1	15	1.593E+00	6.027E-03	1.317E-03	1.574E-03	6.039E-03	4.932E-04	2.643E+02	8.166E-02
1	17	3.879E+00	1.468E-02	3.210E-03	3.834E-03	1.471E-02	1.202E-03	2.643E+02	8.166E-02
1	18	7.212E+00	2.729E-02	5.975E-03	7.140E-03	2.739E-02	2.237E-03	2.643E+02	8.166E-02
1	19	7.395E-01	2.798E-03	6.116E-04	7.305E-04	2.804E-03	2.290E-04	2.643E+02	8.166E-02
1	20	4.269E-01	1.615E-03	3.531E-04	4.218E-04	1.619E-03	1.322E-04	2.643E+02	8.166E-02
1	21	4.351E-01	1.646E-03	3.599E-04	4.298E-04	1.650E-03	1.347E-04	2.643E+02	8.166E-02
1	22	4.183E+00	1.583E-02	3.463E-03	4.137E-03	1.587E-02	1.296E-03	2.643E+02	8.166E-02
1	23	4.110E+00	1.555E-02	3.405E-03	4.068E-03	1.561E-02	1.275E-03	2.643E+02	8.166E-02
1	24	4.809E-01	1.820E-03	3.973E-04	4.745E-04	1.822E-03	1.488E-04	2.643E+02	8.166E-02
1	25	6.837E-01	2.587E-03	5.652E-04	6.751E-04	2.591E-03	2.116E-04	2.643E+02	8.166E-02
1	26	5.130E-01	1.941E-03	4.244E-04	5.070E-04	1.946E-03	1.589E-04	2.643E+02	8.166E-02
1	28	3.574E+00	1.352E-02	2.961E-03	3.538E-03	1.357E-02	1.109E-03	2.643E+02	8.166E-02
1	29	8.795E-01	3.328E-03	7.265E-04	8.676E-04	3.330E-03	2.720E-04	2.643E+02	8.166E-02
1	30	4.983E-01	1.886E-03	4.118E-04	4.918E-04	1.888E-03	1.542E-04	2.643E+02	8.166E-02
1	31	4.437E-01	1.679E-03	3.667E-04	4.379E-04	1.681E-03	1.373E-04	2.643E+02	8.166E-02
1	32	1.065E+00	4.031E-03	8.809E-04	1.052E-03	4.038E-03	3.298E-04	2.643E+02	8.166E-02
1	33	2.963E+00	1.121E-02	2.451E-03	2.928E-03	1.124E-02	9.176E-04	2.643E+02	8.166E-02
1	34	5.890E-01	2.229E-03	4.868E-04	5.814E-04	2.231E-03	1.822E-04	2.643E+02	8.166E-02
1	37	5.543E-01	2.097E-03	4.584E-04	5.476E-04	2.102E-03	1.716E-04	2.643E+02	8.166E-02
1	38	8.344E-01	3.157E-03	6.902E-04	8.244E-04	3.164E-03	2.584E-04	2.643E+02	8.166E-02
1	39	9.348E-01	3.537E-03	7.732E-04	9.236E-04	3.545E-03	2.895E-04	2.643E+02	8.166E-02
1	40	2.790E+00	1.056E-02	2.309E-03	2.758E-03	1.058E-02	8.642E-04	2.643E+02	8.166E-02
1	41	9.545E-01	3.612E-03	7.903E-04	9.442E-04	3.623E-03	2.959E-04	2.643E+02	8.166E-02
1	42	2.657E+00	1.005E-02	2.198E-03	2.625E-03	1.007E-02	8.227E-04	2.643E+02	8.166E-02
1	43	1.005E+00	3.802E-03	8.323E-04	9.944E-04	3.815E-03	3.116E-04	2.643E+02	8.166E-02

RUN	GAGE	Q(CW)	Q(AV)/Q(O)	H(A)	H(B)	H(A)/H(O)	C(H)	Q(O)	C(H(O))
2	1	9.715E-01	3.678E-03	8.056E-04	9.627E-04	3.695E-03	3.018E-04	2.642E+02	8.170E-02
2	2	1.355E+00	5.131E-03	1.123E-03	1.342E-03	5.150E-03	4.208E-04	2.642E+02	8.170E-02
2	3	1.578E+00	5.974E-03	1.307E-03	1.561E-03	5.994E-03	4.897E-04	2.642E+02	8.170E-02
2	4	2.107E+00	7.975E-03	1.744E-03	2.084E-03	8.000E-03	6.536E-04	2.642E+02	8.170E-02
2	5	1.436E+00	5.434E-03	1.189E-03	1.420E-03	5.451E-03	4.454E-04	2.642E+02	8.170E-02
2	6	6.837E-01	2.588E-03	5.659E-04	6.761E-04	2.596E-03	2.121E-04	2.642E+02	8.170E-02
2	7	1.389E+00	5.257E-03	1.149E-03	1.373E-03	5.271E-03	4.306E-04	2.642E+02	8.170E-02
2	8	2.195E+00	8.310E-03	1.816E-03	2.170E-03	8.330E-03	6.805E-04	2.642E+02	8.170E-02
2	10	3.015E+00	1.141E-02	2.496E-03	2.981E-03	1.145E-02	9.351E-04	2.642E+02	8.170E-02
2	11	2.223E+00	8.414E-03	1.838E-03	2.195E-03	8.429E-03	6.887E-04	2.642E+02	8.170E-02
2	12	2.032E+00	7.691E-03	1.679E-03	2.005E-03	7.699E-03	6.290E-04	2.642E+02	8.170E-02
2	13	1.477E+00	5.590E-03	1.221E-03	1.458E-03	5.600E-03	4.575E-04	2.642E+02	8.170E-02
2	14	1.184E+00	4.482E-03	9.792E-04	1.170E-03	4.491E-03	3.669E-04	2.642E+02	8.170E-02
2	15	1.266E+00	4.793E-03	1.047E-03	1.251E-03	4.802E-03	3.924E-04	2.642E+02	8.170E-02
2	16	7.804E-01	2.954E-03	6.454E-04	7.709E-04	2.960E-03	2.418E-04	2.642E+02	8.170E-02
2	17	3.408E+00	1.290E-02	2.820E-03	3.369E-03	1.293E-02	1.057E-03	2.642E+02	8.170E-02
2	18	5.893E+00	2.231E-02	4.881E-03	5.832E-03	2.239E-02	1.829E-03	2.642E+02	8.170E-02
2	19	1.116E+00	4.224E-03	9.229E-04	1.102E-03	4.233E-03	3.458E-04	2.642E+02	8.170E-02
2	20	1.105E+00	4.185E-03	9.144E-04	1.092E-03	4.194E-03	3.426E-04	2.642E+02	8.170E-02
2	21	1.380E+00	5.225E-03	1.142E-03	1.364E-03	5.237E-03	4.279E-04	2.642E+02	8.170E-02
2	22	4.049E+00	1.533E-02	3.352E-03	4.004E-03	1.537E-02	1.256E-03	2.642E+02	8.170E-02
2	23	6.697E+00	2.535E-02	5.551E-03	6.633E-03	2.546E-02	2.080E-03	2.642E+02	8.170E-02
2	24	1.509E+00	5.712E-03	1.247E-03	1.489E-03	5.720E-03	4.673E-04	2.642E+02	8.170E-02
2	25	1.664E+00	6.300E-03	1.376E-03	1.644E-03	6.311E-03	5.156E-04	2.642E+02	8.170E-02
2	26	1.311E+00	4.962E-03	1.085E-03	1.296E-03	4.974E-03	4.064E-04	2.642E+02	8.170E-02
2	27	2.201E+00	8.333E-03	1.822E-03	2.176E-03	8.355E-03	6.826E-04	2.642E+02	8.170E-02
2	28	7.976E+00	3.019E-02	6.613E-03	7.903E-03	3.033E-02	2.478E-03	2.642E+02	8.170E-02
2	29	2.557E+00	9.678E-03	2.113E-03	2.523E-03	9.689E-03	7.916E-04	2.642E+02	8.170E-02
2	30	1.936E+00	7.327E-03	1.600E-03	1.911E-03	7.337E-03	5.994E-04	2.642E+02	8.170E-02
2	31	1.370E+00	5.188E-03	1.133E-03	1.353E-03	5.195E-03	4.245E-04	2.642E+02	8.170E-02
2	32	2.408E+00	9.116E-03	1.992E-03	2.379E-03	9.135E-03	7.464E-04	2.642E+02	8.170E-02
2	33	6.107E+00	2.312E-02	5.056E-03	6.040E-03	2.319E-02	1.894E-03	2.642E+02	8.170E-02
2	34	1.732E+00	6.557E-03	1.432E-03	1.710E-03	6.567E-03	5.365E-04	2.642E+02	8.170E-02
2	35	1.031E+00	3.902E-03	8.523E-04	1.018E-03	3.909E-03	3.193E-04	2.642E+02	8.170E-02
2	37	2.808E+00	1.063E-02	2.323E-03	2.776E-03	1.066E-02	8.706E-04	2.642E+02	8.170E-02
2	38	1.753E+00	6.634E-03	1.450E-03	1.732E-03	6.650E-03	5.433E-04	2.642E+02	8.170E-02
2	40	6.069E+00	2.297E-02	5.024E-03	6.002E-03	2.304E-02	1.883E-03	2.642E+02	8.170E-02
2	41	2.380E+00	9.011E-03	1.972E-03	2.356E-03	9.042E-03	7.388E-04	2.642E+02	8.170E-02
2	42	5.204E+00	1.970E-02	4.306E-03	5.144E-03	1.975E-02	1.613E-03	2.642E+02	8.170E-02
2	43	1.313E+00	4.969E-03	1.087E-03	1.299E-03	4.987E-03	4.075E-04	2.642E+02	8.170E-02

RUN	GAGE	Q(CW)	Q(AV)/Q(O)	H(A)	H(B)	H(A)/H(O)	C(H)	Q(O)	C(H(O))
3	1	2.072E+00	4.452E-03	1.714E-03	2.048E-03	4.473E-03	2.090E-04	4.655E+02	4.672E-02
3	2	2.466E+00	5.298E-03	2.038E-03	2.435E-03	5.320E-03	2.485E-04	4.655E+02	4.672E-02
3	3	3.791E+00	8.145E-03	3.132E-03	3.742E-03	8.175E-03	3.819E-04	4.655E+02	4.672E-02
3	4	4.150E+00	8.914E-03	3.427E-03	4.095E-03	8.946E-03	4.180E-04	4.655E+02	4.672E-02
3	5	2.239E+00	4.809E-03	1.848E-03	2.208E-03	4.824E-03	2.254E-04	4.655E+02	4.672E-02
3	7	2.752E+00	5.913E-03	2.272E-03	2.714E-03	5.930E-03	2.770E-04	4.655E+02	4.672E-02
3	8	3.257E+00	6.996E-03	2.687E-03	3.210E-03	7.015E-03	3.277E-04	4.655E+02	4.672E-02
3	10	3.263E+00	7.011E-03	2.694E-03	3.218E-03	7.032E-03	3.285E-04	4.655E+02	4.672E-02
3	11	3.474E+00	7.464E-03	2.865E-03	3.422E-03	7.479E-03	3.494E-04	4.655E+02	4.672E-02
3	12	3.156E+00	6.779E-03	2.600E-03	3.105E-03	6.787E-03	3.171E-04	4.655E+02	4.672E-02
3	13	3.603E+00	7.740E-03	2.971E-03	3.549E-03	7.756E-03	3.624E-04	4.655E+02	4.672E-02
3	14	2.084E+00	4.476E-03	1.719E-03	2.053E-03	4.486E-03	2.096E-04	4.655E+02	4.672E-02
3	15	2.459E+00	5.283E-03	2.029E-03	2.423E-03	5.295E-03	2.474E-04	4.655E+02	4.672E-02
3	17	7.057E+00	1.516E-02	5.826E-03	6.960E-03	1.521E-02	7.105E-04	4.655E+02	4.672E-02
3	18	1.066E+01	2.290E-02	8.810E-03	1.053E-02	2.300E-02	1.074E-03	4.655E+02	4.672E-02
3	19	2.436E+00	5.233E-03	2.010E-03	2.400E-03	5.245E-03	2.451E-04	4.655E+02	4.672E-02
3	20	2.551E+00	5.480E-03	2.105E-03	2.514E-03	5.494E-03	2.567E-04	4.655E+02	4.672E-02
3	21	3.022E+00	6.493E-03	2.494E-03	2.979E-03	6.509E-03	3.041E-04	4.655E+02	4.672E-02
3	22	8.000E+00	1.719E-02	6.608E-03	7.896E-03	1.725E-02	8.059E-04	4.655E+02	4.672E-02
3	24	2.615E+00	5.618E-03	2.155E-03	2.574E-03	5.626E-03	2.629E-04	4.655E+02	4.672E-02
3	25	3.475E+01	7.464E-02	2.883E-02	3.447E-02	7.524E-02	3.515E-03	4.655E+02	4.672E-02
3	26	2.404E+00	5.163E-03	1.983E-03	2.369E-03	5.177E-03	2.419E-04	4.655E+02	4.672E-02
3	28	1.121E+01	2.408E-02	9.273E-03	1.108E-02	2.420E-02	1.131E-03	4.655E+02	4.672E-02
3	29	3.808E+00	8.180E-03	3.138E-03	3.748E-03	8.191E-03	3.827E-04	4.655E+02	4.672E-02
3	30	3.946E+00	8.476E-03	3.253E-03	3.885E-03	8.491E-03	3.967E-04	4.655E+02	4.672E-02
3	31	3.525E+00	7.573E-03	2.907E-03	3.472E-03	7.588E-03	3.545E-04	4.655E+02	4.672E-02
3	33	1.331E+01	2.859E-02	1.100E-02	1.314E-02	2.871E-02	1.341E-03	4.655E+02	4.672E-02
3	34	4.128E+00	8.868E-03	3.404E-03	4.066E-03	8.885E-03	4.151E-04	4.655E+02	4.672E-02
3	35	3.439E+00	7.387E-03	2.836E-03	3.388E-03	7.404E-03	3.459E-04	4.655E+02	4.672E-02
3	37	5.831E+00	1.253E-02	4.814E-03	5.751E-03	1.257E-02	5.871E-04	4.655E+02	4.672E-02
3	38	4.397E+00	9.445E-03	3.629E-03	4.335E-03	9.471E-03	4.425E-04	4.655E+02	4.672E-02
3	41	6.882E+00	1.478E-02	5.688E-03	6.797E-03	1.485E-02	6.936E-04	4.655E+02	4.672E-02
3	42	3.877E+01	8.328E-02	3.219E-02	3.850E-02	8.401E-02	3.925E-03	4.655E+02	4.672E-02
3	43	4.320E+00	9.281E-03	3.571E-03	4.267E-03	9.320E-03	4.354E-04	4.655E+02	4.672E-02

RUN	GAGE	Q(CW)	Q(AV)/Q(D)	H(A)	H(B)	H(A)/H(D)	C(H)	Q(D)	C(H(D))
4	1	1.822E+01	3.943E-02	1.498E-02	1.798E-02	3.973E-02	1.889E-03	4.619E+02	4.755E-02
4	2	7.509E+00	1.626E-02	6.150E-03	7.376E-03	1.631E-02	7.757E-04	4.619E+02	4.755E-02
4	3	4.830E+00	1.046E-02	3.943E-03	4.726E-03	1.046E-02	4.973E-04	4.619E+02	4.755E-02
4	4	4.752E+00	1.029E-02	3.878E-03	4.647E-03	1.029E-02	4.891E-04	4.619E+02	4.755E-02
4	5	4.243E+00	9.185E-03	3.462E-03	4.148E-03	9.183E-03	4.366E-04	4.619E+02	4.755E-02
4	6	6.647E+00	1.439E-02	5.426E-03	6.503E-03	1.439E-02	6.844E-04	4.619E+02	4.755E-02
4	8	4.389E+00	9.501E-03	3.577E-03	4.285E-03	9.488E-03	4.511E-04	4.619E+02	4.755E-02
4	10	1.767E+01	3.824E-02	1.441E-02	1.727E-02	3.824E-02	1.818E-03	4.619E+02	4.755E-02
4	11	2.489E+01	5.389E-02	2.033E-02	2.436E-02	5.392E-02	2.564E-03	4.619E+02	4.755E-02
4	12	1.593E+01	3.448E-02	1.298E-02	1.555E-02	3.443E-02	1.637E-03	4.619E+02	4.755E-02
4	13	3.136E+00	6.789E-03	2.551E-03	3.056E-03	6.769E-03	3.218E-04	4.619E+02	4.755E-02
4	14	3.009E+00	6.515E-03	2.448E-03	2.932E-03	6.494E-03	3.088E-04	4.619E+02	4.755E-02
4	15	3.872E+00	8.382E-03	3.151E-03	3.774E-03	8.358E-03	3.974E-04	4.619E+02	4.755E-02
4	17	6.552E+00	1.418E-02	5.335E-03	6.391E-03	1.415E-02	6.729E-04	4.619E+02	4.755E-02
4	18	1.673E+01	3.622E-02	1.371E-02	1.644E-02	3.637E-02	1.729E-03	4.619E+02	4.755E-02
4	19	1.320E+00	2.858E-03	1.079E-03	1.285E-03	2.847E-03	1.354E-04	4.619E+02	4.755E-02
4	20	4.354E-01	9.427E-04	3.541E-04	4.241E-04	9.394E-04	4.467E-05	4.619E+02	4.755E-02
4	21	1.077E+00	2.330E-03	8.761E-04	1.049E-03	2.324E-03	1.105E-04	4.619E+02	4.755E-02
4	22	6.501E+00	1.407E-02	5.299E-03	6.350E-03	1.406E-02	6.684E-04	4.619E+02	4.755E-02
4	23	1.257E+01	2.722E-02	1.029E-02	1.234E-02	2.729E-02	1.298E-03	4.619E+02	4.755E-02
4	24	1.328E+00	2.876E-03	1.080E-03	1.293E-03	2.864E-03	1.362E-04	4.619E+02	4.755E-02
4	25	7.920E-01	1.714E-03	6.439E-04	7.711E-04	1.708E-03	8.121E-05	4.619E+02	4.755E-02
4	26	4.658E-01	1.008E-03	3.789E-04	4.537E-04	1.005E-03	4.778E-05	4.619E+02	4.755E-02
4	28	8.744E+00	1.893E-02	7.145E-03	8.564E-03	1.895E-02	9.011E-04	4.619E+02	4.755E-02
4	29	2.547E+00	5.513E-03	2.070E-03	2.479E-03	5.491E-03	2.611E-04	4.619E+02	4.755E-02
4	30	1.088E+00	2.354E-03	8.839E-04	1.058E-03	2.345E-03	1.115E-04	4.619E+02	4.755E-02
4	32	2.105E+00	4.556E-03	1.711E-03	2.049E-03	4.538E-03	2.158E-04	4.619E+02	4.755E-02
4	33	2.011E+01	4.353E-02	1.640E-02	1.965E-02	4.350E-02	2.068E-03	4.619E+02	4.755E-02
4	34	2.524E+00	5.465E-03	2.052E-03	2.457E-03	5.443E-03	2.588E-04	4.619E+02	4.755E-02
4	35	9.319E-01	2.017E-03	7.576E-04	9.072E-04	2.010E-03	9.555E-05	4.619E+02	4.755E-02
4	37	2.814E+00	6.093E-03	2.289E-03	2.742E-03	6.073E-03	2.887E-04	4.619E+02	4.755E-02
4	38	9.140E-01	1.979E-03	7.435E-04	8.905E-04	1.972E-03	9.378E-05	4.619E+02	4.755E-02
4	39	5.657E+00	1.225E-02	4.611E-03	5.525E-03	1.223E-02	5.816E-04	4.619E+02	4.755E-02
4	40	2.182E+00	4.723E-03	1.777E-03	2.129E-03	4.713E-03	2.241E-04	4.619E+02	4.755E-02
4	41	3.040E+00	6.582E-03	2.474E-03	2.963E-03	6.563E-03	3.121E-04	4.619E+02	4.755E-02
4	42	1.689E+00	3.657E-03	1.342E-03	1.600E-03	3.560E-03	1.693E-04	4.619E+02	4.755E-02
4	43	2.575E+00	5.574E-03	2.097E-03	2.512E-03	5.562E-03	2.645E-04	4.619E+02	4.755E-02

RUN	GAGE	Q(CW)	Q(AV)/Q(O)	H(A)	H(B)	H(A)/H(O)	C(H)	Q(O)	C(H(O))
5	1	9.379E+00	3.697E-02	7.861E-03	9.436E-03	3.719E-02	3.111E-03	2.537E+02	8.363E-02
5	2	4.314E+00	1.700E-02	3.605E-03	4.324E-03	1.705E-02	1.426E-03	2.537E+02	8.363E-02
5	3	2.820E+00	1.111E-02	2.349E-03	2.817E-03	1.112E-02	9.296E-04	2.537E+02	8.363E-02
5	4	2.681E+00	1.057E-02	2.232E-03	2.676E-03	1.056E-02	8.833E-04	2.537E+02	8.363E-02
5	5	2.365E+00	9.323E-03	1.969E-03	2.361E-03	9.318E-03	7.792E-04	2.537E+02	8.363E-02
5	6	3.548E+00	1.398E-02	2.955E-03	3.543E-03	1.398E-02	1.169E-03	2.537E+02	8.363E-02
5	7	6.491E+00	2.558E-02	5.407E-03	6.482E-03	2.558E-02	2.139E-03	2.537E+02	8.363E-02
5	8	2.320E+00	9.143E-03	1.929E-03	2.312E-03	9.127E-03	7.633E-04	2.537E+02	8.363E-02
5	10	5.175E+00	2.040E-02	4.301E-03	5.154E-03	2.035E-02	1.702E-03	2.537E+02	8.363E-02
5	11	8.076E+00	3.183E-02	6.713E-03	8.044E-03	3.176E-02	2.656E-03	2.537E+02	8.363E-02
5	12	6.238E+00	2.459E-02	5.181E-03	6.208E-03	2.451E-02	2.050E-03	2.537E+02	8.363E-02
5	13	1.432E+00	5.644E-03	1.189E-03	1.424E-03	5.624E-03	4.704E-04	2.537E+02	8.363E-02
5	14	1.622E+00	6.394E-03	1.347E-03	1.613E-03	6.371E-03	5.328E-04	2.537E+02	8.363E-02
5	15	1.913E+00	7.539E-03	1.588E-03	1.903E-03	7.514E-03	6.284E-04	2.537E+02	8.363E-02
5	16	2.294E+00	9.043E-03	1.906E-03	2.283E-03	9.016E-03	7.540E-04	2.537E+02	8.363E-02
5	17	4.766E+00	1.879E-02	3.960E-03	4.745E-03	1.874E-02	1.567E-03	2.537E+02	8.363E-02
5	18	7.620E+00	3.003E-02	6.363E-03	7.633E-03	3.011E-02	2.518E-03	2.537E+02	8.363E-02
5	19	6.969E-01	2.747E-03	5.782E-04	6.927E-04	2.736E-03	2.288E-04	2.537E+02	8.363E-02
5	20	2.875E-01	1.133E-03	2.387E-04	2.859E-04	1.129E-03	9.444E-05	2.537E+02	8.363E-02
5	21	6.472E-01	2.551E-03	5.376E-04	6.441E-04	2.543E-03	2.127E-04	2.537E+02	8.363E-02
5	22	3.753E+00	1.479E-02	3.121E-03	3.741E-03	1.477E-02	1.235E-03	2.537E+02	8.363E-02
5	23	5.545E+00	2.185E-02	4.627E-03	5.549E-03	2.189E-02	1.831E-03	2.537E+02	8.363E-02
5	24	6.691E-01	2.637E-03	5.550E-04	6.648E-04	2.626E-03	2.196E-04	2.537E+02	8.363E-02
5	25	1.924E-01	7.581E-04	1.596E-04	1.912E-04	7.551E-04	6.315E-05	2.537E+02	8.363E-02
5	26	3.694E-01	1.456E-03	3.066E-04	3.673E-04	1.451E-03	1.213E-04	2.537E+02	8.363E-02
5	27	1.387E+00	5.466E-03	1.153E-03	1.381E-03	5.453E-03	4.561E-04	2.537E+02	8.363E-02
5	28	4.242E+00	1.672E-02	3.536E-03	4.240E-03	1.673E-02	1.399E-03	2.537E+02	8.363E-02
5	29	1.027E+00	4.047E-03	8.518E-04	1.020E-03	4.030E-03	3.370E-04	2.537E+02	8.363E-02
5	30	5.453E-01	2.149E-03	4.523E-04	5.418E-04	2.140E-03	1.790E-04	2.537E+02	8.363E-02
5	31	2.500E-01	9.855E-04	2.074E-04	2.484E-04	9.812E-04	8.206E-05	2.537E+02	8.363E-02
5	32	1.305E+00	5.143E-03	1.083E-03	1.297E-03	5.122E-03	4.284E-04	2.537E+02	8.363E-02
5	33	7.606E+00	2.998E-02	6.319E-03	7.572E-03	2.990E-02	2.500E-03	2.537E+02	8.363E-02
5	34	9.783E-01	3.856E-03	8.115E-04	9.721E-04	3.840E-03	3.211E-04	2.537E+02	8.363E-02
5	35	2.602E-01	1.026E-03	2.159E-04	2.586E-04	1.021E-03	8.541E-05	2.537E+02	8.363E-02
5	37	1.193E+00	4.702E-03	9.902E-04	1.186E-03	4.685E-03	3.918E-04	2.537E+02	8.363E-02
5	38	7.028E-01	2.770E-03	5.835E-04	6.991E-04	2.761E-03	2.309E-04	2.537E+02	8.363E-02
5	39	2.287E+00	9.014E-03	1.902E-03	2.279E-03	8.998E-03	7.525E-04	2.537E+02	8.363E-02
5	40	1.311E+00	5.169E-03	1.090E-03	1.306E-03	5.158E-03	4.313E-04	2.537E+02	8.363E-02
5	41	1.256E+00	4.950E-03	1.043E-03	1.249E-03	4.934E-03	4.126E-04	2.537E+02	8.363E-02
5	42	4.206E-01	1.658E-03	3.408E-04	4.064E-04	1.612E-03	1.349E-04	2.537E+02	8.363E-02
5	43	1.365E+00	5.381E-03	1.135E-03	1.360E-03	5.368E-03	4.489E-04	2.537E+02	8.363E-02

RUN	GAGE	Q(CW)	Q(AV)/Q(O)	H(A)	H(B)	H(A)/H(O)	C(H)	Q(O)	C(H(O))
6	1	5.150E+00	4.143E-02	4.308E-03	5.170E-03	4.166E-02	7.106E-03	1.243E+02	1.706E-01
6	2	2.387E+00	1.920E-02	1.991E-03	2.389E-03	1.926E-02	3.285E-03	1.243E+02	1.706E-01
6	3	1.358E+00	1.093E-02	1.130E-03	1.355E-03	1.093E-02	1.864E-03	1.243E+02	1.706E-01
6	4	1.432E+00	1.152E-02	1.191E-03	1.427E-03	1.151E-02	1.964E-03	1.243E+02	1.706E-01
6	5	1.358E+00	1.092E-02	1.129E-03	1.353E-03	1.092E-02	1.862E-03	1.243E+02	1.706E-01
6	6	1.801E+00	1.449E-02	1.498E-03	1.795E-03	1.448E-02	2.471E-03	1.243E+02	1.706E-01
6	7	2.634E+00	2.119E-02	2.190E-03	2.625E-03	2.118E-02	3.613E-03	1.243E+02	1.706E-01
6	8	1.139E+00	9.161E-03	9.455E-04	1.133E-03	9.142E-03	1.560E-03	1.243E+02	1.706E-01
6	9	9.593E-01	7.718E-03	7.960E-04	9.538E-04	7.697E-03	1.313E-03	1.243E+02	1.706E-01
6	10	1.659E+00	1.335E-02	1.377E-03	1.649E-03	1.331E-02	2.271E-03	1.243E+02	1.706E-01
6	12	1.501E+00	1.207E-02	1.244E-03	1.490E-03	1.203E-02	2.052E-03	1.243E+02	1.706E-01
6	13	5.998E-01	4.826E-03	4.972E-04	5.957E-04	4.808E-03	8.202E-04	1.243E+02	1.706E-01
6	14	7.136E-01	5.741E-03	5.916E-04	7.087E-04	5.720E-03	9.759E-04	1.243E+02	1.706E-01
6	15	1.129E+00	9.083E-03	9.361E-04	1.122E-03	9.052E-03	1.544E-03	1.243E+02	1.706E-01
6	16	1.279E+00	1.029E-02	1.060E-03	1.271E-03	1.025E-02	1.748E-03	1.243E+02	1.706E-01
6	17	1.936E+00	1.558E-02	1.606E-03	1.924E-03	1.553E-02	2.650E-03	1.243E+02	1.706E-01
6	18	3.377E+00	2.717E-02	2.814E-03	3.375E-03	2.721E-02	4.643E-03	1.243E+02	1.706E-01
6	19	3.276E-01	2.636E-03	2.715E-04	3.252E-04	2.625E-03	4.478E-04	1.243E+02	1.706E-01
6	20	2.433E-01	1.957E-03	2.017E-04	2.416E-04	1.950E-03	3.327E-04	1.243E+02	1.706E-01
6	21	4.193E-01	3.373E-03	3.478E-04	4.168E-04	3.364E-03	5.738E-04	1.243E+02	1.706E-01
6	22	1.456E+00	1.171E-02	1.209E-03	1.449E-03	1.169E-02	1.994E-03	1.243E+02	1.706E-01
6	23	2.354E+00	1.894E-02	1.961E-03	2.352E-03	1.896E-02	3.235E-03	1.243E+02	1.706E-01
6	24	3.102E-01	2.496E-03	2.570E-04	3.078E-04	2.485E-03	4.239E-04	1.243E+02	1.706E-01
6	25	2.527E-01	2.033E-03	2.095E-04	2.509E-04	2.025E-03	3.455E-04	1.243E+02	1.706E-01
6	26	2.601E-01	2.092E-03	2.156E-04	2.583E-04	2.085E-03	3.557E-04	1.243E+02	1.706E-01
6	27	6.060E-01	4.875E-03	5.029E-04	6.026E-04	4.863E-03	8.296E-04	1.243E+02	1.706E-01
6	28	1.685E+00	1.355E-02	1.402E-03	1.681E-03	1.356E-02	2.312E-03	1.243E+02	1.706E-01
6	29	2.772E-01	2.230E-03	2.296E-04	2.750E-04	2.220E-03	3.788E-04	1.243E+02	1.706E-01
6	30	1.950E-01	1.569E-03	1.615E-04	1.935E-04	1.562E-03	2.665E-04	1.243E+02	1.706E-01
6	32	5.839E-01	4.698E-03	4.837E-04	5.794E-04	4.678E-03	7.980E-04	1.243E+02	1.706E-01
6	33	2.210E+00	1.778E-02	1.832E-03	2.195E-03	1.772E-02	3.022E-03	1.243E+02	1.706E-01
6	34	1.773E-01	1.426E-03	1.468E-04	1.759E-04	1.420E-03	2.422E-04	1.243E+02	1.706E-01
6	35	2.089E-01	1.680E-03	1.730E-04	2.073E-04	1.673E-03	2.855E-04	1.243E+02	1.706E-01
6	37	2.925E-01	2.353E-03	2.425E-04	2.905E-04	2.345E-03	4.000E-04	1.243E+02	1.706E-01
6	38	2.577E-01	2.073E-03	2.137E-04	2.560E-04	2.067E-03	3.525E-04	1.243E+02	1.706E-01
6	39	6.969E-01	5.607E-03	5.786E-04	6.934E-04	5.595E-03	9.545E-04	1.243E+02	1.706E-01
6	40	7.312E-01	5.883E-03	6.070E-04	7.273E-04	5.869E-03	1.001E-03	1.243E+02	1.706E-01
6	41	2.487E-01	2.001E-03	2.063E-04	2.471E-04	1.994E-03	3.402E-04	1.243E+02	1.706E-01
6	42	3.179E-01	2.558E-03	2.573E-04	3.068E-04	2.488E-03	4.244E-04	1.243E+02	1.706E-01
6	43	2.530E-01	2.035E-03	2.100E-04	2.516E-04	2.030E-03	3.463E-04	1.243E+02	1.706E+01

RUN	GAGE	Q(CW)	Q(AV)/Q(O)	H(A)	H(B)	H(A)/H(O)	C(H)	Q(O)	C(H(O))
7	1	1.036E+01	4.969E-02	8.702E-03	1.045E-02	5.002E-02	5.126E-03	2.085E+02	1.025E-01
7	2	4.380E+00	2.101E-02	3.667E-03	4.400E-03	2.108E-02	2.160E-03	2.085E+02	1.025E-01
7	3	2.504E+00	1.201E-02	2.090E-03	2.506E-03	1.201E-02	1.231E-03	2.085E+02	1.025E-01
7	4	2.428E+00	1.165E-02	2.025E-03	2.428E-03	1.164E-02	1.193E-03	2.085E+02	1.025E-01
7	5	2.429E+00	1.165E-02	2.026E-03	2.429E-03	1.165E-02	1.193E-03	2.085E+02	1.025E-01
7	6	3.259E+00	1.563E-02	2.719E-03	3.260E-03	1.563E-02	1.602E-03	2.085E+02	1.025E-01
7	7	5.408E+00	2.594E-02	4.512E-03	5.410E-03	2.594E-02	2.658E-03	2.085E+02	1.025E-01
7	8	1.893E+00	9.080E-03	1.577E-03	1.890E-03	9.063E-03	9.288E-04	2.085E+02	1.025E-01
7	9	1.354E+00	6.495E-03	1.127E-03	1.351E-03	6.479E-03	6.639E-04	2.085E+02	1.025E-01
7	10	3.083E+00	1.479E-02	2.567E-03	3.076E-03	1.475E-02	1.512E-03	2.085E+02	1.025E-01
7	12	3.672E+00	1.761E-02	3.054E-03	3.659E-03	1.756E-02	1.799E-03	2.085E+02	1.025E-01
7	13	1.101E+00	5.281E-03	9.155E-04	1.097E-03	5.262E-03	5.393E-04	2.085E+02	1.025E-01
7	14	1.173E+00	5.625E-03	9.757E-04	1.169E-03	5.609E-03	5.747E-04	2.085E+02	1.025E-01
7	15	1.783E+00	8.555E-03	1.483E-03	1.777E-03	8.527E-03	8.738E-04	2.085E+02	1.025E-01
7	16	2.449E+00	1.175E-02	2.038E-03	2.442E-03	1.172E-02	1.201E-03	2.085E+02	1.025E-01
7	17	3.669E+00	1.760E-02	3.054E-03	3.659E-03	1.755E-02	1.799E-03	2.085E+02	1.025E-01
7	18	5.281E+00	2.533E-02	4.417E-03	5.298E-03	2.539E-02	2.602E-03	2.085E+02	1.025E-01
7	19	6.785E-01	3.255E-03	5.639E-04	6.756E-04	3.242E-03	3.322E-04	2.085E+02	1.025E-01
7	20	3.583E-01	1.719E-03	2.979E-04	3.569E-04	1.713E-03	1.755E-04	2.085E+02	1.025E-01
7	21	6.355E-01	3.049E-03	5.288E-04	6.337E-04	3.040E-03	3.115E-04	2.085E+02	1.025E-01
7	22	3.025E+00	1.451E-02	2.520E-03	3.021E-03	1.449E-02	1.485E-03	2.085E+02	1.025E-01
7	23	4.556E+00	2.186E-02	3.809E-03	4.568E-03	2.189E-02	2.244E-03	2.085E+02	1.025E-01
7	24	5.370E-01	2.576E-03	4.462E-04	5.345E-04	2.565E-03	2.629E-04	2.085E+02	1.025E-01
7	25	2.543E-01	1.220E-03	2.114E-04	2.532E-04	1.215E-03	1.245E-04	2.085E+02	1.025E-01
7	26	3.259E-01	1.563E-03	2.710E-04	3.247E-04	1.558E-03	1.597E-04	2.085E+02	1.025E-01
7	27	1.383E+00	6.637E-03	1.152E-03	1.380E-03	6.621E-03	6.785E-04	2.085E+02	1.025E-01
7	28	2.992E+00	1.435E-02	2.498E-03	2.995E-03	1.436E-02	1.471E-03	2.085E+02	1.025E-01
7	29	6.720E-01	3.224E-03	5.584E-04	6.689E-04	3.210E-03	3.289E-04	2.085E+02	1.025E-01
7	30	4.215E-01	2.022E-03	3.503E-04	4.196E-04	2.013E-03	2.063E-04	2.085E+02	1.025E-01
7	31	2.353E-01	1.129E-03	1.955E-04	2.342E-04	1.124E-03	1.152E-04	2.085E+02	1.025E-01
7	32	1.075E+00	5.159E-03	8.937E-04	1.071E-03	5.137E-03	5.264E-04	2.085E+02	1.025E-01
7	33	5.682E+00	2.726E-02	4.728E-03	5.665E-03	2.718E-02	2.785E-03	2.085E+02	1.025E-01
7	34	7.571E-01	3.632E-03	6.292E-04	7.537E-04	3.617E-03	3.706E-04	2.085E+02	1.025E-01
7	35	3.673E-01	1.762E-03	3.053E-04	3.657E-04	1.755E-03	1.798E-04	2.085E+02	1.025E-01
7	37	7.800E-01	3.742E-03	6.485E-04	7.770E-04	3.728E-03	3.820E-04	2.085E+02	1.025E-01
7	38	3.045E-01	1.461E-03	2.533E-04	3.034E-04	1.456E-03	1.492E-04	2.085E+02	1.025E-01
7	39	1.542E+00	7.397E-03	1.284E-03	1.539E-03	7.383E-03	7.565E-04	2.085E+02	1.025E-01
7	40	1.124E+00	5.391E-03	9.357E-04	1.121E-03	5.379E-03	5.512E-04	2.085E+02	1.025E-01
7	41	8.567E-01	4.110E-03	7.126E-04	8.538E-04	4.096E-03	4.198E-04	2.085E+02	1.025E-01
7	42	3.794E-01	1.820E-03	3.079E-04	3.672E-04	1.770E-03	1.814E-04	2.085E+02	1.025E-01
7	43	4.401E-01	2.111E-03	3.663E-04	4.390E-04	2.106E-03	2.158E-04	2.085E+02	1.025E-01

RUN	GAGE	Q(CW)	Q(AV)/Q(O)	H(A)	H(B)	H(A)/H(O)	C(H)	Q(O)	C(H(O))
8	1	2.033E+01	4.376E-02	1.753E-02	2.124E-02	4.606E-02	2.163E-03	4.645E+02	4.697E-02
8	2	7.963E+00	1.714E-02	6.817E-03	8.243E-03	1.791E-02	8.410E-04	4.645E+02	4.697E-02
8	3	5.357E+00	1.153E-02	4.526E-03	5.458E-03	1.189E-02	5.584E-04	4.645E+02	4.697E-02
8	4	5.000E+00	1.076E-02	4.200E-03	5.058E-03	1.103E-02	5.181E-04	4.645E+02	4.697E-02
8	5	4.007E+00	8.628E-03	3.365E-03	4.053E-03	8.840E-03	4.152E-04	4.645E+02	4.697E-02
8	6	6.120E+00	1.318E-02	5.151E-03	6.206E-03	1.353E-02	6.355E-04	4.645E+02	4.697E-02
8	7	9.903E+00	2.132E-02	8.336E-03	1.005E-02	2.190E-02	1.029E-03	4.645E+02	4.697E-02
8	8	4.548E+00	9.792E-03	3.774E-03	4.535E-03	9.915E-03	4.657E-04	4.645E+02	4.697E-02
8	9	4.002E+00	8.617E-03	3.307E-03	3.969E-03	8.686E-03	4.080E-04	4.645E+02	4.697E-02
8	10	1.736E+01	3.738E-02	1.431E-02	1.717E-02	3.759E-02	1.765E-03	4.645E+02	4.697E-02
8	12	1.795E+01	3.865E-02	1.474E-02	1.768E-02	3.873E-02	1.819E-03	4.645E+02	4.697E-02
8	13	2.465E+00	5.306E-03	2.014E-03	2.412E-03	5.291E-03	2.485E-04	4.645E+02	4.697E-02
8	14	3.106E+00	6.687E-03	2.541E-03	3.044E-03	6.675E-03	3.135E-04	4.645E+02	4.697E-02
8	15	3.251E+00	6.999E-03	2.662E-03	3.189E-03	6.992E-03	3.284E-04	4.645E+02	4.697E-02
8	16	2.556E+00	5.503E-03	2.095E-03	2.511E-03	5.504E-03	2.585E-04	4.645E+02	4.697E-02
8	17	8.655E+00	1.863E-02	7.104E-03	8.516E-03	1.866E-02	8.764E-04	4.645E+02	4.697E-02
8	18	1.442E+01	3.104E-02	1.186E-02	1.422E-02	3.115E-02	1.463E-03	4.645E+02	4.697E-02
8	19	1.267E+00	2.771E-03	1.047E-03	1.253E-03	2.750E-03	1.292E-04	4.645E+02	4.697E-02
8	20	6.008E-01	1.294E-03	4.902E-04	5.870E-04	1.288E-03	6.048E-05	4.645E+02	4.697E-02
8	21	1.198E+00	2.579E-03	9.809E-04	1.175E-03	2.577E-03	1.210E-04	4.645E+02	4.697E-02
8	22	6.564E+00	1.413E-02	5.404E-03	6.483E-03	1.420E-02	6.668E-04	4.645E+02	4.697E-02
8	23	1.216E+01	2.618E-02	1.014E-02	1.219E-02	2.663E-02	1.251E-03	4.645E+02	4.697E-02
8	24	1.059E+00	2.279E-03	8.595E-04	1.028E-03	2.258E-03	1.060E-04	4.645E+02	4.697E-02
8	25	4.989E-01	1.074E-03	4.061E-04	4.860E-04	1.067E-03	5.010E-05	4.645E+02	4.697E-02
8	26	4.755E-01	1.024E-03	3.881E-04	4.647E-04	1.019E-03	4.788E-05	4.645E+02	4.697E-02
8	27	2.542E+00	5.472E-03	2.082E-03	2.494E-03	5.468E-03	2.568E-04	4.645E+02	4.697E-02
8	28	6.792E+00	1.462E-02	5.633E-03	6.767E-03	1.480E-02	6.950E-04	4.645E+02	4.697E-02
8	29	2.456E+00	5.287E-03	1.989E-03	2.379E-03	5.225E-03	2.454E-04	4.645E+02	4.697E-02
8	30	1.213E+00	2.612E-03	9.837E-04	1.176E-03	2.584E-03	1.214E-04	4.645E+02	4.697E-02
8	32	2.809E+00	6.048E-03	2.283E-03	2.732E-03	5.997E-03	2.817E-04	4.645E+02	4.697E-02
8	33	1.560E+01	3.358E-02	1.277E-02	1.530E-02	3.354E-02	1.575E-03	4.645E+02	4.697E-02
8	35	1.040E+00	2.240E-03	8.447E-04	1.010E-03	2.219E-03	1.042E-04	4.645E+02	4.697E-02
8	37	2.754E+00	5.930E-03	2.237E-03	2.676E-03	5.875E-03	2.760E-04	4.645E+02	4.697E-02
8	38	1.301E+00	2.801E-03	1.059E-03	1.267E-03	2.781E-03	1.306E-04	4.645E+02	4.697E-02
8	39	4.999E+00	1.076E-02	4.076E-03	4.880E-03	1.071E-02	5.028E-04	4.645E+02	4.697E-02
8	40	1.056E+00	2.274E-03	8.678E-04	1.041E-03	2.279E-03	1.071E-04	4.645E+02	4.697E-02
8	41	3.074E+00	6.618E-03	2.498E-03	2.989E-03	6.562E-03	3.032E-04	4.645E+02	4.697E-02
8	42	1.426E+00	3.071E-03	1.182E-03	1.419E-03	3.104E-03	1.458E-04	4.645E+02	4.697E-02
8	43	2.166E+00	4.663E-03	1.763E-03	2.110E-03	4.631E-03	2.175E-04	4.645E+02	4.697E-02

RUN	GAGE	Q(CW)	Q(AV)/Q(O)	H(A)	H(B)	H(A)/H(O)	C(H)	Q(O)	C(H(O))
9	1	1.644E+01	4.269E-02	1.420E-02	1.720E-02	4.490E-02	2.535E-03	3.851E+02	5.647E-02
9	2	6.236E+00	1.619E-02	5.347E-03	6.465E-03	1.691E-02	9.547E-04	3.851E+02	5.647E-02
9	3	4.263E+00	1.107E-02	3.608E-03	4.351E-03	1.141E-02	6.442E-04	3.851E+02	5.647E-02
9	4	4.114E+00	1.068E-02	3.461E-03	4.169E-03	1.094E-02	6.180E-04	3.851E+02	5.647E-02
9	5	3.408E+00	8.849E-03	2.867E-03	3.453E-03	9.066E-03	5.119E-04	3.851E+02	5.647E-02
9	6	5.024E+00	1.304E-02	4.235E-03	5.103E-03	1.339E-02	7.562E-04	3.851E+02	5.647E-02
9	7	8.952E+00	2.324E-02	7.549E-03	9.097E-03	2.387E-02	1.348E-03	3.851E+02	5.647E-02
9	8	3.909E+00	1.015E-02	3.249E-03	3.904E-03	1.028E-02	5.802E-04	3.851E+02	5.647E-02
9	9	3.225E+00	8.374E-03	2.669E-03	3.204E-03	8.440E-03	4.766E-04	3.851E+02	5.647E-02
9	10	1.274E+01	3.309E-02	1.051E-02	1.261E-02	3.325E-02	1.877E-03	3.851E+02	5.647E-02
9	12	1.527E+01	3.965E-02	1.256E-02	1.506E-02	3.972E-02	2.243E-03	3.851E+02	5.647E-02
9	13	2.267E+00	5.887E-03	1.856E-03	2.222E-03	5.867E-03	3.313E-04	3.851E+02	5.647E-02
9	14	2.683E+00	6.967E-03	2.199E-03	2.635E-03	6.953E-03	3.926E-04	3.851E+02	5.647E-02
9	15	2.584E+00	6.706E-03	2.119E-03	2.539E-03	6.700E-03	3.783E-04	3.851E+02	5.647E-02
9	16	2.815E+00	7.308E-03	2.311E-03	2.770E-03	7.309E-03	4.127E-04	3.851E+02	5.647E-02
9	17	7.703E+00	2.000E-02	6.333E-03	7.592E-03	2.003E-02	1.131E-03	3.851E+02	5.647E-02
9	18	1.265E+01	3.285E-02	1.042E-02	1.250E-02	3.295E-02	1.860E-03	3.851E+02	5.647E-02
9	19	1.251E+00	3.249E-03	1.020E-03	1.221E-03	3.225E-03	1.821E-04	3.851E+02	5.647E-02
9	20	4.912E-01	1.275E-03	4.015E-04	4.807E-04	1.269E-03	7.168E-05	3.851E+02	5.647E-02
9	21	1.1[illegible]E+00	2.938E-03	9.282E-04	1.112E-03	2.935E-03	1.657E-04	3.851E+02	5.647E-02
9	22	5.716E+00	1.484E-02	4.714E-03	5.654E-03	1.491E-02	8.416E-04	3.851E+02	5.647E-02
9	23	1.028E+01	2.669E-02	8.586E-03	1.033E-02	2.715E-02	1.533E-03	3.851E+02	5.647E-02
9	24	1.144E+00	2.970E-03	9.304E-04	1.113E-03	2.942E-03	1.661E-04	3.851E+02	5.647E-02
9	25	4.666E-01	1.212E-03	3.805E-04	4.554E-04	1.203E-03	6.793E-05	3.851E+02	5.647E-02
9	26	4.350E-01	1.129E-03	3.557E-04	4.259E-04	1.125E-03	6.3[illegible]E-05	3.851E+02	5.647E-02
9	27	2.227E+00	5.782E-03	1.827E-03	2.189E-03	5.777E-03	3.262E-04	3.851E+02	5.647E-02
9	28	6.201E+00	1.610E-02	5.151E-03	6.189E-03	1.629E-02	9.198E-04	3.851E+02	5.647E-02
9	29	1.948E+00	5.057E-03	1.580E-03	1.890E-03	4.998E-03	2.822E-04	3.851E+02	5.647E-02
9	30	7.928E-01	2.058E-03	6.436E-04	7.700E-04	2.036E-03	1.150E-04	3.851E+02	5.647E-02
9	32	2.285E+00	5.932E-03	1.860E-03	2.226E-03	5.882E-03	3.322E-04	3.851E+02	5.647E-02
9	33	8.617E+00	2.237E-02	7.057E-03	8.455E-03	2.232E-02	1.260E-03	3.851E+02	5.647E-02
9	34	1.852E+00	4.808E-03	1.504E-03	1.799E-03	4.755E-03	2.685E-04	3.851E+02	5.647E-02
9	35	6.334E-01	1.644E-03	5.150E-04	6.161E-04	1.629E-03	9.196E-05	3.851E+02	5.647E-02
9	37	2.123E+00	5.511E-03	1.726E-03	2.065E-03	5.459E-03	3.083E-04	3.851E+02	5.647E-02
9	38	7.903E-01	2.052E-03	6.443E-04	7.712E-04	2.037E-03	1.150E-04	3.851E+02	5.647E-02
9	39	3.726E+00	9.674E-03	3.043E-03	3.643E-03	9.621E-03	5.433E-04	3.851E+02	5.647E-02
9	40	1.813E+00	4.721E-03	1.497E-03	1.795E-03	4.733E-03	2.673E-04	3.851E+02	5.647E-02
9	41	2.121E+00	5.506E-03	1.726E-03	2.065E-03	5.459E-03	3.082E-04	3.851E+02	5.647E-02
9	42	1.154E+00	2.998E-03	9.583E-04	1.151E-03	3.030E-03	1.711E-04	3.851E+02	5.647E-02
9	43	2.268E+00	5.890E-03	1.850E-03	2.214E-03	5.849E-03	3.303E-04	3.851E+02	5.647E-02

RUN	GAGE	Q(CM)	Q(AV)/Q(O)	H(A)	H(B)	H(A)/H(O)	C(H)	Q(O)	C(H(O))
10	1	1.241E+01	5.030E-02	1.105E-02	1.339E-02	5.295E-02	4.450E-03	2.467E+02	8.404E-02
10	2	4.960E+00	2.010E-02	4.385E-03	5.306E-03	2.101E-02	1.766E-03	2.467E+02	8.404E-02
10	3	3.165E+00	1.283E-02	2.761E-03	3.332E-03	1.323E-02	1.112E-03	2.467E+02	8.404E-02
10	4	3.053E+00	1.237E-02	2.647E-03	3.190E-03	1.269E-02	1.066E-03	2.467E+02	8.404E-02
10	5	2.628E+00	1.065E-02	2.279E-03	2.746E-03	1.092E-02	9.178E-04	2.467E+02	8.404E-02
10	6	3.691E+00	1.496E-02	3.206E-03	3.866E-03	1.537E-02	1.291E-03	2.467E+02	8.404E-02
10	7	6.069E+00	2.460E-02	5.272E-03	6.357E-03	2.527E-02	2.123E-03	2.467E+02	8.404E-02
10	8	2.793E+00	1.132E-02	2.392E-03	2.875E-03	1.146E-02	9.632E-04	2.467E+02	8.404E-02
10	9	2.299E+00	9.318E-03	1.960E-03	2.354E-03	9.392E-03	7.893E-04	2.467E+02	8.404E-02
10	10	6.225E+00	2.523E-02	5.285E-03	6.343E-03	2.533E-02	2.129E-03	2.467E+02	8.404E-02
10	12	7.119E+00	2.885E-02	6.022E-03	7.223E-03	2.886E-02	2.426E-03	2.467E+02	8.404E-02
10	13	1.601E+00	6.490E-03	1.349E-03	1.617E-03	6.467E-03	5.435E-04	2.467E+02	8.404E-02
10	14	1.633E+00	6.617E-03	1.378E-03	1.652E-03	6.603E-03	5.549E-04	2.467E+02	8.404E-02
10	15	1.815E+00	7.357E-03	1.533E-03	1.838E-03	7.348E-03	6.175E-04	2.467E+02	8.404E-02
10	16	2.521E+00	1.022E-02	2.132E-03	2.557E-03	1.022E-02	8.587E-04	2.467E+02	8.404E-02
10	17	5.193E+00	2.104E-02	4.395E-03	5.271E-03	2.106E-02	1.770E-03	2.467E+02	8.404E-02
10	18	8.713E+00	3.531E-02	7.366E-03	8.862E-03	3.540E-02	2.975E-03	2.467E+02	8.404E-02
10	19	7.466E-01	3.026E-03	6.265E-04	7.502E-04	3.003E-03	2.523E-04	2.467E+02	8.404E-02
10	20	3.677E-01	1.490E-03	3.094E-04	3.707E-04	1.483E-03	1.246E-04	2.467E+02	8.404E-02
10	21	8.238E-01	3.339E-03	6.959E-04	8.343E-04	3.335E-03	2.803E-04	2.467E+02	8.404E-02
10	22	3.825E+00	1.550E-02	3.248E-03	3.899E-03	1.557E-02	1.308E-03	2.467E+02	8.404E-02
10	24	7.886E-01	3.196E-03	6.604E-04	7.904E-04	3.165E-03	2.660E-04	2.467E+02	8.404E-02
10	25	2.909E-01	1.179E-03	2.442E-04	2.924E-04	1.170E-03	9.835E-05	2.467E+02	8.404E-02
10	26	4.614E-01	1.870E-03	3.885E-04	4.655E-04	1.862E-03	1.565E-04	2.467E+02	8.404E-02
10	27	1.607E+00	6.512E-03	1.357E-03	1.628E-03	6.506E-03	5.467E-04	2.467E+02	8.404E-02
10	28	4.310E+00	1.747E-02	3.688E-03	4.433E-03	1.767E-02	1.485E-03	2.467E+02	8.404E-02
10	29	1.080E+00	4.400E-03	9.068E-04	1.085E-03	4.346E-03	3.652E-04	2.467E+02	8.404E-02
10	30	4.889E-01	1.981E-03	4.087E-04	4.891E-04	1.959E-03	1.646E-04	2.467E+02	8.404E-02
10	31	3.949E-01	1.600E-03	3.305E-04	3.956E-04	1.584E-03	1.331E-04	2.467E+02	8.404E-02
10	32	1.537E+00	6.230E-03	1.289E-03	1.543E-03	6.175E-03	5.190E-04	2.467E+02	8.404E-02
10	33	5.744E+00	2.328E-02	4.843E-03	5.804E-03	2.321E-02	1.951E-03	2.467E+02	8.404E-02
10	34	1.219E+00	4.939E-03	1.019E-03	1.219E-03	4.883E-03	4.104E-04	2.467E+02	8.404E-02
10	35	3.953E-01	1.602E-03	3.309E-04	3.961E-04	1.586E-03	1.333E-04	2.467E+02	8.404E-02
10	37	1.231E+00	4.988E-03	1.030E-03	1.233E-03	4.939E-03	4.150E-04	2.467E+02	8.404E-02
10	38	4.514E-01	1.829E-03	3.789E-04	4.537E-04	1.816E-03	1.526E-04	2.467E+02	8.404E-02
10	39	2.160E+00	8.755E-03	1.816E-03	2.175E-03	8.704E-03	7.315E-04	2.467E+02	8.404E-02
10	40	1.547E+00	6.268E-03	1.311E-03	1.573E-03	6.284E-03	5.281E-04	2.467E+02	8.404E-02
10	42	7.697E-01	3.119E-03	6.562E-04	7.911E-04	3.154E-03	2.651E-04	2.467E+02	8.404E-02
10	43	1.175E+00	4.763E-03	9.866E-04	1.181E-03	4.728E-03	3.974E-04	2.467E+02	8.404E-02

RUN	GAGE	Q(CW)	Q(AV)/Q(D)	H(A)	H(B)	H(A)/H(D)	C(H)	Q(D)	C(H(D))
11	1	5.738E+00	4.882E-02	5.089E-03	6.166E-03	5.133E-02	9.057E-03	1.175E+02	1.765E-01
11	2	2.530E+00	2.153E-02	2.230E-03	2.698E-03	2.249E-02	3.969E-03	1.175E+02	1.765E-01
11	3	1.561E+00	1.328E-02	1.358E-03	1.638E-03	1.369E-02	2.417E-03	1.175E+02	1.765E-01
11	4	1.571E+00	1.337E-02	1.359E-03	1.638E-03	1.370E-02	2.418E-03	1.175E+02	1.765E-01
11	5	1.437E+00	1.222E-02	1.242E-03	1.497E-03	1.253E-02	2.211E-03	1.175E+02	1.765E-01
11	6	1.827E+00	1.555E-02	1.583E-03	1.908E-03	1.596E-02	2.817E-03	1.175E+02	1.765E-01
11	7	2.647E+00	2.252E-02	2.292E-03	2.763E-03	2.312E-02	4.079E-03	1.175E+02	1.765E-01
11	8	1.262E+00	1.073E-02	1.077E-03	1.295E-03	1.087E-02	1.918E-03	1.175E+02	1.765E-01
11	9	1.053E+00	8.957E-03	8.949E-04	1.075E-03	9.026E-03	1.593E-03	1.175E+02	1.765E-01
11	10	1.687E+00	1.435E-02	1.427E-03	1.713E-03	1.440E-02	2.540E-03	1.175E+02	1.765E-01
11	12	1.484E+00	1.263E-02	1.252E-03	1.501E-03	1.262E-02	2.227E-03	1.175E+02	1.765E-01
11	13	5.777E-01	4.915E-03	4.855E-04	5.818E-04	4.897E-03	8.641E-04	1.175E+02	1.765E-01
11	14	6.860E-01	5.836E-03	5.773E-04	6.920E-04	5.823E-03	1.027E-03	1.175E+02	1.765E-01
11	15	1.176E+00	1.000E-02	9.902E-04	1.187E-03	9.987E-03	1.762E-03	1.175E+02	1.765E-01
11	16	1.493E+00	1.271E-02	1.260E-03	1.510E-03	1.270E-02	2.242E-03	1.175E+02	1.765E-01
11	17	2.127E+00	1.810E-02	1.795E-03	2.153E-03	1.810E-02	3.194E-03	1.175E+02	1.765E-01
11	18	3.505E+00	2.982E-02	2.962E-03	3.553E-03	2.987E-02	5.271E-03	1.175E+02	1.765E-01
11	19	4.195E-01	3.569E-03	3.511E-04	4.204E-04	3.541E-03	6.249E-04	1.175E+02	1.765E-01
11	20	3.173E-01	2.700E-03	2.664E-04	3.192E-04	2.687E-03	4.741E-04	1.175E+02	1.765E-01
11	21	4.336E-01	3.689E-03	3.654E-04	4.380E-04	3.685E-03	6.503E-04	1.175E+02	1.765E-01
11	22	1.697E+00	1.444E-02	1.437E-03	1.724E-03	1.449E-02	2.557E-03	1.175E+02	1.765E-01
11	23	2.578E+00	2.194E-02	2.210E-03	2.659E-03	2.229E-02	3.934E-03	1.175E+02	1.765E-01
11	24	3.148E-01	2.678E-03	2.629E-04	3.147E-04	2.652E-03	4.680E-04	1.175E+02	1.765E-01
11	25	2.780E-01	2.365E-03	2.328E-04	2.788E-04	2.348E-03	4.144E-04	1.175E+02	1.765E-01
11	26	2.799E-01	2.382E-03	2.351E-04	2.817E-04	2.371E-03	4.184E-04	1.175E+02	1.765E-01
11	27	7.018E-01	5.971E-03	5.913E-04	7.090E-04	5.964E-03	1.052E-03	1.175E+02	1.765E-01
11	28	2.097E+00	1.784E-02	1.789E-03	2.150E-03	1.804E-02	3.184E-03	1.175E+02	1.765E-01
11	29	3.608E-01	3.070E-03	3.006E-04	3.596E-04	3.032E-03	5.350E-04	1.175E+02	1.765E-01
11	30	2.451E-01	2.085E-03	2.044E-04	2.445E-04	2.061E-03	3.637E-04	1.175E+02	1.765E-01
11	31	2.450E-01	2.085E-03	2.046E-04	2.448E-04	2.063E-03	3.641E-04	1.175E+02	1.765E-01
11	32	6.237E-01	5.306E-03	5.214E-04	6.242E-04	5.259E-03	9.280E-04	1.175E+02	1.765E-01
11	33	2.341E+00	1.991E-02	1.967E-03	2.357E-03	1.984E-02	3.501E-03	1.175E+02	1.765E-01
11	34	3.352E-01	2.852E-03	2.795E-04	3.345E-04	2.819E-03	4.975E-04	1.175E+02	1.765E-01
11	35	2.460E-01	2.093E-03	2.054E-04	2.458E-04	2.072E-03	3.656E-04	1.175E+02	1.765E-01
11	37	3.210E-01	2.731E-03	2.681E-04	3.209E-04	2.704E-03	4.772E-04	1.175E+02	1.765E-01
11	38	2.771E-01	2.357E-03	2.320E-04	2.778E-04	2.340E-03	4.129E-04	1.175E+02	1.765E-01
11	39	6.945E-01	5.909E-03	5.623E-04	6.974E-04	5.873E-03	1.036E-03	1.175E+02	1.765E-01
11	40	8.098E-01	6.890E-03	6.648E-04	8.215E-04	6.906E-03	1.219E-03	1.175E+02	1.765E-01
11	41	3.232E-01	2.750E-03	2.702E-04	3.234E-04	2.725E-03	4.808E-04	1.175E+02	1.765E-01
11	42	4.080E-01	3.472E-03	3.480E-04	4.163E-04	3.510E-03	6.194E-04	1.175E+02	1.765E-01
11	43	3.159E-01	2.688E-03	2.645E-04	3.167E-04	2.668E-03	4.708E-04	1.175E+02	1.765E-01

RUN	GAGE	Q(CW)	Q(AV)/Q(O)	H(A)	H(B)	H(A)/H(O)	C(H)	Q(O)	C(H(O))
12	1	9.858E+00	3.897E-02	8.675E-03	1.051E-02	4.099E-02	3.457E-03	2.529E+02	8.434E-02
12	2	3.493E+00	1.381E-02	3.053E-03	3.694E-03	1.443E-02	1.217E-03	2.529E+02	8.434E-02
12	3	2.507E+00	9.910E-03	2.163E-03	2.609E-03	1.022E-02	8.618E-04	2.529E+02	8.434E-02
12	4	2.565E+00	1.022E-02	2.217E-03	2.671E-03	1.047E-02	8.833E-04	2.529E+02	8.434E-02
12	5	3.183E+00	1.258E-02	2.730E-03	3.290E-03	1.290E-02	1.088E-03	2.529E+02	8.434E-02
12	6	5.147E+00	2.035E-02	4.424E-03	5.333E-03	2.090E-02	1.763E-03	2.529E+02	8.434E-02
12	7	6.168E+00	2.438E-02	5.300E-03	6.389E-03	2.504E-02	2.112E-03	2.529E+02	8.434E-02
12	8	2.403E+00	9.501E-03	2.036E-03	2.447E-03	9.619E-03	8.112E-04	2.529E+02	8.434E-02
12	9	1.726E+00	6.822E-03	1.455E-03	1.747E-03	6.875E-03	5.798E-04	2.529E+02	8.434E-02
12	10	4.677E+00	1.849E-02	3.927E-03	4.719E-03	1.856E-02	1.565E-03	2.529E+02	8.434E-02
12	12	3.428E+00	1.355E-02	2.867E-03	3.438E-03	1.355E-02	1.143E-03	2.529E+02	8.434E-02
12	13	1.532E+00	6.057E-03	1.277E-03	1.531E-03	6.036E-03	5.090E-04	2.529E+02	8.434E-02
12	14	1.691E+00	6.683E-03	1.412E-03	1.692E-03	6.669E-03	5.625E-04	2.529E+02	8.434E-02
12	15	2.148E+00	8.491E-03	1.795E-03	2.151E-03	8.480E-03	7.152E-04	2.529E+02	8.434E-02
12	16	2.765E+00	1.093E-02	2.314E-03	2.774E-03	1.093E-02	9.220E-04	2.529E+02	8.434E-02
12	17	5.490E+00	2.170E-02	4.598E-03	5.514E-03	2.172E-02	1.832E-03	2.529E+02	8.434E-02
12	18	9.082E+00	3.590E-02	7.619E-03	9.139E-03	3.600E-02	3.036E-03	2.529E+02	8.434E-02
12	19	1.120E+00	4.429E-03	9.303E-04	1.114E-03	4.395E-03	3.707E-04	2.529E+02	8.434E-02
12	20	4.654E-01	1.840E-03	3.876E-04	4.643E-04	1.831E-03	1.544E-04	2.529E+02	8.434E-02
12	21	1.023E+00	4.044E-03	8.550E-04	1.025E-03	4.040E-03	3.407E-04	2.529E+02	8.434E-02
12	22	4.330E+00	1.712E-02	3.638E-03	4.366E-03	1.719E-02	1.450E-03	2.529E+02	8.434E-02
12	23	6.703E+00	2.650E-02	5.703E-03	6.861E-03	2.694E-02	2.272E-03	2.529E+02	8.434E-02
12	24	9.465E-01	3.742E-03	7.844E-04	9.397E-04	3.706E-03	3.126E-04	2.529E+02	8.434E-02
12	25	5.027E-01	1.987E-03	4.176E-04	5.000E-04	1.973E-03	1.664E-04	2.529E+02	8.434E-02
12	26	5.714E-01	2.259E-03	4.761E-04	5.703E-04	2.249E-03	1.897E-04	2.529E+02	8.434E-02
12	27	1.664E+00	6.579E-03	1.391E-03	1.668E-03	6.573E-03	5.544E-04	2.529E+02	8.434E-02
12	28	5.075E+00	2.007E-02	4.297E-03	5.164E-03	2.030E-02	1.712E-03	2.529E+02	8.434E-02
12	29	1.231E+00	4.868E-03	1.018E-03	1.218E-03	4.810E-03	4.056E-04	2.529E+02	8.434E-02
12	30	8.253E-01	3.263E-03	6.829E-04	8.170E-04	3.226E-03	2.721E-04	2.529E+02	8.434E-02
12	31	5.003E-01	1.978E-03	4.144E-04	4.959E-04	1.958E-03	1.651E-04	2.529E+02	8.434E-02
12	32	1.771E+00	7.003E-03	1.469E-03	1.759E-03	6.942E-03	5.855E-04	2.529E+02	8.434E-02
12	33	7.850E+00	3.104E-02	6.551E-03	7.851E-03	3.095E-02	2.610E-03	2.529E+02	8.434E-02
12	34	1.449E+00	5.728E-03	1.199E-03	1.434E-03	5.663E-03	4.776E-04	2.529E+02	8.434E-02
12	35	4.658E-01	1.842E-03	3.860E-04	4.619E-04	1.824E-03	1.538E-04	2.529E+02	8.434E-02
12	37	1.348E+00	5.329E-03	1.117E-03	1.337E-03	5.277E-03	4.450E-04	2.529E+02	8.434E-02
12	38	5.557E-01	2.197E-03	4.616E-04	5.526E-04	2.181E-03	1.839E-04	2.529E+02	8.434E-02
12	39	2.506E+00	9.906E-03	2.085E-03	2.497E-03	9.849E-03	8.306E-04	2.529E+02	8.434E-02
12	40	1.781E+00	7.040E-03	1.494E-03	1.792E-03	7.057E-03	5.952E-04	2.529E+02	8.434E-02
12	41	2.097E+00	8.291E-03	1.739E-03	2.082E-03	8.218E-03	6.931E-04	2.529E+02	8.434E-02
12	42	9.999E-01	3.953E-03	8.460E-04	1.017E-03	3.997E-03	3.371E-04	2.529E+02	8.434E-02
12	43	8.737E-01	3.454E-03	7.258E-04	8.689E-04	3.429E-03	2.892E-04	2.529E+02	8.434E-02

RUN	GAGE	Q(CW)	Q(AV)/Q(O)	H(A)	H(B)	H(A)/H(O)	C(H)	Q(O)	C(H(O))
13	1	7.249E+00	3.549E-02	6.432E-03	7.794E-03	3.734E-02	3.840E-03	2.042E+02	1.029E-01
13	2	3.452E+00	1.690E-02	3.043E-03	3.682E-03	1.766E-02	1.817E-03	2.042E+02	1.029E-01
13	3	2.436E+00	1.193E-02	2.119E-03	2.557E-03	1.230E-02	1.265E-03	2.042E+02	1.029E-01
13	4	2.016E+00	9.869E-03	1.743E-03	2.101E-03	1.012E-02	1.041E-03	2.042E+02	1.029E-01
13	5	2.235E+00	1.094E-02	1.933E-03	2.329E-03	1.122E-02	1.154E-03	2.042E+02	1.029E-01
13	6	3.260E+00	1.596E-02	2.825E-03	3.407E-03	1.640E-02	1.687E-03	2.042E+02	1.029E-01
13	7	6.360E+00	3.114E-02	5.512E-03	6.646E-03	3.199E-02	3.291E-03	2.042E+02	1.029E-01
13	8	1.758E+00	8.610E-03	1.502E-03	1.805E-03	8.717E-03	8.966E-04	2.042E+02	1.029E-01
13	9	1.407E+00	6.887E-03	1.196E-03	1.436E-03	6.941E-03	7.139E-04	2.042E+02	1.029E-01
13	10	3.062E+00	1.499E-02	2.592E-03	3.110E-03	1.504E-02	1.547E-03	2.042E+02	1.029E-01
13	12	3.739E+00	1.831E-02	3.154E-03	3.782E-03	1.831E-02	1.883E-03	2.042E+02	1.029E-01
13	13	1.019E+00	4.989E-03	8.565E-04	1.026E-03	4.971E-03	5.113E-04	2.042E+02	1.029E-01
13	14	1.662E+00	8.137E-03	1.399E-03	1.677E-03	8.120E-03	8.352E-04	2.042E+02	1.029E-01
13	15	2.374E+00	1.162E-02	2.000E-03	2.398E-03	1.161E-02	1.194E-03	2.042E+02	1.029E-01
13	16	2.031E+00	9.947E-03	1.714E-03	2.055E-03	9.946E-03	1.023E-03	2.042E+02	1.029E-01
13	17	3.850E+00	1.885E-02	3.250E-03	3.898E-03	1.887E-02	1.940E-03	2.042E+02	1.029E-01
13	18	6.108E+00	2.991E-02	5.164E-03	6.195E-03	2.997E-02	3.083E-03	2.042E+02	1.029E-01
13	19	7.856E-01	3.847E-03	6.577E-04	7.874E-04	3.817E-03	3.926E-04	2.042E+02	1.029E-01
13	20	5.941E-01	2.909E-03	4.988E-04	5.976E-04	2.895E-03	2.978E-04	2.042E+02	1.029E-01
13	21	7.796E-01	3.817E-03	6.570E-04	7.876E-04	3.813E-03	3.922E-04	2.042E+02	1.029E-01
13	22	2.929E+00	1.434E-02	2.461E-03	2.977E-03	1.440E-02	1.481E-03	2.042E+02	1.029E-01
13	23	4.739E+00	2.321E-02	4.065E-03	4.891E-03	2.359E-02	2.427E-03	2.042E+02	1.029E-01
13	24	6.337E-01	3.103E-03	5.294E-04	6.336E-04	3.073E-03	3.160E-04	2.042E+02	1.029E-01
13	25	3.896E-01	1.908E-03	3.263E-04	3.908E-04	1.894E-03	1.948E-04	2.042E+02	1.029E-01
13	26	4.222E-01	2.067E-03	3.546E-04	4.249E-04	2.058E-03	2.117E-04	2.042E+02	1.029E-01
13	27	1.220E+00	5.975E-03	1.028E-03	1.233E-03	5.969E-03	6.139E-04	2.042E+02	1.029E-01
13	28	2.935E+00	1.437E-02	2.505E-03	3.011E-03	1.454E-02	1.495E-03	2.042E+02	1.029E-01
13	29	7.719E-01	3.779E-03	6.432E-04	7.694E-04	3.733E-03	3.839E-04	2.042E+02	1.029E-01
13	30	2.991E-01	1.464E-03	2.494E-04	2.984E-04	1.448E-03	1.489E-04	2.042E+02	1.029E-01
13	31	3.315E-01	1.623E-03	2.768E-04	3.313E-04	1.607E-03	1.652E-04	2.042E+02	1.029E-01
13	32	1.118E+00	5.476E-03	9.351E-04	1.119E-03	5.428E-03	5.582E-04	2.042E+02	1.029E-01
13	33	4.171E+00	2.042E-02	3.507E-03	4.203E-03	2.036E-02	2.094E-03	2.042E+02	1.029E-01
13	34	9.256E-01	4.532E-03	7.719E-04	9.236E-04	4.480E-03	4.608E-04	2.042E+02	1.029E-01
13	37	9.797E-01	4.797E-03	8.184E-04	9.795E-04	4.750E-03	4.885E-04	2.042E+02	1.029E-01
13	38	4.743E-01	2.322E-03	3.972E-04	4.756E-04	2.305E-03	2.371E-04	2.042E+02	1.029E-01
13	39	1.484E+00	7.268E-03	1.245E-03	1.491E-03	7.225E-03	7.430E-04	2.042E+02	1.029E-01
13	40	1.068E+00	5.229E-03	9.031E-04	1.084E-03	5.242E-03	5.391E-04	2.042E+02	1.029E-01
13	41	1.060E+00	5.189E-03	8.859E-04	1.060E-03	5.142E-03	5.288E-04	2.042E+02	1.029E-01
13	43	7.337E-01	3.592E-03	6.144E-04	7.357E-04	3.566E-03	3.668E-04	2.042E+02	1.029E-01

RUN	GAGE	Q(CW)	Q(AV)/Q(D)	H(A)	H(B)	H(A)/H(D)	C(H)	Q(D)	C(H(D))
14	1	1.861E+01	4.439E-02	1.611E-02	1.952E-02	4.671E-02	2.392E-03	4.193E+02	5.121E-02
14	2	6.948E+00	1.657E-02	5.971E-03	7.221E-03	1.731E-02	8.864E-04	4.193E+02	5.121E-02
14	3	4.559E+00	1.087E-02	3.867E-03	4.664E-03	1.121E-02	5.741E-04	4.193E+02	5.121E-02
14	4	6.059E+00	1.445E-02	5.110E-03	6.156E-03	1.481E-02	7.586E-04	4.193E+02	5.121E-02
14	5	5.588E+00	1.333E-02	4.713E-03	5.677E-03	1.366E-02	6.996E-04	4.193E+02	5.121E-02
14	6	3.875E+00	9.243E-03	3.273E-03	3.944E-03	9.489E-03	4.859E-04	4.193E+02	5.121E-02
14	7	8.194E+00	1.954E-02	6.923E-03	8.343E-03	2.007E-02	1.028E-03	4.193E+02	5.121E-02
14	9	4.445E+00	1.060E-02	3.687E-03	4.426E-03	1.069E-02	5.473E-04	4.193E+02	5.121E-02
14	10	1.822E+01	4.346E-02	1.508E-02	1.809E-02	4.371E-02	2.238E-03	4.193E+02	5.121E-02
14	12	1.444E+01	3.445E-02	1.190E-02	1.427E-02	3.450E-02	1.767E-03	4.193E+02	5.121E-02
14	13	2.919E+00	6.963E-03	2.394E-03	2.863E-03	6.940E-03	3.554E-04	4.193E+02	5.121E-02
14	14	3.627E+00	8.651E-03	2.979E-03	3.570E-03	8.636E-03	4.423E-04	4.193E+02	5.121E-02
14	15	3.659E+00	8.728E-03	3.008E-03	3.605E-03	8.720E-03	4.466E-04	4.193E+02	5.121E-02
14	17	8.792E+00	2.097E-02	7.245E-03	8.686E-03	2.100E-02	1.075E-03	4.193E+02	5.121E-02
14	18	1.459E+01	3.480E-02	1.205E-02	1.445E-02	3.492E-02	1.788E-03	4.193E+02	5.121E-02
14	19	1.623E+00	3.872E-03	1.326E-03	1.587E-03	3.843E-03	1.968E-04	4.193E+02	5.121E-02
14	20	8.834E-01	2.107E-03	7.235E-04	8.664E-04	2.097E-03	1.074E-04	4.193E+02	5.121E-02
14	21	1.344E+00	3.207E-03	1.105E-03	1.324E-03	3.204E-03	1.641E-04	4.193E+02	5.121E-02
14	22	7.357E+00	1.755E-02	6.081E-03	7.296E-03	1.763E-02	9.028E-04	4.193E+02	5.121E-02
14	23	9.201E+00	2.195E-02	7.699E-03	9.259E-03	2.232E-02	1.143E-03	4.193E+02	5.121E-02
14	25	6.153E-01	1.468E-03	5.027E-04	6.018E-04	1.457E-03	7.463E-05	4.193E+02	5.121E-02
14	26	3.523E-01	8.404E-04	2.887E-04	3.457E-04	8.368E-04	4.285E-05	4.193E+02	5.121E-02
14	27	2.978E+00	7.104E-03	2.449E-03	2.935E-03	7.099E-03	3.635E-04	4.193E+02	5.121E-02
14	28	3.869E+00	9.227E-03	3.219E-03	3.868E-03	9.333E-03	4.779E-04	4.193E+02	5.121E-02
14	29	2.885E+00	6.881E-03	2.346E-03	2.806E-03	6.801E-03	3.483E-04	4.193E+02	5.121E-02
14	30	7.909E-01	1.886E-03	6.436E-04	7.697E-04	1.866E-03	9.554E-05	4.193E+02	5.121E-02
14	31	5.350E-01	1.276E-03	4.359E-04	5.214E-04	1.263E-03	6.470E-05	4.193E+02	5.121E-02
14	32	1.988E+00	4.743E-03	1.622E-03	1.941E-03	4.702E-03	2.408E-04	4.193E+02	5.121E-02
14	33	9.210E+00	2.197E-02	7.560E-03	9.057E-03	2.192E-02	1.122E-03	4.193E+02	5.121E-02
14	34	1.756E+00	4.188E-03	1.429E-03	1.709E-03	4.142E-03	2.121E-04	4.193E+02	5.121E-02
14	35	9.036E-01	2.155E-03	7.363E-04	8.808E-04	2.134E-03	1.093E-04	4.193E+02	5.121E-02
14	37	2.664E+00	6.355E-03	2.172E-03	2.598E-03	6.295E-03	3.224E-04	4.193E+02	5.121E-02
14	38	8.473E-01	2.021E-03	6.922E-04	8.285E-04	2.007E-03	1.028E-04	4.193E+02	5.121E-02
14	39	4.489E+00	1.071E-02	3.673E-03	4.398E-03	1.065E-02	5.453E-04	4.193E+02	5.121E-02
14	40	1.702E+00	4.059E-03	1.403E-03	1.683E-03	4.068E-03	2.083E-04	4.193E+02	5.121E-02
14	41	2.016E+00	4.808E-03	1.644E-03	1.967E-03	4.766E-03	2.441E-04	4.193E+02	5.121E-02
14	42	1.326E+00	3.164E-03	1.103E-03	1.325E-03	3.198E-03	1.638E-04	4.193E+02	5.121E-02
14	43	2.105E+00	5.022E-03	1.720E-03	2.059E-03	4.987E-03	2.554E-04	4.193E+02	5.121E-02

RUN	GAGE	Q(CH)	Q(AV)/Q(D)	H(A)	H(B)	H(A)/H(D)	C(H)	Q(D)	C(H(D))
15	1	1.250E+01	4.352E-02	1.104E-02	1.337E-02	4.580E-02	3.318E-03	2.873E+02	7.246E-02
15	2	6.176E+00	2.150E-02	5.416E-03	6.553E-03	2.247E-02	1.628E-03	2.873E+02	7.246E-02
15	3	4.977E+00	1.732E-02	4.307E-03	5.197E-03	1.787E-02	1.295E-03	2.873E+02	7.246E-02
15	4	4.603E+00	1.602E-02	3.959E-03	4.772E-03	1.643E-02	1.191E-03	2.873E+02	7.246E-02
15	5	4.720E+00	1.643E-02	4.061E-03	4.894E-03	1.685E-02	1.221E-03	2.873E+02	7.246E-02
15	6	4.103E+00	1.428E-02	3.536E-03	4.263E-03	1.467E-02	1.063E-03	2.873E+02	7.246E-02
15	7	7.105E+00	2.473E-02	6.124E-03	7.383E-03	2.541E-02	1.841E-03	2.873E+02	7.246E-02
15	8	3.989E+00	1.389E-02	3.389E-03	4.074E-03	1.406E-02	1.019E-03	2.873E+02	7.246E-02
15	9	2.800E+00	9.746E-03	2.368E-03	2.843E-03	9.824E-03	7.119E-04	2.873E+02	7.246E-02
15	10	8.198E+00	2.854E-02	6.907E-03	8.288E-03	2.866E-02	2.077E-03	2.873E+02	7.246E-02
15	12	5.270E+00	1.835E-02	4.422E-03	5.302E-03	1.835E-02	1.330E-03	2.873E+02	7.246E-02
15	13	1.995E+00	6.943E-03	1.668E-03	1.998E-03	6.919E-03	5.014E-04	2.873E+02	7.246E-02
15	14	2.284E+00	7.949E-03	1.912E-03	2.292E-03	7.933E-03	5.749E-04	2.873E+02	7.246E-02
15	15	3.764E+00	1.310E-02	3.155E-03	3.782E-03	1.309E-02	9.486E-04	2.873E+02	7.246E-02
15	16	1.923E+00	6.695E-03	1.613E-03	1.935E-03	6.695E-03	4.851E-04	2.873E+02	7.246E-02
15	17	5.603E+00	1.950E-02	4.705E-03	5.642E-03	1.952E-02	1.415E-03	2.873E+02	7.246E-02
15	18	8.154E+00	2.839E-02	6.857E-03	8.226E-03	2.845E-02	2.062E-03	2.873E+02	7.246E-02
15	19	1.180E+00	4.110E-03	9.829E-04	1.177E-03	4.078E-03	2.955E-04	2.873E+02	7.246E-02
15	20	4.411E-01	1.536E-03	3.683E-04	4.412E-04	1.528E-03	1.108E-04	2.873E+02	7.246E-02
15	21	9.179E-01	3.195E-03	7.693E-04	9.222E-04	3.192E-03	2.313E-04	2.873E+02	7.246E-02
15	22	4.491E+00	1.563E-02	3.783E-03	4.540E-03	1.570E-02	1.138E-03	2.873E+02	7.246E-02
15	23	7.024E+00	2.445E-02	5.992E-03	7.210E-03	2.486E-02	1.802E-03	2.873E+02	7.246E-02
15	24	1.246E+00	4.336E-03	1.035E-03	1.239E-03	4.295E-03	3.112E-04	2.873E+02	7.246E-02
15	25	8.105E-01	2.821E-03	6.752E-04	8.084E-04	2.802E-03	2.030E-04	2.873E+02	7.246E-02
15	26	4.117E-01	1.433E-03	3.439E-04	4.120E-04	1.427E-03	1.034E-04	2.873E+02	7.246E-02
15	27	1.987E+00	6.917E-03	1.666E-03	1.997E-03	6.911E-03	5.008E-04	2.873E+02	7.246E-02
15	28	5.117E+00	1.781E-02	4.344E-03	5.221E-03	1.802E-02	1.306E-03	2.873E+02	7.246E-02
15	29	2.071E+00	7.209E-03	1.717E-03	2.053E-03	7.123E-03	5.161E-04	2.873E+02	7.246E-02
15	30	1.419E+00	4.939E-03	1.177E-03	1.408E-03	4.884E-03	3.539E-04	2.873E+02	7.246E-02
15	31	5.215E-01	1.815E-03	4.331E-04	5.183E-04	1.797E-03	1.302E-04	2.873E+02	7.246E-02
15	32	1.644E+00	5.724E-03	1.368E-03	1.637E-03	5.674E-03	4.112E-04	2.873E+02	7.246E-02
15	34	1.825E+00	6.352E-03	1.514E-03	1.811E-03	6.281E-03	4.551E-04	2.873E+02	7.246E-02
15	35	1.326E+00	4.616E-03	1.102E-03	1.318E-03	4.571E-03	3.312E-04	2.873E+02	7.246E-02
15	37	1.868E+00	6.501E-03	1.552E-03	1.857E-03	6.438E-03	4.666E-04	2.873E+02	7.246E-02
15	38	9.216E-01	3.208E-03	7.676E-04	9.190E-04	3.185E-03	2.308E-04	2.873E+02	7.246E-02
15	39	2.583E+00	8.990E-03	2.154E-03	2.580E-03	8.938E-03	6.477E-04	2.873E+02	7.246E-02
15	40	1.698E+00	5.912E-03	1.428E-03	1.714E-03	5.927E-03	4.295E-04	2.873E+02	7.246E-02
15	41	1.572E+00	5.472E-03	1.307E-03	1.564E-03	5.423E-03	3.930E-04	2.873E+02	7.246E-02
15	42	7.755E-01	2.700E-03	6.579E-04	7.906E-04	2.730E-03	1.978E-04	2.873E+02	7.246E-02
15	43	1.514E+00	5.272E-03	1.262E-03	1.511E-03	5.235E-03	3.793E-04	2.873E+02	7.246E-02

RUN	GAGE	Q(CW)	Q(AV)/Q(O)	H(A)	H(B)	H(A)/H(O)	C(H)	Q(O)	C(H(O))
16	1	5.134E+00	4.181E-02	3.763E-03	4.536E-03	4.358E-02	9.792E-03	1.228E+02	2.247E-01
16	2	2.804E+00	2.284E-02	2.045E-03	2.463E-03	2.369E-02	5.322E-03	1.228E+02	2.247E-01
16	3	1.855E+00	1.510E-02	1.338E-03	1.607E-03	1.549E-02	3.481E-03	1.228E+02	2.247E-01
16	4	1.732E+00	1.410E-02	1.243E-03	1.492E-03	1.440E-02	3.235E-03	1.228E+02	2.247E-01
16	5	1.859E+00	1.514E-02	1.334E-03	1.602E-03	1.545E-02	3.472E-03	1.228E+02	2.247E-01
16	6	2.308E+00	1.879E-02	1.659E-03	1.992E-03	1.921E-02	4.317E-03	1.228E+02	2.247E-01
16	7	3.296E+00	2.684E-02	2.369E-03	2.844E-03	2.743E-02	6.164E-03	1.228E+02	2.247E-01
16	8	1.520E+00	1.238E-02	1.080E-03	1.293E-03	1.250E-02	2.809E-03	1.228E+02	2.247E-01
16	9	1.294E+00	1.054E-02	9.157E-04	1.096E-03	1.060E-02	2.383E-03	1.228E+02	2.247E-01
16	10	1.761E+00	1.434E-02	1.242E-03	1.485E-03	1.438E-02	3.231E-03	1.228E+02	2.247E-01
16	12	1.473E+00	1.199E-02	1.035E-03	1.237E-03	1.199E-02	2.694E-03	1.228E+02	2.247E-01
16	13	6.746E-01	5.494E-03	4.729E-04	5.650E-04	5.477E-03	1.231E-03	1.228E+02	2.247E-01
16	14	8.993E-01	7.323E-03	6.312E-04	7.542E-04	7.309E-03	1.642E-03	1.228E+02	2.247E-01
16	15	1.400E+00	1.140E-02	9.824E-04	1.175E-03	1.139E-02	2.559E-03	1.228E+02	2.247E-01
16	16	1.859E+00	1.514E-02	1.307E-03	1.562E-03	1.513E-02	3.400E-03	1.228E+02	2.247E-01
16	17	2.704E+00	2.202E-02	1.902E-03	2.274E-03	2.203E-02	4.950E-03	1.228E+02	2.247E-01
16	18	4.057E+00	3.304E-02	2.857E-03	3.416E-03	3.308E-02	7.433E-03	1.228E+02	2.247E-01
16	19	4.326E-01	3.523E-03	3.023E-04	3.609E-04	3.500E-03	7.865E-04	1.228E+02	2.247E-01
16	20	4.415E-01	3.596E-03	3.093E-04	3.694E-04	3.581E-03	8.047E-04	1.228E+02	2.247E-01
16	21	6.021E-01	4.903E-03	4.230E-04	5.055E-04	4.898E-03	1.101E-03	1.228E+02	2.247E-01
16	22	1.960E+00	1.596E-02	1.383E-03	1.654E-03	1.601E-02	3.598E-03	1.228E+02	2.247E-01
16	23	3.431E+00	2.794E-02	2.445E-03	2.931E-03	2.832E-02	6.363E-03	1.228E+02	2.247E-01
16	24	3.438E-01	2.800E-03	2.396E-04	2.862E-04	2.777E-03	6.240E-04	1.228E+02	2.247E-01
16	25	3.280E-01	2.671E-03	2.293E-04	2.738E-04	2.655E-03	5.966E-04	1.228E+02	2.247E-01
16	26	3.988E-01	3.247E-03	2.794E-04	3.337E-04	3.235E-03	7.270E-04	1.228E+02	2.247E-01
16	27	8.359E-01	6.807E-03	5.872E-04	7.018E-04	6.800E-03	1.528E-03	1.228E+02	2.247E-01
16	28	2.488E+00	2.026E-02	1.766E-03	2.115E-03	2.045E-02	4.595E-03	1.228E+02	2.247E-01
16	29	3.714E-01	3.025E-03	2.585E-04	3.084E-04	2.994E-03	6.726E-04	1.228E+02	2.247E-01
16	30	3.204E-01	2.609E-03	2.232E-04	2.663E-04	2.585E-03	5.807E-04	1.228E+02	2.247E-01
16	31	3.718E-01	3.028E-03	2.593E-04	3.094E-04	3.002E-03	6.746E-04	1.228E+02	2.247E-01
16	32	7.494E-01	6.103E-03	5.231E-04	6.243E-04	6.057E-03	1.361E-03	1.228E+02	2.247E-01
16	33	2.525E+00	2.057E-02	1.770E-03	2.115E-03	2.050E-02	4.607E-03	1.228E+02	2.247E-01
16	34	4.219E-01	3.435E-03	2.938E-04	3.505E-04	3.402E-03	7.645E-04	1.228E+02	2.247E-01
16	35	3.081E-01	2.509E-03	2.146E-04	2.564E-04	2.488E-03	5.590E-04	1.228E+02	2.247E-01
16	37	3.943E-01	3.211E-03	2.750E-04	3.281E-04	3.184E-03	7.154E-04	1.228E+02	2.247E-01
16	38	3.532E-01	2.876E-03	2.468E-04	2.947E-04	2.858E-03	6.422E-04	1.228E+02	2.247E-01
16	39	7.239E-01	5.895E-03	5.064E-04	6.047E-04	5.865E-03	1.318E-03	1.228E+02	2.247E-01
16	40	1.006E+00	8.207E-03	7.101E-04	8.491E-04	8.223E-03	1.848E-03	1.228E+02	2.247E-01
16	41	3.835E-01	3.123E-03	2.676E-04	3.194E-04	3.099E-03	6.963E-04	1.228E+02	2.247E-01
16	42	6.215E-01	5.061E-03	4.411E-04	5.282E-04	5.108E-03	1.148E-03	1.228E+02	2.247E-01
16	43	4.568E-01	3.720E-03	3.192E-04	3.811E-04	3.697E-03	8.306E-04	1.228E+02	2.247E-01

RUN	GAGE	Q(CW)	Q(AV)/Q(D)	H(A)	H(B)	H(A)/H(D)	C(H)	Q(D)	C(H(D))
17	1	5.823E+00	2.284E-02	4.920E-03	5.906E-03	2.297E-02	1.886E-03	2.549E+02	8.209E-02
17	2	2.552E+00	1.001E-02	2.150E-03	2.579E-03	1.004E-02	8.241E-04	2.549E+02	8.209E-02
17	3	2.356E+00	9.243E-03	1.980E-03	2.374E-03	9.243E-03	7.588E-04	2.549E+02	8.209E-02
17	4	2.517E+00	9.871E-03	2.113E-03	2.534E-03	9.868E-03	8.100E-04	2.549E+02	8.209E-02
17	5	1.193E+00	4.678E-03	1.001E-03	1.200E-03	4.675E-03	3.837E-04	2.549E+02	8.209E-02
17	6	2.069E+00	8.118E-03	1.738E-03	2.084E-03	8.114E-03	6.661E-04	2.549E+02	8.209E-02
17	7	3.882E+00	1.523E-02	3.260E-03	3.908E-03	1.522E-02	1.249E-03	2.549E+02	8.209E-02
17	8	2.778E+00	1.090E-02	2.330E-03	2.793E-03	1.088E-02	8.931E-04	2.549E+02	8.209E-02
17	9	3.448E+00	1.352E-02	2.890E-03	3.464E-03	1.349E-02	1.108E-03	2.549E+02	8.209E-02
17	10	9.958E+00	3.906E-02	8.353E-03	1.001E-02	3.900E-02	3.202E-03	2.549E+02	8.209E-02
17	12	7.139E+00	2.800E-02	5.981E-03	7.167E-03	2.792E-02	2.292E-03	2.549E+02	8.209E-02
17	13	1.273E+00	4.994E-03	1.066E-03	1.277E-03	4.976E-03	4.085E-04	2.549E+02	8.209E-02
17	14	1.223E+00	4.797E-03	1.024E-03	1.227E-03	4.779E-03	3.923E-04	2.549E+02	8.209E-02
17	15	9.375E-01	3.677E-03	7.849E-04	9.405E-04	3.665E-03	3.008E-04	2.549E+02	8.209E-02
17	16	1.413E+00	5.543E-03	1.183E-03	1.418E-03	5.525E-03	4.536E-04	2.549E+02	8.209E-02
17	17	4.168E+00	1.635E-02	3.492E-03	4.185E-03	1.631E-02	1.339E-03	2.549E+02	8.209E-02
17	18	8.290E+00	3.252E-02	6.983E-03	8.378E-03	3.260E-02	2.676E-03	2.549E+02	8.209E-02
17	19	5.624E-01	2.206E-03	4.705E-04	5.638E-04	2.197E-03	1.803E-04	2.549E+02	8.209E-02
17	20	3.006E-01	1.179E-03	2.517E-04	3.016E-04	1.175E-03	9.647E-05	2.549E+02	8.209E-02
17	21	4.552E-01	1.786E-03	3.813E-04	4.570E-04	1.780E-03	1.462E-04	2.549E+02	8.209E-02
17	22	4.075E+00	1.599E-02	3.419E-03	4.098E-03	1.596E-02	1.310E-03	2.549E+02	8.209E-02
17	23	5.700E+00	2.236E-02	4.798E-03	5.755E-03	2.240E-02	1.839E-03	2.549E+02	8.209E-02
17	24	4.302E-01	1.688E-03	3.599E-04	4.311E-04	1.680E-03	1.379E-04	2.549E+02	8.209E-02
17	25	3.778E-01	1.482E-03	3.161E-04	3.788E-04	1.476E-03	1.212E-04	2.549E+02	8.209E-02
17	26	3.040E-01	1.192E-03	2.545E-04	3.049E-04	1.188E-03	9.753E-05	2.549E+02	8.209E-02
17	27	1.529E+00	5.999E-03	1.282E-03	1.536E-03	5.985E-03	4.913E-04	2.549E+02	8.209E-02
17	28	5.995E+00	2.351E-02	5.040E-03	6.045E-03	2.353E-02	1.932E-03	2.549E+02	8.209E-02
17	29	4.761E-01	1.867E-03	3.982E-04	4.771E-04	1.859E-03	1.526E-04	2.549E+02	8.209E-02
17	30	4.724E-01	1.853E-03	3.952E-04	4.735E-04	1.845E-03	1.515E-04	2.549E+02	8.209E-02
17	31	4.022E-01	1.578E-03	3.364E-04	4.030E-04	1.571E-03	1.289E-04	2.549E+02	8.209E-02
17	32	1.983E+00	7.779E-03	1.659E-03	1.988E-03	7.747E-03	6.360E-04	2.549E+02	8.209E-02
17	33	4.493E+00	1.762E-02	3.762E-03	4.508E-03	1.756E-02	1.442E-03	2.549E+02	8.209E-02
17	34	6.986E-01	2.740E-03	5.844E-04	7.002E-04	2.729E-03	2.240E-04	2.549E+02	8.209E-02
17	35	3.589E-01	1.408E-03	3.003E-04	3.597E-04	1.402E-03	1.151E-04	2.549E+02	8.209E-02
17	37	8.703E-01	3.414E-03	7.285E-04	8.729E-04	3.401E-03	2.792E-04	2.549E+02	8.209E-02
17	38	4.862E-01	1.907E-03	4.071E-04	4.879E-04	1.901E-03	1.561E-04	2.549E+02	8.209E-02
17	39	1.638E+00	6.426E-03	1.374E-03	1.646E-03	6.413E-03	5.265E-04	2.549E+02	8.209E-02
17	40	8.601E-01	3.374E-03	7.209E-04	8.641E-04	3.366E-03	2.763E-04	2.549E+02	8.209E-02
17	41	1.419E+00	5.565E-03	1.188E-03	1.424E-03	5.547E-03	4.554E-04	2.549E+02	8.209E-02
17	42	5.342E-01	2.096E-03	4.478E-04	5.367E-04	2.091E-03	1.716E-04	2.549E+02	8.209E-02
17	43	2.273E+00	8.915E-03	1.905E-03	2.283E-03	8.895E-03	7.302E-04	2.549E+02	8.209E-02

RUN	GAGE	Q(CW)	Q(AV)/Q(O)	H(A)	H(B)	H(A)/H(O)	C(H)	Q(O)	C(H(O))
18	1	9.488E+00	1.995E-02	8.077E-03	9.775E-03	2.095E-02	9.774E-04	4.756E+02	4.666E-02
18	2	5.036E+00	1.059E-02	4.261E-03	5.150E-03	1.105E-02	5.156E-04	4.756E+02	4.666E-02
18	3	6.408E+00	1.347E-02	5.355E-03	6.456E-03	1.389E-02	6.481E-04	4.756E+02	4.666E-02
18	4	7.505E+00	1.578E-02	6.236E-03	7.510E-03	1.617E-02	7.547E-04	4.756E+02	4.666E-02
18	5	2.426E+00	5.101E-03	2.014E-03	2.425E-03	5.224E-03	2.437E-04	4.756E+02	4.666E-02
18	6	3.218E+00	6.767E-03	2.677E-03	3.225E-03	6.944E-03	3.240E-04	4.756E+02	4.666E-02
18	7	7.091E+00	1.491E-02	5.901E-03	7.108E-03	1.530E-02	7.141E-04	4.756E+02	4.666E-02
18	8	8.655E+00	1.820E-02	7.109E-03	8.540E-03	1.844E-02	8.603E-04	4.756E+02	4.666E-02
18	9	1.094E+01	2.300E-02	8.948E-03	1.074E-02	2.321E-02	1.083E-03	4.756E+02	4.666E-02
18	10	3.516E+01	7.393E-02	2.875E-02	3.450E-02	7.455E-02	3.479E-03	4.756E+02	4.666E-02
18	12	1.858E+01	3.906E-02	1.519E-02	1.810E-02	3.915E-02	1.827E-03	4.756E+02	4.666E-02
18	13	3.137E+00	6.596E-03	2.565E-03	3.036E-03	6.575E-03	3.068E-04	4.756E+02	4.666E-02
18	14	2.272E+00	4.778E-03	1.859E-03	2.203E-03	4.769E-03	2.225E-04	4.756E+02	4.666E-02
18	15	3.020E+00	6.351E-03	2.446E-03	2.931E-03	6.344E-03	2.960E-04	4.756E+02	4.666E-02
18	16	1.758E+00	3.696E-03	1.425E-03	1.707E-03	3.695E-03	1.724E-04	4.756E+02	4.666E-02
18	17	8.341E+00	1.754E-02	6.772E-03	8.117E-03	1.756E-02	8.195E-04	4.756E+02	4.666E-02
18	18	1.604E+01	3.374E-02	1.306E-02	1.566E-02	3.386E-02	1.580E-03	4.756E+02	4.666E-02
18	19	9.304E-01	1.956E-03	7.488E-04	8.960E-04	1.942E-03	9.062E-05	4.756E+02	4.666E-02
18	20	1.187E+00	2.497E-03	9.585E-04	1.147E-03	2.486E-03	1.160E-04	4.756E+02	4.666E-02
18	21	7.628E-01	1.604E-03	6.178E-04	7.402E-04	1.602E-03	7.477E-05	4.756E+02	4.666E-02
18	22	7.402E+00	1.556E-02	6.028E-03	7.230E-03	1.563E-02	7.295E-04	4.756E+02	4.666E-02
18	23	1.173E+01	2.467E-02	9.675E-03	1.163E-02	2.509E-02	1.171E-03	4.756E+02	4.666E-02
18	24	7.856E-01	1.652E-03	6.311E-04	7.548E-04	1.637E-03	7.637E-05	4.756E+02	4.666E-02
18	25	1.301E+00	2.736E-03	1.048E-03	1.254E-03	2.717E-03	1.268E-04	4.756E+02	4.666E-02
18	26	5.794E-01	1.218E-03	4.678E-04	5.601E-04	1.213E-03	5.662E-05	4.756E+02	4.666E-02
18	27	2.880E+00	6.056E-03	2.333E-03	2.796E-03	6.052E-03	2.824E-04	4.756E+02	4.666E-02
18	28	7.341E+00	1.544E-02	6.022E-03	7.233E-03	1.562E-02	7.289E-04	4.756E+02	4.666E-02
18	29	1.285E+00	2.702E-03	1.030E-03	1.231E-03	2.671E-03	1.246E-04	4.756E+02	4.666E-02
18	30	2.047E+00	4.305E-03	1.642E-03	1.964E-03	4.259E-03	1.987E-04	4.756E+02	4.666E-02
18	31	5.296E-01	1.112E-03	4.247E-04	5.079E-04	1.101E-03	5.140E-05	4.756E+02	4.666E-02
18	32	3.509E+00	7.379E-03	2.822E-03	3.376E-03	7.319E-03	3.415E-04	4.756E+02	4.666E-02
18	33	7.480E+00	1.573E-02	6.048E-03	7.244E-03	1.569E-02	7.320E-04	4.756E+02	4.666E-02
18	34	1.604E+00	3.541E-03	1.359E-03	1.615E-03	3.502E-03	1.634E-04	4.756E+02	4.666E-02
18	35	1.476E+00	3.104E-03	1.186E-03	1.418E-03	3.075E-03	1.435E-04	4.756E+02	4.666E-02
18	37	1.717E+00	3.610E-03	1.379E-03	1.649E-03	3.576E-03	1.669E-04	4.756E+02	4.666E-02
18	38	1.819E+00	3.825E-03	1.465E-03	1.753E-03	3.799E-03	1.773E-04	4.756E+02	4.666E-02
18	39	2.860E+00	6.013E-03	2.306E-03	2.760E-03	5.980E-03	2.790E-04	4.756E+02	4.666E-02
18	40	1.808E+00	3.803E-03	1.470E-03	1.762E-03	3.812E-03	1.779E-04	4.756E+02	4.666E-02
18	41	3.576E+00	7.518E-03	2.875E-03	3.439E-03	7.456E-03	3.479E-04	4.756E+02	4.666E-02
18	42	1.157E+00	2.434E-03	9.486E-04	1.139E-03	2.460E-03	1.148E-04	4.756E+02	4.666E-02
18	43	6.259E+00	1.316E-02	5.044E-03	6.036E-03	1.308E-02	6.104E-04	4.756E+02	4.666E-02

RUN	GAGE	Q(CW)	Q(AV)/Q(O)	H(A)	H(B)	H(A)/H(O)	C(H)	Q(O)	C(H(O))
19	1	5.793E+00	2.244E-02	5.112E-03	6.196E-03	2.367E-02	1.932E-03	2.581E+02	8.161E-02
19	2	2.792E+00	1.081E-02	2.450E-03	2.967E-03	1.135E-02	9.260E-04	2.581E+02	8.161E-02
19	3	2.548E+00	9.871E-03	2.204E-03	2.660E-03	1.021E-02	8.328E-04	2.581E+02	8.161E-02
19	4	2.705E+00	1.048E-02	2.330E-03	2.811E-03	1.079E-02	8.807E-04	2.581E+02	8.161E-02
19	6	2.219E+00	8.596E-03	1.915E-03	2.311E-03	8.868E-03	7.237E-04	2.581E+02	8.161E-02
19	7	4.024E+00	1.559E-02	3.476E-03	4.194E-03	1.610E-02	1.314E-03	2.581E+02	8.161E-02
19	8	2.945E+00	1.141E-02	2.507E-03	3.017E-03	1.161E-02	9.476E-04	2.581E+02	8.161E-02
19	9	3.630E+00	1.406E-02	3.072E-03	3.692E-03	1.423E-02	1.161E-03	2.581E+02	8.161E-02
19	10	1.004E+01	3.887E-02	8.463E-03	1.016E-02	3.919E-02	3.198E-03	2.581E+02	8.161E-02
19	12	1.019E+01	3.947E-02	8.552E-03	1.026E-02	3.960E-02	3.232E-03	2.581E+02	8.161E-02
19	13	1.315E+00	5.092E-03	1.096E-03	1.313E-03	5.074E-03	4.141E-04	2.581E+02	8.161E-02
19	14	1.243E+00	4.815E-03	1.037E-03	1.243E-03	4.804E-03	3.921E-04	2.581E+02	8.161E-02
19	15	1.115E+00	4.319E-03	9.314E-04	1.116E-03	4.313E-03	3.520E-04	2.581E+02	8.161E-02
19	16	2.035E+00	7.885E-03	1.703E-03	2.041E-03	7.884E-03	6.434E-04	2.581E+02	8.161E-02
19	17	4.628E+00	1.793E-02	3.874E-03	4.646E-03	1.794E-02	1.464E-03	2.581E+02	8.161E-02
19	18	9.078E+00	3.517E-02	7.613E-03	9.133E-03	3.526E-02	2.877E-03	2.581E+02	8.161E-02
19	19	5.471E-01	2.119E-03	4.541E-04	5.436E-04	2.103E-03	1.716E-04	2.581E+02	8.161E-02
19	20	4.197E-01	1.626E-03	3.494E-04	4.186E-04	1.618E-03	1.321E-04	2.581E+02	8.161E-02
19	21	6.027E-01	2.335E-03	5.036E-04	6.037E-04	2.332E-03	1.903E-04	2.581E+02	8.161E-02
19	22	4.122E+00	1.597E-02	3.462E-03	4.154E-03	1.603E-02	1.308E-03	2.581E+02	8.161E-02
19	23	6.656E+00	2.579E-02	5.662E-03	6.811E-03	2.622E-02	2.140E-03	2.581E+02	8.161E-02
19	24	5.271E-01	2.042E-03	4.367E-04	5.225E-04	2.022E-03	1.650E-04	2.581E+02	8.161E-02
19	25	4.414E-01	1.710E-03	3.680E-04	4.410E-04	1.704E-03	1.391E-04	2.581E+02	8.161E-02
19	26	4.740E-01	1.836E-03	3.963E-04	4.751E-04	1.835E-03	1.498E-04	2.581E+02	8.161E-02
19	27	1.745E+00	6.761E-03	1.465E-03	1.758E-03	6.786E-03	5.538E-04	2.581E+02	8.161E-02
19	28	5.349E+00	2.072E-02	4.555E-03	5.481E-03	2.109E-02	1.721E-03	2.581E+02	8.161E-02
19	29	6.785E-01	2.628E-03	5.640E-04	6.754E-04	2.612E-03	2.131E-04	2.581E+02	8.161E-02
19	30	6.445E-01	2.497E-03	5.364E-04	6.425E-04	2.484E-03	2.027E-04	2.581E+02	8.161E-02
19	31	4.607E-01	1.785E-03	3.841E-04	4.603E-04	1.779E-03	1.452E-04	2.581E+02	8.161E-02
19	32	2.048E+00	7.936E-03	1.712E-03	2.052E-03	7.927E-03	6.469E-04	2.581E+02	8.161E-02
19	33	4.776E+00	1.850E-02	4.032E-03	4.844E-03	1.867E-02	1.524E-03	2.581E+02	8.161E-02
19	34	8.054E-01	3.120E-03	6.702E-04	8.027E-04	3.104E-03	2.533E-04	2.581E+02	8.161E-02
19	35	4.173E-01	1.617E-03	3.480E-04	4.170E-04	1.612E-03	1.315E-04	2.581E+02	8.161E-02
19	37	9.690E-01	3.754E-03	8.065E-04	9.660E-04	3.735E-03	3.048E-04	2.581E+02	8.161E-02
19	38	5.598E-01	2.168E-03	4.667E-04	5.592E-04	2.161E-03	1.764E-04	2.581E+02	8.161E-02
19	39	2.028E+00	7.854E-03	1.697E-03	2.035E-03	7.859E-03	6.413E-04	2.581E+02	8.161E-02
19	40	1.162E+00	4.502E-03	9.806E-04	1.178E-03	4.541E-03	3.706E-04	2.581E+02	8.161E-02
19	41	1.604E+00	6.212E-03	1.335E-03	1.600E-03	6.184E-03	5.046E-04	2.581E+02	8.161E-02
19	42	7.783E-01	3.015E-03	6.583E-04	7.911E-04	3.049E-03	2.488E-04	2.581E+02	8.161E-02
19	43	1.499E+00	5.807E-03	1.250E-03	1.499E-03	5.791E-03	4.726E-04	2.581E+02	8.161E-02

RUN	GAGE	Q(CW)	Q(AV)/Q(D)	H(A)	H(B)	H(A)/H(D)	C(H)	Q(D)	C(H(D))
20	1	2.628E+00	2.277E-02	2.345E-03	2.841E-03	2.393E-02	4.263E-03	1.154E+02	1.781E-01
20	2	1.326E+00	1.149E-02	1.176E-03	1.423E-03	1.200E-02	2.139E-03	1.154E+02	1.781E-01
20	3	1.030E+00	8.921E-03	8.997E-04	1.085E-03	9.183E-03	1.636E-03	1.154E+02	1.781E-01
20	4	9.674E-01	8.383E-03	8.423E-04	1.015E-03	8.596E-03	1.531E-03	1.154E+02	1.781E-01
20	6	1.198E+00	1.038E-02	1.044E-03	1.259E-03	1.066E-02	1.899E-03	1.154E+02	1.781E-01
20	7	1.869E+00	1.619E-02	1.630E-03	1.966E-03	1.664E-02	2.964E-03	1.154E+02	1.781E-01
20	8	8.695E-01	7.535E-03	7.475E-04	8.967E-04	7.629E-03	1.359E-03	1.154E+02	1.781E-01
20	9	8.482E-01	7.351E-03	7.257E-04	8.717E-04	7.407E-03	1.320E-03	1.154E+02	1.781E-01
20	10	1.291E+00	1.118E-02	1.100E-03	1.320E-03	1.123E-02	2.000E-03	1.154E+02	1.781E-01
20	12	1.356E+00	1.175E-02	1.151E-03	1.380E-03	1.174E-02	2.092E-03	1.154E+02	1.781E-01
20	13	5.079E-01	4.401E-03	4.297E-04	5.150E-04	4.386E-03	7.813E-04	1.154E+02	1.781E-01
20	14	5.024E-01	4.353E-03	4.253E-04	5.098E-04	4.341E-03	7.734E-04	1.154E+02	1.781E-01
20	15	8.249E-01	7.148E-03	6.989E-04	8.378E-04	7.133E-03	1.271E-03	1.154E+02	1.781E-01
20	16	1.094E+00	9.483E-03	9.283E-04	1.113E-03	9.475E-03	1.688E-03	1.154E+02	1.781E-01
20	17	1.962E+00	1.700E-02	1.665E-03	1.997E-03	1.699E-02	3.027E-03	1.154E+02	1.781E-01
20	18	3.597E+00	3.117E-02	3.055E-03	3.664E-03	3.118E-02	5.555E-03	1.154E+02	1.781E-01
20	19	2.550E-01	2.210E-03	2.165E-04	2.554E-04	2.180E-03	3.883E-04	1.154E+02	1.781E-01
20	20	2.652E-01	2.298E-03	2.243E-04	2.688E-04	2.289E-03	4.078E-04	1.154E+02	1.781E-01
20	21	2.897E-01	2.511E-03	2.457E-04	2.947E-04	2.508E-03	4.468E-04	1.154E+02	1.781E-01
20	22	1.733E+00	1.502E-02	1.477E-03	1.772E-03	1.507E-02	2.685E-03	1.154E+02	1.781E-01
20	23	2.863E+00	2.481E-02	2.471E-03	2.973E-03	2.522E-02	4.492E-03	1.154E+02	1.781E-01
20	24	2.863E-01	2.481E-03	2.415E-04	2.892E-04	2.464E-03	4.390E-04	1.154E+02	1.781E-01
20	25	2.263E-01	1.961E-03	1.912E-04	2.291E-04	1.952E-03	3.477E-04	1.154E+02	1.781E-01
20	26	2.280E-01	1.976E-03	1.931E-04	2.314E-04	1.971E-03	3.511E-04	1.154E+02	1.781E-01
20	27	7.214E-01	6.251E-03	6.130E-04	7.354E-04	6.257E-03	1.115E-03	1.154E+02	1.781E-01
20	28	2.628E+00	2.277E-02	2.263E-03	2.721E-03	2.309E-02	4.114E-03	1.154E+02	1.781E-01
20	29	3.364E-01	2.915E-03	2.834E-04	3.394E-04	2.893E-03	5.153E-04	1.154E+02	1.781E-01
20	30	2.265E-01	1.963E-03	1.910E-04	2.287E-04	1.949E-03	3.473E-04	1.154E+02	1.781E-01
20	32	8.366E-01	7.250E-03	7.074E-04	8.477E-04	7.220E-03	1.286E-03	1.154E+02	1.781E-01
20	33	2.342E+00	2.029E-02	1.997E-03	2.397E-03	2.038E-02	3.631E-03	1.154E+02	1.781E-01
20	34	3.014E-01	2.612E-03	2.541E-04	3.044E-04	2.594E-03	4.621E-04	1.154E+02	1.781E-01
20	35	2.612E-01	2.263E-03	2.206E-04	2.643E-04	2.251E-03	4.011E-04	1.154E+02	1.781E-01
20	37	3.416E-01	2.960E-03	2.881E-04	3.451E-04	2.941E-03	5.239E-04	1.154E+02	1.781E-01
20	38	2.639E-01	2.287E-03	2.230E-04	2.673E-04	2.277E-03	4.056E-04	1.154E+02	1.781E-01
20	39	6.554E-01	5.679E-03	5.551E-04	6.654E-04	5.666E-03	1.009E-03	1.154E+02	1.781E-01
20	40	5.963E-01	5.167E-03	5.098E-04	6.123E-04	5.204E-03	9.270E-04	1.154E+02	1.781E-01
20	41	3.129E-01	2.711E-03	2.641E-04	3.163E-04	2.695E-03	4.801E-04	1.154E+02	1.781E-01
20	42	3.811E-01	3.302E-03	3.272E-04	3.932E-04	3.339E-03	5.949E-04	1.154E+02	1.781E-01
20	43	2.342E-01	2.029E-03	1.979E-04	2.372E-04	2.020E-03	3.599E-04	1.154E+02	1.781E-01

RUN	GAGE	Q(CW)	Q(AV)/Q(O)	H(A)	H(B)	H(A)/H(O)	C(H)	Q(O)	C(H(O))
21	1	4.435E+00	2.153E-02	3.959E-03	4.804E-03	2.279E-02	2.324E-03	2.059E+02	1.020E-01
21	2	2.354E+00	1.143E-02	2.087E-03	2.529E-03	1.202E-02	1.225E-03	2.059E+02	1.020E-01
21	3	1.792E+00	8.700E-03	1.562E-03	1.886E-03	8.993E-03	9.170E-04	2.059E+02	1.020E-01
21	4	1.958E+00	9.511E-03	1.686E-03	2.034E-03	9.705E-03	9.896E-04	2.059E+02	1.020E-01
21	6	2.062E+00	1.001E-02	1.794E-03	2.165E-03	1.033E-02	1.053E-03	2.059E+02	1.020E-01
21	7	3.650E+00	1.772E-02	3.175E-03	3.832E-03	1.828E-02	1.864E-03	2.059E+02	1.020E-01
21	8	1.853E+00	8.996E-03	1.588E-03	1.910E-03	9.141E-03	9.321E-04	2.059E+02	1.020E-01
21	9	1.674E+00	8.130E-03	1.426E-03	1.714E-03	8.210E-03	8.372E-04	2.059E+02	1.020E-01
21	10	4.114E+00	1.998E-02	3.491E-03	4.191E-03	2.009E-02	2.049E-03	2.059E+02	1.020E-01
21	12	4.393E+00	2.133E-02	3.710E-03	4.450E-03	2.136E-02	2.178E-03	2.059E+02	1.020E-01
21	13	1.347E+00	6.541E-03	1.132E-03	1.357E-03	6.519E-03	6.648E-04	2.059E+02	1.020E-01
21	14	6.724E-01	3.265E-03	5.663E-04	6.788E-04	3.260E-03	3.324E-04	2.059E+02	1.020E-01
21	15	8.480E-01	4.118E-03	7.148E-04	8.570E-04	4.114E-03	4.196E-04	2.059E+02	1.020E-01
21	16	1.735E+00	8.425E-03	1.465E-03	1.757E-03	8.431E-03	8.597E-04	2.059E+02	1.020E-01
21	17	3.519E+00	1.709E-02	2.972E-03	3.566E-03	1.711E-02	1.745E-03	2.059E+02	1.020E-01
21	18	7.109E+00	3.452E-02	6.007E-03	7.207E-03	3.458E-02	3.526E-03	2.059E+02	1.020E-01
21	19	7.741E-01	3.759E-03	6.505E-04	7.794E-04	3.744E-03	3.818E-04	2.059E+02	1.020E-01
21	20	2.329E-01	1.131E-03	1.956E-04	2.343E-04	1.126E-03	1.148E-04	2.059E+02	1.020E-01
21	21	4.969E-01	2.413E-03	4.169E-04	5.023E-04	2.412E-03	2.459E-04	2.059E+02	1.020E-01
21	22	3.187E+00	1.548E-02	2.702E-03	3.244E-03	1.556E-02	1.586E-03	2.059E+02	1.020E-01
21	23	4.896E+00	2.377E-02	4.207E-03	5.063E-03	2.422E-02	2.469E-03	2.059E+02	1.020E-01
21	24	7.874E-01	3.824E-03	6.586E-04	7.884E-04	3.791E-03	3.866E-04	2.059E+02	1.020E-01
21	25	4.543E-01	2.206E-03	3.807E-04	4.560E-04	2.192E-03	2.235E-04	2.059E+02	1.020E-01
21	26	4.349E-01	2.112E-03	3.655E-04	4.380E-04	2.104E-03	2.146E-04	2.059E+02	1.020E-01
21	28	4.879E+00	2.369E-02	4.165E-03	5.006E-03	2.398E-02	2.445E-03	2.059E+02	1.020E-01
21	29	8.925E-01	4.334E-03	7.450E-04	8.915E-04	4.288E-03	4.373E-04	2.059E+02	1.020E-01
21	30	8.313E-01	4.037E-03	6.948E-04	8.316E-04	4.000E-03	4.078E-04	2.059E+02	1.020E-01
21	31	3.430E-01	1.665E-03	2.869E-04	3.435E-04	1.652E-03	1.684E-04	2.059E+02	1.020E-01
21	32	1.785E+00	8.670E-03	1.495E-03	1.791E-03	8.608E-03	8.778E-04	2.059E+02	1.020E-01
21	33	3.358E+00	1.631E-02	2.818E-03	3.375E-03	1.622E-02	1.654E-03	2.059E+02	1.020E-01
21	34	1.063E+00	5.162E-03	8.880E-04	1.063E-03	5.112E-03	5.213E-04	2.059E+02	1.020E-01
21	35	6.705E-01	3.256E-03	5.612E-04	6.719E-04	3.230E-03	3.294E-04	2.059E+02	1.020E-01
21	37	1.244E+00	6.040E-03	1.040E-03	1.245E-03	5.988E-03	6.106E-04	2.059E+02	1.020E-01
21	38	5.700E-01	2.768E-03	4.820E-04	5.782E-04	2.774E-03	2.829E-04	2.059E+02	1.020E-01
21	39	1.449E+00	7.037E-03	1.218E-03	1.460E-03	7.012E-03	7.150E-04	2.059E+02	1.020E-01
21	40	6.614E-01	3.212E-03	5.609E-04	6.733E-04	3.229E-03	3.292E-04	2.059E+02	1.020E-01
21	41	1.497E+00	7.271E-03	1.253E-03	1.500E-03	7.214E-03	7.357E-04	2.059E+02	1.020E-01
21	42	5.805E-01	2.819E-03	4.951E-04	5.950E-04	2.850E-03	2.906E-04	2.059E+02	1.020E-01
21	43	8.968E-01	4.355E-03	7.519E-04	9.006E-04	4.329E-03	4.414E-04	2.059E+02	1.020E-01

RUN	GAGE	Q(CW)	Q(AV)/Q(O)	H(A)	H(B)	H(A)/H(O)	C(H)	Q(O)	C(H(O))
22	1	6.329E+00	2.083E-02	5.361E-03	6.484E-03	2.180E-02	1.579E-03	3.038E+02	7.241E-02
22	2	3.184E+00	1.048E-02	2.679E-03	3.235E-03	1.089E-02	7.888E-04	3.038E+02	7.241E-02
22	3	2.568E+00	8.453E-03	2.131E-03	2.567E-03	8.667E-03	6.276E-04	3.038E+02	7.241E-02
22	4	3.354E+00	1.104E-02	2.775E-03	3.339E-03	1.128E-02	8.170E-04	3.038E+02	7.241E-02
22	6	2.507E+00	8.254E-03	2.076E-03	2.499E-03	8.441E-03	6.112E-04	3.038E+02	7.241E-02
22	7	6.233E+00	2.052E-02	5.165E-03	6.218E-03	2.100E-02	1.521E-03	3.038E+02	7.241E-02
22	8	4.604E+00	1.516E-02	3.768E-03	4.524E-03	1.532E-02	1.109E-03	3.038E+02	7.241E-02
22	9	4.764E+00	1.568E-02	3.883E-03	4.659E-03	1.579E-02	1.143E-03	3.038E+02	7.241E-02
22	10	9.895E+00	3.257E-02	8.047E-03	9.651E-03	3.272E-02	2.369E-03	3.038E+02	7.241E-02
22	12	1.136E+01	3.738E-02	9.210E-03	1.104E-02	3.745E-02	2.712E-03	3.038E+02	7.241E-02
22	13	3.066E+00	1.009E-02	2.478E-03	2.968E-03	1.008E-02	7.296E-04	3.038E+02	7.241E-02
22	14	1.691E+00	5.566E-03	1.367E-03	1.638E-03	5.560E-03	4.026E-04	3.038E+02	7.241E-02
22	15	1.699E+00	5.593E-03	1.375E-03	1.648E-03	5.592E-03	4.049E-04	3.038E+02	7.241E-02
22	16	2.003E+00	6.595E-03	1.623E-03	1.945E-03	6.599E-03	4.779E-04	3.038E+02	7.241E-02
22	17	4.392E+00	1.446E-02	3.561E-03	4.269E-03	1.448E-02	1.049E-03	3.038E+02	7.241E-02
22	18	7.677E+00	2.527E-02	6.229E-03	7.467E-03	2.533E-02	1.834E-03	3.038E+02	7.241E-02
22	19	1.496E+00	4.925E-03	1.207E-03	1.445E-03	4.907E-03	3.553E-04	3.038E+02	7.241E-02
22	20	7.750E-01	2.551E-03	6.252E-04	7.486E-04	2.542E-03	1.841E-04	3.038E+02	7.241E-02
22	21	6.046E-01	1.990E-03	4.902E-04	5.875E-04	1.993E-03	1.443E-04	3.038E+02	7.241E-02
22	22	4.283E+00	1.410E-02	3.490E-03	4.187E-03	1.419E-02	1.028E-03	3.038E+02	7.241E-02
22	23	5.630E+00	1.853E-02	4.628E-03	5.562E-03	1.882E-02	1.363E-03	3.038E+02	7.241E-02
22	24	1.783E+00	5.870E-03	1.438E-03	1.722E-03	5.847E-03	4.234E-04	3.038E+02	7.241E-02
22	25	8.695E-01	2.862E-03	7.024E-04	8.413E-04	2.856E-03	2.068E-04	3.038E+02	7.241E-02
22	26	5.209E-01	1.712E-03	4.208E-04	5.041E-04	1.711E-03	1.239E-04	3.038E+02	7.241E-02
22	27	2.063E+00	6.792E-03	1.674E-03	2.007E-03	6.808E-03	4.930E-04	3.038E+02	7.241E-02
22	28	5.105E+00	1.681E-02	4.192E-03	5.037E-03	1.704E-02	1.234E-03	3.038E+02	7.241E-02
22	29	2.501E+00	8.232E-03	2.013E-03	2.409E-03	8.186E-03	5.927E-04	3.038E+02	7.241E-02
22	30	9.976E-01	3.284E-03	8.034E-04	9.616E-04	3.267E-03	2.366E-04	3.038E+02	7.241E-02
22	31	5.192E-01	1.709E-03	4.185E-04	5.011E-04	1.702E-03	1.232E-04	3.038E+02	7.241E-02
22	32	2.901E+00	9.549E-03	2.341E-03	2.804E-03	9.520E-03	6.894E-04	3.038E+02	7.241E-02
22	33	5.300E+00	1.745E-02	4.292E-03	5.144E-03	1.745E-02	1.264E-03	3.038E+02	7.241E-02
22	34	2.259E+00	7.437E-03	1.816E-03	2.176E-03	7.394E-03	5.354E-04	3.038E+02	7.241E-02
22	35	4.438E-01	1.461E-03	3.576E-04	4.282E-04	1.454E-03	1.053E-04	3.038E+02	7.241E-02
22	37	1.844E+00	6.070E-03	1.484E-03	1.776E-03	6.033E-03	4.369E-04	3.038E+02	7.241E-02
22	38	7.698E-01	2.534E-03	6.204E-04	7.427E-04	2.523E-03	1.827E-04	3.038E+02	7.241E-02
22	39	1.811E+00	5.962E-03	1.463E-03	1.753E-03	5.950E-03	4.308E-04	3.038E+02	7.241E-02
22	40	2.752E-01	9.061E-04	2.241E-04	2.689E-04	9.114E-04	6.600E-05	3.038E+02	7.241E-02
22	41	1.849E+00	6.085E-03	1.486E-03	1.781E-03	6.049E-03	4.381E-04	3.038E+02	7.241E-02
22	42	7.721E-01	2.542E-03	6.318E-04	7.586E-04	2.569E-03	1.860E-04	3.038E+02	7.241E-02
22	43	2.406E+00	7.919E-03	1.938E-03	2.321E-03	7.882E-03	5.708E-04	3.038E+02	7.241E-02

RUN	GAGE	Q(CW)	Q(AV)/Q(O)	H(A)	H(B)	H(A)/H(O)	C(H)	Q(O)	C(H(O))
23	1	2.948E+00	3.816E-02	2.773E-03	3.363E-03	4.007E-02	9.926E-03	7.726E+01	2.477E-01
23	2	1.374E+00	1.778E-02	1.281E-03	1.551E-03	1.852E-02	4.587E-03	7.726E+01	2.477E-01
23	3	1.098E+00	1.421E-02	1.008E-03	1.216E-03	1.457E-02	3.609E-03	7.726E+01	2.477E-01
23	4	8.403E-01	1.088E-02	7.689E-04	9.271E-04	1.111E-02	2.752E-03	7.726E+01	2.477E-01
23	6	8.486E-01	1.098E-02	7.767E-04	9.395E-04	1.125E-02	2.787E-03	7.726E+01	2.477E-01
23	7	1.224E+00	1.584E-02	1.123E-03	1.355E-03	1.623E-02	4.020E-03	7.726E+01	2.477E-01
23	8	6.748E-01	8.735E-03	6.100E-04	7.338E-04	8.815E-03	2.184E-03	7.726E+01	2.477E-01
23	9	6.646E-01	8.602E-03	5.988E-04	7.198E-04	8.653E-03	2.143E-03	7.726E+01	2.477E-01
23	10	8.707E-01	1.127E-02	7.816E-04	9.367E-04	1.129E-02	2.798E-03	7.726E+01	2.477E-01
23	12	1.002E+00	1.296E-02	8.946E-04	1.073E-03	1.293E-02	3.202E-03	7.726E+01	2.477E-01
23	13	4.040E-01	5.229E-03	3.596E-04	4.312E-04	5.197E-03	1.287E-03	7.726E+01	2.477E-01
23	14	4.589E-01	5.940E-03	4.095E-04	4.913E-04	5.917E-03	1.466E-03	7.726E+01	2.477E-01
23	15	6.683E-01	8.651E-03	5.970E-04	7.164E-04	8.628E-03	2.137E-03	7.726E+01	2.477E-01
23	16	9.997E-01	1.294E-02	8.950E-04	1.074E-03	1.293E-02	3.204E-03	7.726E+01	2.477E-01
23	17	1.546E+00	2.002E-02	1.386E-03	1.664E-03	2.003E-02	4.961E-03	7.726E+01	2.477E-01
23	18	2.315E+00	2.997E-02	2.077E-03	2.495E-03	3.002E-02	7.436E-03	7.726E+01	2.477E-01
23	20	2.195E-01	2.841E-03	1.954E-04	2.343E-04	2.824E-03	6.994E-04	7.726E+01	2.477E-01
23	21	3.207E-01	4.151E-03	2.865E-04	3.438E-04	4.140E-03	1.026E-03	7.726E+01	2.477E-01
23	22	1.081E+00	1.400E-02	9.710E-04	1.166E-03	1.403E-02	3.476E-03	7.726E+01	2.477E-01
23	23	1.572E+00	2.035E-02	1.426E-03	1.717E-03	2.061E-02	5.106E-03	7.726E+01	2.477E-01
23	24	2.518E-01	3.259E-03	2.231E-04	2.673E-04	3.224E-03	7.985E-04	7.726E+01	2.477E-01
23	26	2.662E-01	3.472E-03	2.389E-04	2.865E-04	3.452E-03	8.551E-04	7.726E+01	2.477E-01
23	27	5.173E-01	6.696E-03	4.622E-04	5.546E-04	6.679E-03	1.654E-03	7.726E+01	2.477E-01
23	28	1.297E+00	1.679E-02	1.172E-03	1.410E-03	1.694E-02	4.196E-03	7.726E+01	2.477E-01
23	29	2.477E-01	3.207E-03	2.191E-04	2.624E-04	3.167E-03	7.844E-04	7.726E+01	2.477E-01
23	30	2.103E-01	2.723E-03	1.863E-04	2.231E-04	2.692E-03	6.667E-04	7.726E+01	2.477E-01
23	31	2.235E-01	2.893E-03	1.981E-04	2.374E-04	2.863E-03	7.093E-04	7.726E+01	2.477E-01
23	32	4.539E-01	5.875E-03	4.030E-04	4.830E-04	5.824E-03	1.443E-03	7.726E+01	2.477E-01
23	33	1.371E+00	1.775E-02	1.226E-03	1.471E-03	1.772E-02	4.388E-03	7.726E+01	2.477E-01
23	34	2.320E-01	3.002E-03	2.053E-04	2.459E-04	2.967E-03	7.349E-04	7.726E+01	2.477E-01
23	35	1.496E-01	1.936E-03	1.326E-04	1.589E-04	1.917E-03	4.748E-04	7.726E+01	2.477E-01
23	37	2.460E-01	3.185E-03	2.178E-04	2.609E-04	3.147E-03	7.796E-04	7.726E+01	2.477E-01
23	38	2.220E-01	2.874E-03	1.969E-04	2.359E-04	2.845E-03	7.048E-04	7.726E+01	2.477E-01
23	39	4.720E-01	6.109E-03	4.199E-04	5.035E-04	6.068E-03	1.503E-03	7.726E+01	2.477E-01
23	40	7.098E-01	9.188E-03	6.365E-04	7.643E-04	9.197E-03	2.278E-03	7.726E+01	2.477E-01
23	41	2.290E-01	2.965E-03	2.029E-04	2.430E-04	2.932E-03	7.262E-04	7.726E+01	2.477E-01
23	43	1.726E-01	2.234E-03	1.531E-04	1.835E-04	2.213E-03	5.480E-04	7.726E+01	2.477E-01

RUN	GAGE	Q(CW)	Q(AV)/Q(O)	H(A)	H(B)	H(A)/H(O)	C(H)	Q(O)	C(H(O))
24	1	4.539E+00	4.005E-02	3.902E-03	4.723E-03	4.201E-02	8.153E-03	1.133E+02	1.941E-01
24	2	2.171E+00	1.916E-02	1.852E-03	2.237E-03	1.994E-02	3.869E-03	1.133E+02	1.941E-01
24	3	1.382E+00	1.219E-02	1.162E-03	1.400E-03	1.251E-02	2.429E-03	1.133E+02	1.941E-01
24	4	1.395E+00	1.231E-02	1.170E-03	1.408E-03	1.259E-02	2.444E-03	1.133E+02	1.941E-01
24	6	1.542E+00	1.360E-02	1.294E-03	1.559E-03	1.393E-02	2.704E-03	1.133E+02	1.941E-01
24	7	1.376E+00	1.214E-02	1.154E-03	1.390E-03	1.243E-02	2.412E-03	1.133E+02	1.941E-01
24	8	1.206E+00	1.065E-02	1.001E-03	1.202E-03	1.077E-02	2.090E-03	1.133E+02	1.941E-01
24	9	9.733E-01	8.588E-03	8.042E-04	9.654E-04	8.658E-03	1.680E-03	1.133E+02	1.941E-01
24	10	1.494E+00	1.318E-02	1.230E-03	1.476E-03	1.324E-02	2.570E-03	1.133E+02	1.941E-01
24	12	1.943E+00	1.714E-02	1.595E-03	1.912E-03	1.717E-02	3.332E-03	1.133E+02	1.941E-01
24	13	5.397E-01	4.763E-03	4.417E-04	5.292E-04	4.755E-03	9.228E-04	1.133E+02	1.941E-01
24	14	6.059E-01	5.347E-03	4.962E-04	5.946E-04	5.342E-03	1.037E-03	1.133E+02	1.941E-01
24	15	1.020E+00	9.004E-03	8.365E-04	1.003E-03	9.005E-03	1.748E-03	1.133E+02	1.941E-01
24	16	1.805E+00	1.593E-02	1.482E-03	1.777E-03	1.596E-02	3.097E-03	1.133E+02	1.941E-01
24	17	1.666E+00	1.470E-02	1.369E-03	1.641E-03	1.473E-02	2.859E-03	1.133E+02	1.941E-01
24	20	3.474E-01	3.066E-03	2.843E-04	3.406E-04	3.060E-03	5.940E-04	1.133E+02	1.941E-01
24	21	4.137E-01	3.650E-03	3.396E-04	4.072E-04	3.656E-03	7.096E-04	1.133E+02	1.941E-01
24	22	1.476E+00	1.302E-02	1.217E-03	1.461E-03	1.311E-02	2.544E-03	1.133E+02	1.941E-01
24	23	2.611E+00	2.304E-02	2.175E-03	2.615E-03	2.341E-02	4.544E-03	1.133E+02	1.941E-01
24	24	3.301E-01	2.913E-03	2.691E-04	3.221E-04	2.897E-03	5.622E-04	1.133E+02	1.941E-01
24	25	2.512E-01	2.217E-03	2.052E-04	2.457E-04	2.209E-03	4.287E-04	1.133E+02	1.941E-01
24	26	3.073E-01	2.711E-03	2.516E-04	3.014E-04	2.708E-03	5.256E-04	1.133E+02	1.941E-01
24	27	6.792E-01	5.994E-03	5.579E-04	6.689E-04	6.006E-03	1.166E-03	1.133E+02	1.941E-01
24	28	2.207E+00	1.947E-02	1.837E-03	2.208E-03	1.977E-02	3.838E-03	1.133E+02	1.941E-01
24	29	3.304E-01	3.092E-03	2.851E-04	3.411E-04	3.069E-03	5.956E-04	1.133E+02	1.941E-01
24	30	2.176E-01	1.920E-03	1.772E-04	2.122E-04	1.908E-03	3.703E-04	1.133E+02	1.941E-01
24	31	2.342E-02	2.067E-04	1.910E-05	2.287E-05	2.056E-04	3.991E-05	1.133E+02	1.941E-01
24	32	6.527E-01	5.759E-03	5.330E-04	6.384E-04	5.739E-03	1.114E-03	1.133E+02	1.941E-01
24	33	2.672E+00	2.358E-02	2.197E-03	2.635E-03	2.365E-02	4.590E-03	1.133E+02	1.941E-01
24	34	3.492E-01	3.082E-03	2.843E-04	3.403E-04	3.061E-03	5.940E-04	1.133E+02	1.941E-01
24	35	2.143E-01	1.891E-03	1.747E-04	2.092E-04	1.881E-03	3.651E-04	1.133E+02	1.941E-01
24	37	2.910E-01	2.567E-03	2.369E-04	2.836E-04	2.551E-03	4.950E-04	1.133E+02	1.941E-01
24	38	2.618E-01	2.311E-03	2.135E-04	2.557E-04	2.299E-03	4.462E-04	1.133E+02	1.941E-01
24	39	6.541E-01	5.772E-03	5.300E-04	6.338E-04	5.706E-03	1.107E-03	1.133E+02	1.941E-01
24	40	8.079E-01	7.129E-03	6.656E-04	7.985E-04	7.165E-03	1.391E-03	1.133E+02	1.941E-01
24	41	2.808E-01	2.478E-03	2.287E-04	2.737E-04	2.462E-03	4.778E-04	1.133E+02	1.941E-01
24	42	3.745E-01	3.304E-03	3.102E-04	3.726E-04	3.340E-03	6.482E-04	1.133E+02	1.941E-01
24	43	1.475E-01	1.301E-03	1.203E-04	1.440E-04	1.295E-03	2.514E-04	1.133E+02	1.941E-01

RUN	GAGE	Q(CW)	Q(AV)/Q(O)	H(A)	H(B)	H(A)/H(O)	C(H)	Q(O)	C(H(O))
26	1	8.606E-01	3.986E-03	7.996E-04	9.628E-04	4.033E-03	3.408E-04	2.159E+02	8.453E-02
26	2	9.455E-01	4.379E-03	8.752E-04	1.053E-03	4.414E-03	3.731E-04	2.159E+02	8.453E-02
26	3	1.533E+00	7.098E-03	1.414E-03	1.700E-03	7.130E-03	6.026E-04	2.159E+02	8.453E-02
26	4	1.790E+00	8.288E-03	1.650E-03	1.984E-03	8.322E-03	7.034E-04	2.159E+02	8.453E-02
26	6	5.976E-01	2.768E-03	5.510E-04	6.625E-04	2.779E-03	2.349E-04	2.159E+02	8.453E-02
26	7	1.299E+00	6.015E-03	1.198E-03	1.440E-03	6.040E-03	5.105E-04	2.159E+02	8.453E-02
26	8	1.864E+00	8.631E-03	1.715E-03	2.062E-03	8.651E-03	7.312E-04	2.159E+02	8.453E-02
26	10	2.353E+00	1.090E-02	2.165E-03	2.601E-03	1.092E-02	9.228E-04	2.159E+02	8.453E-02
26	12	3.096E+00	1.434E-02	2.848E-03	3.422E-03	1.436E-02	1.214E-03	2.159E+02	8.453E-02
26	13	1.497E+00	6.934E-03	1.377E-03	1.654E-03	6.942E-03	5.868E-04	2.159E+02	8.453E-02
26	14	1.434E+00	6.643E-03	1.318E-03	1.584E-03	6.649E-03	5.620E-04	2.159E+02	8.453E-02
26	15	9.425E-01	4.365E-03	8.666E-04	1.041E-03	4.370E-03	3.694E-04	2.159E+02	8.453E-02
26	16	6.382E-01	2.956E-03	5.870E-04	7.054E-04	2.961E-03	2.502E-04	2.159E+02	8.453E-02
26	17	2.970E+00	1.376E-02	2.734E-03	3.285E-03	1.379E-02	1.165E-03	2.159E+02	8.453E-02
26	19	8.234E-01	3.813E-03	7.573E-04	9.099E-04	3.819E-03	3.228E-04	2.159E+02	8.453E-02
26	20	1.005E+00	4.653E-03	9.240E-04	1.110E-03	4.660E-03	3.939E-04	2.159E+02	8.453E-02
26	21	1.122E+00	5.197E-03	1.033E-03	1.241E-03	5.207E-03	4.401E-04	2.159E+02	8.453E-02
26	22	3.906E+00	1.809E-02	3.598E-03	4.325E-03	1.815E-02	1.534E-03	2.159E+02	8.453E-02
26	23	6.039E+00	2.797E-02	5.580E-03	6.711E-03	2.814E-02	2.379E-03	2.159E+02	8.453E-02
26	24	1.209E+00	5.601E-03	1.113E-03	1.337E-03	5.611E-03	4.742E-04	2.159E+02	8.453E-02
26	25	1.418E+00	6.567E-03	1.304E-03	1.568E-03	6.579E-03	5.561E-04	2.159E+02	8.453E-02
26	26	1.174E+00	5.438E-03	1.080E-03	1.298E-03	5.449E-03	4.606E-04	2.159E+02	8.453E-02
26	27	2.010E+00	9.311E-03	1.851E-03	2.225E-03	9.335E-03	7.891E-04	2.159E+02	8.453E-02
26	28	6.639E+00	3.075E-02	6.130E-03	7.372E-03	3.091E-02	2.613E-03	2.159E+02	8.453E-02
26	29	1.561E+00	7.322E-03	1.454E-03	1.747E-03	7.334E-03	6.199E-04	2.159E+02	8.453E-02
26	30	1.419E+00	6.574E-03	1.306E-03	1.569E-03	6.585E-03	5.566E-04	2.159E+02	8.453E-02
26	31	1.330E+00	6.161E-03	1.224E-03	1.470E-03	6.171E-03	5.216E-04	2.159E+02	8.453E-02
26	32	2.130E+00	9.864E-03	1.959E-03	2.354E-03	9.881E-03	8.352E-04	2.159E+02	8.453E-02
26	33	6.946E+00	3.217E-02	6.397E-03	7.689E-03	3.226E-02	2.727E-03	2.159E+02	8.453E-02
26	34	1.623E+00	7.515E-03	1.493E-03	1.794E-03	7.529E-03	6.364E-04	2.159E+02	8.453E-02
26	35	1.341E+00	6.209E-03	1.233E-03	1.482E-03	6.220E-03	5.258E-04	2.159E+02	8.453E-02
26	37	2.759E+00	1.278E-02	2.538E-03	3.049E-03	1.280E-02	1.082E-03	2.159E+02	8.453E-02
26	38	1.386E+00	6.420E-03	1.275E-03	1.533E-03	6.432E-03	5.436E-04	2.159E+02	8.453E-02
26	39	2.098E+00	9.718E-03	1.931E-03	2.321E-03	9.741E-03	8.233E-04	2.159E+02	8.453E-02
26	40	6.260E+00	2.899E-02	5.772E-03	6.939E-03	2.911E-02	2.460E-03	2.159E+02	8.453E-02
26	41	1.680E+00	7.781E-03	1.545E-03	1.856E-03	7.791E-03	6.585E-04	2.159E+02	8.453E-02
26	42	7.595E+00	3.518E-02	6.967E-03	8.367E-03	3.513E-02	2.970E-03	2.159E+02	8.453E-02
26	43	7.628E-01	3.533E-03	7.016E-04	8.430E-04	3.538E-03	2.991E-04	2.159E+02	8.453E-02

RUN	GAGE	Q(CW)	Q(AV)/Q(O)	H(A)	H(B)	H(A)/H(O)	C(H)	Q(O)	C(H(O))
27	1	2.123E+00	4.478E-03	1.853E-03	2.252E-03	4.798E-03	2.230E-04	4.741E+02	4.648E-02
27	2	2.968E+00	6.261E-03	2.576E-03	3.127E-03	6.672E-03	3.101E-04	4.741E+02	4.648E-02
27	3	5.198E+00	1.096E-02	4.514E-03	5.482E-03	1.169E-02	5.435E-04	4.741E+02	4.648E-02
27	4	5.546E+00	1.170E-02	4.689E-03	5.663E-03	1.215E-02	5.646E-04	4.741E+02	4.648E-02
27	6	1.962E+00	4.139E-03	1.665E-03	2.011E-03	4.311E-03	2.004E-04	4.741E+02	4.648E-02
27	7	1.993E+00	4.203E-03	1.689E-03	2.041E-03	4.375E-03	2.034E-04	4.741E+02	4.648E-02
27	8	3.607E+00	7.607E-03	3.005E-03	3.618E-03	7.785E-03	3.619E-04	4.741E+02	4.648E-02
27	9	3.757E+00	7.924E-03	3.110E-03	3.739E-03	8.054E-03	3.744E-04	4.741E+02	4.648E-02
27	10	4.048E+00	8.538E-03	3.307E-03	3.966E-03	8.567E-03	3.982E-04	4.741E+02	4.648E-02
27	12	7.672E+00	1.618E-02	6.287E-03	7.543E-03	1.628E-02	7.569E-04	4.741E+02	4.648E-02
27	13	1.359E+00	2.867E-03	1.107E-03	1.327E-03	2.869E-03	1.333E-04	4.741E+02	4.648E-02
27	14	3.718E+00	7.841E-03	3.037E-03	3.642E-03	7.867E-03	3.657E-04	4.741E+02	4.648E-02
27	15	3.260E+00	6.877E-03	2.665E-03	3.196E-03	6.903E-03	3.209E-04	4.741E+02	4.648E-02
27	17	7.332E+00	1.546E-02	5.998E-03	7.195E-03	1.554E-02	7.222E-04	4.741E+02	4.648E-02
27	19	3.262E+00	6.880E-03	2.642E-03	3.163E-03	6.845E-03	3.182E-04	4.741E+02	4.648E-02
27	20	3.467E+00	7.313E-03	2.818E-03	3.376E-03	7.300E-03	3.393E-04	4.741E+02	4.648E-02
27	21	3.366E+00	7.099E-03	2.745E-03	3.291E-03	7.111E-03	3.306E-04	4.741E+02	4.648E-02
27	22	8.807E+00	1.857E-02	7.220E-03	8.663E-03	1.870E-02	8.693E-04	4.741E+02	4.648E-02
27	23	1.633E+01	3.444E-02	1.360E-02	1.637E-02	3.522E-02	1.637E-03	4.741E+02	4.648E-02
27	24	3.899E+00	8.224E-03	3.145E-03	3.761E-03	8.145E-03	3.786E-04	4.741E+02	4.648E-02
27	25	4.683E+00	9.878E-03	3.792E-03	4.539E-03	9.822E-03	4.566E-04	4.741E+02	4.648E-02
27	26	3.801E+00	8.018E-03	3.066E-03	3.696E-03	7.993E-03	3.715E-04	4.741E+02	4.648E-02
27	27	4.095E+00	8.637E-03	3.335E-03	3.996E-03	8.638E-03	4.015E-04	4.741E+02	4.648E-02
27	28	1.645E+01	3.469E-02	1.360E-02	1.635E-02	3.523E-02	1.638E-03	4.741E+02	4.648E-02
27	29	3.722E+00	7.850E-03	2.990E-03	3.574E-03	7.746E-03	3.601E-04	4.741E+02	4.648E-02
27	30	3.448E+00	7.273E-03	2.773E-03	3.314E-03	7.182E-03	3.338E-04	4.741E+02	4.648E-02
27	31	4.006E+00	8.450E-03	3.225E-03	3.856E-03	8.354E-03	3.883E-04	4.741E+02	4.648E-02
27	32	4.673E+00	9.857E-03	3.767E-03	4.505E-03	9.758E-03	4.536E-04	4.741E+02	4.648E-02
27	33	1.813E+01	3.825E-02	1.477E-02	1.770E-02	3.826E-02	1.778E-03	4.741E+02	4.648E-02
27	34	3.726E+00	7.860E-03	2.996E-03	3.581E-03	7.760E-03	3.607E-04	4.741E+02	4.648E-02
27	35	3.700E+00	7.804E-03	2.980E-03	3.563E-03	7.718E-03	3.588E-04	4.741E+02	4.648E-02
27	37	5.238E+00	1.105E-02	4.225E-03	5.054E-03	1.094E-02	5.087E-04	4.741E+02	4.648E-02
27	38	4.894E+00	1.032E-02	3.953E-03	4.730E-03	1.024E-02	4.760E-04	4.741E+02	4.648E-02
27	39	4.175E+00	8.806E-03	3.382E-03	4.049E-03	8.761E-03	4.072E-04	4.741E+02	4.648E-02
27	40	1.425E+01	3.005E-02	1.164E-02	1.396E-02	3.015E-02	1.402E-03	4.741E+02	4.648E-02
27	41	1.108E+01	2.336E-02	8.947E-03	1.071E-02	2.318E-02	1.077E-03	4.741E+02	4.648E-02
27	42	2.181E+01	4.600E-02	1.801E-02	2.165E-02	4.666E-02	2.169E-03	4.741E+02	4.648E-02
27	43	5.306E+00	1.119E-02	4.291E-03	5.136E-03	1.112E-02	5.167E-04	4.741E+02	4.648E-02

RUN	GAGE	Q(CW)	Q(AV)/Q(O)	H(A)	H(B)	H(A)/H(O)	C(H)	Q(O)	C(H(O))
28	1	1.287E+00	5.328E-03	1.147E-03	1.390E-03	5.592E-03	4.767E-04	2.416E+02	8.524E-02
28	2	1.733E+00	7.175E-03	1.536E-03	1.858E-03	7.487E-03	6.382E-04	2.416E+02	8.524E-02
28	3	2.381E+00	9.858E-03	2.030E-03	2.510E-03	1.014E-02	8.644E-04	2.416E+02	8.524E-02
28	4	3.002E+00	1.243E-02	2.610E-03	3.146E-03	1.272E-02	1.085E-03	2.416E+02	8.524E-02
28	6	7.699E-01	3.187E-03	6.706E-04	8.084E-04	3.268E-03	2.786E-04	2.416E+02	8.524E-02
28	7	1.938E+00	8.021E-03	1.687E-03	2.033E-03	8.221E-03	7.008E-04	2.416E+02	8.524E-02
28	8	3.616E+00	1.497E-02	3.107E-03	3.735E-03	1.514E-02	1.291E-03	2.416E+02	8.524E-02
28	10	6.492E+00	2.687E-02	5.538E-03	6.647E-03	2.699E-02	2.301E-03	2.416E+02	8.524E-02
28	12	5.316E+00	2.200E-02	4.514E-03	5.413E-03	2.200E-02	1.875E-03	2.416E+02	8.524E-02
28	13	2.889E+00	1.196E-02	2.443E-03	2.927E-03	1.191E-02	1.015E-03	2.416E+02	8.524E-02
28	14	2.117E+00	8.761E-03	1.792E-03	2.148E-03	8.736E-03	7.446E-04	2.416E+02	8.524E-02
28	15	1.781E+00	7.372E-03	1.509E-03	1.809E-03	7.355E-03	6.269E-04	2.416E+02	8.524E-02
28	16	9.290E-01	3.845E-03	7.879E-04	9.448E-04	3.841E-03	3.274E-04	2.416E+02	8.524E-02
28	17	4.151E+00	1.718E-02	3.524E-03	4.225E-03	1.717E-02	1.464E-03	2.416E+02	8.524E-02
28	19	2.361E+00	9.773E-03	1.995E-03	2.391E-03	9.726E-03	8.290E-04	2.416E+02	8.524E-02
28	20	1.551E+00	6.421E-03	1.308E-03	1.567E-03	6.376E-03	5.435E-04	2.416E+02	8.524E-02
28	21	1.485E+00	6.146E-03	1.256E-03	1.506E-03	6.124E-03	5.220E-04	2.416E+02	8.524E-02
28	22	5.002E+00	2.071E-02	4.250E-03	5.098E-03	2.072E-02	1.766E-03	2.416E+02	8.524E-02
28	23	9.027E+00	3.737E-02	7.773E-03	9.349E-03	3.789E-02	3.230E-03	2.416E+02	8.524E-02
28	24	2.611E+00	1.081E-02	2.186E-03	2.614E-03	1.065E-02	9.082E-04	2.416E+02	8.524E-02
28	25	1.807E+00	7.480E-03	1.518E-03	1.816E-03	7.398E-03	6.306E-04	2.416E+02	8.524E-02
28	26	2.082E+00	8.620E-03	1.756E-03	2.103E-03	8.559E-03	7.295E-04	2.416E+02	8.524E-02
28	27	2.595E+00	1.074E-02	2.195E-03	2.630E-03	1.070E-02	9.119E-04	2.416E+02	8.524E-02
28	28	8.702E+00	3.602E-02	7.462E-03	8.967E-03	3.637E-02	3.100E-03	2.416E+02	8.524E-02
28	29	2.478E+00	1.026E-02	2.068E-03	2.471E-03	1.008E-02	8.591E-04	2.416E+02	8.524E-02
28	30	2.185E+00	9.043E-03	1.825E-03	2.181E-03	8.894E-03	7.581E-04	2.416E+02	8.524E-02
28	31	1.791E+00	7.414E-03	1.497E-03	1.790E-03	7.299E-03	6.222E-04	2.416E+02	8.524E-02
28	32	1.687E+00	6.981E-03	1.412E-03	1.688E-03	6.881E-03	5.865E-04	2.416E+02	8.524E-02
28	33	5.604E+00	2.320E-02	4.716E-03	5.646E-03	2.299E-02	1.959E-03	2.416E+02	8.524E-02
28	34	2.016E+00	8.346E-03	1.693E-03	2.012E-03	8.205E-03	6.994E-04	2.416E+02	8.524E-02
28	35	1.686E+00	6.977E-03	1.409E-03	1.685E-03	6.870E-03	5.856E-04	2.416E+02	8.524E-02
28	37	2.934E+00	1.215E-02	2.459E-03	2.941E-03	1.198E-02	1.021E-03	2.416E+02	8.524E-02
28	38	2.032E+00	8.410E-03	1.706E-03	2.041E-03	8.315E-03	7.088E-04	2.416E+02	8.524E-02
28	39	2.420E+00	1.002E-02	2.039E-03	2.441E-03	9.937E-03	8.470E-04	2.416E+02	8.524E-02
28	40	9.604E+00	3.976E-02	8.142E-03	9.761E-03	3.968E-02	3.383E-03	2.416E+02	8.524E-02
28	41	2.320E+00	9.602E-03	1.946E-03	2.328E-03	9.486E-03	8.086E-04	2.416E+02	8.524E-02
28	42	1.095E+01	4.533E-02	9.421E-03	1.133E-02	4.592E-02	3.914E-03	2.416E+02	8.524E-02
28	43	1.891E+00	7.829E-03	1.590E-03	1.903E-03	7.750E-03	6.606E-04	2.416E+02	8.524E-02

RUN	GAGE	Q(CW)	Q(AV)/Q(O)	H(A)	H(B)	H(A)/H(O)	C(H)	Q(O)	C(H(O))
29	1	6.970E-01	6.026E-03	6.237E-04	7.554E-04	6.318E-03	1.113E-03	1.157E+02	1.761E-01
29	2	8.587E-01	7.424E-03	7.653E-04	9.261E-04	7.752E-03	1.365E-03	1.157E+02	1.761E-01
29	3	7.171E-01	6.199E-03	6.296E-04	7.596E-04	6.378E-03	1.123E-03	1.157E+02	1.761E-01
29	4	7.748E-01	6.699E-03	6.769E-04	8.158E-04	6.857E-03	1.208E-03	1.157E+02	1.761E-01
29	6	6.061E-01	5.240E-03	5.308E-04	6.399E-04	5.376E-03	9.470E-04	1.157E+02	1.761E-01
29	7	1.137E+00	9.831E-03	9.945E-04	1.199E-03	1.007E-02	1.775E-03	1.157E+02	1.761E-01
29	8	8.719E-01	7.538E-03	7.523E-04	9.043E-04	7.621E-03	1.342E-03	1.157E+02	1.761E-01
29	9	1.037E+00	8.970E-03	8.915E-04	1.071E-03	9.031E-03	1.591E-03	1.157E+02	1.761E-01
29	10	1.389E+00	1.201E-02	1.169E-03	1.427E-03	1.204E-02	2.122E-03	1.157E+02	1.761E-01
29	12	1.214E+00	1.049E-02	1.034E-03	1.240E-03	1.048E-02	1.846E-03	1.157E+02	1.761E-01
29	13	6.711E-01	5.802E-03	5.702E-04	6.833E-04	5.775E-03	1.017E-03	1.157E+02	1.761E-01
29	14	4.046E-01	3.498E-03	3.444E-04	4.128E-04	3.488E-03	6.145E-04	1.157E+02	1.761E-01
29	15	4.513E-01	3.902E-03	3.844E-04	4.609E-04	3.894E-03	6.859E-04	1.157E+02	1.761E-01
29	16	8.049E-01	6.959E-03	6.865E-04	8.233E-04	6.954E-03	1.225E-03	1.157E+02	1.761E-01
29	17	2.003E+00	1.732E-02	1.709E-03	2.049E-03	1.731E-02	3.049E-03	1.157E+02	1.761E-01
29	19	4.972E-01	4.299E-03	4.204E-04	5.034E-04	4.259E-03	7.502E-04	1.157E+02	1.761E-01
29	20	6.407E-01	5.540E-03	5.439E-04	6.517E-04	5.510E-03	9.705E-04	1.157E+02	1.761E-01
29	21	4.151E-01	3.589E-03	3.539E-04	4.244E-04	3.585E-03	6.315E-04	1.157E+02	1.761E-01
29	22	2.142E+00	1.852E-02	1.836E-03	2.204E-03	1.859E-02	3.275E-03	1.157E+02	1.761E-01
29	23	3.560E+00	3.078E-02	3.090E-03	3.719E-03	3.130E-02	5.514E-03	1.157E+02	1.761E-01
29	24	8.224E-01	7.110E-03	6.930E-04	8.291E-04	7.019E-03	1.236E-03	1.157E+02	1.761E-01
29	25	6.681E-01	5.776E-03	5.650E-04	6.764E-04	5.723E-03	1.008E-03	1.157E+02	1.761E-01
29	26	4.444E-01	3.842E-03	3.768E-04	4.513E-04	3.817E-03	6.723E-04	1.157E+02	1.761E-01
29	27	1.274E+00	1.101E-02	1.085E-03	1.301E-03	1.099E-02	1.936E-03	1.157E+02	1.761E-01
29	28	4.062E+00	3.512E-02	3.505E-03	4.213E-03	3.550E-02	6.253E-03	1.157E+02	1.761E-01
29	29	1.465E+00	1.267E-02	1.230E-03	1.470E-03	1.246E-02	2.195E-03	1.157E+02	1.761E-01
29	30	1.283E+00	1.110E-02	1.078E-03	1.269E-03	1.092E-02	1.924E-03	1.157E+02	1.761E-01
29	31	6.750E-01	5.836E-03	5.676E-04	6.788E-04	5.749E-03	1.013E-03	1.157E+02	1.761E-01
29	32	1.456E+00	1.260E-02	1.227E-03	1.467E-03	1.243E-02	2.189E-03	1.157E+02	1.761E-01
29	33	4.448E+00	3.845E-02	3.751E-03	4.489E-03	3.800E-02	6.693E-03	1.157E+02	1.761E-01
29	34	1.137E+00	9.831E-03	9.555E-04	1.143E-03	9.679E-03	1.705E-03	1.157E+02	1.761E-01
29	35	4.189E-01	3.622E-03	3.525E-04	4.216E-04	3.570E-03	6.289E-04	1.157E+02	1.761E-01
29	37	9.411E-01	8.137E-03	7.933E-04	9.492E-04	8.036E-03	1.415E-03	1.157E+02	1.761E-01
29	38	9.381E-01	8.110E-03	7.924E-04	9.484E-04	8.026E-03	1.414E-03	1.157E+02	1.761E-01
29	39	1.252E+00	1.083E-02	1.061E-03	1.271E-03	1.075E-02	1.893E-03	1.157E+02	1.761E-01
29	40	3.700E+00	3.199E-02	3.156E-03	3.785E-03	3.197E-02	5.631E-03	1.157E+02	1.761E-01
29	41	6.484E-01	5.606E-03	5.472E-04	6.549E-04	5.543E-03	9.764E-04	1.157E+02	1.761E-01
29	42	4.984E+00	4.309E-02	4.305E-03	5.176E-03	4.361E-02	7.682E-03	1.157E+02	1.761E-01
29	43	4.777E-01	4.130E-03	4.039E-04	4.836E-04	4.091E-03	7.207E-04	1.157E+02	1.761E-01

RUN	GAGE	Q(CW)	Q(AV)/Q(O)	H(A)	H(B)	H(A)/H(O)	C(H)	Q(O)	C(H(O))
30	1	1.130E+00	5.443E-03	9.870E-04	1.193E-03	5.662E-03	5.767E-04	2.075E+02	1.019E-01
30	2	1.358E+00	6.542E-03	1.180E-03	1.425E-03	6.769E-03	6.895E-04	2.075E+02	1.019E-01
30	3	1.824E+00	8.786E-03	1.564E-03	1.883E-03	8.970E-03	9.136E-04	2.075E+02	1.019E-01
30	4	2.126E+00	1.024E-02	1.813E-03	2.181E-03	1.040E-02	1.060E-03	2.075E+02	1.019E-01
30	6	7.476E-01	3.602E-03	6.393E-04	7.694E-04	3.667E-03	3.736E-04	2.075E+02	1.019E-01
30	7	1.717E+00	8.274E-03	1.467E-03	1.765E-03	8.414E-03	8.570E-04	2.075E+02	1.019E-01
30	8	2.331E+00	1.123E-02	1.967E-03	2.361E-03	1.128E-02	1.149E-03	2.075E+02	1.019E-01
30	9	2.960E+00	1.426E-02	2.488E-03	2.984E-03	1.427E-02	1.454E-03	2.075E+02	1.019E-01
30	10	3.696E+00	1.782E-02	3.100E-03	3.715E-03	1.778E-02	1.811E-03	2.075E+02	1.019E-01
30	12	3.640E+00	1.754E-02	3.039E-03	3.639E-03	1.743E-02	1.775E-03	2.075E+02	1.019E-01
30	13	2.137E+00	1.030E-02	1.780E-03	2.132E-03	1.021E-02	1.040E-03	2.075E+02	1.019E-01
30	14	1.567E+00	7.549E-03	1.307E-03	1.565E-03	7.497E-03	7.636E-04	2.075E+02	1.019E-01
30	15	7.791E-01	3.754E-03	6.500E-04	7.784E-04	3.729E-03	3.798E-04	2.075E+02	1.019E-01
30	16	1.106E+00	5.327E-03	9.238E-04	1.107E-03	5.299E-03	5.398E-04	2.075E+02	1.019E-01
30	17	3.481E+00	1.677E-02	2.912E-03	3.488E-03	1.670E-02	1.701E-03	2.075E+02	1.019E-01
30	19	1.811E+00	8.726E-03	1.506E-03	1.802E-03	8.638E-03	8.799E-04	2.075E+02	1.019E-01
30	20	1.189E+00	5.729E-03	9.896E-04	1.184E-03	5.677E-03	5.782E-04	2.075E+02	1.019E-01
30	21	8.814E-01	4.247E-03	7.365E-04	8.821E-04	4.225E-03	4.303E-04	2.075E+02	1.019E-01
30	22	3.743E+00	1.803E-02	3.143E-03	3.769E-03	1.803E-02	1.836E-03	2.075E+02	1.019E-01
30	23	5.964E+00	2.874E-02	5.080E-03	6.109E-03	2.914E-02	2.968E-03	2.075E+02	1.019E-01
30	24	1.445E+00	6.961E-03	1.196E-03	1.429E-03	6.858E-03	6.985E-04	2.075E+02	1.019E-01
30	25	1.292E+00	6.227E-03	1.073E-03	1.283E-03	6.152E-03	6.267E-04	2.075E+02	1.019E-01
30	26	7.235E-01	3.486E-03	6.023E-04	7.209E-	3.455E-03	3.519E-04	2.075E+02	1.019E-01
30	27	2.128E+00	1.025E-02	1.777E-03	2.129E-03	1.019E-02	1.038E-03	2.075E+02	1.019E-01
30	28	7.537E+00	3.632E-02	6.363E-03	7.638E-03	3.650E-02	3.718E-03	2.075E+02	1.019E-01
30	29	1.476E+00	7.111E-03	1.218E-03	1.455E-03	6.985E-03	7.115E-04	2.075E+02	1.019E-01
30	30	1.507E+00	7.260E-03	1.244E-03	1.487E-03	7.138E-03	7.270E-04	2.075E+02	1.019E-01
30	31	7.855E-01	3.785E-03	6.494E-04	7.762E-04	3.725E-03	3.794E-04	2.075E+02	1.019E-01
30	32	1.658E+00	7.990E-03	1.372E-03	1.641E-03	7.873E-03	8.019E-04	2.075E+02	1.019E-01
30	33	6.191E+00	2.983E-02	5.148E-03	6.161E-03	2.953E-02	3.008E-03	2.075E+02	1.019E-01
30	34	8.398E-01	4.046E-03	6.934E-04	8.286E-04	3.977E-03	4.051E-04	2.075E+02	1.019E-01
30	35	4.613E-01	2.222E-03	3.814E-04	4.559E-04	2.188E-03	2.228E-04	2.075E+02	1.019E-01
30	37	9.194E-01	4.430E-03	7.610E-04	9.099E-04	4.365E-03	4.447E-04	2.075E+02	1.019E-01
30	38	9.319E-01	4.490E-03	7.729E-04	9.245E-04	4.434E-03	4.516E-04	2.075E+02	1.019E-01
30	39	2.141E+00	1.032E-02	1.778E-03	2.126E-03	1.020E-02	1.039E-03	2.075E+02	1.019E-01
30	40	7.198E+00	3.468E-02	6.036E-03	7.235E-03	3.462E-02	3.527E-03	2.075E+02	1.019E-01
30	42	7.981E+00	3.846E-02	6.787E-03	8.158E-03	3.893E-02	3.965E-03	2.075E+02	1.019E-01
30	43	1.568E+00	7.555E-03	1.303E-03	1.559E-03	7.474E-03	7.613E-04	2.075E+02	1.019E-01

RUN	GAGE	Q(CW)	Q(AV)/Q(O)	H(A)	H(B)	H(A)/H(O)	C(H)	Q(O)	C(H(O))
31	1	2.634E+00	5.440E-03	2.125E-03	2.545E-03	5.436E-03	2.509E-04	4.841E+02	4.615E-02
31	2	3.499E+00	7.228E-03	2.820E-03	3.378E-03	7.215E-03	3.330E-04	4.841E+02	4.615E-02
31	3	3.669E+00	7.577E-03	2.950E-03	3.532E-03	7.548E-03	3.484E-04	4.841E+02	4.615E-02
31	4	4.254E+00	8.787E-03	3.420E-03	4.094E-03	8.751E-03	4.039E-04	4.841E+02	4.615E-02
31	6	2.193E+00	4.529E-03	1.762E-03	2.109E-03	4.508E-03	2.080E-04	4.841E+02	4.615E-02
31	7	2.361E+00	4.878E-03	1.896E-03	2.269E-03	4.851E-03	2.239E-04	4.841E+02	4.615E-02
31	8	3.486E+00	7.201E-03	2.799E-03	3.350E-03	7.162E-03	3.305E-04	4.841E+02	4.615E-02
31	9	3.406E+00	7.036E-03	2.732E-03	3.270E-03	6.991E-03	3.226E-04	4.841E+02	4.615E-02
31	10	3.347E+00	6.914E-03	2.684E-03	3.211E-03	6.867E-03	3.169E-04	4.841E+02	4.615E-02
31	12	4.999E+00	1.033E-02	4.003E-03	4.769E-03	1.024E-02	4.727E-04	4.841E+02	4.615E-02
31	13	2.883E+00	5.955E-03	2.309E-03	2.762E-03	5.908E-03	2.727E-04	4.841E+02	4.615E-02
31	14	2.137E+00	4.413E-03	1.712E-03	2.048E-03	4.380E-03	2.021E-04	4.841E+02	4.615E-02
31	15	2.747E+00	5.674E-03	2.201E-03	2.634E-03	5.632E-03	2.599E-04	4.841E+02	4.615E-02
31	16	2.104E+00	4.345E-03	1.686E-03	2.017E-03	4.313E-03	1.991E-04	4.841E+02	4.615E-02
31	17	5.695E+00	1.176E-02	4.566E-03	5.463E-03	1.168E-02	5.392E-04	4.841E+02	4.615E-02
31	19	3.551E+00	7.334E-03	2.841E-03	3.399E-03	7.270E-03	3.355E-04	4.841E+02	4.615E-02
31	20	2.623E+00	5.418E-03	2.101E-03	2.513E-03	5.375E-03	2.481E-04	4.841E+02	4.615E-02
31	21	3.020E+00	6.238E-03	2.421E-03	2.897E-03	6.195E-03	2.859E-04	4.841E+02	4.615E-02
31	22	7.120E+00	1.471E-02	5.717E-03	6.843E-03	1.463E-02	6.751E-04	4.841E+02	4.615E-02
31	23	1.230E+01	2.541E-02	9.921E-03	1.188E-02	2.538E-02	1.172E-03	4.841E+02	4.615E-02
31	24	4.246E+00	8.770E-03	3.396E-03	4.062E-03	8.690E-03	4.011E-04	4.841E+02	4.615E-02
31	25	3.072E+00	6.346E-03	2.459E-03	2.941E-03	6.292E-03	2.904E-04	4.841E+02	4.615E-02
31	26	3.279E+00	6.774E-03	2.626E-03	3.141E-03	6.719E-03	3.101E-04	4.841E+02	4.615E-02
31	27	3.383E+00	6.988E-03	2.713E-03	3.247E-03	6.942E-03	3.204E-04	4.841E+02	4.615E-02
31	28	1.443E+01	2.981E-02	1.163E-02	1.393E-02	2.975E-02	1.373E-03	4.841E+02	4.615E-02
31	29	4.810E+00	9.935E-03	3.845E-03	4.599E-03	9.839E-03	4.541E-04	4.841E+02	4.615E-02
31	30	4.383E+00	9.053E-03	3.506E-03	4.193E-03	8.971E-03	4.140E-04	4.841E+02	4.615E-02
31	31	3.154E+00	6.515E-03	2.523E-03	3.018E-03	6.456E-03	2.980E-04	4.841E+02	4.615E-02
31	32	3.667E+00	7.575E-03	2.934E-03	3.509E-03	7.506E-03	3.464E-04	4.841E+02	4.615E-02
31	33	1.281E+01	2.646E-02	1.027E-02	1.229E-02	2.627E-02	1.212E-03	4.841E+02	4.615E-02
31	34	4.516E+00	9.329E-03	3.613E-03	4.321E-03	9.244E-03	4.266E-04	4.841E+02	4.615E-02
31	35	3.053E+00	6.306E-03	2.442E-03	2.921E-03	6.248E-03	2.884E-04	4.841E+02	4.615E-02
31	37	4.761E+00	9.833E-03	3.814E-03	4.563E-03	9.759E-03	4.504E-04	4.841E+02	4.615E-02
31	38	3.451E+00	7.129E-03	2.765E-03	3.308E-03	7.075E-03	3.265E-04	4.841E+02	4.615E-02
31	39	3.420E+00	7.065E-03	2.746E-03	3.287E-03	7.026E-03	3.243E-04	4.841E+02	4.615E-02
31	40	1.200E+01	2.479E-02	9.639E-03	1.154E-02	2.466E-02	1.138E-03	4.841E+02	4.615E-02
31	41	1.309E+01	2.703E-02	1.051E-02	1.258E-02	2.689E-02	1.241E-03	4.841E+02	4.615E-02
31	42	1.420E+01	2.934E-02	1.147E-02	1.374E-02	2.934E-02	1.354E-03	4.841E+02	4.615E-02
31	43	5.981E+00	1.235E-02	4.802E-03	5.748E-03	1.229E-02	5.671E-04	4.841E+02	4.615E-02

RUN	GAGE	Q(CW)	Q(AV)/Q(O)	H(A)	H(B)	H(A)/H(O)	C(H)	Q(O)	C(H(O))
32	1	9.323E+00	3.686E-02	8.299E-03	1.004E-02	3.839E-02	3.093E-03	2.529E+02	8.056E-02
32	2	3.779E+00	1.494E-02	3.353E-03	4.053E-03	1.551E-02	1.250E-03	2.529E+02	8.056E-02
32	3	2.531E+00	1.001E-02	2.218E-03	2.675E-03	1.026E-02	8.267E-04	2.529E+02	8.056E-02
32	4	2.484E+00	9.821E-03	2.166E-03	2.609E-03	1.002E-02	8.072E-04	2.529E+02	8.056E-02
32	6	3.458E+00	1.367E-02	3.023E-03	3.642E-03	1.398E-02	1.126E-03	2.529E+02	8.056E-02
32	7	5.788E+00	2.288E-02	5.056E-03	6.091E-03	2.338E-02	1.884E-03	2.529E+02	8.056E-02
32	8	2.422E+00	9.576E-03	2.087E-03	2.507E-03	9.654E-03	7.777E-04	2.529E+02	8.056E-02
32	9	1.835E+00	7.256E-03	1.575E-03	1.890E-03	7.283E-03	5.867E-04	2.529E+02	8.056E-02
32	10	5.603E+00	2.215E-02	4.793E-03	5.750E-03	2.217E-02	1.786E-03	2.529E+02	8.056E-02
32	12	8.206E+00	3.244E-02	6.993E-03	8.383E-03	3.235E-02	2.606E-03	2.529E+02	8.056E-02
32	13	1.879E+00	7.429E-03	1.595E-03	1.911E-03	7.378E-03	5.944E-04	2.529E+02	8.056E-02
32	14	1.819E+00	7.191E-03	1.547E-03	1.854E-03	7.157E-03	5.766E-04	2.529E+02	8.056E-02
32	15	1.825E+00	7.214E-03	1.553E-03	1.861E-03	7.184E-03	5.787E-04	2.529E+02	8.056E-02
32	16	2.390E+00	9.449E-03	2.036E-03	2.441E-03	9.418E-03	7.587E-04	2.529E+02	8.056E-02
32	17	4.760E+00	1.882E-02	4.058E-03	4.865E-03	1.877E-02	1.512E-03	2.529E+02	8.056E-02
32	19	1.244E+00	4.916E-03	1.052E-03	1.260E-03	4.868E-03	3.922E-04	2.529E+02	8.056E-02
32	20	5.103E-01	2.017E-03	4.328E-04	5.184E-04	2.002E-03	1.613E-04	2.529E+02	8.056E-02
32	21	5.069E-01	2.004E-03	4.316E-04	5.173E-04	1.996E-03	1.608E-04	2.529E+02	8.056E-02
32	22	3.723E+00	1.472E-02	3.188E-03	3.825E-03	1.475E-02	1.188E-03	2.529E+02	8.056E-02
32	23	5.949E+00	2.352E-02	5.169E-03	6.221E-03	2.391E-02	1.926E-03	2.529E+02	8.056E-02
32	24	1.008E+00	3.984E-03	8.487E-04	1.015E-03	3.926E-03	3.163E-04	2.529E+02	8.056E-02
32	25	4.733E-01	1.871E-03	3.998E-04	4.785E-04	1.850E-03	1.490E-04	2.529E+02	8.056E-02
32	26	5.309E-01	2.099E-03	4.501E-04	5.390E-04	2.082E-03	1.677E-04	2.529E+02	8.056E-02
32	27	1.477E+00	5.837E-03	1.256E-03	1.506E-03	5.811E-03	4.682E-04	2.529E+02	8.056E-02
32	28	4.459E+00	1.763E-02	3.842E-03	4.616E-03	1.777E-02	1.432E-03	2.529E+02	8.056E-02
32	29	1.466E+00	5.797E-03	1.231E-03	1.471E-03	5.692E-03	4.585E-04	2.529E+02	8.056E-02
32	30	8.536E-01	3.375E-03	7.170E-04	8.571E-04	3.317E-03	2.672E-04	2.529E+02	8.056E-02
32	31	3.972E-01	1.570E-03	3.338E-04	3.991E-04	1.544E-03	1.244E-04	2.529E+02	8.056E-02
32	32	1.571E+00	6.212E-03	1.322E-03	1.580E-03	6.113E-03	4.925E-04	2.529E+02	8.056E-02
32	33	4.385E+00	1.734E-02	3.691E-03	4.415E-03	1.708E-02	1.376E-03	2.529E+02	8.056E-02
32	34	1.096E+00	4.334E-03	9.208E-04	1.101E-03	4.259E-03	3.431E-04	2.529E+02	8.056E-02
32	35	8.979E-01	3.550E-03	7.555E-04	9.034E-04	3.495E-03	2.815E-04	2.529E+02	8.056E-02
32	37	1.468E+00	5.802E-03	1.237E-03	1.479E-03	5.720E-03	4.608E-04	2.529E+02	8.056E-02
32	38	1.188E+00	4.696E-03	1.003E-03	1.200E-03	4.640E-03	3.738E-04	2.529E+02	8.056E-02
32	39	1.269E+00	5.016E-03	1.076E-03	1.288E-03	4.976E-03	4.009E-04	2.529E+02	8.056E-02
32	40	3.581E+00	1.416E-02	3.057E-03	3.666E-03	1.414E-02	1.139E-03	2.529E+02	8.056E-02
32	41	1.899E+00	7.507E-03	1.602E-03	1.917E-03	7.412E-03	5.971E-04	2.529E+02	8.056E-02
32	42	5.104E+00	2.018E-02	4.415E-03	5.308E-03	2.042E-02	1.645E-03	2.529E+02	8.056E-02
32	43	1.372E+00	5.424E-03	1.160E-03	1.388E-03	5.365E-03	4.322E-04	2.529E+02	8.056E-02

RUN	GAGE	Q(CW)	Q(AV)/Q(O)	H(A)	H(B)	H(A)/H(O)	C(H)	Q(O)	C(H(C))
33	1	1.539E+01	3.188E-02	1.236E-02	1.477E-02	3.205E-02	1.513E-03	4.827E+02	4.719E-02
33	2	6.557E+00	1.358E-02	5.252E-03	6.274E-03	1.362E-02	6.429E-04	4.827E+02	4.719E-02
33	3	4.320E+00	8.950E-03	3.459E-03	4.132E-03	8.973E-03	4.235E-04	4.827E+02	4.719E-02
33	4	4.116E+00	8.528E-03	3.294E-03	3.933E-03	8.543E-03	4.032E-04	4.827E+02	4.719E-02
33	6	5.492E+00	1.138E-02	4.396E-03	5.251E-03	1.140E-02	5.382E-04	4.827E+02	4.719E-02
33	7	8.804E+00	1.824E-02	7.047E-03	8.417E-03	1.828E-02	8.627E-04	4.827E+02	4.719E-02
33	8	3.896E+00	8.071E-03	3.116E-03	3.721E-03	8.083E-03	3.815E-04	4.827E+02	4.719E-02
33	9	3.549E+00	7.352E-03	2.837E-03	3.387E-03	7.359E-03	3.473E-04	4.827E+02	4.719E-02
33	10	1.626E+01	3.369E-02	1.303E-02	1.557E-02	3.381E-02	1.595E-03	4.827E+02	4.719E-02
33	12	1.634E+01	3.384E-02	1.307E-02	1.561E-02	3.391E-02	1.600E-03	4.827E+02	4.719E-02
33	13	2.251E+00	4.662E-03	1.798E-03	2.147E-03	4.664E-03	2.201E-04	4.827E+02	4.719E-02
33	14	2.946E+00	6.104E-03	2.355E-03	2.812E-03	6.109E-03	2.883E-04	4.827E+02	4.719E-02
33	15	3.779E+00	7.830E-03	3.022E-03	3.608E-03	7.838E-03	3.699E-04	4.827E+02	4.719E-02
33	16	1.733E+00	3.591E-03	1.385E-03	1.654E-03	3.594E-03	1.696E-04	4.827E+02	4.719E-02
33	17	8.283E+00	1.716E-02	6.627E-03	7.914E-03	1.719E-02	8.112E-04	4.827E+02	4.719E-02
33	19	1.138E+00	2.357E-03	9.101E-04	1.087E-03	2.361E-03	1.114E-04	4.827E+02	4.719E-02
33	20	5.690E-01	1.179E-03	4.548E-04	5.430E-04	1.180E-03	5.567E-05	4.827E+02	4.719E-02
33	21	1.053E+00	2.183E-03	8.422E-04	1.006E-03	2.185E-03	1.031E-04	4.827E+02	4.719E-02
33	22	5.940E+00	1.231E-02	4.752E-03	5.675E-03	1.233E-02	5.818E-04	4.827E+02	4.719E-02
33	23	1.050E+01	2.175E-02	8.410E-03	1.005E-02	2.181E-02	1.029E-03	4.827E+02	4.719E-02
33	24	1.351E+00	2.798E-03	1.079E-03	1.288E-03	2.798E-03	1.321E-04	4.827E+02	4.719E-02
33	25	5.428E-01	1.124E-03	4.336E-04	5.177E-04	1.125E-03	5.308E-05	4.827E+02	4.719E-02
33	26	4.551E-01	9.426E-04	3.632E-04	4.335E-04	9.420E-04	4.446E-05	4.827E+02	4.719E-02
33	27	2.262E+00	4.685E-03	1.808E-03	2.159E-03	4.691E-03	2.214E-04	4.827E+02	4.719E-02
33	28	6.667E+00	1.381E-02	5.337E-03	6.375E-03	1.385E-02	6.534E-04	4.827E+02	4.719E-02
33	29	2.729E+00	5.654E-03	2.207E-03	2.642E-03	5.726E-03	2.702E-04	4.827E+02	4.719E-02
33	30	8.707E-01	1.804E-03	6.953E-04	8.301E-04	1.804E-03	8.512E-05	4.827E+02	4.719E-02
33	31	3.710E-01	7.686E-04	2.963E-04	3.537E-04	7.685E-04	3.627E-05	4.827E+02	4.719E-02
33	32	1.948E+00	4.036E-03	1.557E-03	1.858E-03	4.038E-03	1.906E-04	4.827E+02	4.719E-02
33	33	1.594E+01	3.303E-02	1.277E-02	1.525E-02	3.312E-02	1.563E-03	4.827E+02	4.719E-02
33	34	1.669E+00	3.872E-03	1.493E-03	1.783E-03	3.873E-03	1.828E-04	4.827E+02	4.719E-02
33	35	8.415E-01	1.743E-03	6.723E-04	8.027E-04	1.744E-03	8.230E-05	4.827E+02	4.719E-02
33	39	4.529E+00	9.383E-03	3.619E-03	4.320E-03	9.387E-03	4.430E-04	4.827E+02	4.719E-02
33	40	1.964E+00	4.069E-03	1.570E-03	1.875E-03	4.072E-03	1.922E-04	4.827E+02	4.719E-02
33	41	5.700E+00	1.181E-02	4.562E-03	5.449E-03	1.183E-02	5.585E-04	4.827E+02	4.719E-02
33	42	2.265E+00	4.693E-03	1.810E-03	2.161E-03	4.695E-03	2.216E-04	4.827E+02	4.719E-02
33	43	1.686E+00	3.493E-03	1.349E-03	1.612E-03	3.500E-03	1.652E-04	4.827E+02	4.719E-02

RUN	GAGE	Q(CN)	Q(AV)/Q(O)	H(A)	H(B)	H(A)/H(O)	C(H)	Q(O)	C(H(O))
34	1	9.927E+00	3.837E-02	8.316E-03	9.947E-03	3.862E-02	3.181E-03	2.587E+02	8.237E-02
34	2	4.316E+00	1.668E-02	3.609E-03	4.315E-03	1.676E-02	1.380E-03	2.587E+02	8.237E-02
34	3	2.773E+00	1.072E-02	2.316E-03	2.768E-03	1.076E-02	8.859E-04	2.587E+02	8.237E-02
34	4	2.416E+00	9.338E-03	2.017E-03	2.411E-03	9.368E-03	7.716E-04	2.587E+02	8.237E-02
34	6	3.409E+00	1.318E-02	2.847E-03	3.403E-03	1.322E-02	1.089E-03	2.587E+02	8.237E-02
34	7	5.591E+00	2.161E-02	4.669E-03	5.581E-03	2.168E-02	1.786E-03	2.587E+02	8.237E-02
34	8	2.169E+00	8.383E-03	1.809E-03	2.162E-03	8.402E-03	6.921E-04	2.587E+02	8.237E-02
34	10	5.139E+00	1.987E-02	4.291E-03	5.128E-03	1.993E-02	1.641E-03	2.587E+02	8.237E-02
34	12	8.375E+00	3.237E-02	6.984E-03	8.347E-03	3.244E-02	2.672E-03	2.587E+02	8.237E-02
34	13	1.352E+00	5.226E-03	1.136E-03	1.357E-03	5.274E-03	4.344E-04	2.587E+02	8.237E-02
34	14	1.473E+00	5.693E-03	1.230E-03	1.470E-03	5.711E-03	4.704E-04	2.587E+02	8.237E-02
34	15	1.694E+00	6.547E-03	1.425E-03	1.705E-03	6.616E-03	5.449E-04	2.587E+02	8.237E-02
34	16	2.160E+00	8.346E-03	1.801E-03	2.153E-03	8.366E-03	6.891E-04	2.587E+02	8.237E-02
34	17	4.567E+00	1.765E-02	3.811E-03	4.555E-03	1.770E-02	1.458E-03	2.587E+02	8.237E-02
34	19	6.101E-01	2.358E-03	5.084E-04	6.075E-04	2.361E-03	1.945E-04	2.587E+02	8.237E-02
34	20	3.690E-01	1.426E-03	3.077E-04	3.677E-04	1.429E-03	1.177E-04	2.587E+02	8.237E-02
34	21	6.795E-01	2.627E-03	5.668E-04	6.773E-04	2.632E-03	2.168E-04	2.587E+02	8.237E-02
34	22	3.416E+00	1.321E-02	2.852E-03	3.409E-03	1.324E-02	1.091E-03	2.587E+02	8.237E-02
34	23	5.278E+00	2.040E-02	4.412E-03	5.275E-03	2.049E-02	1.688E-03	2.587E+02	8.237E-02
34	24	6.283E-01	2.429E-03	5.233E-04	6.252E-04	2.430E-03	2.002E-04	2.587E+02	8.237E-02
34	25	2.354E-01	9.099E-04	1.962E-04	2.344E-04	9.110E-04	7.504E-05	2.587E+02	8.237E-02
34	26	2.998E-01	1.159E-03	2.501E-04	2.988E-04	1.161E-03	9.566E-05	2.587E+02	8.237E-02
34	27	1.365E+00	5.275E-03	1.138E-03	1.361E-03	5.287E-03	4.355E-04	2.587E+02	8.237E-02
34	28	3.998E+00	1.545E-02	3.341E-03	3.995E-03	1.552E-02	1.278E-03	2.587E+02	8.237E-02
34	29	9.251E-01	3.576E-03	7.701E-04	9.199E-04	3.576E-03	2.946E-04	2.587E+02	8.237E-02
34	30	4.062E-01	1.570E-03	3.382E-04	4.041E-04	1.571E-03	1.294E-04	2.587E+02	8.237E-02
34	31	2.416E-01	9.336E-04	2.013E-04	2.405E-04	9.348E-04	7.700E-05	2.587E+02	8.237E-02
34	32	1.109E+00	4.286E-03	9.239E-04	1.104E-03	4.291E-03	3.534E-04	2.587E+02	8.237E-02
34	33	7.757E+00	2.998E-02	6.472E-03	7.735E-03	3.006E-02	2.476E-03	2.587E+02	8.237E-02
34	34	8.475E-01	3.276E-03	7.059E-04	8.434E-04	3.278E-03	2.700E-04	2.587E+02	8.237E-02
34	35	3.276E-01	1.266E-03	2.730E-04	3.262E-04	1.268E-03	1.044E-04	2.587E+02	8.237E-02
34	39	1.923E+00	7.434E-03	1.607E-03	1.921E-03	7.463E-03	6.147E-04	2.587E+02	8.237E-02
34	40	1.327E+00	5.131E-03	1.107E-03	1.323E-03	5.140E-03	4.234E-04	2.587E+02	8.237E-02
34	41	1.005E+00	3.887E-03	8.393E-04	1.003E-03	3.898E-03	3.211E-04	2.587E+02	8.237E-02
34	42	7.068E-01	2.732E-03	5.896E-04	7.032E-04	2.734E-03	2.252E-04	2.587E+02	8.237E-02
34	43	9.673E-01	3.739E-03	8.080E-04	9.658E-04	3.752E-03	3.091E-04	2.587E+02	8.237E-02

C3

RUN	GAGE	Q(CW)	Q(AV)/Q(O)	H(A)	H(B)	H(A)/H(O)	C(H)	Q(O)	C(H(O))
35	1	4.872E+00	4.087E-02	4.064E-03	4.858E-03	4.109E-02	7.372E-03	1.192E+02	1.794E-01
35	2	2.341E+00	1.964E-02	1.950E-03	2.331E-03	1.972E-02	3.538E-03	1.192E+02	1.794E-01
35	3	1.468E+00	1.232E-02	1.223E-03	1.461E-03	1.236E-02	2.218E-03	1.192E+02	1.794E-01
35	4	1.343E+00	1.127E-02	1.118E-03	1.336E-03	1.131E-02	2.028E-03	1.192E+02	1.794E-01
35	6	1.735E+00	1.456E-02	1.444E-03	1.726E-03	1.461E-02	2.620E-03	1.192E+02	1.794E-01
35	7	2.562E+00	2.150E-02	2.133E-03	2.548E-03	2.157E-02	3.869E-03	1.192E+02	1.794E-01
35	8	1.154E+00	9.678E-03	9.597E-04	1.147E-03	9.705E-03	1.741E-03	1.192E+02	1.794E-01
35	9	9.482E-01	7.954E-03	7.886E-04	9.422E-04	7.975E-03	1.431E-03	1.192E+02	1.794E-01
35	10	1.603E+00	1.345E-02	1.335E-03	1.595E-03	1.350E-02	2.421E-03	1.192E+02	1.794E-01
35	12	2.332E+00	1.956E-02	1.937E-03	2.314E-03	1.959E-02	3.514E-03	1.192E+02	1.794E-01
35	13	5.471E-01	4.589E-03	4.549E-04	5.434E-04	4.600E-03	8.252E-04	1.192E+02	1.794E-01
35	14	7.150E-01	5.998E-03	5.946E-04	7.104E-04	6.013E-03	1.079E-03	1.192E+02	1.794E-01
35	15	1.173E+00	9.836E-03	9.754E-04	1.165E-03	9.864E-03	1.769E-03	1.192E+02	1.794E-01
35	16	1.436E+00	1.204E-02	1.194E-03	1.427E-03	1.208E-02	2.166E-03	1.192E+02	1.794E-01
35	17	2.178E+00	1.827E-02	1.812E-03	2.165E-03	1.833E-02	3.287E-03	1.192E+02	1.794E-01
35	19	3.276E-01	2.748E-03	2.724E-04	3.255E-04	2.755E-03	4.942E-04	1.192E+02	1.794E-01
35	20	3.152E-01	2.644E-03	2.622E-04	3.133E-04	2.652E-03	4.757E-04	1.192E+02	1.794E-01
35	21	4.198E-01	3.521E-03	3.492E-04	4.173E-04	3.532E-03	6.335E-04	1.192E+02	1.794E-01
35	22	1.501E+00	1.259E-02	1.250E-03	1.493E-03	1.264E-02	2.267E-03	1.192E+02	1.794E-01
35	23	2.313E+00	1.941E-02	1.927E-03	2.303E-03	1.949E-02	3.496E-03	1.192E+02	1.794E-01
35	24	2.985E-01	2.504E-03	2.481E-04	2.964E-04	2.509E-03	4.501E-04	1.192E+02	1.794E-01
35	25	2.492E-01	2.091E-03	2.072E-04	2.476E-04	2.096E-03	3.759E-04	1.192E+02	1.794E-01
35	26	2.008E-01	1.684E-03	1.671E-04	1.997E-04	1.690E-03	3.032E-04	1.192E+02	1.794E-01
35	27	5.584E-01	4.684E-03	4.646E-04	5.551E-04	4.698E-03	8.428E-04	1.192E+02	1.794E-01
35	28	1.835E+00	1.540E-02	1.534E-03	1.834E-03	1.551E-02	2.782E-03	1.192E+02	1.794E-01
35	29	2.963E-01	2.486E-03	2.462E-04	2.941E-04	2.490E-03	4.466E-04	1.192E+02	1.794E-01
35	30	1.922E-01	1.612E-03	1.597E-04	1.908E-04	1.615E-03	2.897E-04	1.192E+02	1.794E-01
35	31	2.012E-01	1.688E-03	1.672E-04	1.998E-04	1.691E-03	3.034E-04	1.192E+02	1.794E-01
35	32	5.803E-01	4.868E-03	4.827E-04	5.767E-04	4.881E-03	8.757E-04	1.192E+02	1.794E-01
35	33	2.242E+00	1.881E-02	1.865E-03	2.229E-03	1.886E-02	3.384E-03	1.192E+02	1.794E-01
35	34	3.076E-01	2.580E-03	2.557E-04	3.055E-04	2.586E-03	4.639E-04	1.192E+02	1.794E-01
35	35	2.551E-01	2.140E-03	2.122E-04	2.535E-04	2.145E-03	3.849E-04	1.192E+02	1.794E-01
35	39	6.971E-01	5.848E-03	5.817E-04	6.955E-04	5.883E-03	1.055E-03	1.192E+02	1.794E-01
35	40	7.510E-01	6.300E-03	6.247E-04	7.464E-04	6.318E-03	1.133E-03	1.192E+02	1.794E-01
35	41	3.000E-01	2.517E-03	2.498E-04	2.985E-04	2.526E-03	4.531E-04	1.192E+02	1.794E-01
35	42	4.538E-01	3.807E-03	3.773E-04	4.507E-04	3.815E-03	6.844E-04	1.192E+02	1.794E-01
35	43	2.850E-01	2.390E-03	2.373E-04	2.836E-04	2.400E-03	4.306E-04	1.192E+02	1.794E-01

RUN	GAGE	Q(CW)	Q(AV)/Q(O)	H(A)	H(B)	H(A)/H(O)	C(H)	Q(O)	C(H(O))
36	1	9.098E+00	3.642E-02	7.746E-03	9.262E-03	3.662E-02	3.079E-03	2.498E+02	8.409E-02
36	2	4.108E+00	1.644E-02	3.490E-03	4.172E-03	1.650E-02	1.387E-03	2.498E+02	8.409E-02
36	3	2.565E+00	1.027E-02	2.178E-03	2.602E-03	1.029E-02	8.656E-04	2.498E+02	8.409E-02
36	4	2.405E+00	9.629E-03	2.041E-03	2.440E-03	9.650E-03	8.115E-04	2.498E+02	8.409E-02
36	6	3.461E+00	1.385E-02	2.938E-03	3.512E-03	1.389E-02	1.168E-03	2.498E+02	8.409E-02
36	7	4.956E+00	1.984E-02	4.207E-03	5.027E-03	1.989E-02	1.672E-03	2.498E+02	8.409E-02
36	8	2.092E+00	8.373E-03	1.774E-03	2.119E-03	8.385E-03	7.051E-04	2.498E+02	8.409E-02
36	9	1.507E+00	6.034E-03	1.278E-03	1.527E-03	6.041E-03	5.079E-04	2.498E+02	8.409E-02
36	10	4.381E+00	1.754E-02	3.719E-03	4.444E-03	1.758E-02	1.478E-03	2.498E+02	8.409E-02
36	12	7.284E+00	2.916E-02	6.172E-03	7.373E-03	2.918E-02	2.453E-03	2.498E+02	8.409E-02
36	13	1.165E+00	4.662E-03	9.870E-04	1.179E-03	4.666E-03	3.923E-04	2.498E+02	8.409E-02
36	14	1.424E+00	5.701E-03	1.207E-03	1.443E-03	5.708E-03	4.800E-04	2.498E+02	8.409E-02
36	15	1.687E+00	6.754E-03	1.431E-03	1.709E-03	6.763E-03	5.687E-04	2.498E+02	8.409E-02
36	16	2.180E+00	8.726E-03	1.848E-03	2.208E-03	8.738E-03	7.347E-04	2.498E+02	8.409E-02
36	17	4.355E+00	1.743E-02	3.695E-03	4.415E-03	1.747E-02	1.469E-03	2.498E+02	8.409E-02
36	19	6.338E-01	2.537E-03	5.372E-04	6.418E-04	2.540E-03	2.135E-04	2.498E+02	8.409E-02
36	20	2.750E-01	1.101E-03	2.332E-04	2.786E-04	1.102E-03	9.269E-05	2.498E+02	8.409E-02
36	21	7.432E-01	2.975E-03	6.303E-04	7.531E-04	2.980E-03	2.506E-04	2.498E+02	8.409E-02
36	22	3.397E+00	1.360E-02	2.883E-03	3.446E-03	1.363E-02	1.146E-03	2.498E+02	8.409E-02
36	23	5.116E+00	2.048E-02	4.346E-03	5.195E-03	2.055E-02	1.728E-03	2.498E+02	8.409E-02
36	24	6.705E-01	2.684E-03	5.679E-04	6.784E-04	2.685E-03	2.257E-04	2.498E+02	8.409E-02
36	25	3.796E-01	1.520E-03	3.218E-04	3.844E-04	1.521E-03	1.279E-04	2.498E+02	8.409E-02
36	26	5.232E-01	2.094E-03	4.439E-04	5.304E-04	2.098E-03	1.764E-04	2.498E+02	8.409E-02
36	27	1.375E+00	5.503E-03	1.166E-03	1.394E-03	5.513E-03	4.636E-04	2.498E+02	8.409E-02
36	28	3.855E+00	1.543E-02	3.275E-03	3.914E-03	1.548E-02	1.302E-03	2.498E+02	8.409E-02
36	29	9.990E-01	3.999E-03	8.459E-04	1.010E-03	3.999E-03	3.362E-04	2.498E+02	8.409E-02
36	30	6.331E-01	2.534E-03	5.363E-04	6.406E-04	2.535E-03	2.132E-04	2.498E+02	8.409E-02
36	31	3.961E-01	1.593E-03	3.373E-04	4.029E-04	1.594E-03	1.341E-04	2.498E+02	8.409E-02
36	32	1.306E+00	5.228E-03	1.107E-03	1.322E-03	5.233E-03	4.400E-04	2.498E+02	8.409E-02
36	33	7.185E+00	2.876E-02	6.098E-03	7.287E-03	2.893E-02	2.424E-03	2.498E+02	8.409E-02
36	34	1.046E+00	4.187E-03	8.862E-04	1.059E-03	4.189E-03	3.523E-04	2.498E+02	8.409E-02
36	35	4.524E-01	1.811E-03	3.834E-04	4.580E-04	1.812E-03	1.524E-04	2.498E+02	8.409E-02
36	39	1.877E+00	7.512E-03	1.599E-03	1.912E-03	7.557E-03	6.355E-04	2.498E+02	8.409E-02
36	40	1.345E+00	5.385E-03	1.141E-03	1.363E-03	5.392E-03	4.534E-04	2.498E+02	8.409E-02
36	42	5.700E-01	2.282E-03	4.829E-04	5.769E-04	2.283E-03	1.920E-04	2.498E+02	8.409E-02
36	43	8.576E-01	3.433E-03	7.282E-04	8.703E-04	3.442E-03	2.895E-04	2.498E+02	8.409E-02

RUN	GAGE	Q(CW)	Q(AV)/Q(O)	H(A)	H(B)	H(A)/H(O)	C(H)	Q(O)	C(H(O))
37	1	7.932E+00	3.777E-02	6.602E-03	7.890E-03	3.794E-02	3.912E-03	2.100E+02	1.031E-01
37	2	3.645E+00	1.736E-02	3.029E-03	3.619E-03	1.741E-02	1.795E-03	2.100E+02	1.031E-01
37	3	2.228E+00	1.061E-02	1.850E-03	2.210E-03	1.063E-02	1.096E-03	2.100E+02	1.031E-01
37	4	2.067E+00	9.842E-03	1.716E-03	2.049E-03	9.859E-03	1.017E-03	2.100E+02	1.031E-01
37	6	2.764E+00	1.316E-02	2.294E-03	2.741E-03	1.318E-02	1.359E-03	2.100E+02	1.031E-01
37	7	4.278E+00	2.037E-02	3.550E-03	4.241E-03	2.040E-02	2.104E-03	2.100E+02	1.031E-01
37	8	1.769E+00	8.425E-03	1.468E-03	1.753E-03	8.433E-03	8.695E-04	2.100E+02	1.031E-01
37	9	1.312E+00	6.246E-03	1.088E-03	1.299E-03	6.250E-03	6.444E-04	2.100E+02	1.031E-01
37	10	3.268E+00	1.556E-02	2.713E-03	3.241E-03	1.559E-02	1.607E-03	2.100E+02	1.031E-01
37	12	5.574E+00	2.654E-02	4.620E-03	5.517E-03	2.655E-02	2.737E-03	2.100E+02	1.031E-01
37	13	1.131E+00	5.387E-03	9.379E-04	1.120E-03	5.390E-03	5.557E-04	2.100E+02	1.031E-01
37	14	1.148E+00	5.466E-03	9.518E-04	1.137E-03	5.469E-03	5.639E-04	2.100E+02	1.031E-01
37	15	1.510E+00	7.190E-03	1.252E-03	1.495E-03	7.193E-03	7.417E-04	2.100E+02	1.031E-01
37	16	2.035E+00	9.691E-03	1.688E-03	2.015E-03	9.698E-03	9.999E-04	2.100E+02	1.031E-01
37	17	3.673E+00	1.749E-02	3.047E-03	3.640E-03	1.751E-02	1.806E-03	2.100E+02	1.031E-01
37	19	5.816E-01	2.769E-03	4.823E-04	5.759E-04	2.771E-03	2.857E-04	2.100E+02	1.031E-01
37	20	3.608E-01	1.718E-03	2.992E-04	3.573E-04	1.719E-03	1.773E-04	2.100E+02	1.031E-01
37	21	6.504E-01	3.097E-03	5.394E-04	6.441E-04	3.099E-03	3.196E-04	2.100E+02	1.031E-01
37	22	2.862E+00	1.363E-02	2.375E-03	2.836E-03	1.365E-02	1.407E-03	2.100E+02	1.031E-01
37	23	4.225E+00	2.012E-02	3.508E-03	4.191E-03	2.016E-02	2.079E-03	2.100E+02	1.031E-01
37	24	5.777E-01	2.751E-03	4.787E-04	5.716E-04	2.751E-03	2.836E-04	2.100E+02	1.031E-01
37	25	2.729E-01	1.300E-03	2.262E-04	2.701E-04	1.300E-03	1.340E-04	2.100E+02	1.031E-01
37	26	3.706E-01	1.765E-03	3.073E-04	3.670E-04	1.766E-03	1.821E-04	2.100E+02	1.031E-01
37	27	1.072E+00	5.107E-03	8.894E-04	1.062E-03	5.111E-03	5.270E-04	2.100E+02	1.031E-01
37	28	3.227E+00	1.536E-02	2.678E-03	3.199E-03	1.539E-02	1.587E-03	2.100E+02	1.031E-01
37	29	6.648E-01	3.166E-03	5.507E-04	6.575E-04	3.164E-03	3.263E-04	2.100E+02	1.031E-01
37	30	2.981E-01	1.419E-03	2.470E-04	2.949E-04	1.419E-03	1.463E-04	2.100E+02	1.031E-01
37	31	3.588E-01	1.709E-03	2.973E-04	3.551E-04	1.709E-03	1.762E-04	2.100E+02	1.031E-01
37	32	9.947E-01	4.737E-03	8.248E-04	9.849E-04	4.739E-03	4.887E-04	2.100E+02	1.031E-01
37	33	5.544E+00	2.640E-02	4.602E-03	5.497E-03	2.645E-02	2.727E-03	2.100E+02	1.031E-01
37	34	6.185E-01	2.945E-03	5.125E-04	6.119E-04	2.945E-03	3.037E-04	2.100E+02	1.031E-01
37	35	4.041E-01	1.924E-03	3.350E-04	4.000E-04	1.925E-03	1.985E-04	2.100E+02	1.031E-01
37	40	1.138E+00	5.421E-03	9.439E-04	1.127E-03	5.424E-03	5.592E-04	2.100E+02	1.031E-01
37	42	4.319E-01	2.056E-03	3.580E-04	4.275E-04	2.057E-03	2.121E-04	2.100E+02	1.031E-01
37	43	5.873E-01	2.797E-03	4.877E-04	5.826E-04	2.802E-03	2.890E-04	2.100E+02	1.031E-01

RUN	GAGE	Q(CW)	Q(AV)/Q(O)	H(A)	H(B)	H(A)/H(O)	C(H)	Q(O)	C(H(O))
38	1	9.440E+00	3.453E-02	8.468E-03	1.013E-02	3.466E-02	2.399E-03	2.734E+02	6.922E-02
38	2	4.299E+00	1.572E-02	3.850E-03	4.604E-03	1.576E-02	1.091E-03	2.734E+02	6.922E-02
38	3	2.754E+00	1.007E-02	2.465E-03	2.948E-03	1.009E-02	6.985E-04	2.734E+02	6.922E-02
38	4	2.519E+00	9.215E-03	2.255E-03	2.696E-03	9.229E-03	6.389E-04	2.734E+02	6.922E-02
38	6	3.421E+00	1.251E-02	3.061E-03	3.661E-03	1.253E-02	8.673E-04	2.734E+02	6.922E-02
38	7	5.266E+00	1.926E-02	4.711E-03	5.634E-03	1.929E-02	1.335E-03	2.734E+02	6.922E-02
38	8	2.182E+00	7.980E-03	1.951E-03	2.332E-03	7.985E-03	5.527E-04	2.734E+02	6.922E-02
38	9	1.806E+00	6.605E-03	1.614E-03	1.930E-03	6.607E-03	4.573E-04	2.734E+02	6.922E-02
38	10	6.687E+00	2.446E-02	5.988E-03	7.161E-03	2.451E-02	1.697E-03	2.734E+02	6.922E-02
38	12	1.094E+01	4.001E-02	9.781E-03	1.169E-02	4.004E-02	2.771E-03	2.734E+02	6.922E-02
38	13	1.541E+00	5.637E-03	1.377E-03	1.646E-03	5.637E-03	3.902E-04	2.734E+02	6.922E-02
38	14	1.691E+00	6.186E-03	1.512E-03	1.807E-03	6.188E-03	4.283E-04	2.734E+02	6.922E-02
38	15	1.599E+00	5.847E-03	1.429E-03	1.709E-03	5.850E-03	4.050E-04	2.734E+02	6.922E-02
38	16	2.071E+00	7.574E-03	1.851E-03	2.213E-03	7.577E-03	5.245E-04	2.734E+02	6.922E-02
38	17	4.768E+00	1.744E-02	4.265E-03	5.099E-03	1.746E-02	1.208E-03	2.734E+02	6.922E-02
38	19	4.437E-01	1.623E-03	3.965E-04	4.740E-04	1.623E-03	1.123E-04	2.734E+02	6.922E-02
38	20	4.448E-01	1.627E-03	3.977E-04	4.755E-04	1.628E-03	1.127E-04	2.734E+02	6.922E-02
38	21	7.627E-01	2.790E-03	6.818E-04	8.151E-04	2.791E-03	1.932E-04	2.734E+02	6.922E-02
38	22	3.657E+00	1.338E-02	3.271E-03	3.911E-03	1.339E-02	9.267E-04	2.734E+02	6.922E-02
38	23	5.528E+00	2.022E-02	4.947E-03	5.916E-03	2.025E-02	1.402E-03	2.734E+02	6.922E-02
38	24	7.053E-01	2.580E-03	6.299E-04	7.530E-04	2.578E-03	1.785E-04	2.734E+02	6.922E-02
38	25	2.917E-01	1.067E-03	2.606E-04	3.115E-04	1.067E-03	7.383E-05	2.734E+02	6.922E-02
38	26	3.537E-01	1.294E-03	3.163E-04	3.782E-04	1.295E-03	8.962E-05	2.734E+02	6.922E-02
38	27	1.320E+00	4.829E-03	1.181E-03	1.413E-03	4.836E-03	3.347E-04	2.734E+02	6.922E-02
38	28	3.965E+00	1.450E-02	3.550E-03	4.245E-03	1.453E-02	1.006E-03	2.734E+02	6.922E-02
38	29	9.910E-01	3.625E-03	8.851E-04	1.058E-03	3.623E-03	2.508E-04	2.734E+02	6.922E-02
38	30	5.543E-01	2.027E-03	4.951E-04	5.918E-04	2.027E-03	1.403E-04	2.734E+02	6.922E-02
38	31	3.289E-01	1.203E-03	2.938E-04	3.512E-04	1.203E-03	8.325E-05	2.734E+02	6.922E-02
36	32	1.156E+00	4.227E-03	1.033E-03	1.235E-03	4.228E-03	2.926E-04	2.734E+02	6.922E-02
38	34	9.903E-01	3.622E-03	8.847E-04	1.058E-03	3.621E-03	2.507E-04	2.734E+02	6.922E-02
38	35	5.015E-01	1.834E-03	4.482E-04	5.358E-04	1.835E-03	1.270E-04	2.734E+02	6.922E-02
38	39	2.579E+00	9.434E-03	2.320E-03	2.777E-03	9.495E-03	6.573E-04	2.734E+02	6.922E-02
38	40	1.451E+00	5.308E-03	1.297E-03	1.551E-03	5.310E-03	3.675E-04	2.734E+02	6.922E-02
38	42	7.196E-01	2.632E-03	6.430E-04	7.666E-04	2.632E-03	1.822E-04	2.734E+02	6.922E-02
38	43	1.266E+00	4.630E-03	1.133E-03	1.355E-03	4.638E-03	3.211E-04	2.734E+02	6.922E-02

RUN	GAGE	Q(CW)	Q(AV)/Q(D)	H(A)	H(B)	H(A)/H(D)	C(H)	Q(D)	C(H(D))
39	1	6.086E+00	2.340E-02	5.091E-03	6.085E-03	2.350E-02	1.920E-03	2.600E+02	8.171E-02
39	2	2.847E+00	1.095E-02	2.378E-03	2.842E-03	1.098E-02	8.969E-04	2.600E+02	8.171E-02
39	3	2.607E+00	1.002E-02	2.176E-03	2.600E-03	1.004E-02	8.206E-04	2.600E+02	8.171E-02
39	4	2.623E+00	1.009E-02	2.188E-03	2.614E-03	1.010E-02	8.253E-04	2.600E+02	8.171E-02
39	6	2.153E+00	8.280E-03	1.797E-03	2.147E-03	8.293E-03	6.776E-04	2.600E+02	8.171E-02
39	7	3.888E+00	1.495E-02	3.243E-03	3.875E-03	1.497E-02	1.223E-03	2.600E+02	8.171E-02
39	8	2.781E+00	1.069E-02	2.319E-03	2.770E-03	1.070E-02	8.746E-04	2.600E+02	8.171E-02
39	9	3.556E+00	1.368E-02	2.967E-03	3.544E-03	1.369E-02	1.119E-03	2.600E+02	8.171E-02
39	10	1.089E+01	4.188E-02	9.097E-03	1.087E-02	4.199E-02	3.431E-03	2.600E+02	8.171E-02
39	12	1.578E+01	6.069E-02	1.317E-02	1.573E-02	6.077E-02	4.965E-03	2.600E+02	8.171E-02
39	13	1.295E+00	4.979E-03	1.079E-03	1.288E-03	4.979E-03	4.068E-04	2.600E+02	8.171E-02
39	14	1.147E+00	4.410E-03	9.555E-04	1.141E-03	4.410E-03	3.604E-04	2.600E+02	8.171E-02
39	15	9.094E-01	3.497E-03	7.577E-04	9.049E-04	3.497E-03	2.858E-04	2.600E+02	8.171E-02
39	16	1.976E+00	7.601E-03	1.647E-03	1.967E-03	7.603E-03	6.212E-04	2.600E+02	8.171E-02
39	17	4.252E+00	1.635E-02	3.545E-03	4.235E-03	1.636E-02	1.337E-03	2.600E+02	8.171E-02
39	19	5.177E-01	1.991E-03	4.312E-04	5.150E-04	1.990E-03	1.626E-04	2.600E+02	8.171E-02
39	20	4.502E-01	1.731E-03	3.752E-04	4.481E-04	1.732E-03	1.415E-04	2.600E+02	8.171E-02
39	21	5.557E-01	2.137E-03	4.631E-04	5.532E-04	2.138E-03	1.747E-04	2.600E+02	8.171E-02
39	24	5.141E-01	1.977E-03	4.280E-04	5.111E-04	1.975E-03	1.614E-04	2.600E+02	8.171E-02
39	25	4.204E-01	1.617E-03	3.501E-04	4.181E-04	1.616E-03	1.320E-04	2.600E+02	8.171E-02
39	26	4.153E-01	1.597E-03	3.465E-04	4.140E-04	1.600E-03	1.307E-04	2.600E+02	8.171E-02
39	27	1.456E+00	5.599E-03	1.213E-03	1.449E-03	5.600E-03	4.576E-04	2.600E+02	8.171E-02
39	28	5.087E+00	1.956E-02	4.236E-03	5.059E-03	1.955E-02	1.598E-03	2.600E+02	8.171E-02
39	29	5.245E-01	2.017E-03	4.365E-04	5.212E-04	2.015E-03	1.646E-04	2.600E+02	8.171E-02
39	30	5.550E-01	2.134E-03	4.621E-04	5.519E-04	2.133E-03	1.743E-04	2.600E+02	8.171E-02
39	31	3.980E-01	1.531E-03	3.315E-04	3.958E-04	1.530E-03	1.250E-04	2.600E+02	8.171E-02
39	32	1.951E+00	7.501E-03	1.626E-03	1.942E-03	7.503E-03	6.131E-04	2.600E+02	8.171E-02
39	33	5.095E+00	1.959E-02	4.250E-03	5.078E-03	1.962E-02	1.603E-03	2.600E+02	8.171E-02
39	34	7.072E-01	2.719E-03	5.899E-04	7.033E-04	2.718E-03	2.221E-04	2.600E+02	8.171E-02
39	35	3.983E-01	1.532E-03	3.318E-04	3.963E-04	1.531E-03	1.251E-04	2.600E+02	8.171E-02
39	39	1.341E+00	5.158E-03	1.121E-03	1.340E-03	5.176E-03	4.230E-04	2.600E+02	8.171E-02
39	40	1.052E+00	4.047E-03	8.770E-04	1.047E-03	4.048E-03	3.308E-04	2.600E+02	8.171E-02
39	42	7.454E-01	2.867E-03	6.211E-04	7.419E-04	2.867E-03	2.343E-04	2.600E+02	8.171E-02
39	43	7.323E-01	2.816E-03	6.114E-04	7.306E-04	2.822E-03	2.306E-04	2.600E+02	8.171E-02

RUN	GAGE	Q(CW)	Q(AV)/Q(O)	H(A)	H(B)	H(A)/H(O)	C(H)	Q(O)	C(H(O))
40	1	4.952E+00	2.302E-02	4.091E-03	4.891E-03	2.314E-02	2.359E-03	2.152E+02	1.020E-01
40	2	2.335E+00	1.085E-02	1.926E-03	2.302E-03	1.089E-02	1.111E-03	2.152E+02	1.020E-01
40	3	1.838E+00	8.542E-03	1.515E-03	1.810E-03	8.568E-03	8.736E-04	2.152E+02	1.020E-01
40	4	1.661E+00	7.722E-03	1.369E-03	1.636E-03	7.745E-03	7.896E-04	2.152E+02	1.020E-01
40	6	1.808E+00	8.402E-03	1.490E-03	1.780E-03	8.426E-03	8.591E-04	2.152E+02	1.020E-01
40	7	3.176E+00	1.476E-02	2.617E-03	3.127E-03	1.480E-02	1.509E-03	2.152E+02	1.020E-01
40	8	1.614E+00	7.499E-03	1.329E-03	1.588E-03	7.516E-03	7.663E-04	2.152E+02	1.020E-01
40	9	1.893E+00	8.800E-03	1.558E-03	1.861E-03	8.813E-03	8.985E-04	2.152E+02	1.020E-01
40	10	5.111E+00	2.375E-02	4.210E-03	5.031E-03	2.382E-02	2.428E-03	2.152E+02	1.020E-01
40	12	8.471E+00	3.937E-02	6.969E-03	8.326E-03	3.942E-02	4.019E-03	2.152E+02	1.020E-01
40	13	9.377E-01	4.358E-03	7.713E-04	9.213E-04	4.363E-03	4.448E-04	2.152E+02	1.020E-01
40	14	8.357E-01	3.884E-03	6.875E-04	8.213E-04	3.889E-03	3.965E-04	2.152E+02	1.020E-01
40	15	8.984E-01	4.175E-03	7.394E-04	8.834E-04	4.182E-03	4.264E-04	2.152E+02	1.020E-01
40	16	1.719E+00	7.989E-03	1.415E-03	1.690E-03	8.002E-03	8.158E-04	2.152E+02	1.020E-01
40	17	3.307E+00	1.537E-02	2.722E-03	3.252E-03	1.540E-02	1.570E-03	2.152E+02	1.020E-01
40	19	5.346E-01	2.485E-03	4.396E-04	5.251E-04	2.487E-03	2.535E-04	2.152E+02	1.020E-01
40	20	2.957E-01	1.374E-03	2.432E-04	2.905E-04	1.376E-03	1.403E-04	2.152E+02	1.020E-01
40	21	4.375E-01	2.033E-03	3.599E-04	4.300E-04	2.036E-03	2.076E-04	2.152E+02	1.020E-01
40	22	2.817E+00	1.309E-02	2.319E-03	2.771E-03	1.312E-02	1.338E-03	2.152E+02	1.020E-01
40	23	4.747E+00	2.206E-02	3.911E-03	4.674E-03	2.212E-02	2.256E-03	2.152E+02	1.020E-01
40	24	4.605E-01	2.140E-03	3.785E-04	4.520E-04	2.141E-03	2.183E-04	2.152E+02	1.020E-01
40	25	2.445E-01	1.136E-03	2.010E-04	2.402E-04	1.137E-03	1.159E-04	2.152E+02	1.020E-01
40	26	3.137E-01	1.458E-03	2.581E-04	3.083E-04	1.460E-03	1.489E-04	2.152E+02	1.020E-01
40	28	4.945E+00	2.298E-02	4.074E-03	4.869E-03	2.305E-02	2.350E-03	2.152E+02	1.020E-01
40	29	5.679E-01	2.639E-03	4.666E-04	5.572E-04	2.639E-03	2.691E-04	2.152E+02	1.020E-01
40	30	4.593E-01	2.135E-03	3.774E-04	4.507E-04	2.135E-03	2.176E-04	2.152E+02	1.020E-01
40	31	4.021E-01	1.869E-03	3.305E-04	3.948E-04	1.870E-03	1.906E-04	2.152E+02	1.020E-01
40	32	1.412E+00	6.561E-03	1.161E-03	1.387E-03	6.569E-03	6.698E-04	2.152E+02	1.020E-01
40	33	3.435E+00	1.596E-02	2.828E-03	3.378E-03	1.599E-02	1.631E-03	2.152E+02	1.020E-01
40	34	6.915E-01	3.214E-03	5.686E-04	6.791E-04	3.216E-03	3.279E-04	2.152E+02	1.020E-01
40	35	3.364E-01	1.564E-03	2.767E-04	3.305E-04	1.565E-03	1.596E-04	2.152E+02	1.020E-01
40	39	9.873E-01	4.589E-03	8.192E-04	9.803E-04	4.634E-03	4.725E-04	2.152E+02	1.020E-01
40	40	4.326E-01	2.011E-03	3.558E-04	4.250E-04	2.013E-03	2.052E-04	2.152E+02	1.020E-01
40	42	4.549E-01	2.114E-03	3.740E-04	4.467E-04	2.116E-03	2.157E-04	2.152E+02	1.020E-01
40	43	3.722E-01	1.730E-03	3.068E-04	3.667E-04	1.735E-03	1.769E-04	2.152E+02	1.020E-01

RUN	GAGE	M	P(M)	C(P)	P(M)/P	P(M)/PITOT	P(M)/POP(M
1	1	1.226E+01	7.817E-02	2.449E-02	3.580E+00	1.813E-02	1.753E-02
1	2	1.226E+01	6.827E-02	2.019E-02	3.127E+00	1.584E-02	1.531E-02
1	4	1.226E+01	4.172E-02	8.645E-03	1.911E+00	9.677E-03	9.354E-03
1	5	1.226E+01	3.301E-02	4.859E-03	1.512E+00	7.658E-03	7.402E-03
1	101	1.226E+01	4.462E+00	1.931E+00	2.044E+02	1.035E+00	1.001E+00
1	102	1.226E+01	4.422E+00	1.913E+00	2.025E+02	1.026E+00	9.914E-01
2	1	1.226E+01	5.022E-02	1.236E-02	2.302E+00	1.166E-02	1.019E-02
2	2	1.226E+01	5.924E-02	1.629E-02	2.715E+00	1.375E-02	1.202E-02
2	101	1.226E+01	5.074E+00	2.199E+00	2.326E+02	1.178E+00	1.029E+00
2	102	1.226E+01	4.741E+00	2.054E+00	2.173E+02	1.101E+00	9.618E-01
3	1	1.187E+01	1.732E-01	1.440E-02	2.423E+00	1.308E-02	1.255E-02
3	2	1.187E+01	1.876E-01	1.644E-02	2.624E+00	1.417E-02	1.359E-02
3	3	1.187E+01	2.339E-01	2.300E-02	3.272E+00	1.767E-02	1.695E-02
3	4	1.187E+01	2.515E-01	2.549E-02	3.519E+00	1.900E-02	1.823E-02
3	5	1.187E+01	2.026E-01	1.857E-02	2.834E+00	1.530E-02	1.468E-02
3	101	1.187E+01	1.414E+01	1.992E+00	1.978E+02	1.068E+00	1.025E+00
3	102	1.187E+01	1.333E+01	1.877E+00	1.864E+02	1.007E+00	9.658E-01
4	2	1.180E+01	1.764E-01	1.523E-02	2.485E+00	1.359E-02	1.233E-02
4	4	1.180E+01	2.639E-02	-6.441E-03	3.718E-01	2.032E-03	1.845E-03
4	5	1.180E+01	8.849E-02	2.532E-03	1.247E+00	6.816E-03	6.188E-03
4	101	1.180E+01	1.485E+01	2.135E+00	2.092E+02	1.144E+00	1.038E+00
4	102	1.180E+01	1.369E+01	1.967E+00	1.929E+02	1.054E+00	9.571E-01
5	2	1.224E+01	6.507E-02	2.021E-02	3.124E+00	1.586E-02	1.350E-02
5	3	1.224E+01	1.817E-02	-1.214E-03	8.725E-01	4.429E-03	3.771E-03
5	4	1.224E+01	1.245E-02	-3.828E-03	5.978E-01	3.035E-03	2.584E-03
5	5	1.224E+01	2.847E-02	3.490E-03	1.367E+00	6.938E-03	5.907E-03
5	101	1.224E+01	5.048E+00	2.297E+00	2.423E+02	1.230E+00	1.047E+00
5	102	1.224E+01	4.574E+00	2.080E+00	2.196E+02	1.115E+00	9.469E-01

RUN	GAGE	M	P(M)	C(P)	P(M)/P	P(M)/PITOT	P(M)/POP(M
6	2	1.167E+01	1.406E-02	1.632E-02	2.558E+00	1.430E-02	1.436E-02
6	3	1.167E+01	5.083E-03	-7.867E-04	9.249E-01	5.170E-03	5.192E-03
6	4	1.167E+01	3.432E-03	-3.935E-03	6.245E-01	3.491E-03	3.506E-03
6	5	1.167E+01	5.367E-03	-2.452E-04	9.766E-01	5.459E-03	5.482E-03
6	101	1.167E+01	1.007E+00	1.910E+00	1.832E+02	1.024E+00	1.029E+00
6	102	1.167E+01	9.469E-01	1.795E+00	1.723E+02	9.630E-01	9.672E-01
7	2	1.571E+01	3.677E-02	1.909E-02	4.303E+00	1.327E-02	1.398E-02
7	3	1.571E+01	7.835E-03	-4.810E-04	9.168E-01	2.827E-03	2.979E-03
7	4	1.571E+01	6.674E-03	-1.266E-03	7.810E-01	2.408E-03	2.538E-03
7	101	1.571E+01	2.729E+00	1.840E+00	3.194E+02	9.847E-01	1.038E+00
7	102	1.571E+01	2.505E+00	1.689E+00	2.931E+02	9.039E-01	9.525E-01
8	2	1.181E+01	1.329E-01	8.583E-03	1.839E+00	1.003E-02	9.292E-03
8	3	1.181E+01	5.116E-02	-2.997E-03	7.072E-01	3.858E-03	3.574E-03
8	4	1.181E+01	3.666E-02	-5.042E-03	5.073E-01	2.768E-03	2.564E-03
8	5	1.181E+01	8.903E-02	2.374E-03	1.232E+00	6.722E-03	6.226E-03
8	101	1.181E+01	1.485E+01	2.093E+00	2.055E+02	1.121E+00	1.039E+00
8	102	1.181E+01	1.360E+01	1.915E+00	1.882E+02	1.027E+00	9.511E-01
9	2	1.161E+01	1.087E-01	1.172E-02	2.107E+00	1.189E-02	1.119E-02
9	3	1.161E+01	3.048E-02	-4.333E-03	5.908E-01	3.336E-03	3.139E-03
9	4	1.161E+01	2.214E-02	-6.046E-03	4.290E-01	2.422E-03	2.280E-03
9	5	1.161E+01	6.066E-02	1.860E-03	1.176E+00	6.638E-03	6.247E-03
9	101	1.161E+01	1.024E+01	2.091E+00	1.984E+02	1.120E+00	1.055E+00
9	102	1.161E+01	9.211E+00	1.880E+00	1.785E+02	1.008E+00	9.486E-01
10	2	1.226E+01	5.505E-02	1.629E-02	2.717E+00	1.375E-02	1.184E-02
10	3	1.226E+01	1.767E-02	-1.213E-03	8.722E-01	4.416E-03	3.801E-03
10	4	1.226E+01	1.276E-02	-3.515E-03	6.296E-01	3.187E-03	2.744E-03
10	5	1.226E+01	2.538E-02	2.393E-03	1.252E+00	6.340E-03	5.457E-03
10	101	1.226E+01	4.811E+00	2.243E+00	2.374E+02	1.202E+00	1.035E+00
10	102	1.226E+01	4.467E+00	2.082E+00	2.204E+02	1.116E+00	9.606E-01

RUN	GAGE	M	P(M)	C(P)	P(M)/P	P(M)/PITOT	P(M)/POP(M
11	3	1.164E+01	5.206E-03	2.400E-04	1.023E+00	5.751E-03	5.903E-03
11	4	1.164E+01	3.655E-03	-2.972E-03	7.181E-01	4.038E-03	4.144E-03
11	5	1.164E+01	5.017E-03	-1.516E-04	9.856E-01	5.542E-03	5.689E-03
11	101	1.164E+01	9.111E-01	1.876E+00	1.790E+02	1.006E+00	1.033E+00
11	102	1.164E+01	8.535E-01	1.757E+00	1.677E+02	9.428E-01	9.677E-01
12	2	1.601E+01	5.458E-02	1.942E-02	4.488E+00	1.333E-02	1.358E-02
12	3	1.601E+01	9.231E-02	3.670E-02	7.590E+00	2.255E-02	2.296E-02
12	4	1.601E+01	4.763E-03	-3.388E-03	3.916E-01	1.163E-03	1.185E-03
12	101	1.601E+01	4.093E+00	1.869E+00	3.366E+02	1.000E+00	1.018E+00
12	102	1.601E+01	3.918E+00	1.789E+00	3.222E+02	9.572E-01	9.747E-01
13	5	1.571E+01	1.311E-02	3.251E-03	1.562E+00	4.819E-03	5.266E-03
13	101	1.571E+01	2.622E+00	1.801E+00	3.125E+02	9.638E-01	1.053E+00
13	102	1.571E+01	2.510E+00	1.723E+00	2.991E+02	9.225E-01	1.008E+00
14	2	1.016E+01	1.252E-01	7.667E-03	1.555E+00	1.146E-02	1.052E-02
14	4	1.016E+01	3.363E-02	-8.049E-03	4.177E-01	3.079E-03	2.826E-03
14	5	1.016E+01	7.829E-02	-3.806E-04	9.725E-01	7.169E-03	6.579E-03
14	101	1.016E+01	1.201E+01	2.049E+00	1.492E+02	1.100E+00	1.009E+00
14	102	1.016E+01	1.165E+01	1.987E+00	1.448E+02	1.067E+00	9.794E-01
15	2	1.005E+01	8.190E-02	1.462E-02	2.035E+00	1.534E-02	1.424E-02
15	4	1.005E+01	1.854E-02	-7.617E-03	4.607E-01	3.472E-03	3.224E-03
15	5	1.005E+01	3.466E-02	-1.960E-03	8.613E-01	6.490E-03	6.027E-03
15	101	1.005E+01	6.037E+00	2.105E+00	1.500E+02	1.131E+00	1.050E+00
15	102	1.005E+01	5.446E+00	1.898E+00	1.354E+02	1.020E+00	9.474E-01
16	4	1.581E+01	3.628E-03	4.314E-03	1.755E+00	5.328E-03	9.231E-03
16	101	1.581E+01	3.938E-01	1.082E+00	1.906E+02	5.784E-01	1.002E+00
16	102	1.581E+01	3.924E-01	1.079E+00	1.899E+02	5.764E-01	9.985E-01

RUN	GAGE	M	P(M)	C(P)	P(M)/P	P(M)/PITOT	P(M)/POP(M
17	2	1.224E+01	4.518E-02	1.054E-02	2.106E+00	1.071E-02	1.027E-02
17	4	1.224E+01	1.415E-02	-3.24 E-03	6.595E-01	3.353E-03	3.215E-03
17	5	1.224E+01	3.127E-02	4.362E-03	1.458E+00	7.412E-03	7.107E-03
17	101	1.224E+01	4.584E+00	2.027E+00	2.137E+02	1.087E+00	1.042E+00
17	102	1.224E+01	4.210E+00	1.861E+00	1.963E+02	9.979E-01	9.569E-01
18	2	1.182E+01	8.533E-02	1.586E-03	1.155E+00	6.287E-03	5.845E-03
18	3	1.182E+01	2.715E-02	-6.455E-03	3.676E-01	2.000E-03	1.859E-03
18	4	1.182E+01	3.219E-02	-5.758E-03	4.359E-01	2.372E-03	2.205E-03
18	5	1.182E+01	1.002E-01	3.641E-03	1.357E+00	7.382E-03	6.863E-03
18	101	1.182E+01	1.514E+01	2.082E+00	2.050E+02	1.115E+00	1.037E+00
18	102	1.182E+01	1.415E+01	1.945E+00	1.916E+02	1.042E+00	9.691E-01
19	2	1.223E+01	1.607E-02	-2.511E-03	7.366E-01	3.747E-03	3.562E-03
19	4	1.223E+01	1.361E-02	-3.587E-03	6.238E-01	3.173E-03	3.017E-03
19	5	1.223E+01	3.193E-02	4.427E-03	1.464E+00	7.448E-03	7.081E-03
19	101	1.223E+01	4.629E+00	2.015E+00	2.123E+02	1.080E+00	1.026E+00
19	102	1.223E+01	4.383E+00	1.907E+00	2.010E+02	1.022E+00	9.719E-01
20	4	1.168E+01	4.234E-03	-1.472E-03	8.592E-01	4.792E-03	5.040E-03
20	5	1.168E+01	8.078E-03	6.682E-03	1.639E+00	9.143E-03	9.617E-03
20	101	1.168E+01	8.574E-01	1.808E+00	1.740E+02	9.704E-01	1.021E+00
20	102	1.168E+01	8.176E-01	1.724E+00	1.659E+02	9.254E-01	9.734E-01
21	2	1.570E+01	5.097E-03	-2.336E-03	5.964E-01	1.642E-03	1.916E-03
21	4	1.570E+01	1.100E-02	1.660E-03	1.287E+00	3.974E-03	4.134E-03
21	5	1.570E+01	2.047E-02	8.074E-03	2.395E+00	7.396E-03	7.694E-03
21	101	1.570E+01	2.664E+00	1.799E+00	3.118E+02	9.629E-01	1.002E+00
21	102	1.570E+01	2.644E+00	1.785E+00	3.093E+02	9.554E-01	9.938E-01
22	2	1.001E+01	8.980E-03	-1.121E-02	2.133E-01	1.619E-03	1.311E-03
22	3	1.001E+01	3.023E-02	-4.015E-03	7.181E-01	5.453E-03	4.414E-03
22	4	1.001E+01	2.393E-02	-6.147E-03	5.684E-01	4.316E-03	3.494E-03
22	5	1.001E+01	3.973E-02	-8.035E-04	9.436E-01	7.165E-03	5.799E-03
22	101	1.001E+01	6.646E+00	2.234E+00	1.579E+02	1.199E+00	9.702E-01
22	102	1.001E+01	5.782E+00	1.942E+00	1.373E+02	1.043E+00	8.441E-01

RUN	GAGE	M	P(M)	C(P)	P(M)/P	P(M)/PITOT	P(M)/PDP(M
23	4	1.826E+01	2.451E-03	6.096E-03	2.425E+00	5.541E-03	6.366E-03
23	5	1.826E+01	2.815E-03	7.635E-03	2.785E+00	6.363E-03	7.310E-03
23	101	1.826E+01	4.001E-01	1.689E+00	3.959E+02	9.046E-01	1.039E+00
23	102	1.826E+01	3.714E-01	1.568E+00	3.675E+02	8.398E-01	9.648E-01
24	2	1.859E+01	9.386E-03	1.614E-02	5.395E+00	1.188E-02	1.175E-02
24	4	1.859E+01	2.982E-03	2.947E-03	1.714E+00	3.773E-03	3.732E-03
24	5	1.859E+01	4.164E-03	5.753E-03	2.393E+00	5.269E-03	5.211E-03
24	101	1.859E+01	8.286E-01	1.962E+00	4.762E+02	1.048E+00	1.037E+00
24	102	1.859E+01	7.692E-01	1.821E+00	4.421E+02	9.734E-01	9.628E-01
26	101	1.232E+01	4.262E+00	2.182E+00	2.330E+02	1.171E+00	1.076E+00
26	102	1.232E+01	3.919E+00	2.006E+00	2.143E+02	1.077E+00	9.897E-01
27	3	1.181E+01	2.185E-01	1.987E-02	2.944E+00	1.605E-02	1.896E-02
27	4	1.181E+01	2.608E-01	2.571E-02	3.515E+00	1.916E-02	2.266E-02
27	5	1.181E+01	2.252E-01	2.080E-02	3.035E+00	1.654E-02	1.957E-02
27	101	1.181E+01	1.430E+01	1.960E+00	1.927E+02	1.051E+00	1.243E+00
27	102	1.181E+01	1.383E+01	1.895E+00	1.863E+02	1.016E+00	1.201E+00
28	2	1.224E+01	8.629E-02	3.224E-02	4.385E+00	2.228E-02	1.832E-02
28	4	1.224E+01	9.616E-02	3.702E-02	4.887E+00	2.483E-02	2.042E-02
28	5	1.224E+01	8.242E-02	3.037E-02	4.188E+00	2.128E-02	1.750E-02
28	101	1.224E+01	4.736E+00	2.283E+00	2.407E+02	1.223E+00	1.006E+00
28	102	1.224E+01	4.657E+00	2.244E+00	2.367E+02	1.203E+00	9.888E-01
29	2	1.166E+01	1.565E-02	2.215E-02	3.111E+00	1.742E-02	1.549E-02
29	4	1.166E+01	2.319E-02	3.789E-02	4.611E+00	2.582E-02	2.296E-02
29	5	1.166E+01	2.020E-02	3.165E-02	4.016E+00	2.249E-02	2.000E-02
29	101	1.166E+01	9.495E-01	1.971E+00	1.688E+02	1.057E+00	9.401E-01
29	102	1.166E+01	8.962E-01	1.859E+00	1.782E+02	9.979E-01	8.874E-01
30	2	1.570E+01	2.470E-02	1.083E-02	2.869E+00	8.867E-03	9.648E-03
30	5	1.570E+01	3.834E-02	2.001E-02	4.454E+00	1.376E-02	1.498E-02
30	101	1.570E+01	2.947E+00	1.977E+00	3.423E+02	1.058E+00	1.151E+00
30	102	1.570E+01	2.715E+00	1.821E+00	3.153E+02	9.745E-01	1.060E+00

RUN	GAGE	M	P(M)	C(P)	P(M)/P	P(M)/PITOT	P(M)/POP(M
31	2	1.183E+01	1.409E-01	8.767E-03	1.860E+00	1.011E-02	9.885E-03
31	3	1.183E+01	2.382E-01	2.187E-02	3.146E+00	1.709E-02	1.671E-02
31	4	1.183E+01	2.768E-01	2.707E-02	3.656E+00	1.986E-02	1.943E-02
31	5	1.183E+01	2.229E-01	1.981E-02	2.944E+00	1.599E-02	1.564E-02
31	101	1.183E+01	1.442E+01	1.931E+00	1.905E+02	1.035E+00	1.012E+00
31	102	1.183E+01	1.410E+01	1.888E+00	1.863E+02	1.012E+00	9.898E-01
32	4	1.226E+01	4.352E-02	9.445E-03	1.995E+00	1.011E-02	9.670E-03
32	5	1.226E+01	4.193E-02	8.757E-03	1.922E+00	9.741E-03	9.318E-03
32	101	1.226E+01	4.730E+00	2.049E+00	2.168E+02	1.099E+00	1.051E+00
32	102	1.226E+01	4.279E+00	1.853E+00	1.961E+02	9.940E-01	9.509E-01
33	4	1.180E+01	3.868E-05	-1.024E-02	5.289E-04	2.889E-06	2.817E-06
33	5	1.180E+01	8.060E-02	1.046E-03	1.102E+00	6.019E-03	5.870E-03
33	101	1.180E+01	1.470E+01	2.049E+00	2.011E+02	1.098E+00	1.071E+00
33	102	1.180E+01	1.272E+01	1.772E+00	1.739E+02	9.499E-01	9.264E-01
34	2	1.228E+01	5.615E-02	1.556E-02	2.644E+00	1.335E-02	1.245E-02
34	3	1.228E+01	1.652E-02	-2.100E-03	7.780E-01	3.928E-03	3.663E-03
34	4	1.228E+01	1.232E-02	-3.971E-03	5.803E-01	2.929E-03	2.732E-03
34	5	1.228E+01	2.120E-02	-1.445E-05	9.985E-01	5.041E-03	4.701E-03
34	101	1.228E+01	4.536E+00	2.012E+00	2.136E+02	1.078E+00	1.006E+00
34	102	1.228E+01	4.297E+00	1.905E+00	2.023E+02	1.021E+00	9.527E-01
35	2	1.170E+01	1.400E-02	1.919E-02	2.842E+00	1.580E-02	1.394E-02
35	3	1.170E+01	4.232E-03	-1.467E-03	8.592E-01	4.776E-03	4.215E-03
35	4	1.170E+01	3.568E-03	-2.872E-03	7.243E-01	4.026E-03	3.554E-03
35	5	1.170E+01	3.789E-03	-2.405E-03	7.692E-01	4.276E-03	3.774E-03
35	101	1.170E+01	9.288E-01	1.954E+00	1.886E+02	1.048E+00	9.251E-01
35	102	1.170E+01	8.181E-01	1.720E+00	1.661E+02	9.232E-01	8.148E-01

RUN	GAGE	M	P(M)	C(P)	P(M)/P	P(M)/PITOT	P(M)/POP(M
36	2	1.609E+01	5.183E-02	1.854E-02	4.363E+00	1.284E-02	1.183E-02
36	4	1.609E+01	1.096E-02	-4.253E-04	9.228E-01	2.715E-03	2.503E-03
36	101	1.609E+01	4.130E+00	1.911E+00	3.477E+02	1.023E+00	9.430E-01
36	102	1.609E+01	4.048E+00	1.873E+00	3.407E+02	1.003E+00	9.242E-01
37	2	1.570E+01	3.698E-02	1.954E-02	4.376E+00	1.352E-02	1.306E-02
37	4	1.570E+01	7.754E-03	-4.758E-04	9.178E-01	2.834E-03	2.738E-03
37	101	1.570E+01	2.838E+00	1.938E+00	3.359E+02	1.037E+00	1.002E+00
38	2	1.016E+01	8.516E-02	1.546E-02	2.119E+00	1.564E-02	1.357E-02
38	4	1.016E+01	1.415E-02	-8.951E-03	3.521E-01	2.599E-03	2.255E-03
38	5	1.016E+01	2.591E-02	-4.907E-03	6.448E-01	4.760E-03	4.130E-03
38	101	1.016E+01	5.784E+00	1.975E+00	1.440E+02	1.063E+00	9.221E-01
38	102	1.016E+01	5.776E+00	1.973E+00	1.438E+02	1.061E+00	9.210E-01
39	2	1.223E+01	5.487E-02	1.459E-02	2.529E+00	1.287E-02	1.328E-02
39	5	1.223E+01	2.678E-02	2.236E-03	1.234E+0	6.285E-03	6.485E-03
39	101	1.223E+01	4.490E+00	1.965E+00	2.069E+02	1.054E+00	1.087E+00
39	102	1.223E+01	4.171E+00	1.825E+00	1.922E+02	9.787E-01	1.010E+00
40	2	1.570E+01	1.285E-02	2.738E-03	1.473E+00	4.548E-03	4.589E-03
40	4	1.570E+01	8.142E-03	-3.855E-04	9.334E-01	2.882E-03	2.908E-03
40	101	1.570E+01	2.837E+00	1.877E+00	3.253E+02	1.004E+00	1.013E+00
40	102	1.570E+01	2.755E+00	1.823E+00	3.159E+02	9.754E-01	9.841E-01